Towards understanding selective neuronal vulnerability: Establishing an *in-vitro* model for strain selection

A thesis submitted in partial fulfilment of the requirements for the degree of Doctor of Philosophy from University College London

Alexandra Philiastides

MRC Prion Unit at UCL

Institute of Prion Diseases

University College London

2018

Declaration

I, Alexandra Philiastides, confirm that the work presented in this thesis is my own. Where information has been derived from other sources, I confirm that this has been indicated in the thesis.

Dedication

This thesis is dedicated to the memory of my dearest grandfather Andreas Philiastides and to my beloved grandparents Michalis and Theano Themistokleous.

Acknowledgments

Firstly, I would like to express my sincere gratitude to my PhD supervisor Dr. Peter-Christian Kloehn, for the continuous support, scientific input, encouragement and patience throughout my PhD.

I would like to thank my previous supervisor Dr. Sarah Lloyd, for her great support, guidance and kind advice during the first 18 months of my PhD.

A special thank you to Dr. Craig Brown, who introduced me to cell culture and molecular cloning. It was a real privilege for me to share of his exceptional scientific knowledge which was pivotal for the accomplishment of the work presented in this thesis.

I would also like to thank Dr. Juan Ribes, for his continuous support, help with data analysis, experimental planning and protocols and for his encouragement when the PhD seemed like an unending struggle.

I would like to express my special appreciation and thanks to my secondary supervisor Prof. Parmjit Jat, for his valuable advice on my research as well as on my career. I am also grateful to my departmental graduate tutor Prof. Elizabeth Fisher, for her tremendous support and advice during the difficult times of my PhD. Many thanks are due to Dr. Graham Jackson, for his insightful comments and valuable suggestions which helped me during the write up of this thesis.

This work would not have been possible without the invaluable scientific input and patience of Daniel Yip, Christian Schmidt and Parvin Ahmed who carried out the automated Scrapie Cell assays and devoted their time to help me collect data for my PhD thesis.

I am grateful to Nunu Arora, Mark Batchelor, Susan Joiner, Jessica Sells, Adam Wenborn, Dr. Emmanuelle Vire, Emma Quarterman and Gary Adamson for the scientific input, encouragement and help throughout the past four years.

I am thankful to my friends Luke Dabin, Laura Pulford, Justin Tosh, Lucy Sheytanova, Nora Thoeng, Matt Rickman, Dr. Karen Cleverley, Billy West, Xun Yu Choong, Julia Ravey, Madeleine Reilly and Shaheen Akhtar, with whom I have shared many happy moments and who were always encouraging throughout my PhD. I would also like to thank my colleagues with whom I have shared the PhD office, for the support and the happy memories which I treasure so much: Lucianne Dobson, James Miller, Charlotte Ridler, Prasanth Sivakumar, David Thomas, Grace O'Regan, Karolin Koriath, Caroline

Casey, Angelos Armen, Rachele Saccon, Daniel Wright, Francesca De Giorgio, Rhia Ghosh, Marta Benedekova, Claudia Cannavo, Heather Whittaker, Thanos Dimitriadis, Ines Whitworth, Bernie Simone and Emma Jones.

I am grateful to the people in the IT and administration office who were always friendly and happy to help: Ryan Peter, Samantha MacLeod, Amir Mayahi, David Ruegg, Alison Church and Oke Avwenagha.

This work would not have been possible without the funding provided by John Collinge through the Medical Research Council.

I am thankful and grateful beyond words to my best friend Ruchi Kumari for her immense support and love, and for being the most amazing, caring, genuine and loving friend I could ever ask for. Thank you for the love, the patience, the endless deep conversations, the daily coffee breaks and for believing in me and reminding me that things will always be ok in the end. I would not have been able to go through this without you.

To my dearest parents, Antony and Stalo, and to my precious brothers Andreas and Michalis, thank you for the continuous support, the endless love and for helping me overcome situations when continuing seemed impossible.
To my amazing fiancé, Charlie, thank you for the love, support, encouragement and never-ending patience.

Abstract

Prion diseases are fatal neurodegenerative diseases that affect humans and animals. Prion strains, conformational variants of misfolded prion proteins, are thought to be associated with distinct clinical and pathological phenotypes. Why prion strains cause damage in particular areas of the brain is poorly understood. Although prions are innocuous to most cell lines, differences in their tropism to mouse-adapted prion strains have been broadly observed. While some cell lines show broad susceptibility to prion strains, others are highly selective, suggesting that susceptibility to a specific prion strain is determined by distinct cellular factors.

The neuroblastoma cell line N2aPK1 (PK1) is refractory to the murine prion strain Me7, but highly susceptible to RML. Intracerebral inoculation of mice with Me7 induces hippocampal neuronal loss, whereas RML does not cause degeneration in this brain region. The PME2 subclone, is a PK1-derived subclone with low susceptibility to Me7 and this was used as the parental line to derive highly Me7-susceptible cells. To understand the molecular underpinning of selective neuronal vulnerability and cell tropism of prion strains, respectively, we first undertook a series of successive sub cloning experiments to identify rare PK1 cell clones that are susceptible to Me7. Initially, Me7-susceptible clones were identified at a frequency of only $4x10^{-3}$. The percentage of Me7-susceptible cells increased by 6-fold and 20-fold, respectively, and by the third and final round of sub cloning, 63% of cell clones were highly susceptible to Me7. Persistently infected PME2 cell clones deposited disease-associated PrP (PrP^{d}) in perinuclear and extracellular stores. Strikingly, Me7-refractory PK1 cells were found to be highly susceptible to prions derived from homogenates of chronically Me7-infected PME2 cells, suggesting that a single passage in PME2 cells changed the strain properties of brain-adapted Me7. This cell model provides the first evidence for prion strain adaptation in genetically similar cell clones. The identification of genetically similar cell clones that differ in their ability to adapt prion strains lays the foundation for future work to gain insights into the molecular mechanisms that underlie prion strain adaptation.

During the second half of my PhD, I worked on a separate project, investigating the role of Fkbp proteins in molecular mechanisms of prion propagation. While the prion protein gene is the major genetic determinant of susceptibility to prion disease, several studies have identified additional modifier genes that also influence susceptibility and modify the disease phenotype.

A microarray gene expression study which correlated the level of mRNA expression, in uninfected brains, from 5 inbred lines of mice, with their respective incubation times identified several potential prion modifier genes including *Fkbp9*. Lower levels of expression of *Fkbp9* correlated with shorter incubation times in mice, following prion infection. These findings were validated *in vitro* where Scrapie Cell Assays (SCA) in *Fkbp9* stably knocked down cell lines showed a significant increase prion propagation. The Fkbp9 protein is part of the immunophilin family of proteins which are peptidyl-propyl cis-trans isomerases. Fkbp proteins have been implicated in aspects of neurodegenerative disease, including accelerating α-synuclein fibrillisation and aggregation (primarily Fkbp12 but also Fkbp38, 52 and 65) and inhibiting tau induced tubulin polymerisation (Fkbp52) *in vitro*. Fkbp52 also reduced Aβ levels in a fly model of Alzheimer's disease and Fkbp51 was shown to block tau clearance through the proteasome resulting in oligomerisation.

The aim of this project was to characterise the functional roles of Fkbp family members in prion propagation. I generated a panel of N2aPK1 cell lines by stable gene silencing of four different *Fkbp* genes and employed the SCA to test whether *Fkbp* knock down (KD) influences prion propagation. For each *Fkbp* gene, four to eight KD cell lines were generated. Three out of four *Fkbp4* (Fkbp52) KD cell lines with over 50% KD of mRNA expression levels showed a significant reduction in the number of PrP^{Sc}-positive cells, as quantified in the SCA. Additionally, KD of *Fkbp8* in PK1 cells led to a significant reduction in the number of PrP^{Sc}-positive cells in four out of the five cell lines screened in the SCA. In contrast to these findings, in some cell lines with a significant reduction in mRNA expression levels (>60%) of the target *Fkbp* gene, there was no corresponding decrease in the number of PrP^{Sc}-positive cells. We reasoned that shRNA off-target effects arising when an shRNA downregulates unintended gene targets through partial sequence complementarity, may mask the effect of KD of the gene of interest. To examine whether an independent gene silencing approach for the examined gene targets recapitulates the results of stable gene silencing, siRNAs were used to transiently knock down *Fkbp* genes in chronically RML-infected PK1 cells (iS7 cells). Surprisingly, none of the siRNAs against the specified *Fkbp* genes reduced the number of PrP^{Sc}-positive iS7 cells. After establishing which Fkbp proteins affect prion propagation in the SCA, we aimed to carry out *in vitro* studies to understand the molecular mechanisms by which Fkbp proteins influence prion propagation. After optimisation of expression and cloning strategies, I successfully induced the expression of recombinant Fkbp9 and Fkbp52 proteins. The aim was to use the recombinant proteins in cell-free assays to test whether Fkbp proteins affect prion

replication and/or modulate the fibrillisation of recombinant PrP^C. *In vitro* assays with recombinant Fkbp proteins were not carried out as the project was terminated shortly after my primary supervisor left the Unit.

Impact statement

In neurodegenerative diseases, neuronal populations of distinct brain areas degenerate, a phenomenon known as selective neuronal vulnerability. While amyotrophic lateral sclerosis is associated with selective degeneration of motor neurones, disease progression in Parkinson's disease leads to degeneration of dopaminergic neurones in a specific brain area termed substantia nigra.
In prion diseases, the cellular prion protein PrP^{C}, is converted into its pathological, misfolded isoform PrP^{Sc}. Prion strains are conformational variants of PrP^{Sc} that are associated with degeneration of distinct brain areas. The inherited prion disease fatal familial insomnia (FFI), is characterised by prominent degeneration of the thalamus, whereas Gerstmann-Straussler-Scheinker disease (GSS), a different type of human prion disease, is characterised by progressive degeneration of the cerebellum.

The murine prion strains Me7 and 22L cause hippocampal and cerebellar degeneration respectively, following intracerebral inoculation in mice. It is thought that, by targeting specific brain areas, prion strains are associated with distinct clinical and pathological phenotypes. Additionally, it has been reported that in diseased mouse brains, distinct prion strains accumulate in different cell types. While prion toxicity is not readily observed in most cell lines *in vitro*, differences in their susceptibility to prion strains have been broadly observed. Collectively, these findings suggest that susceptibility to a prion strain is determined by cell-specific genetic or epigenetic factors.

The aim of this PhD project was to isolate a panel of genetically similar (cognate) sub lines that are differentially susceptible to the murine prion strains Me7 and RML. Additionally, we aimed to investigate whether cells with exclusive susceptibility to any one of the prion strains Me7, RML and 22L can be isolated to identify cell-specific factors that determine susceptibility to distinct prion strains. The final aim of this study was to examine whether passage of murine prion strains in susceptible cells changes the biochemical properties and virulence of prions, a phenomenon known as strain adaptation.

To isolate cognate cell clones that are differentially susceptible to Me7 and RML, I employed single cell cloning and successfully isolated highly Me7-susceptible cell clones from Me7-refractory neuroblastoma cells. While in the initial subcloning experiment poorly Me7-susceptible cell clones (PME2) were identified at a frequency of only $4x10^{-3}$, repeated subcloning of PME2 clones yielded highly Me7-susceptible

cells in subsequent rounds. Unexpectedly, the prion strain properties of brain-adapted Me7 were altered upon passage in permissive PME2 cells as cell-adapted Me7 was able to infect a panel of cell lines that are resistant to brain-adapted Me7.

Isolation of cognate cells that differ in their susceptibility to a single prion strain may enable identification of cellular factors for prion strain selectivity. Understanding the mechanisms which underlie cell tropism of prion strains may lay the foundation to understand the more complex mechanisms which underlie brain tropism of prion strains and hence, selective neuronal vulnerability in prion diseases. Additionally, the isolation of Me7-susceptible and Me7-resistant cell clones suggests that prion strain adaptation is determined by cellular factors expressed in Me7-susceptible cells. Such cell clones will be invaluable for future studies to identify host factors that govern prion strain adaptation.

Table of Contents

List of Figures

List of Tables

List of Acronyms and Abbreviations

AD	Alzheimer's disease
AFM	Atomic Force Microscopy
ALS	Amyotrophic Lateral Sclerosis
ApoE	Apolipoprotein E
APP	Amyloid Precursor Protein
ATP	Adenosine Triphosphate
Aβ	Amyloid beta
BACE	Beta-secretase
BCA	Bicinchoninic acid assay
BDNF	Brain-derived neurotrophic factor
BGS	Bovine growth serum
BSE	Bovine Spongiform Encephalopathy
C.P.A	Cell Panel Assay
$Ca2^{+}$	Calcium ion
CAA	Cerebral amyloid angiopathy
CAD5	Murine catecholaminergic neuroblastoma cells
CaN	Calcineurin
CD-1	Inbred laboratory mouse strain
cDNA	Complementary DNA
CHO	Chinese hamster ovary cells
CJD	Creutzfeldt-Jakob disease
CLDs	Calveolae-like domains
CNS	Central nervous system
DAPI	4',6-diamidino-2-phenylindole

DaSNc	Dopaminergic substantia nigra - pars compacta neurones
DC	Dendritic cells
DMSO	Dimethyl sulfoxide
DNA	Deoxyribonucleic acid
DY	Drowsy prion strain
EDTA	Ethylene diamine tetra-acetic acid
ELISA	Enzyme-linked immunosorbent assay
Elispot	Enzyme Linked Immunospot Assay
EOAD	Early-onset Alzheimer's disease
FBS	Fetal bovine serum
FFI	Fatal familial insomnia
FTD	Frontotemporal dementia
GABA	Gamma-Aminobutyric acid
GAG	Glycosaminoglycan
GdnHCl	Guanidine hydrochloride
GPI	Glycosylphosphatidylinositol
GR	Glucocorticoid receptor
GSS	Gerstmann–Sträussler–Scheinker syndrome
GT1-1	Mouse hypothalamic neuronal cell line
GTC	Guanidinium thiocyanate
GTP	Guanosine-5'-triphosphate
GWAS	Genome Wide Association Study
HD	Huntington's disease
HEK293	Human embryonic kidney cells
hGH	Human growth hormone
HTT	Huntingtin gene, human

Htt	Huntingtin gene, mouse
HY	Hyper prion strain
iCJD	Iatrogenic Creutzfeldt-Jakob disease
IP_3R	Inositol trisphosphate receptor
iPSCs	Induced pluripotent stem cells
iS7	RML-infected S7 cells
LB/LN	Lewy bodies/Lewy neurites
LD9	Murine fibroblast cell line
LOAD	Late-onset Alzheimer's disease
LRP/LR	Laminin receptor
LTCC	L-type calcium channel
MMLV	Moloney murine leukemia virus
MMP14	Matrix metalloproteinase-14
MN	Motor neurone
MND	Motor neurone disease
MPTP	1-methyl-4-phenyl-1,2,3,6-tetrahydropyridine
MRI	Magnetic resonance imaging
mRNA	Messenger RNA
MSA	Multiple system atrophy
mTOR	Mammalian target of rapamycin
NFT	Neurofibrillary tangle
NMR	Nuclear magnetic resonance
OBGS	OptiMEM supplemented 10% BGS + 1% PenStrep
OFCS	OptiMEM supplemented 10% FBS + 1% PenStrep
PBS	Phosphate-buffered saline
PBST	Phosphate Buffered Saline with Tween

PC12	Rat pheochromocytoma cell line
PCA	Posterior cortical atrophy
PCR	Polymerase chain reaction
PD	Parkinson's disease
PK	Proteinase K
PK1	N2a cell prion susceptible subclone
PMCA	Prion misfolding cyclic amplification
PMSF	Phenylmethylsulfonyl fluoride
PolyQ	Polyglutamine
PPIase	Peptidyl prolyl cis/trans isomerase
PRNP	Prion protein gene, human
Prnp	Prion protein gene, mouse
PrP^{27-30}	Protease-resistant core of PrP^{Sc}
PrP^{c}	Cellular prion protein
PrP^{d}	Disease-associated deposits of PrP
PrP^{Sc}	Disease-related, PK-resistant form of the prion protein
PSP	Progressive Supranuclear Palsy
PVDF	Polyvinylidene fluoride
qRT-PCR	Quantitative reverse transcription polymerase chain reaction
QTL	Quantitative trait loci
R33	N2a prion resistant subclone cells
RNA	Ribonucleic acid
ROS	Reactive oxygen species
RT	Reverse transcription
RyR	Ryanodine receptor
sCJD	Sporadic Creutzfeldt-Jakob disease

ScN2a	Scrapie infected N2a cells
SDS	Sodium dodecyl sulphate
SDS-PAGE	Sodium dodecyl sulphate–polyacrylamide gel electrophoresis
SEPP1	Selenoprotein P
shRNA	Short hairpin RNA
SH-SY5Y	Human Neuroblastoma cells
siRNA	Small interfering RNA
SNP	Single-nucleotide polymorphism
SOD1	Superoxide dismutase 1
SS	Selectivity score
SSCA	Standard scrapie cell assay
SUMO	Small Ubiquitin-like Modifier
S7	N2a-PK1 prion susceptible subclone 7 cells
TBST	Tris-buffered saline with Tween
TDP-43	Transactive response DNA binding protein 43 kDa
Tg	Transgenic
TGF-β	Transforming growth factor β
TNTs	Tunneling nanotubes
TRPC1	Transient receptor potential channel 1
TSE	Transmissible spongiform encephalopathy
v/v	Volume per volume
vCJD	Variant Creutzfeldt-Jakob disease
w/v	Weight per volume
WT	Wild type
α-Syn	Alpha synuclein

1 Introduction

1.1 Prion diseases

Prion diseases, also known as Transmissible Spongiform Encephalopathies (TSEs), are a family of rare, progressive neurodegenerative diseases that affect humans and animals. The prototypic disease scrapie is a naturally occurring disease affecting sheep and goats. More recently recognised prion diseases in animals include transmissible mink encephalopathy, chronic wasting disease in mule, deer, and elk, and bovine spongiform encephalopathy (BSE) in cattle. Prion diseases in humans include familial Creutzfeldt Jakob disease (CJD), Gerstmann-Staussler-Scheinker (GSS) syndrome and Fatal Familial Insomnia (FFI). These inherited forms of the disease arise as a result of pathogenic mutations in the prion protein gene, *PRNP* (Mastrianni, 2010). Sporadic forms of human prion disease include sporadic CJD and sporadic fatal insomnia and these arise as result of spontaneous conversion of the Proteinase-K sensitive, cellular prion protein (PrP^{C}), to its misfolded, pathogenic and partially Proteinase-K resistant form, PrP^{Sc} (Puoti *et al.*, 2012). Acquired forms of human prion diseases include iatrogenic CJD and kuru. Iatrogenic CJD can develop years after treatment with intramuscular injections of prion-infected growth hormone preparations from cadaver-derived pituitary glands and kuru disease arises as a result of endo-cannibalistic rituals amongst the Fore people of Papua New Guinea (Collinge, 2001). A novel human prion disease, variant CJD (vCJD), emerged in the United Kingdom (UK) in 1995 and is caused by the dietary exposure to BSE prions as a result of interspecies transmission from cattle to humans (Collinge, 1999). Importantly, a common PrP polymorphism at residue 129, where either methionine or valine can be encoded, is a key determinant of genetic susceptibility to both acquired and sporadic prion diseases (Collinge, Palmer, & Dryden, 1991; Palmer, Dryden, Hughes, & Collinge, 1991). The large majority of these diseases occur in methionine homozygous individuals whereas heterozygosity in codon 129 of *PRNP* has a protective effect (Windl *et al.*, 1996).

Clinical features vary, depending on the type of human prion disease. Classical (sporadic) CJD presents as rapidly progressive, multifocal dementia, usually with myoclonus. The central clinical feature of Kuru is progressive cerebellar ataxia and in sharp contrast to CJD, dementia is often absent in this acquired form of prion disease (Gambetti *et al.*, 2003). The clinical manifestation of vCJD differs from other forms of CJD. Patients present with behavioural and psychiatric disturbances, including

depression, anxiety, withdrawal, aggression and visual hallucinations (Collinge, 1999). Dementia usually develops later during the clinical course of disease which is unusually prolonged (9-35 months). The classical diagnostic triad of prion diseases is spongiform vacuolation, neuronal loss and astrogliosis (Collinge, 2005). These neuropathological features might be accompanied by amyloid plaques composed of the misfolded PrP conformer, PrP^{Sc} (Collinge, 2005).

1.2 The protein-only hypothesis

The nature of the transmissible agent in prion diseases has been subject to debate for many years. The initial assumption that the agent must be a form of slow virus (Sigurdsson, 1954) was challenged, both by the failure to demonstrate such a virus or any immunological response to it, and by evidence showing that the transmissible agent was exceptionally resistant to treatment that would otherwise inactivate nucleic acids (Alper, Haig, & Clarke, 1966; Alper, Cramp, Haig, & Clarke, 1967). These findings led to suggestions in 1966 by Tikvar Alper and others that the transmissible agent may be devoid of nucleic acid (Alper, Haig, & Clarke, 1966; Alper, Cramp, Haig, & Clarke, 1967). The protein-only hypothesis was first proposed by Griffith in 1967 and was later supported by Stanley Prusiner's work in 1982, which led to the identification and purification of the scrapie agent (Griffith, 1967; Prusiner, 1982). Because of its novel properties, resistance to treatments that would otherwise inactivate nucleic acids and resistance to Proteinase K digestion, the scrapie agent could be distinguished from viruses, plasmids and viroids (Prusiner, 1982). Additionally, procedures that could modify or destroy proteins could abolish the infectivity. It was concluded that this novel infectious agent was composed solely of protein and it was termed prion, denoting a *small proteinaceous infectious particle* (Prusiner, 1982).

The protease resistant PrP core extracted from affected hamster brains was of 27–30 kDa and was termed $PrP^{27–30}$ (Oesch *et al.*, 1985). Work by Charles Weissmann and colleagues in 1985 demonstrated that PrP^{Sc} is encoded by a single copy host chromosomal gene, *PRNP*, contrary to previous assumptions that PrP is encoded by a putative viral nucleic acid (Oesch et al., 1985; Basler et al., 1986). It was demonstrated that the normal product of the *PRNP* gene is protease-sensitive and was designated PrP^{C}, denoting the cellular isoform of the protein (Caughey and Raymond, 1991). PrP is a glycoprotein with two asparagine linked glycosylation sites (Riesner, 2003). A glycosylphosphatidylinositol (GPI) anchor attaches the protein to the external cell surface but is not required for prion conversion (Stahl, Borchelt, Hsiao, & Prusiner, 1987; Baron & Caughey, 2003; Lewis PA et al., 2006). As there were no differences in

the amino acid sequence between PrP^C and PrP^{Sc}, it was postulated that PrP^{Sc} was derived from PrP^c by a post-translational process (Basler *et al.*, 1986). It was proposed that PrP^{Sc} acts as a template, promoting the conversion of PrP^C to PrP^{Sc} and that the difference between the two isoforms lies purely in their conformation and state of aggregation (Prusiner, 1991). As a result of this conversion process, the predominantly alpha helical PrP^C undergoes a conformational change to PrP^{Sc}, which is characterised by increased beta sheet content (Pan *et al.*, 1993). The accumulation and spread of disease-associated PrP^{Sc} in prion diseases occurs through the process of seeded polymerisation. Seeded polymerisation of PrP^{Sc} involves several monomeric PrP^{Sc} which are mounted into a highly ordered and infectious seed (Aguzzi, Montrasio and Kaeser, 2001). The seed can recruit more PrP^{Sc} and eventually aggregate to form an amyloid. Amyloid fibrils can fragment and recruit further PrP^{Sc}, resulting in replication of the agent (Aguzzi, Montrasio and Kaeser, 2001). The current models for the conversion of PrP^C to PrP^{Sc} are described in **Figure 1.1**.

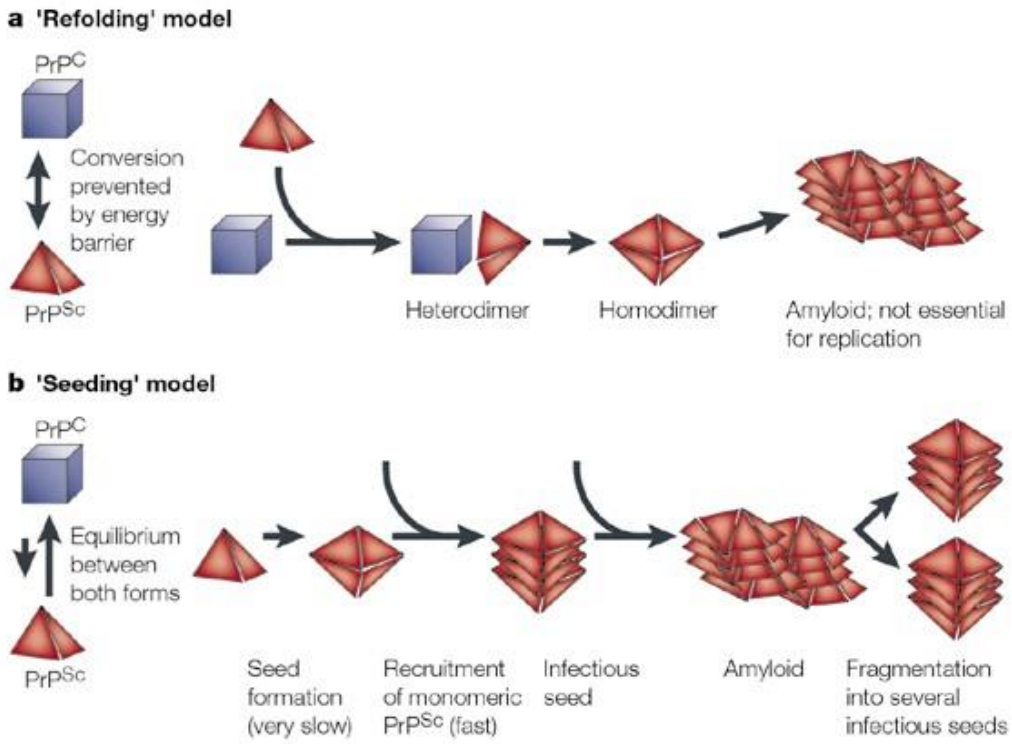

Figure 1.1 Models for the conformational conversion of PrP^C into PrP^{Sc} (taken from Aguzzi et al., 2001). (a) In the refolding model, a high activation energy barrier prevents the spontaneous misfolding of PrP^C to PrP^{Sc}. Direct interaction between exogenously introduced PrP^{Sc} and endogenous PrP^C induces a conformational change in PrP^C, causing the latter to transform into PrP^{Sc}. It is possible that the interaction between PrP^C and PrP^{Sc} is facilitated by

an enzyme or a chaperone protein. (b) In the seeding or nucleation model, PrP^{C} and PrP^{Sc} are in a reversible equilibrium which strongly favours PrP^{C}. When several monomeric PrP^{Sc} molecules are mounted into a highly ordered seed, PrP^{Sc} is stabilised and the seed recruits further monomeric PrP^{Sc}. This process of seeded polymerisation converts the seed into an amyloid through aggregation. Fragmentation of PrP^{Sc} aggregates yields several infectious seeds, generating more surfaces for the recruitment of further Prp^{Sc}. This self-propagating prion replication explains the exponential conversion rates of PrP^{C} to PrP^{Sc}.

Work by Bueler and colleagues showed that the development of prion disease requires the expression of the endogenous prion protein, PrP^{C}, as *Prnp* knock out mice are resistant to scrapie and survive without pathology within their natural lifespan (Büeler *et al.*, 1993). Additionally, depletion of endogenous neuronal PrP^{C} in mice with established prion infection, reversed spongiosis, prevented neuronal loss and halted progression to clinical disease (Mallucci *et al.*, 2003).

1.3 Prion disease genetic modifiers

PrP is central to the pathogenesis of prion diseases as mutations in the prion protein gene *PRNP* are the only cause factors in inherited prion diseases (Owen et al., 1990; Hsiao et al., 1989). Octapeptide repeat insertions within the unstable region of *PRNP* result in a variable clinical and pathologic phenotype.

The common M129V polymorphism in the prion protein influences the risk of sporadic and acquired iatrogenic CJD (Palmer, Dryden, Hughes, & Collinge, 1991;Collinge, 2005).

Several studies suggest that genes other than *PRNP* can also influence susceptibility and modify the disease phenotype. The use of human genome-wide association studies (GWAS) and complementary mouse studies (single nucleotide polymorphism (SNP) association studies, quantitative trait loci (QTL) mapping studies and microarray expression studies) have reinforced the critical role of *PRNP* and have identified additional genetic modifiers (Lloyd, Mead, & Collinge, 2013;Lloyd, Uphill, Targonski, Fisher, & Collinge, 2002;Lloyd et al., 2001). In the Ethiopian vCJD GWAS, two non-*PRNP* loci were identified, *MTMR7*, encoding myotubularin-related protein 7, and *NPAS2*, encoding domain-containing protein 2 (Sanchez-Juan et al., 2012). The gene product of *MTMR7* dephosphorylates phosphatidylinositol-3-phosphate and inositol 1, 3-bisphosphate and the gene product of *NPAS2* belongs to a family of transcription factors. In an independent GWAS study, single nucleotide polymorphisms (SNPs) at the *ZBTB38-RASA2* locus were associated with sCJD in the UK (Mead et al., 2012).

ZBTB38 is a transcriptional activator that binds methylated DNA and RASA2 is a member of a family of GTPase-activating proteins.

Screening genes that may contribute to prion pathogenesis is important to understand their function in PrP conversion and their role as mediators of neurotoxic mechanisms.

A study to investigate the role of Cx3cl1/Cx3cr1 (a signalling cascade thought to maintain microglia in their resting state) in prion disease showed that *Cx3cr1* null mice exhibited a significant reduction in incubation period for two mouse-adapted scrapie strains and a mouse-passaged BSE strain. The results showed that Cx3cl1/Cx3cr1 signalling is partially protective in prion disease (Grizenkova *et al.*, 2014). This pathway, which involves neuron-microglial interaction, has previously been implicated in the modulation of neurotoxicity (Limatola and Ransohoff, 2014).

The metalloproteinase ADAM10 has been shown to modulate prion disease pathogenesis in mice (Altmeppen *et al.*, 2015). In conditional Nestin *ADAM10* knock out (KO) mice, prion infection led to elevated membrane levels of PrP^{c} (others detected PrP^{c} accumulation in intracellular compartments (Altmeppen *et al.*, 2011)), significantly shortened incubation time and enhanced prion conversion relative to control mice.

ATPase Heat-Shock proteins (HSPs) are chaperone proteins that have previously been implicated in prion propagation. Hsp40 molecular chaperones emerged as critical regulators of prion propagation in yeast (Summers, Douglas and Cyr, 2009). Hsp70 proteins are a family of heat shock proteins that interact with peptide segments to mediate protein folding, prevent protein aggregation and regulate protein activity (Mashaghi *et al.*, 2016). A transgenic mouse model with 8-fold overexpression of mouse Hspa13 (encoding Heat shock 70 kDa protein 13) exhibited significant reduction in incubation time of 16, 15 and 7% following infection with Chandler/RML, ME7 and MRC2 prion strains respectively (Grizenkova *et al.*, 2012).

Copper-Zinc superoxide dismutase (SOD1) has been implicated in the pathogenesis of amyotrophic lateral sclerosis (ALS), as mutations in SOD1 are causative factors in ALS. It is becoming apparent that mutant SOD1 causes disease through a gain-of-function mechanism of neurotoxicity (Banci *et al.*, 2008). SOD1 was also identified as a modulator of prion disease pathogenesis. SOD1-deficient mice exhibit significantly reduced incubation times following infection with different prion strains, highlighting the protective role played by the endogenous SOD1 protein as well as the importance of oxidative damage in prion disease (Akhtar *et al.*, 2013). Another study showed that

Tg(SOD)3Cje mice overexpressing human SOD1 showed prolonged incubation periods when inoculated with RML prions (Tamgüney *et al.*, 2008).

Given that the cellular prion protein is membrane-anchored, it is tempting to speculate that proteins involved in the regulation of membrane trafficking dynamics may modulate prion propagation and disease. Copines are calcium-dependent phospholipid binding proteins that have not been linked to neurodegenerative disease. The observation that Cpne8 mRNA is upregulated at the terminal stage of prion disease in mice, points towards the putative involvement of copine family members in prion disease (Lloyd *et al.*, 2010). Cpne8, a poorly characterised protein is thought to have a role in membrane trafficking. Newly synthesised PrP is trafficked through the ER and Golgi towards the plasma membrane where it associates with lipid rafts through its GPI anchor (Harris, 2003). Pathogenic mutations in PrP, associated with familial prion disease have shown abnormal cellular localisations of PrP (Petersen *et al.*, 1996). CPN8 may therefore be important in regulating the correct trafficking of PrP, which might explain its deregulation in gene expression at end-stage disease.

Clusterin (apolipoprotein J) is a heterodimeric protein associated with the clearance of cellular debris and apoptosis. As a molecular chaperone, it facilitates the folding of secreted proteins. A considerable amount of evidence exists for the involvement of clusterin in prion disease pathogenesis (Xu, Karnaukhova, & Vostal, 2008;Kempster et al., 2004;Sasaki, Doh-ura, Ironside, & Iwaki, 2002). Clusterin was shown to interact directly with the prion protein (Xu, Karnaukhova and Vostal, 2008). Clusterin KO mice exhibited prolonged incubation times compared to wild-type mice, following prion infection. Also, the deposition of PrP^{BSE} in the brains of clusterin KO mice was less aggregated compared to that of wild-type mice (Kempster *et al.*, 2004). Clusterin was shown to co localise with PrP^{Sc} plaques in the brains of individuals with CJD and clusterin associated with PrP^{Sc} plaques was found to be resistant to protease digestion (Freixes *et al.*, 2004). Collectively, these findings suggest that clusterin interacts with PrP and participates in PrP sequestration, thereby modifying PrP toxicity in prion diseases.

Another candidate gene associated with prion disease incubation time in the mouse is the *Rarb* gene, encoding the nuclear receptor, retinoic acid receptor beta. In the mouse brain, *Rarb* mRNA levels were significantly elevated in prion-infected mice compared to uninfected controls (Grizenkova *et al.*, 2010), whereas in prion-infected GT-1 (mouse hypothalamic neuronal) cells, no difference was detected for Rarb

expression (Mead *et al.*, 2009). It is likely however, that a cell system will not faithfully recapitulate the situation *in vivo* at end-stage disease.

There is increasing evidence for the effect of genetic background in prion disease susceptibility. RNAseq experiments in two closely related ovine microglia clones with different prion susceptibility identified 22 genes with consistently altered transcription and known biological function (following prion infection of the cells) (Muñoz-Gutiérrez *et al.*, 2016). There were no PrP^c expression level differences between the clones. Amongst the genes with altered transcription profiles were MMP14 (Matrix metalloproteinase-14) and SEPP1 (Selenoprotein P). SEPP1 was the gene with the most dramatic fold change in transcription. Selenoprotein P, an extracellular selenium transporter glycoprotein has been implicated in AD pathology. AD patient brains have elevated levels of SEPP1, which is thought to be upregulated in response to oxidative stress/inflammation resulting from AD pathology (Rueli *et al.*, 2015). SEPP1 was found to colocalize with amyloid β (Aβ) and NFTs in individuals with AD (Bellinger *et al.*, 2008) and to inhibit the metal-induced aggregation and toxicity of Aβ, as well as promote Abeta clearance (Du *et al.*, 2014).

Hectd2 has previously been identified as a candidate susceptibility gene for AD (Lloyd, Rossor, *et al.*, 2009). Hectd2, an E3 ubiquitin ligase, was shown to be associated with an increased risk of two human prion diseases, vCJD and Kuru. Additionally, incubation time data following Chandler/RML infection, showed that mice expressing higher levels of Hectd2 exhibited shorter incubation time relative to control mice (Lloyd, Maytham, *et al.*, 2009). Importantly, Hectd2 mRNA expression levels were significantly upregulated in mice with end-stage prion disease.

The membrane-bound enzyme complex NADPH oxidase has also been studied in the context of prion disease. Upon challenge with prions, mice lacking NADPH oxidase, showed delayed onset of motor deficits and a modest but significant prolongation of survival (Sorce *et al.*, 2014). Being a major source of reactive oxygen species (ROS) production, NOX2 can contribute to oxidative stress and neuroinflammation in prion disease.

Trascriptome analysis of rare prion-resistant revertants isolated from highly susceptible mouse neuroblastoma N2a PK1 cells revealed significant gene expression differences between resistant and susceptible cells (Marbiah *et al.*, 2014). These differences were independent on PrP^c expression. The gene regulatory network associated with susceptibility to prion replication was shown to be associated with the

differentiation state of cells and involved the expression of genes with a role in extracellular matrix (ECM) remodelling. Importantly, The ECM is a compartment that accumulates disease-associated PrP.

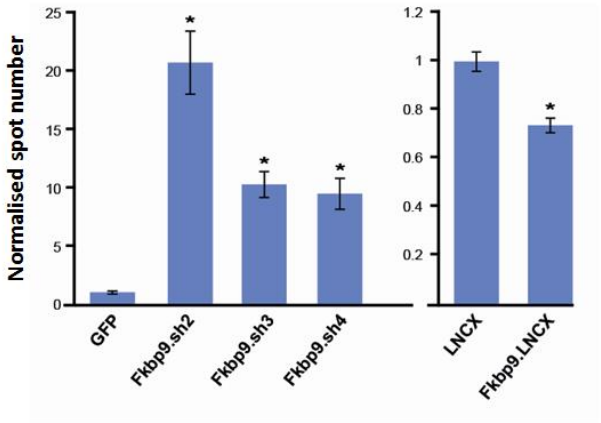

Figure 1.2 Silencing of *Fkbp9* in PK1 cells leads to an increase in prion propagation. Stable *Fkbp9* gene silenced (shRNA) or overexpressing (LNCX) N2aPK1 cell lines were tested in the SCA (1x10 ^{5} RML dilution) together with a control cell line (*GFP* shRNA or LNCX vector). PrP^{Sc} spot numbers from three independent assays are shown normalised to the control line (which precedes it in the graph) ± sem. * P<0.001. *Figure taken from Brown et al., 2014.*

An *in vitro* bioassay, the Scrapie Cell Assay (SCA) uses a subclone of neuroblastoma cells (N_2a PK1) that is susceptible to Chandler/RML prions and can propagate prions at high levels (Klohn *et al.*, 2003). The generation of stable gene silenced and/or overexpressing PK1-derived cell lines allows for the screening of candidate genes that affect prion susceptibility. A study identified a number of genes, which significantly affect prion propagation (represented by the number of PrP^{Sc}-positive cells). For two of these genes, *Fkbp9* and *Actr10*, stable knock down led to a significant increase in prion propagation whereas the converse was observed in their respective overexpressing cell lines (Brown et al., 2014, **Figure 1.2**). These observations suggest a role for these genes in fundamental processes such as infectivity, prion uptake and propagation, PrP^{Sc} accumulation, clearance and cell-to-cell spread. These data are consistent with the original observation that for both *Fkbp9* and *Actr10*, a lower mRNA expression level correlated with a shorter incubation time in RML-infected mice (Grizenkova *et al.*, 2012). Actr10 is a component of the dynactin complex (Zhang *et al.*, 2008). The complex binds to cytoplasmic dynein and activates cytoplasmic dynein-mediated vesicular transport. Changes in Actr10 levels may therefore perturb the trafficking of the cellular prion protein. Fkbp9 is a chaperone protein with peptidyl-

propyl *cis-trans* isomerase activity. Fkbp family members have a well-established role in neurodegeneration (Chambraud *et al.*, 2007; Fusco *et al.*, 2010; Suzuki *et al.*, 2012; Giustiniani *et al.*, 2015).

1.4 Physiological functions of Fkbp proteins

Fkbp proteins are part of a family of highly conserved proteins known as immunophilins. These proteins possess peptidyl-propyl *cis-trans* isomerase activity by catalysing the *cis-trans* interconversion of peptide bonds of proline residues in proteins, a rate-limiting process that can influence protein folding and function (Tong and Jiang, 2015). The *cis-trans* interconversion of X-Pro peptide groups can be catalysed by disruption of the partial double-bond character of the peptide bond. This chaperone activity is an important component of the proteostasis network in living cells (Wedemeyer, Welker, & Scheraga, 2002; Schmidpeter, Koch, & Schmid, 2015). The two prototypic members of the immunophilin family, Fkbp12 and Cyclophilin A were discovered on the basis of their ability to bind the drugs cyclosporine, FK506 and rapamycin and to mediate their immunosuppressive effects (Marks, 1996). The enzymatic activity of Fkbp proteins is not involved in their ability to mediate immune system suppression.

Their high expression in the brain and peripheral nerves renders Fkbp proteins appealing targets for neuroimmunophilin ligand analogues that lack immunosuppressive capacity, yet still bind to Fkbp proteins, resulting in potent neuroprotective and neurotrophic effects (Sabatini, Lai and Snyder, 1997). Surprisingly, the levels of Fkbp12 in the brain are up to 50 times higher than those in tissues in the immune system (Snyder *et al.*, 1998).

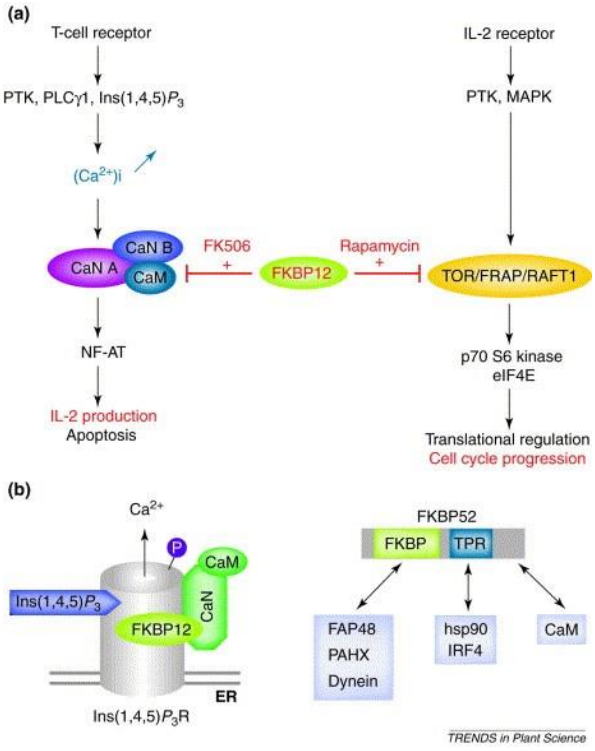

Figure 1.3 The association of Fkbp proteins with signalling partners. (a). The binding of FK506 to Fkbp12 creates a binding platform which then binds to and inhibits the regulatory subunit of calcineurin (CaN). This in turn blocks substrate access to the catalytic subunit, suppressing T-cell activation. The binding of rapamycin to Fkbp12 inhibits mTOR and downstream cell cycle progression. (b) Examples of Fkbp-interacting proteins; Fkbp12 acts as a scaffold protein to stabilize calcium channels [Ins(1,4,5)P_3R]. Fkbp52 associates with multiple proteins via its different domains. Abbreviations: CaM, calmodulin; CaN, calcineurin; CaN A, CaN catalytic subunit; CaN B, CaN regulatory subunit; ER, endoplasmic reticulum; FAP48, FKBP-associated protein 48; FRAP, FK506 and rapamycin-associated protein; hsp90, heat-shock protein 90; Ins(1,4,5)P3, inositol-(1,4,5)-trisphosphate; Ins(1,4,5)P3R, inositol-(1,4,5)-trisphosphate receptor; IL-2, interleukin 2; IRF4, interferon response factor 4; MAPK, mitogen-activated protein kinase; NF-AT, nuclear factor of activated T cells; PAHX, phytanoyl-CoA α-hydroxylase; PLCγ1, phospholipase C γ1; PTK, protein tyrosine kinase; RAFT, rapamycin and FKBP target; TOR, target of rapamycin; TPR, tetratricopeptide repeat. *Figure taken from Harrar et al., 2001*.

Fkbp12 was originally identified as the major receptor protein for FK506 (Snyder *et al.*, 1998). The Fkbp12-FK506 complex creates a binding platform for interaction with the regulatory subunit of the phosphatase calcineurin (CaN) ((Harrar et al., 2001; **Figure 1.3**). This in turn blocks substrate access to the catalytic subunit of calcineurin. The nuclear factor of activated T-cells (NF-AT) remains phosphorylated and T-cell activation is blocked due to inhibition of interleukin-2 production (Harrar, Bellini and

Faure, 2001). When rapamycin binds to Fkbp12, the complex interacts with and inactivates the mammalian target of rapamycin (mTOR). The most well characterised function of mTOR is translational control as well as regulation of cell cycle progression (Harrar et al., 2001; Laplante & Sabatini, 2012). It has been shown that the Fkbp12-rapamycin complex inhibits progression through the G1 phase of the cell cycle in osteosarcoma, liver, T-cells as well as in yeast. The complex interferes with mitogenic signalling pathways involved in G1 progression (Brown *et al.*, 1994).

Fkbp12 is dispensable for transforming growth factor beta (TGF-β) mediated signalling (Shou *et al.*, 1998). A well–established molecular function of Fkbp12 and Fkbp12.6 is the stabilisation of ryanodine receptors in both skeletal and cardiac tissue, which enables them to prevent the passive leakage of calcium ions from the endoplasmic reticulum (Hausch, 2015). Fkbp12 control of these important functions might explain the embryonic and neonatal lethality of Fkbp12-deficient mice (Shou *et al.*, 1998). Ryanodine receptors (RyR1 and RyR2) are tetrameric structures and this structure is stabilised by the binding of Fkbp12 (Marks, 1997). Fkbp12 was also identified as an adaptor protein for the inositol 1, 4, 5-trisphosphate receptor (IP_3R) (Cameron *et al.*, 1997). A yeast two-hybrid system identified a site in IP_3R that binds Fkbp12, allowing the IP_3R to function as an “endogenous FK506”. The binding to IP_3R enables Fkbp12 to interact with calcineurin, anchoring this phosphatase to IP_3R and modulating the phosphorylation status of the receptor. The functional significance of this interaction is the regulation of calcium flux of the receptor. Importantly, Fkbp12- IP_3R-CN complex is independent of Fkbp12’s rotamase activity (Cameron *et al.*, 1997). Fkbp proteins can therefore act as stabiliser proteins and participate in signalling cascades and these functions can be at least partly uncoupled from their PPIase activity. The complex molecular structure and the diverse subcellular localisation of immunophilins allows these proteins to play an essential role in various biochemical pathways (Barik, 2006).

Fkbps have been shown to influence the folding of a number of synthetic peptides and natural proteins like carbonic anhydrase and ribonuclease (Kiefhaber *et al.*, 1990). The exact catalytic mechanism of their PPIase activity remains poorly characterised and there is still no convincing evidence that this enzymatic activity is an absolute requirement *in vivo* (Barik, 2006).

Fkbp52 levels are high in neurons and are further elevated in facial or sciatic nerve injuries. Importantly, FK506 promotes nerve regeneration in a mechanism independent of calcineurin (Toll, Seifalian and Birchall, 2011). It is thought that the addition of FK506 disrupts steroid receptor complexes in the cell, releasing chaperones such as

Fkbp52 which is then made available for neurotrophic signalling pathways (Barik, 2006). Mice that lack Fkbp52 grow normally but are infertile and exhibit several functional and anatomical abnormalities of the reproductive organs (Toll, Seifalian and Birchall, 2011).

It has been well established that Fkbp52 potentiates glucocorticoid receptor (GR) signalling by regulating receptor maturation and hormone binding (Silverstein *et al.*, 1999; Cheung-Flynn *et al.*, 2005). This process requires the binding of Hsp90 and drives hormone-dependent gene activation in a *Saccharomyces Cerevisiae* model for glucocorticoid receptor function (Riggs *et al.*, 2003). The proposed model is that the FK1 region (the region where the PPIase activity resides) of Fkbp52 binds to dynein. The interaction between Fkbp52, dynein and receptor-bound Hsp90 is thought to assist the transport of GR from the cytoplasm to the nucleus (Pratt, Silverstein and Galigniana, 1999). The formation of the transportosome determines the attachment of steroid receptors to microtubule-based movement machinery (Pratt, Silverstein and Galigniana, 1999). In the yeast model (Riggs *et al.*, 2003), Fkbp51 blocked Fkbp52-mediated potentiation of reporter gene activation in an antagonistic manner. Interestingly, human glucocorticoid receptor interacts poorly with steroid hormone when complexed with Fkbp51 (Reynolds *et al.*, 1999) and human Fkbp51 gene expression is highly inducible by glucocorticoids (Yoshida *et al.*, 2002). These observations suggest that a negative feedback loop exists, in which responsiveness to steroid hormones can be downregulated by hormone-induced expression of Fkbp51 (Scammell, 2000). Upon steroid binding, Fkbp51 is released from the receptor-Hsp90 heterocomplex and replaced by Fkbp52. The latter then recruits dynein-dynactin motor proteins that promote the transport of the GR on a microtubule network (Erlejman *et al.*, 2014).

The cellular functions of immunophilins and their substrates have been partly characterised but most remain elusive (Guy *et al.*, 2015). It has been shown that the PPIase activity of Fkbp52 regulates neuronal growth cone responses to netrin 1 both *in vitro* and *in vivo* by catalysing the *cis-trans* isomerisation of regions in the transient receptor potential channel 1 (TRPC1) to control channel opening (Shim *et al.*, 2009).

The loss of both Fkbp51 and Fkbp52 in mice results in embryonic lethality, implying that Fkbp51 and Fkbp52 have redundant roles in embryonic development (Storer *et al.*, 2011).

Fkbp38 is a non-canonical Fkbp protein whose PPIase activity is dependent on the binding of the calcium-calmodulin complex (Cao and Konsolaki, 2011). Lack of Fkbp38 in mice results in neonatal lethality with severe malformation of the nervous system (Shirane-Kitsuji and Nakayama, 2014). Importantly, Fkbp38 was identified as an anti-apoptotic protein. Fkbp38 associates with Bcl2 and Bcl-x and co-localises with these proteins in mitochondria, possibly anchoring them to the mitochondria (Shirane and Nakayama, 2003). Overexpression of Fkbp38 prevents apoptosis whereas a dominant negative Fkbp38 protein promotes apoptosis (Shirane and Nakayama, 2003). Although Fkbp38 does not control the induction of mitophagy, Fkbp38 deficiency in a cell system sensitises cells to apoptosis during mitophagy (Saita, Shirane and Nakayama, 2013). Fkbp38 and Bcl-2 escape from mitochondria to the endoplasmic reticulum (ER) during mitophagy, resulting in the degradation of most other proteins, and thereby helping to prevent unwanted apoptosis during this process (Vervliet, Parys and Bultynck, 2015).

Cyclophilins constitute the second largest family of immunophilins. Cyclophilin A plays an important role in the maturation of oligomeric receptors (Helekar *et al.*, 1994) and the activity of essential zinc finger proteins like Zpr1 (Ansari, Greco and Luban, 2002). Cyclophilin D, which is a component of the mitochondrial membrane permeability transition pore, plays an important role in apoptosis induced by calcium and reactive oxygen species (ROS) and in cardiac ischemia-perfusion injury (Nakagawa *et al.*, 2005).

A considerable body of evidence supports the involvement of Fkbp proteins in neurodegenerative diseases.

The immunophilin Fkbp52 has been implicated in the pathogenesis of Alzheimer's disease (AD) and Parkinson's disease (PD). It has been shown that the receptor tyrosine kinase Ret51 is a binding partner of Fkbp52, the complex formation induced by Ret51 phosphorylation (Fusco *et al.*, 2010). This interaction and its downstream signalling cascade may play an important role in the development and maintenance of dopaminergic neurones. In support of the above statement, mutations in Fkbp52 and Ret can disrupt complex formation and cause early onset PD (Fusco *et al.*, 2010).

Studies have demonstrated a direct interaction of Fkbp52 with the microtubule-associated protein tau (Giustiniani *et al.*, 2015). Binding of recombinant Fkbp52 to a functional tau fragment (TauF4) induced tau oligomerization and aggregation as detected by electron microscopy. Interestingly, Fkbp52-induced TauF4 oligomers

could seed the aggregation of endogenous tau in SH-SYSY cells (Giustiniani *et al.*, 2015). Fkbp52 binds directly to the hyper phosphorylated tau protein and antagonizes the ability of tau to promote microtubule assembly (Blair *et al.*, 2015b). In agreement with these findings, stable expression of Fkbp52 in PC12 cells prevented tau accumulation and reduced neurite length (Chambraud *et al.*, 2010). Conversely, depletion of Fkbp52 expression via siRNA led to a differentiated phenotype in PC12 cells, characterized by neurite extension (Chambraud *et al.*, 2007).

It has been reported that in human AD brains, neurofibrillary tangles (NFTs) do not coincide topologically with Fkbp52 and Fkbp52 protein levels are reduced in the frontal cortex of AD patients (Giustiniani *et al.*, 2012). The decrease in Fkbp52 may underlie a number of pathogenic mechanisms in AD, including defects in axonal guidance resulting from loss of its interaction with the TPRC1 calcium channel as well as destabilization of the microtubule network leading to synaptic dysfunction and neuronal loss.

The cytoplasmic immunophilin Fkbp52 was also shown to modify Aβ toxicity in Aβ-transgenic Drosophila (expressing human Aβ using an eye-specific promoter that causes progressive degeneration of the eye (rough eye phenotype). Loss of function mutations in Fkbp52 exacerbated Aβ toxicity whereas gain of function mutations suppressed the rough eye phenotype and prolonged the lifespan of Aβ42-expressing flies (Sanokawa-Akakura *et al.*, 2010). In contrast to the findings that Fkbp52 protects against Aβ toxicity, Fkbp51 was shown to block tau clearance through the proteasome, resulting in oligomerisation (Blair *et al.*, 2013). These findings associate Fkbp51 levels with AD progression. The interaction of Fkbp51 with Hsp90 blocked tau degradation, resulting in neurotoxic tau accumulation (Blair *et al.*, 2013). The synergistic interaction between recombinant Fkbp51 and Hsp90 acted on the modulation of tau conformation and aggregation kinetics, promoting the generation of oligomeric tau species. Importantly, higher Fkbp51 levels have been associated with AD progression (Blair, 2015a). The upregulation of Fkbp51 expression in AD brains was explained by a decrease in *Fkbp5* DNA methylation. Consistent with these observations, tau levels are reduced in the brains of Fkbp51 knock out mice (Blair, 2015a).

Fkbp14 has also been implicated in AD as a regulator of presenilin protein levels in Drosophila. Presenilin protein levels and gamma secretase activity were reduced in Fkbp14 null mutant flies and this observation is consistent with the reduction in the levels of Aβ42 in these flies (van de Hoef, Bonner and Boulianne, 2013).

Fkbp52 can induce the aggregation of TauF4 by a process that is independent on the former's *cis-trans* isomerase activity (Kamah *et al.*, 2016). This physical interaction can lead to the stabilization and oligomerization of these aggregation-prone forms of tau. Fkbp52 is not the only peptidyl-propyl isomerase (PPIase) that can modify tau and Aβ toxicity. The proline isomerase Pin1 is downregulated and/or inhibited by oxidation in AD and Pin1 depletion causes tauopathy and neurodegeneration (Lu, Wulf, Zhou, Davies, & Lu, 1999; Liou et al., 2003; Sultana et al., 2006). Pin1 binds directly to the Amyloid Precursor Protein (APP) and accelerates the isomerisation of its Thr668-Pro motif by over 1000-fold (Pastorino *et al.*, 2006). Importantly, Pin1 overexpression decreased Aβ secretion from cultured cells whereas depletion increased its secretion. Pin1 knock out in mice increased amyloidogenic APP processing and the production of Aβ42, the major toxic species in AD (Pastorino *et al.*, 2006).

The PPIase Pin1 is not the only proline isomerase to interact with APP. Fkbp12 has also been shown to interact directly with the intracellular domain of APP (Liu *et al.*, 2006). This interaction may have relevance in the amyloidogenic APP processing and Aβ production. Further studies have shown that Fkbp12 overexpression in HEK293T cells shifted the APP processing towards the amyloidogenic pathway without inducing any subsequent changes in the messenger RNA (mRNA) levels of beta-secretase (BACE) and presenillins (Liu, Liu and Kung, 2014).

Studies have shown that although the Fkbp12 protein appeared to be reduced in AD patient brains, it highly accumulated in intracellular NFTs (Sugata *et al.*, 2009). If Fkbp12 catalyses tau folding in an analogous fashion to Pin1, then low levels of Fkbp12 in AD brains are likely to impair tau folding, leading to the formation of NFTs. Fkbp12 also serves to anchor calcineurin, a tau phosphatase, to a calcium channel, possibly enabling the dephosphorylation of tau (Jayaraman *et al.*, 1992). Reduced Fkbp12 levels may therefore compromise this process, leading to abnormally phosphorylated tau protein and its deposition in NFTs. Fkbp12 accumulation in NFTs may serve to refold and dephosphorylate the tau protein together with calcineurin. The protective role of Fkbp12 and its association with the tau protein has also been studied by other groups where it was shown that Fkbp12 completely prevented the R3 peptide (main factor for tau aggregation (Perez *et al.*, 2007) from aggregation (Ikura and Ito, 2013). It was confirmed that this was not due to a putative chaperone effect of Fkbp12 but rather its PPIase activity was essential to prevent aggregation.

Fkbp12 and Fkbp12.6 proteins regulate the release of intracellular calcium by either binding directly to the cytoplasmic domains of the Ryanodine (RyR) and Inositol

Trisphosphate (IP_3) receptors or indirectly by modulating the phosphatase calcineurin (MacMillan, 2013; Gaburjakova et al., 2001). The expression of Fkbp12, a RyR stabilizer, attenuated mutant huntingtin-induced calcium leak and cell death in the R6/2HD mouse model (Suzuki *et al.*, 2012). A study to identify proteins in the striatum that are critical for the progression of Huntington's disease found that Fkbp12 levels were markedly downregulated (Chiang *et al.*, 2007). Expression of Fkbp12 in a striatal cell line, harbouring mutant huntingtin with polyQ expansion reduced the formation of huntingtin aggregates, denoting the functional significance of Fkbp12 in HD pathogenesis (Chiang *et al.*, 2007). More recent findings demonstrated that Fkbp12 decreases the amyloidogenicity of mutant huntingtin and induces the formation of amorphous deposits *in vitro*, as determined by Thioflavin T fluorescence and transmission electron microscopy analysis (C.-S. Sun *et al.*, 2015). In the same study, Fkbp12 conferred neuroprotection against polyQ-mediated neurotoxicity in mutant-huntingtin-expressing N2a cells and *C. elegans*.

Fkbp12 has been implicated in Parkinson's disease pathogenesis and more specifically in the fibrillisation of alpha synuclein. Addition of the inhibitor compound FK506 strongly reduced the pro-aggregatory effect of Fkbp12, suggesting a role of Fkbp12 in alpha synuclein fibril formation (Gerard *et al.*, 2008). Importantly, the enzymatically inactive Fkbp12 had no effect on the aggregation of alpha synuclein at low concentrations, while at micromolar concentrations, an accelerated aggregation was observed. The authors concluded that the effect on early aggregation may therefore be due to a combination of both, enzymatic and non-enzymatic chaperone activity of Fkbp12 (Gerard *et al.*, 2008). A number of Fkbp proteins were tested for their ability to affect the aggregation of recombinant alpha synuclein. Fkbp12 was identified as the most potent enhancer of alpha synuclein aggregation, both *in vitro* and in cell culture experiments (Gerard et al., 2006; Deleersnijder et al., 2011). The accelerating effect on alpha synuclein fibril formation was detected at sub-nanomolar concentrations, pointing towards an enzymatic effect rather than a putative chaperone effect (Deleersnijder *et al.*, 2011). Inhibition by FK506 or downregulation of endogenous Fkbp12 or Fkbp52 reduced alpha synuclein aggregation and concomitant neuronal death in a cell culture model for synucleopathy (Gerard *et al.*, 2010). Fkbp12 was found to co-localise with alpha synuclein inclusions in the brains of aged, alpha synuclein transgenic mice. Treatment of these mice with FK506 reduced the number of alpha synuclein inclusions and reduced neurodegeneration (Gerard *et al.*, 2010). In agreement with these findings, the stable overexpression of Fkbp12 and to a lesser

extent Fkbp52 enhanced the aggregation of alpha synuclein and cell death in a neuronal cell line (Gerard *et al.*, 2010).

A study by Stocki and co-workers showed that Fkbp proteins are involved in prion propagation *in vitro* (Stocki *et al.*, 2016). Knock down of one of the 6 Endoplasmic Reticulum (ER) luminar Fkbps, Fkbp10, induced PrP^{c} degradation. At the same time, Fkbp10 depletion efficiently inhibited PrP^{Sc} propagation in scrapie-infected cells (**Figure 1.4**). This occurred after the translocation of PrP^{c} into the ER and was dependent on both proteasomal and lysosomal degradation.

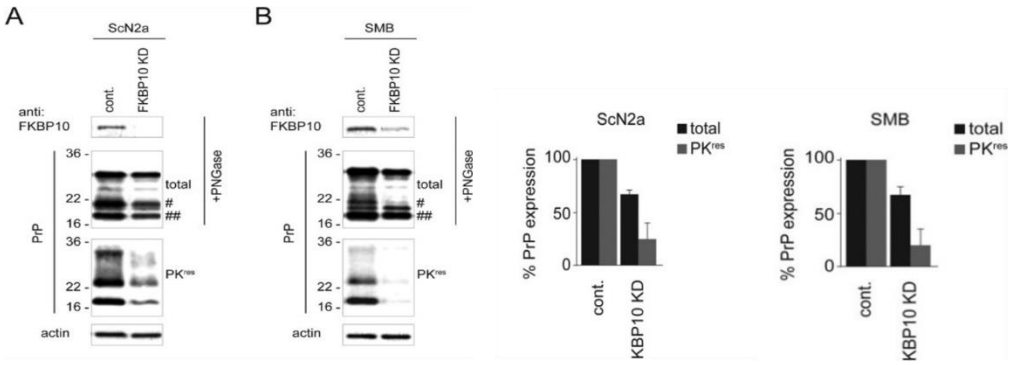

Figure 1.4 Transcriptional silencing of *Fkbp10* in scrapie-infected cells inhibits prion propagation. Transient *Fkbp10* silencing in scrapie-infected mouse neuroblastoma (ScN_2a) cells (A) and scrapie-infected mouse brain (SMB) cells (B) cells inhibits PrP^{Sc} propagation. Total PrP and PrP^{Sc} were quantified and expressed as a percentage of the level of total PrP and PrP^{Sc} in control cells for ScN_2a and SMB cell lines. *Figure taken from Stocki et al., 2016*

1.5 Proline residues in the prion protein

As previously mentioned, Fkbp proteins possess peptidylpropyl *cis/trans* isomerase activity (Kang *et al.*, 2008). In folded proteins, peptide bonds exist either in the *cis* or *trans* conformation. While most peptide bonds exist in the *trans* conformation in folded proteins, 6% of all Xaa-Proline peptide bonds (where X represents any amino acid) are found in the *cis* conformation (Fischer, Michnick and Karplus, 1993). Importantly, *cis/trans* proline isomerisation is a rate-limiting step that can impede the process of protein folding (Galat, 2003). Proline residues impose unique structural constraints on protein secondary structure, and proline isomerisation (Eichner *et al.*, 2011; Nakamura *et al.*, 2012) and the composition of proline vs glycine residues are known to influence amyloid assembly (Rauscher *et al.*, 2006).

The human prion protein is composed of 15 proline residues. The genetic prion disease Gerstmann-Straussler-Scheinker syndrome can arise from point mutations of proline residues at positions 102 or 105 (Young *et al.*, 1995; Wadsworth and Collinge, 2007). The P101L mutation in mouse PrP, is homologous to the P102L disease-linked mutation in humans. A synthetic 55-residue peptide harbouring the P101L mutation converted into a β-sheet -rich conformation and induced clinical signs characteristic of a prion disease following inoculation in transgenic mice carrying the P101L mutation (TgMoPrP-P101L) (Kaneko *et al.*, 2000). The P102L substitution in the PrP(89–143) peptide enhanced the folding of extensive β-sheet fibrils (Inouye *et al.*, 2000; Wan *et al.*, 2015). In an independent study, circular dichroism was employed to examine the effect of the P102L mutation on the secondary structure of PrP. The GSS mutation (proline 102 to leucine) in *E. coli* expressed mouse PrP (residues 23−231) decreased the α-helical content of PrP, without altering protease sensitivity (Cappai *et al.*, 1999). Structural studies to investigate the effect of the P102L and P105L mutations on PrP amyloid formation, showed that proline residues impede amyloid formation by PrP (Kraus *et al.*, 2015). Additionally, substitution of proline residues accelerated PrP conversion and increased the PK-resistance of the N-terminally extended amyloid core. A more recent study by Kraus and co-workers demonstrated that the P102L mutation promotes the formation of infectious, recombinant prion amyloids (Kraus *et al.*, 2017). Following inoculation into wild-type hamsters, synthetic prions harbouring the P102L mutation initiated seeding activity, leading to the accumulation of protease-resistant PrP, without inducing clinical TSE disease. Collectively, these findings suggest that proline residues impose structural constraints and act as key modulators in the conversion of PrP to pathogenic amyloid types.

A study conducted by Cohen and Taraboulos, investigated the role of cyclophilins in the normal folding of PrP^{C} (Cohen and Taraboulos, 2003). Cyclophilins are peptidylpropyl *cis/trans* isomerases and like Fkbp proteins, act by accelerating the isomerisation of X-Proline bonds, a rate-limiting step in the folding of many proteins (Wang and Heitman, 2005). Treatment of cells with cyclosporin A, an inhibitor of the cyclophilin family, caused the accumulation of protease-resistant PrP in aggresomes. Additionally, the expression of disease-linked proline mutants, P101L and P104L, which are homologous to the disease-linked mutations in humans, mimicked the cyclosporin-induced PrP species that accumulated in aggresomes in these cells. These findings suggest that that the PPIase activity of cyclophilins could influence the isomerisation of X-proline bonds in PrP and may in turn have a crucial role in the

folding and processing of PrP^C. When this activity is compromised, it may lead to the abnormal folding of PrP and the development of sporadic prion diseases.

1.6 Prion strains

The existence of multiple prion strains can be accommodated within the "protein-only" hypothesis (Collinge, 2001). Prion strains are defined as conformational variants of PrP^{Sc}, that when transmitted to identical hosts, exhibit distinct prion disease phenotypes (Aguzzi, Heikenwalder, & Polymenidou, 2007, **Figure 1.5 A**). This definition is consistent with the protein-only hypothesis, as it explains how a single polypeptide chain can encode multiple disease phenotypes. The phenotypic traits include incubation times and patterns of neuropathological targeting (lesion profiles) in the brains of affected animals (Aguzzi et al., 2007, **Figure 1.5 A, Table 1.1**). These strain-specific characteristics are thought to be encoded by the distinct conformations of various PrP^{Sc} isotypes that can be stably and faithfully propagated (Collinge, 2005). The first evidence for the existence of prion strains was described by Pattison and Millson in 1961, who showed that goats infected by the same batch of scrapie agent developed two different clinical phenotypes (Pattison & Millson, 1961). The authors termed these as "nervous" and "scratching" syndromes, depending on each disease's manifestation. The differences between these strains were thought to have arisen as a consequence of differences in the genetic background of the host. *In vivo*, prion strains can be discriminated by clinical signs and symptoms, and lesion profiles (Bessen & Marsh, 1992b; Fraser, 1993; DeArmond et al., 1997, **Figure 1.5 A, Table 1.1**). *In vitro*, prion strains can be discriminated by differences in biochemical features including patterns of electrophoretic mobility following PK digestion, glycosylation profiles and extent of resistance to proteolytic digestion by proteases (**Figure 1.5 B**). Variant CJD is associated with PrP^{Sc} glycoform ratios which are distinct from those seen in classical CJD but similar to those seen in cattle BSE and BSE when transmitted to several other species (Collinge *et al.*, 1996). Importantly, the clinicopathological presentation of vCJD is distinct from other forms of CJD, owing to the fact that the former is caused by a different prion strain (Hill *et al.*, 1999). It has also been demonstrated that multiple PrP^{Sc} types co-exist in the brains of individuals with sCJD, justifying, in part, the heterogeneity in clinicopathological phenotypes seen in human prion diseases (Polymenidou et al., 2005; Puoti et al., 1999; Parchi et al., 1996). Polymenidou and colleagues have developed monoclonal antibodies that differentiate between sCJD types 1 and 2 and found that all sCJD type 2 and vCJD

cases analysed contain small amounts of type 1 in distinct brain areas (Polymenidou *et al.*, 2005).

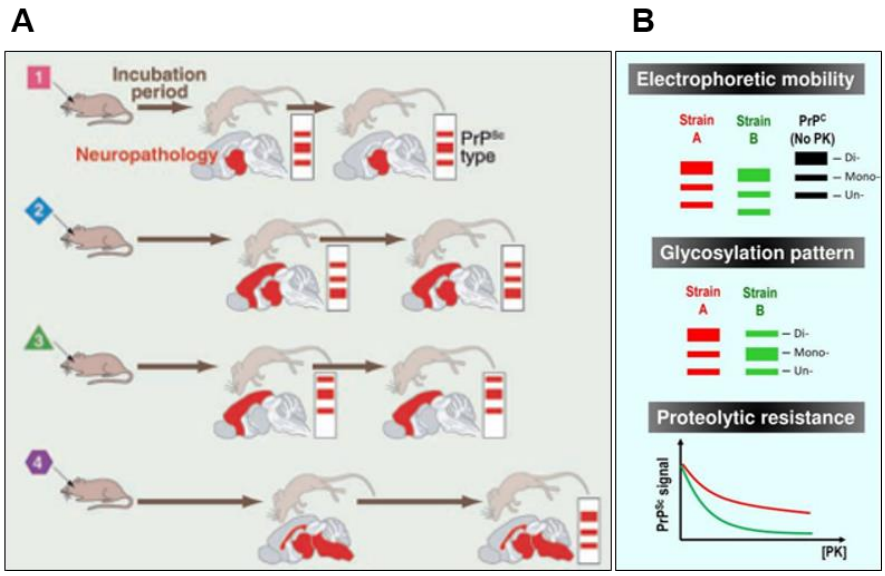

Figure 1.5 ***In vivo*** **and** ***in vitro*** **discrimination of prion strains A** (from John Collinge & Clarke, 2007) Prion strains can be discriminated by patterns of spongiform degeneration in different brain areas (neuropathological lesion profiles) as well as by differences in incubation times. **B** (from Morales, 2017) Biochemical features used to discriminate between prion strains include patterns of electrophoretic mobility following PK digestion, glycosylation profiles and extent of resistance to proteolytic digestion by increasing concentration of proteases such as PK.

Differential targeting of brain regions by prion strains has been demonstrated in experimental models of prion disease (DeArmond et al., 1997; Hecker et al., 1992). Prion strains can be discriminated by differences in the distribution of PrP^{Sc} deposition and the degree of vacuolation in specific brain regions (Fraser & Dickinson, 1973; Morales, Abid, & Soto, 2007). For example, in prion-infected mice, the mouse-adapted scrapie strain 22L targets the cerebellum whereas Me7 primarily targets the hippocampus, demonstrating differential brain region tropism of prion strains (Karapetyan et al., 2009; Brown, 2005, **Table 1.1**). Prion strains can also be discriminated *in vitro*, and it was shown that different cell lines are differentially susceptible to specific prion strains (see chapter **1.11.3**). Organ tropism of prion strains has also been described. For example, vCJD is a lymphotropic strain which rapidly colonises lymphoid tissues before neuroinvasion (Hilton *et al.*, 1998). Collectively, these findings suggest that specific cell types or tissues, contain cofactors or express cell-specific factors that permit the replication of some strains but not of others (Aguzzi, Heikenwalder and Polymenidou, 2007).

Prion strains may impede the replication of another strain, a phenomenon termed strain interference. Prion strain interference results in the emergence of a dominant strain from a mixture (Dickinson *et al.*, 1972). Experiments by Kimberlin and Walker have shown that the 22A prion strain blocks infection of the 22C strain and the blocking effect of 22A was only reversed with 6M urea (Kimberlin and Walker, 1985). In an independent study, the Drowsy (DY) strain was able to block infection with the Hyper (HY) strain (Shikiya *et al.*, 2010). Notably DY PrP^{Sc} did not deplete all of the available PrP^{c} by converting it into PrP^{Sc} in PMCA, suggesting that the blocking effect of DY might be due its ability to sequester PrP^{c} or that both DY and HY compete for a limiting cellular resource.

Prion strains have also been described in yeast. For example, [URE3] results from the prion-like, autocatalytic conversion of the Ure2 protein (Ure2p) into an inactive form and allows yeast cells to take up carbamoyl aspartic acid in the presence of ammonia (Schlumpberger, Prusiner, & Herskowitz, 2001; Wickner, 1994). Importantly, different [URE3] variants have been described. The different strain variants, resulting from different modes of aggregation, could stably maintain their specific characteristics (Schlumpberger, Prusiner and Herskowitz, 2001). In [PSI+] yeast cells, Sup35 exists in an amyloid state that can be propagated and passed to daughter cells (Wickner, 1994). Strain specific infectivity was demonstrated when infectious yeast [*PSI*] particles were used to nucleate the assembly of a bacterially expressed Sup35 in uninfected yeast hosts (King and Diaz-Avalos, 2004). It was shown that the first 61 amino acid residues of Sup35 are sufficient for encoding strain-specific infectivity. Strain-specific characteristics arose as a result of structural differences in the cross-beta folding patterns of the Sup35 protein fragment (King and Diaz-Avalos, 2004).

Prion strain/Prion disease	Derived from/natural host	Neuropathologic lesion profile
Me7	Derived from the spleen of scrapie-infected sheep that has been passaged in mice (Zlotnik I et al., 1963)	CA1 region of hippocampus in mice (Cunningham et al., 2003; Jeffrey et al., 2001)
22L	Derived from the brain of scrapie-infected sheep that has been passaged in mice (Dickinson, 1976)	The strain mainly targets the cerebellum in mice (Siskova et al., 2013)
RML	Derived from the brain of scrapie-infected sheep passaged in goats followed by several passages in mice (Kimberlin and Walker, 1978)	Targets the corterx, hippocampus and brainstem in mice (Karapetyan et al., 2009)
Chronic Wasting Disease (CWD)	Natural hosts are mule, elk, deer and moose (Williams et al., 2002)	Targets the olfactory tubercle, cortex, hypothalamus and parasympathetic vegal nucleus (Williams et al., 1993)
Variant Creutzfeldt Jakob Disease (vCJD)	Disease affects humans that have been infected with BSE prions (Collinge, 1999)	Spongiform change is most prominent in the basal ganglia while the thalamus exhibits severe neuronal loss and gliosis (Ironside, 2004)
Bovine Spongiform Encephalopathy (BSE)	Disease affects domestic cattle (Wells et al., 1987), captive exotic bovids (Jeffrey et al., 1988), domestic cat (Pearson et al., 1992)	Vacuolar changes are most prominent in medulla oblongata, midbrain and thalamus (Wells et al., 1991)

Table 1.1 Prion diseases and prion strains, their natural hosts and neuropathologic lesion profiles.

1.7 Selective neuronal vulnerability in neurogenerative diseases

In neurodegenerative diseases, distinct subpopulations of neurons are targeted, leading to the progressive failure of defined brain regions, a phenomenon known as selective neuronal vulnerability.

1.7.1 Parkinson's disease

Parkinson's disease is a multifactorial neurodegenerative disease characterised by motor dysfunction and by the accumulation of pathological alpha synuclein (α-Syn) in the brain of affected individuals (Kalia and Lang, 2015).

Mutations in several genes account for the relatively rare, familial forms of PD. Additionally, the identification of numerous genetic risk factors that increase the risk of developing PD, led to a better understanding of the molecular mechanisms that underlie the pathogenesis of PD. Mutations in the *SNCA* gene that encodes the α-synuclein protein, cause autosomal-dominant, early-onset PD (Klein and Westenberger, 2012). Alpha synuclein mutations perturb specific tertiary interactions which are required to maintain the native state of α-Syn, which is soluble and innocuous. Mutations including Ala30Pro and Ala53Thr promote the formation of β-sheet-rich conformations, increasing oligomerisation as well as the formation of protofibrils and fibrils (Bertoncini et al., 2005).
Mutations in *PARK6* and *PARK2*, encoding the proteins PINK1 and Parkin respectively, cause autosomal recessive forms of PD. Pink and Parkin work together in the same pathway to regulate mitochondrial quality control, supporting previous evidence that mitochondrial damage is directly involved in PD (Pickrell et al., 2015). Mutations in the *LRRK2* gene are known to cause late-onset autosomal and sporadic PD (Brice A, 2005). The gene encodes the cytoplasmic protein leucine-rich repeat kinase 2 (LRRK2), consisting of a leucine-rich repeat and a kinase domain. Studies have indicated that the protein is involved in cellular functions such as cytoskeletal maintenance, vescicle trafficking as well as protein degradation by autophagy. The precise physiological function of LRRK2 and its involvement in PD remain unclear. It has been reported that inhibition of LRRK2 kinase activity stimulates macroautophagy (Manzoni et al., 2016). Importantly, the most common familial mutation in LRRK2, Gly2019Ser, was shown to increase LRRK2 kinase activity, suggesting a gain-of-function mechanism for LRRK2-linked disease (West et al., 2005). A study conducted

by Manzoni et al., has shown that mutations in the three functional domains of LRRK2 resulted in changes in autophagy/lysosomal markers, linking LRRK2 mutations to the autopghagy-lysosomal pathway (Manzoni et al., 2013).

Another gene involved in PD is *PARK15*, wich encodes the F-box only protein 7 (Fbxo7). Mutations in *PARK15* cause an early-onset parkinsonian-pyramidal syndrome (Di Fonzo et al., 2009). The Fbxo7 protein belongs to a family of proteins that function as adaptors for a class of ubiquitin E3 ligases. Together with Pink and Parkin, Fbxo7 acts to regulate mitophagy, a process which involves the selective clearance of depolarised mitochondria through autophagy (Burchell et al., 2013). A study conducted by Delgado-Camprubi et al., showed that Fbxo7 deficiency, which mimicks the Fbxo7 Arg378Gly mutation in PD patients, leads to a reduced cellular NAD+ levels and impaired activity of Complex I in the mitochondrial electron transport chain, highlighting the importance of mitochondrial impairment in PD (Dalgado-Camprubi et al., 2017).

The loss of dopaminergic substantia nigra pars compacta (DA SNc) neurons accounts for the major clinicopathological manifestations of Parkinson's disease (PD). Mitochondrial dysfunction plays a key role in the pathogenesis of PD (Winklhofer and Haass, 2010; Tufi *et al.*, 2014; Delgado-Camprubi *et al.*, 2017). Evidence suggests that DA SNc neurons are particularly vulnerable to mitochondrial stress and dysfunction. In sporadic PD patients, specific deficiency of mitochondrial Complex I catalytic activity has been found in the SN (Gu *et al.*, 1997). In animal models of PD, the neurotoxins MPTP and rotenone increase the production of reactive oxygen species in the SNc, cause parkinsonism, loss of DA SNc neurons and accumulation of Lewy bodies, all of which are hallmarks of PD. Both neurotoxins act by targeting the mitochondrial electron transport chain and inhibiting Complex I, fuelling the possibility that an oxidative phosphorylation defect plays a key role in the pathogenesis of PD (Keeney, Xie, Capaldi, & Bennett, 2006; Dauer & Przedborski, 2003). Further work disproved the widely accepted hypothesis that inhibition of Complex I induced by these agents is directly linked to dopaminergic neuron death as the genetic depletion of Complex I in mice did not affect the survival of dopaminergic neurons in culture (Choi *et al.*, 2008).

The fact that selective vulnerability of DA SNc neurons to PD is linked to mitochondrial dysfunction does not explain why DA SNc neurons are more vulnerable to mitochondrial dysfunction compared to other neurons. DA SNc neurones have extraordinarily long and branched axons, sustained autonomous spiking, and elevated levels of cytosolic Ca^{2+} (Surmeier *et al.*, 2016). These neurones are Ca^{2+} -dependent

pacemakers and their activity is dependent on $Ca_v1.3$ low-voltage dependent L-type Ca^{2+} channels. These channels allow for high Ca^{2+} flux loads in DA SNc neurones. DA SNc neurons are autonomously active and generate continuous low frequency activity in the absence of synaptic input that is dependent on L-type Ca^{2+} channels. During this autonomous activity to maintain calcium homeostasis, these channels generate mitochondrial-mediated oxidative stress (Schapira, 2013).

Evidence suggested that the susceptibility of these neurones to parkinsonism-inducing drugs is reduced with L-type Ca^{2+} channel antagonists that reduce Ca^{2+} load (Chan *et al.*, 2007). Experiments using transgenic mice showed that, the engagement of plasma membrane L-type calcium channels during normal autonomous pacemaking leads to oxidative stress specifically in vulnerable SNc dopaminergic neurons (Guzman *et al.*, 2010). This oxidative stress activates defences that induce mild uncoupling and depolarization of mitochondria. Importantly, knock out of protein deglycase *DJ-1*, a gene associated with an early-onset form of Parkinson's disease, exacerbated oxidative stress by downregulating the expression of two uncoupling proteins and reducing calcium-induced uncoupling, specifically in SNc dopaminergic neurons (Guzman *et al.*, 2010). These findings provide sufficient evidence to suggest that L-type calcium channels (LTCCs), at least partly underlie selective neuronal vulnerability in Parkinson's disease, making them promising targets for therapeutic intervention in Parkinson's disease (Kang *et al.*, 2012).

PTEN-induced putative kinase 1 (*PINK1*) mutations cause familial recessive PD (Valente *et al.*, 2004). A study by Yao and colleagues demonstrated that PINK1 deficiency, led to increased basal mitochondrial membrane potential in skeletal myocytes and decreased basal mitochondrial membrane potential in neurons (Yao *et al.*, 2011). Importantly, this difference in basal mitochondrial membrane potential between myocytes and midbrain neurons (substantia nigra forms part of the midbrain), had an opposing effect on the aforementioned cell types. PINK1 deficiency induced impaired respiration in both cell types, and this was accompanied by an increase in glycolytic activity. Myocytes possess higher glycolytic capacity compared to neurons, enabling them to produce more ATP and compensate for the metabolic impairment induced by PINK1 deficiency. Additionally, the increased basal mitochondrial membrane potential in skeletal myocytes, as opposed to neurons, conferred myocytes a higher mitochondrial Ca^{2+} buffering capacity, rendering them resistant to Ca^{2+} stress. Contrary to this finding, *PINK1* deficiency in neurons increased reactive oxygen production and mitochondrial Ca^{2+} overload (Gandhi *et al.*, 2009). The above findings

provide a mechanism by which *PINK1* deficiency results in differential susceptibility to cell death in different cell types.

1.7.2 Amyotrophic Lateral Sclerosis (ALS)

Amyotrophic lateral sclerosis leads to the selective degeneration of upper motor neurones in the brain and lower motor neurones in the spinal cord. As these neurones control voluntary muscles, their death leads to gradual muscle weakness due to muscle atrophy. The most common clinical manifestations of ALS include difficulty speaking, swallowing and breathing (Zarei et al., 2015; Kiernan et al., 2011).

To date, at least fifteen candidate genes have been identified, that are associated with both familial and sporadic cases of ALS. Importantly, 20% of familial ALS cases are caused by a mutation in the *SOD1* gene which leads to the expression of a mutant, toxic superoxide dismutase 1 (SOD1) protein that causes disease through a gain-of-function mechanism. More than 30% of ALS cases that show familial inheritance are associated with a hexanucleotide repeat expansion mutation in the *C9orf72* gene (Renton et al., 2011). It has been shown that the expanded GGGGCC repeat leads to the formation of toxic dipeptide-repeat proteins such as poly-(Gly-Arg), through non-ATG-initiated translation (Mori et al., 2013). Mutations in several other genes account for the remaining cases of familial ALS. Some of the resulting mutant proteins are alsin, senataxin, spatascin, vescicle-associated membrane protein-associated protein B (VAPB), TAR DNA-binding protein 43 (TDP43), Fused in Sarcoma (Fus), angiogenin, factor induced gene 4 (FIG4), optineurin (OPTN) and ubiquilin 2 (Sheng et al., 2013). Some of these genes cause motor neurone degeneration by acting in the same molecular pathway. Such pathways include protein aggregation, aberrant RNA processing, oxidative stress, mitochondrial impairment and metabolic disturbance.

ALS leads to the extensive loss of motor neurones in the cerebrospinal axis but motor neurones that control eye movements and bladder contraction are spared, raising the question as to why some populations of motor neurones are resistant to degeneration while others die. Gene expression analysis of susceptible and resistant motor neurones revealed over a thousand differentially expressed genes associated with processes such as synaptic transmission, ubiquitin-dependent proteolysis and mitochondrial function (Brockington *et al.*, 2013). Significant differences in genes encoding several glutamate and gamma-aminobutyric acid (GABA) receptor subunits were identified. The authors showed that resistant motor neurones exhibited reduced

α-amino-3-hydroxy-5-methyl-4-isoxazolepropionic acid (AMPA) receptor-mediated inward calcium current and a higher GABA-mediated inhibitory chloride current, than vulnerable spinal motor neurons, suggesting that enhanced susceptibility to excitotoxicity mediated partly through reduced GABAergic transmission renders spinal motor neurones vulnerable to degeneration (Brockington *et al.*, 2013).

Other studies have also attributed the resistance of oculomotor motor neurones to disease to inhibitory synaptic transmission mediated by GABA and glycine neurotransmission (Comley *et al.*, 2015). This is further supported by the finding that *Gabra1*, which encodes a subunit of GABA receptors, is preferentially expressed in oculomotor motor neurons in symptomatic superoxide dismutase-1 (SOD1) transgenic mice and in end-stage ALS patients, conferring resistance to these neurones (Comley *et al.*, 2015). The expression of glycine receptors, that also mediate inhibitory neurotransmission in the spinal cord and brainstem, was shown to be significantly downregulated in mice expressing a mutant form of human SOD1 with a Gly93-->Ala substitution (G93A-SOD1) (Chang and Martin, 2009). Additionally, glycine-induced current density was significantly smaller in the G93A-SOD1 motor neurons compared with control, non-mutant motor neurones (Chang and Martin, 2011). Studies provided evidence that the resistance of oculomotor neurones to disease is also due to the significantly higher calcium buffering capacities of these neurones, originating from a specialised calcium homeostasis (Vanselow and Keller, 2000). The absence of strong intracellular Ca^{2+} buffers in vulnerable motor neurones renders them particularly reliant on mitochondrial signal cascades to regulate cytosolic calcium. Excessive calcium excitotoxicity makes these neurones even more vulnerable upon mitochondrial dysfunction (Lewinski & Keller, 2005, Spät, Szanda, Csordás, & Hajnóczky, 2008). These findings suggest that imbalances in the excitation of motor neurones underlie selective neuronal vulnerability in ALS.

It has been shown that within motor neurone (MN) pools in disease, high threshold fast-fatigable MNs are particularly vulnerable and are affected in early stages of ALS. In contrast, low-threshold slow MNs are resistant and still innervate muscle at end-stage disease (Saxena and Caroni, 2011). The two types of MNs differ in firing patterns and morphology. With increasing firing rates and decreasing ATP production, the amount of ATP produced is insufficient to sustain the activity of Na+/K+-ATPase and the ion balance is perturbed in vulnerable MNs (LeMasson, Przedborski and Abbott, 2014). Reductions in energy metabolism are a common occurrence in ALS (LeMasson, Przedborski and Abbott, 2014). These findings propose a model whereby vulnerable MNs with high energetic demands per action potential, eventually become

ATP-deficient (Le Masson et al., 2014, Roselli & Caroni, 2014). The ATP required to restore ion homeostasis through ion pumps fail, leading to cation accumulation and sustained depolarisation upon neuronal firing. This process puts an increasing burden on mitochondrial function and ATP production, leading to instability and ion imbalance that spreads within the MN. The energetic imbalance is further amplified by the rising calcium concentration due to mitochondrial overload, as described above, compromising ATP synthesis even more. The synergism between the direct interaction of misfolded, mutant SOD1 with mitochondria, and the secondary overload by ion uptake, could account for mitochondrial metabolism failure, leading to reduced ATP availability and eventually to neuronal dysfunction (Israelson et al., 2010; Roselli & Caroni, 2014). Aberrations in mitochondrial morphology, biochemistry and transport, have been a recurring finding in human and animal samples of ALS (Israelson *et al.*, 2010).

1.7.3 Alzheimer's disease (AD)

AD is the most common neurodegenerative disease, accounting for 60-70% of cases of dementia, and is characterised by progressive cognitive and functional impairment (Masters et al., 2015; Reitz, 2012). The pathological hallmarks of AD are extracellular plaques composed of amyloid β-protein (Aβ) and neurofibrillary tangles consisting of abnormal, hyperphosphorylated tau.

Autosomal dominant AD accounts for <1% of AD cases. Pathogenioc mutations in Amyloid Precursor Protein (APP), Presenilin 1 and Presenilin 2 cause autosomal dominant AD and explain 5-10% of the occurrence of early-onset AD (Cauwenberghe et al., 2016). All mutations that have been identified in APP favour the amyloidogenic processing of APP, leading to an increased production of Aβ42, the main component of neuritic plaques in AD (Cauwenberghe et al., 2016). *PSEN1* and *PSEN2*, encoding presenilin 1 and presenilin 2 respectively, are essential components of the gamma-secretase complex, which catalyses the proteolytic processing of APP to a mixture of Aβ peptides. Mutations in *PSEN1* and *PSEN2* lead to an increased Aβ42 to Aβ40 ratio by impairing the gamma-secretase cleavage of APP (De Strooper, 2007). In addition to the fully penetrant mutations in PSEN1, PSEN2 and APP, the ε4 allele of apolipoprotein E has been identified as a strong genetic risk factor for both early-onset and late-onset AD (Saunders et al., 1993). Studies including genome-wide association studies (GWAS), have identified at least 21 additional AD-susceptibility genes, some of which clustered within pathways such as lipid metabolism and vescicle trafficking

(Cauwenberghe et al., 2016). For example, the AD-susceptibility genes *SORL1*, *BIN1* and *PICALM*, encode the proteins Sortlin-Related Receptor-1, Bridging Integrator 1 and Phosphatidylinositol Binding Clathrin Assembly Protein respectively, all of which are involved in endosomal vesicle trafficking.

It remains unanswered why distinct brain regions are differentially vulnerable to plaque accumulation and tau-related neurodegeneration in AD. Neurones in the hippocampus, amygdala, and cerebral cortex are particularly vulnerable, whereas neurons in the basal ganglia, cerebellum, brain stem, and spinal cord remain relatively unaffected (Muratore *et al.*, 2017). The neurons at higher risk in AD, including entorhinal cortex and hippocampal CA1 projection neurons (Hof and Morrison, 2004), are particularly vulnerable to reduced glucose and oxygen supply through the vasculature and thus to energy deprivation. It has been reported that mild cognitive deficits correlate with reduced glucose utilization in the brain, in early onset cases that frequently progress to AD (Mosconi et al., 2008; Rabinovici & Jagust, 2009).
A study by Muratore et al. with human induced pluripotent stem cells (iPSCs) from AD patients showed that neurons directed to rostral versus caudal fates exhibit marked differences in both their generation of and responses to Aβ (Muratore *et al.*, 2017). Rostral cultures consisted of a mixture of upper and lower layer cortical neurons of both inhibitory and excitatory fates. Treatment with AD brain extracts, elevated levels of phosphorylated tau in rostral, forebrain neurones in an Aβ-dependent manner but this response was absent in caudal neurones after the same treatment. Caudal neurones expressed markers of hindbrain and spinal cord, thereby representing AD-resistant neurones. These findings demonstrated that different neuronal subtypes that are vulnerable or resistant to AD are markedly different with regards to APP processing and tau proteostasis.

A growing body of evidence suggests patients with quite different clinical disease presentations share similar neuropathological profiles of Aβ and neurofibrillary tangle (NFT) accumulation (Ryan & Rossor, 2011; Schott & Warren, 2012; Rossor, Fox, Mummery, Schott, & Warren, 2010). Late-onset AD (LOAD) is the most common variant, presenting with episodic memory deficits. Early-onset AD (EOAD) is a less common variant, characterised by impaired attention, language and visuo-spatial abilities (Sá *et al.*, 2012). Other AD variants have also been described, including a group of rare AD patients that have predominantly behavioural/dysexecutive symptoms (“Frontal variant”) (Ossenkoppele *et al.*, 2015).

The presence of Aβ pathology is a prerequisite for the development of symptomatic AD (Montine *et al.*, 2012). The existence of different AD variants may in part arise from differences in the regulation of Aβ production, accumulation and spread throughout the brain. Current evidence suggests that the regional pattern of Aβ accumulation provides little information about AD phenotypes and that variations in Aβ pathology do not explain phenotypical variations (de Souza et al., 2011; Lehmann, Ghosh, et al., 2013; Rosenbloom et al., 2011). Instead, Aβ deposition appears to be diffusely distributed, without marked differences between clinical variants of AD (Lehmann, Ghosh, et al., 2013; Rosenbloom et al., 2011; Rabinovici et al., 2010). However, these studies were carried out on patients with established disease, whereas Aβ pathology likely develops over several years prior to clinical onset. With this in mind, it is likely that in different clinical variants of AD, Aβ pathology starts to develop in different brain networks, reminiscent of what is observed in prion disease, where different prion strains target distinct brain areas (see chapters **1.8** and **1.11.2**). This might explain why in posterior cortical atrophy (PCA), which is considered an atypical variant of AD, patients have slightly increased occipital Aβ accumulation compared to other AD variants (Lehmann *et al.*, 2013). Overall, it has been established that different AD variants that are associated with different clinicopathological manifestations, show different patterns of brain atrophy. For example, logopenic variant primary progressive aphasia, an atypical form of AD, is associated with atrophy in regions of the left hemisphere whereas in PCA patients, atrophy is predominantly focused to the occipital, parietal and occipitotemporal cortices (Mesulam et al., 2008; Gorno-Tempini et al., 2008; Benson, Davis, & Snyder, 1988).

Additional studies have provided evidence for syndrome-specific patterns of hypometabolism and atrophy in different AD variants, which in contrast to fibrillar Aβ deposition, much more closely mirrored the clinical symptoms (Lehmann, Ghosh, et al., 2013; Gil D. Rabinovici et al., 2010; Migliaccio et al., 2009). Importantly, when comparing EOAD patients and LOAD patients, a study has found more severe metabolic deficits in distinct brain regions of the former group, highlighting that impaired glucose metabolism in posterior brain regions was positively correlated with age-at-onset and with degree of cognitive impairment (Lehmann *et al.*, 2013). It has also been shown that EOAD patients exhibit more apparent deficits in cholinergic and other neurotransmitter systems (Bird, Stranahan, Sumi, & Raskind, 1983; Rossor, Iversen, Reynolds, Mountjoy, & Roth, 1984).

Tau and Aβ deposition originate in different regions of the brain. Tau deposition starts in the entorhinal cortex and then spreads to the hippocampus whereas Aβ plaques are initially deposited in the isocortex and deposition in the hippocampus follows this first stage (Braak & Braak, 1995; Serrano-Pozo, Frosch, Masliah, & Hyman, 2011). The molecular mechanisms that explain the initial sites of Aβ and tau deposition and how Aβ and tau pathologies converge in specific brain regions remain elusive (Jagust, 2018). In contrast to Aβ pathology, tau pathology is more closely linked to neuronal loss and clinical symptoms (Roberson *et al.*, 2007). To explain clinical variability, Mattsson et al proposed a model that links Aβ pathology, tau pathology and regional atrophy distribution (Mattsson *et al.*, 2016). The model postulates that Aβ aggregation is induced by the total neuronal activity in highly connected cortical networks, which explains the broadly similar diffuse pattern of Aβ pathology in AD variants. However, tau pathology develops in specific vulnerable brain regions, its progression being enhanced by amyloid pathology, and spreads from cell-to-cell, through trans-synaptic neural connections, to closely linked brain networks. Patterns of tau deposition correlate more closely with specific functional networks and neuronal loss, suggesting that this may underlie clinical variability (Lehmann *et al.*, 2013).

A growing body of evidence suggests that prion-like mechanisms may underlie tau and Aβ aggregation and spread (see chapters **1.9.2** and **1.9.3**). It has been shown that, similarly to prion strains, different conformational assemblies of tau and Aβ are associated with different neuropathological phenotypes (Eisenberg and Jucker, 2012)(see chapters **1.10.2** and **1.10.3**). It is possible that each AD subtype is characterised by a unique spectrum of Aβ and tau species. Aβ and tau strains may govern the toxicity and variable rates of spread of the aforementioned proteins, or they may exhibit tropism to specific brain regions, giving rise to different disease manifestations.

1.7.4 Huntington's disease

Huntington's disease (HD) is a progressive, fatal neurodegenerative disease caused by an expanded CAG repeat in the huntingtin gene (Ross and Tabrizi, 2011). This expansion results in a long polyglutamine repeat in the huntingtin protein, rendering the mutant huntingtin (mHtt) cytotoxic (Yu et al., 2003; Fu et al., 2017). Some of the most common symptoms include chorea, dystonia and impaired gait, posture and balance. The disease is characterised by highly selective and profound degeneration of the brain's corpus striatum (Mealer *et al.*, 2014). Despite the selective striatal

degeneration in Huntington's disease, wild-type and mutant Htt are expressed ubiquitously throughout the brain and many body tissues (Li *et al.*, 1993). Several studies have implicated Rhes, the striatal-specific guanosine triphosphate (GTP)-binding protein, in the selective, striatal pathology of HD (Subramaniam, Sixt, Barrow, & Snyder, 2009; Steffan et al., 2004; Seredenina, Gokce, & Luthi-Carter, 2011; Lu & Palacino, 2013). It has been shown that Rhes binds to mutant Htt and acts as a SUMO (Small Ubiquitin-like MOdifier) E3 ligase to stimulate sumoylation of mutant Htt, a post-translational modification known to enhance the cytotoxicity of mutant Htt (Steffan et al., 2004; Subramaniam et al., 2009). In Rhes-deleted mice, striatal degeneration and motor dysfunction are dramatically reduced in a striatal-specific model of HD elicited by 3-nitropropionic acid (Mealer, Subramaniam, & Snyder, 2013; Ghiglieri & Calabresi, 2013). The deletion of Rhes in mice delayed the onset of symptoms in a genetic model of HD (Baiamonte *et al.*, 2013).

More recent findings have implicated Rhes in autophagy (Srinivasa Subramaniam et al., 2011; Mealer et al., 2014). Autophagy is a lysosomal degradation pathway with a well-established role in aging and neurodegeneration. Mutant Htt is a well-established substrate of autophagy and activation of this pathway is protective in both cell and animal models of HD (Sarkar & Rubinsztein, 2008; Harris & Rubinsztein, 2012; Jimenez-Sanchez, Thomson, Zavodszky, & Rubinsztein, 2012). In rat pheochromocytoma PC12 cells, deletion of endogenous Rhes was shown to decrease autophagy, whereas Rhes overexpression augmented autophagy (Mealer *et al.*, 2014). The co-expression of mutant Htt blocked Rhes-induced autophagy activation (Mealer *et al.*, 2014). Importantly, these findings demonstrated that the activation of autophagy by Rhes may explain the delay of symptom onset in HD. These findings propose a model whereby both Rhes and mHtt are expressed within the striatum for years, long before neuronal dysfunction and degeneration is evident, but changes in the autophagic activity of Rhes overtime lead to the selective degeneration of the brain's corpus striatum and symptomatology.

Transcriptional dysregulation is a central pathogenic mechanism in Huntington's disease (Benn et al., 2008) Mutant Htt acquires a gain of function and alters the normal expression of specific mRNAs at least partly, by disrupting the binding activities of many transcription factors (Benn *et al.*, 2008). It has been shown that wild-type huntingtin up-regulated the transcription of brain-derived neurotrophic factor (BDNF), a pro-survival factor produced by cortical neurons that was indispensable for the survival of striatal neurons in the brain (Zuccato *et al.*, 2001). This beneficial activity of huntingtin was abrogated when the protein was mutated, leading to reduced

production of cortical BDNF (Zuccato *et al.*, 2001). Reduced levels of BDNF reduced neurotrophic support for striatal neurones, impairing adaptive plasticity and leading to their degeneration.

1.8 Selective neuronal vulnerability in prion diseases

In prion diseases, selective neuronal vulnerability is linked to degeneration of particular brain areas in a strain-dependent manner. Sporadic and iatrogenic CJD cases are associated with three distinct types of PrP^{Sc}, as seen on a Western blot, following proteolytic cleavage (Collinge *et al.*, 1996). PrP^{Sc} types 1 and 2 are linked to different clinicopathological phenotypes of sCJD (Parchi *et al.*, 1996). Type 3 PrP^{Sc} is associated with iCJD cases where exposure to prions occurred via a peripheral route such as intramuscular injection of human cadaveric pituitary-derived growth hormone rather than via a central nervous system (CNS) route (dura mater grafts) (Collinge *et al.*, 1996). Type 4 PrP^{Sc} is uniquely seen in vCJD brain (Collinge, Sidle, Meads, Ironside, & Hill, 1996; Wadsworth et al., 1999; Hill et al., 2003) and is clearly distinguished from other PrP^{Sc} types seen in classical CJD by a predominance of the di-glycosylated PrP glycoform (Hill *et al.*, 2003). This unique glycoform signature of vCJD resembles that of BSE (Hill *et al.*, 1997). Notably, vCJD, which is caused by the BSE strain, is atypical both in its clinical features and neuropathology (Collinge *et al.*, 1996). Importantly, peripherally acquired cases of prion disease such as by oral exposure, exhibit a distinct clinicopathological phenotype characterised by cerebellar ataxia and psychiatric symptoms rather than a dementing illness (Brown, Preece and Will, 1992). Contrary to this observation, iCJD caused by direct CNS exposure, bears resemblance to sporadic CJD (Brown, Preece and Will, 1992).

In natural sheep scrapie and experimental rodent scrapie, the early stage of prion replication occurs in the lymphoreticular system but detectable neuroinvasion occurs at a later stage in the disease (Fraser and Dickinson, 1978). In cattle BSE cases, prion infectivity is primarily detected in Peyer's patches in the distal ileum (Wells *et al.*, 1994). Peripheral pathology and lymphoreticular deposition of PrP^{Sc} are features observed in all vCJD patients that have been studied so far, in striking contrast to other forms of CJD, which lack this prominent lymphoreticular phase (Hill et al., 1999; Hill, Zeidler, Ironside, & Collinge, 1997a). The recognisable differences in tropism of vCJD prions for lymphoreticular organs and neural tissues provide further evidence, alongside with conventional strain typing approaches, that vCJD cases are associated with a distinct strain of PrP^{Sc}. Additionally, the above findings suggest that the route of

exposure to prions may influence strain properties, and initial replication in the peripheral nervous system might change prion strain characteristics.

1.8.1 Fatal Familial Insomnia (FFI)

Fatal familial insomnia is an autosomal dominant inherited prion disease with a variable age of onset ranging from 18 to 60. It is commonly caused by a missense mutation at codon 178 when aspartic acid is replaced by an asparagine residue (Medori *et al.*, 1992). The presentation of the disease is considerably variable from person to person but it is typically characterised by increasing, untreatable insomnia, dysautonomia, hallucinations and rapid weight loss (Gambetti, Parchi, Petersen, Chen, & Lugaresi, 1995; Lugaresi et al., 1986). The disease primarily targets the thalamus, causing severe neuronal loss and reactive gliosis but relatively little PrP deposition or spongiosis (Gambetti et al., 1995; Gambetti, Kong, Zou, Parchi, & Chen, 2003).

A study has found that the D178N mutation, 129M allele segregates with FFI while patients carrying the D178N mutation with the 129V allele are diagnosed with familial CJD (Gambetti *et al.*, 1995). Importantly, the PK resistant isoforms found in FFI and CJD are different in regard to their size and degree of glycosylation. The two diseases caused by the same mutation, but distinct genotypes generated by the methionine-valine polymorphism at codon 129 (129M or 129V) in the mutant allele of the PrP gene, exhibit a different spectrum of clinical and pathological features. The authors have not excluded the possibility that the PrP^{Sc} isoforms in FFI and CJD represent two different prion strains with two different protein conformations responsible for distinct pathological profiles. The existence of FFI strains is further supported by the finding that an FFI patient with the D178N mutation and homozygosity for Met at codon 129, exhibited atypical clinical features including rapidly progressive dementia combined with behavioural disturbances and paroxysmal limb myoclonus (Sun *et al.*, 2015). The patient did not exhibit typical refractory insomnia in the early stage of the disease or observable MRI changes in the thalamus. A patient with the D178N-129M genotype, exhibited cerebellar ataxia but no insomnia, further highlighting the diversity in clinical presentations partly explained by the existence of different prion strains (Taniwaki *et al.*, 2000).

1.8.2 Gerstmann–Sträussler–Scheinker syndrome (GSS)

GSS is associated with autosomal dominant inheritance of a mutation in the prion protein gene, where proline is replaced by a leucine residue in codon 102 (Young *et al.*, 1995). Patients typically experience slowly developing dysarthria and cerebellar

ataxia. Pyramidal features with dementia occur much later in the clinical course of the disease which is longer than that seen in classical CJD (Wadsworth *et al.*, 2003).
Some patients show considerable phenotypic variation which can encompass both CJD- and GSS-like cases (Collinge *et al.*, 1990). For example, prion disease with a 144 base pair insertion in a Japanese family line presented with patchy and regional neuronal loss with marked astrocytosis in the frontal lobe and regional neuronal loss in the hippocampus. These features are not generally observed in CJD and GSS cases caused by point mutations (Oda et al., 1995; Wadsworth et al., 2003; Collinge et al., 1992). An atypical case of GSS has also been described in a patient who carried the P102L mutation but had severe muscular atrophy and vertical gaze palsy, features that are not seen in classical GSS (Oba *et al.*, 2000). Based on the above findings, it is possible that prion strains underlie the extensive phenotypic variability which is seen in human prion diseases. This is clearer in patients that carry the same mutation on *PRNP* yet exhibit a different spectrum of clinicopathological features.

1.8.3 Sporadic CJD

Sporadic CJD occurs as a result of the spontaneous conversion of PrP^{C} into PrP^{Sc} as a rare stochastic event, in the absence of a pathogenic *PRNP* mutation. The disease presents as rapidly progressive dementia, usually with myoclonus. Most cases are aged 45-75 years at onset and the clinical progression is typically over weeks progressing to akinetic mutism and death often in 2–3 months (Wadsworth *et al.*, 2003).
There is now increasing evidence for the co-existence of different PrP^{Sc} types within the same sCJD brain (Puoti et al., 1999; Wadsworth & Collinge, 2007; Polymenidou et al., 2005). Transmission experiments to wild-type and transgenic mice strengthened the hypothesis that alternative conformations of PrP provide the molecular basis for the marked clinicopathological heterogeneity seen in human prion diseases. In sCJD, two different types of PrP^{Sc} with distinct physicochemical properties are found associated with distinct phenotypes (Parchi *et al.*, 1996).

Even though in sporadic CJD, 70% of cases die in under 6 months, around 10% of patients have a clinical course that extends for two years or more and present with cerebellar ataxia rather than cognitive impairment (Gomori, Partnow, Horoupian, & Hirano, 1973; Brown, Rodgers-Johnson, Cathala, Gibbs, & Gajdusek, 1984). Another subtype of CJD, the panencephalopathic type, is characterised by severe and extensive degeneration of the cerebral white matter. These cases have been

predominantly reported from Japan (Mizutani, 1981, Matsusue., Kinoshita, Sugihara, Fujii, Ogawa, Ohama, 2004). Cases of amyotrophic CJD are characterised by a syndrome of slowly progressive dementia with lower motor neuron signs (Salazar *et al.*, 1983). To define the full spectrum of sCJD variants, Parchi and colleagues performed a detailed phenotypic and molecular analysis of 300 sCJD patients (Parchi *et al.*, 1999). The study identified six distinct clinicopathological variants of CJD, arising from at least three distinct prion strains. These variants include the myoclonic type and the ataxic variant. Rarer variants include the kuru-plaque variant, which is linked to MV at codon 129 and PrP^{Sc} type 2 and is characterised by a longer mean duration of symptoms and the presence of kuru-like amyloid plaques. The MM2 thalamic phenotype is indistinguishable from that of fatal familial insomnia and is characterised by thalamic and olivary atrophy. The six sCJD cases were selected for transmission to transgenic mice, each of which showed the typical characteristics of that subgroup (Bishop, Will and Manson, 2010). Several other studies have explored the heterogeneity in sCJD, identifying clinical and pathological phenotypes associated with specific sCJD subtypes (Pierluigi Gambetti et al., 2003; Castellani et al., 2004; Collins et al., 2006).

1.8.4 Codon 129 polymorphism and selective neuronal vulnerability

Notably, methionine (Met) homozygosity at codon 129 confers susceptibility to prion diseases (Collinge et al., 1991; Mead et al., 2009; Palmer, Dryden, Hughes, & Collinge, 1991; Lee et al., 2001; Mead et al., 2003).

While all definite cases of vCJD have occurred in patients with the MM genotype at *PRNP* codon 129 (Will *et al.*, 2000), a single case of vCJD was reported in a patient with heterozygosity at *PRNP* codon 129 (Mok *et al.*, 2017). Notably, the patient's clinical features differed from those of typical vCJD and his neuroimaging features resembled those seen in sCJD patients. However, results of neuropathological examination and molecular strain typing were consistent with a diagnosis of vCJD (Collinge *et al.*, 1996). Immunoblotting revealed type 4 PrP^{Sc} deposits in the patient's brain and PrP^{Sc} was also detectable in lymphoid tissue of the spleen. These findings suggest that polymorphism at codon 129 of the human PrP gene (*PRNP*), where methionine (Met) or valine (Val) can be encoded, might influence prion strain properties, giving rise to vCJD with a different clinicopathological phenotype.

A study has found that 16 out of 22 sCJD patients and a further 11 out of 23 sCJD suspected cases of sCJD were Met-29 homozygotes, whereas 51% of the normal

population were heterozygous at this site (Palmer *et al.*, 1991). These findings imply that homozygosity predisposes to sCJD (Palmer *et al.*, 1991). A number of studies provided evidence that the clinical expression of sCJD is influenced by codon 129 polymorphism. In individuals with sCJD that are homozygous for Met at codon 129 of *PRNP*, brains showed accumulation of type 1 PrP^{Sc} (unglycosylated band of 21.5KDa) and the patients presented with classic CJD symptoms including subacute dementia and myoclonus (Plaitakis *et al.*, 2001). In contrast to these observations, 2 sCJD cases, both homozygous for valine at codon 129, presented with cerebellar ataxia and later dementias and the brains of these patients showed accumulation of PrP^{Sc} type 2 (unglycosylated band of 19.4kDa) (Plaitakis *et al.*, 2001). In addition to these findings, codon 129 valine homozygote cases of sCJD exhibit a neuropathological phenotype characterised by spongiform degeneration and prion protein deposition in the hippocampus, which is rarely reported in sCJD (Kovacs *et al.*, 2000).

In a separate study, a sCJD patient heterozygous at codon 129 presented with cerebellar ataxia and dementia that appeared simultaneously (Tranchant, Geranton, Guiraud- Chaumeil, Mohr, & Warter, 1999). Immunoblot analysis of brain extracts revealed the presence of PrP^{Sc} type 1. The patient had many kuru-like plaques in the cerebellar cortex and many PrP amyloid plaques were present in the basal ganglia.

Importantly, codon 129 genotype has strong implications in prion strain propagation. Certain prion strains only occur in individuals with specific *PRNP* codon 129 genotypes (Collinge et al., 1996; Wadsworth et al., 1999; Hill & Collinge, 2003), suggesting that *PRNP* codon 129 accounts, at least partly, for prion strain selection and the variability in clinicopathological phenotypes in human prion diseases. Additional studies have shown that inoculation of mice with BSE and vCJD prions resulted in the propagation of distinct molecular and neuropathological phenotypes dependent on host PrP codon 129 status (Asante et al., 2002; Wadsworth et al., 2004). Collectively, these data suggest a pivotal role for codon 129 in governing prion strain selection and restricting the repertoire of thermodynamically permissible PrP^{Sc} conformers (Collinge, 1999; Collinge, 2001). Collectively, the above findings are consistent with the conformational selection model of prion transmission barriers. According to this model, ease of transmission of prions between species (or also within species as a result of PrP polymorphisms), is dependent on overlap of permissible PrP^{Sc} conformations between the donor and recipient (Collinge & Clarke, 2007).

1.9 Prion-like mechanisms in neurodegenerative diseases

A number of studies have demonstrated that seeded protein aggregation is not a feature unique to prion diseases and a similar mechanism may account for the accumulation of pathogenic, misfolded proteins in a number of neurodegenerative diseases including Parkinson's disease (PD), Alzheimer's disease (AD) and Amyotrophic Lateral Sclerosis (ALS) (Frost & Diamond, 2010; Goedert, Clavaguera, & Tolnay, 2010; Paumier et al., 2015; Meyer-Luehmann et al., 2006).

1.9.1 Alpha synuclein

PD is a neurodegenerative disease that leads to the progressive loss of neurones in the substantia nigra (Beitz, 2014). PD mainly affects the motor system and the movement difficulties found in PD are called parkinsonism. PD is characterised by the accumulation of aggregated alpha synuclein (α-Syn) in the brains of affected individuals. Cytoplasmic inclusions composed of α-Syn fibrils are referred to as Lewy Bodies (LB) and are the signature neuropathological hallmarks of PD (Wakabayashi *et al.*, 2007).

The spatiotemporal progression of alpha synuclein (α-Syn) pathology in Parkinson's disease (PD) patients is notably stereotypical. Braak staging describes in detail the progression of Parkinson's disease pathology, spreading from the lower brainstem and olfactory bulb into the limbic system and, eventually, to the neocortex (Braak et al., 2003). Alpha synuclein aggregation was observed in the grafted fetal mesencephalic neurons in PD patients, a phenomenon which suggests host-to-graft transmission of misfolded α-Syn (Kordower, Chu, Hauser, Freeman, & Olanow; 2008, J.-Y. Li et al., 2008; Hansen et al., 2011). It was later shown that α-Syn pathology can be propagated by direct neuron-to-neuron transmission of α-synuclein aggregates, reminiscent of prion propagation (Desplats *et al.*, 2009). This mechanism may in turn explain the topographical progression of Lewy pathology in PD suggested by Braak et al (Braak et al., 2003).

The prion-like spreading of misfolded alpha synuclein has been demonstrated in both cell and animal models (Volpicelli-Daley et al., 2011; Paumier et al., 2015). It has been shown, that in healthy, non-transgenic mice, intrastriatal inoculation of synthetic α-Syn fibrils initiated the formation of PD-like Lewy-bodies/Lewy-neurites (LB/LNs) and subsequent cell-to-cell transmission of pathologic α-Syn to anatomically interconnected regions (Luk *et al.*, 2012). The neurodegenerative cascade was

characterised by selective loss of substantia nigra pars compacta (SNpc) DA neurons, and impaired motor coordination (Luk *et al.*, 2012). In a separate study, fibrillar α-Syn seeds were internalised by cells and converted soluble, endogenous α-Syn into insoluble, hyperphosphorylated and ubiquitinated pathological species, resembling LBs in the brains of PD patients (Luk *et al.*, 2009). Similar findings were reported by Volpicelli-Daley and colleagues. Preformed fibrils of α-Syn were internalised by primary neurones, causing α-Syn to form inclusions, probably by promoting recruitment of soluble endogenous α-Syn into insoluble PD-like LBs and LNs (Volpicelli-Daley *et al.*, 2011). Importantly, the aggregates formed first in axons, and propagated throughout the entire neuron. The accumulation of pathologic α-Syn led to a reduction in synaptic proteins and progressively impaired neuronal function, eventually leading to neuronal death (Volpicelli-Daley *et al.*, 2011).

Peripheral inoculation of amyloidogenic alpha synuclein induced pathology in the Central Nervous System (CNS) in the human A53T and wild-type α-Syn transgenic (Tg) mouse models (Sacino *et al.*, 2014). Inoculated animals developed rapid and synchronised hind limb motor weakness and widespread CNS α-Syn inclusion pathology. These findings highlight that seeded aggregation of alpha synuclein can facilitate its spread from the peripheral nervous system to the central nervous system (Sacino *et al.*, 2014).

Alpha synuclein is not only implicated in the pathogenesis of Parkinson's disease. Multiple System Atrophy (MSA) is a slow progressive neurodegenerative disorder characterised by parkinsonism and progressive decline of autonomic nervous system function (Stefanova *et al.*, 2009). The defining histopathologic hallmark of MSA is glial and neuronal cytoplasmic inclusions of filamentous alpha synuclein (Stefanova *et al.*, 2009). Brain extracts from MSA patients were transmissible to transgenic mice harbouring the A53T mutation, a causative factor of Parkinson's disease. All extracts transmitted neurodegeneration and caused neurological dysfunction to mice and this was accompanied by intraneuronal deposition of mutant alpha synuclein aggregates (Prusiner *et al.*, 2015).

1.9.2 Tau

Tauopathies are a class of neurodegenerative diseases including Alzheimer's disease, the most common tauopathy, progressive supranuclear palsy (PSP) and Pick's disease. These diseases are characterised by the pathological aggregation of tau

protein in neurofibrillary or gliofibrillary tangles in the human brain (Orr, Sullivan, & Frost, 2017; Kovacs, 2015).

During AD progression, pathological tau inclusions appear to spread in a predictable pattern throughout the brain, along trans-synaptic neural connections (Braak and Braak, 1991). An increasing body of evidence suggests that prion-like propagation may underlie tau aggregation and spread (Clavaguera et al., 2009; Iba et al., 2013; Ahmed et al., 2014; Peeraer et al., 2015). Studies have demonstrated that the injection of samples containing recombinant tau aggregated *in vitro*, can accelerate tau pathology in transgenic mice that overexpress human tau (Iba et al., 2013; Peeraer et al., 2015). Synthetic tau fibrils were shown to transmit tau inclusions in a transgenic mouse model (Iba *et al.*, 2013). Intracerebral injection of tau fibrils in the brains of young PS19 mice that overexpress mutant human tau, resulted in the induction of neurofibrillary tangle (NFT)-like inclusions (Iba *et al.*, 2013). These inclusions propagated from the sites of injection to more distant, synaptically connected brain regions. In a separate study, intracerebral inoculation of tau fibrils purified from AD brains, but not tau fibrils of synthetic origin, resulted in the formation of tau inclusions in anatomically connected brain regions in non-transgenic mice (Guo *et al.*, 2016). Aggregated tau from brain extracts of P301S tau-expressing transgenic mice could also seed tau pathology when injected into the brains of mice transgenic for human wild-type tau (Clavaguera *et al.*, 2009). Experimental transmission of tau pathology was also demonstrated following intracerebral injection of brain homogenates from human tauopathies into non-transgenic mice (Clavaguera *et al.*, 2013). Importantly, the induced formation of tau aggregates could be propagated by serial injection into mouse brains (Clavaguera *et al.*, 2013).

Work by Jackson and colleagues showed that large tau aggregates are the major species that underlie the spreading of tau pathology in the P301S transgenic model (Jackson *et al.*, 2016). In contrast, small, oligomeric tau species could not initiate the formation and spread of tau pathology (Jackson *et al.*, 2016).

Collectively, these findings support a prion-like spread of tau pathology by a local cell-to-cell and distant axonal spread of inclusions.

1.9.3 Amyloid beta (Aβ)

AD is the most common neurodegenerative disease, accounting for 60-70% of cases of dementia, and is characterised by progressive cognitive and functional impairment (Masters et al., 2015; Reitz, 2012). The pathological hallmarks of AD are extracellular

plaques composed of amyloid β-protein (Aβ) and neurofibrillary tangles consisting of intraneuronal aggregates of hyperphosphorylated and misfolded tau (Serrano-Pozo, Frosch, *et al.*, 2011).

Numerous studies provide evidence for the transmissible nature of Aβ. It has been systematically shown that injecting young mice that naturally deposit Aβ with human AD brain-derived homogenates or extracts accelerates amyloid deposition, which spreads through interconnected regions in the brain (Kane *et al.*, 2000; Meyer-Luehmann *et al.*, 2006; Eisele *et al.*, 2009, 2010; Heilbronner *et al.*, 2013; Fritschi *et al.*, 2014). Intracerebral infusion of dilute brain extracts from AD patient brains can seed cerebral Aβ in β-amyloid precursor protein (βAPP)-transgenic mice (Kane *et al.*, 2000). In agreement with tau findings, even though synthetic Aβ can induce AD pathology *in vivo,* synthetic Aβ is much less effective than brain-derived Aβ aggregates (Stohr *et al.*, 2012). Brain homogenates from autopsied AD patients (AD extract) or from aged, transgenic mice expressing mutant Amyloid Precursor Protein (APP), induced cerebral β-amyloidosis and associated pathology in young APP transgenic mice (Meyer-Luehmann *et al.*, 2006). In this study, the exogenous induction of Aβ deposition *in vivo* was time and concentration dependent. Immunodepletion of Aβ from brain extracts of transgenic mice completely abolished the amyloid-inducing activity of the extract, highlighting that Aβ is the agent that induces seeding. The neuropathological phenotype of the induced amyloidosis depended on the host and the source of agent (Meyer-Luehmann *et al.*, 2006).

Adding to the growing weight of experimental evidence for the prion-like transmission and propagation of Aβ in mice, recent studies have also provided evidence for prion-like iatrogenic transmission of Aβ in humans (Kovacs et al., 2016; Hamaguchi et al., 2016; Jaunmuktane et al., 2015). Post mortem examination of patients, who died of iatrogenic Creutzfeldt-Jakob disease (iCJD) years after having received cadaveric growth hormone or dura mater, revealed that they harboured Aβ seeds from donors who had died of CJD (Jaunmuktane *et al.*, 2015). In this study, patients who died of iCJD had significant Aβ deposition. Examination of patients who died of other prion diseases showed minimal or no Aβ pathology whereas the iCJD patients exhibited grey matter and vascular Aβ pathology. The authors speculated that had these patients lived long enough, they would have developed Cerebral Amyloid Angiopathy (CAA). Further studies were conducted, showing that CAA and brain parenchymal Aβ plaques were significantly more frequent in iCJD than in age-matched sCJD (Frontzek *et al.*, 2016). Importantly, these patients had no family history of early-onset dementia or prominent AD-related tau pathology, had no pathogenic mutations, ε4 allele of

Apolipoprotein E (ApoE) or other high-risk alleles associated with early-onset Alzheimer's disease. The above findings provide evidence that the amyloid beta pathology in these patients may have resulted from seeding of Aβ aggregates from the grafts to host tissues. In addition to these findings, a recent study has reported the accumulation of Aβ in the brains of human Growth Hormone (hGH) recipients who died from causes other than CJD, providing further evidence that the Aβ present in the inoculated hGH preparations had a seeding effect in the brains of around half of all the hGH recipients, producing an AD-like neuropathology and cerebral amyloid angiopathy (CAA), regardless of whether CJD neuropathology had occurred (Ritchie *et al.*, 2017). Importantly, even though these findings prove evidence for the transmissibility of Aβ in humans, there is no evidence to suggest that AD is transmissible or that iCJD patients who received Aβ-contaminated cadaveric growth hormone or dura mater would have gone to develop AD had they lived long enough.

1.9.4 Polyglutamine (PolyQ)

Huntington's disease (HD) is an inherited, progressive, fatal neurodegenerative disease characterised by motor and cognitive dysfunction (Ross and Tabrizi, 2011). The disease is caused by an expanded polyglutamine repeat in exon 1 of the huntingtin (HTT) gene. The expansion of PolyQ increases the propensity of huntingtin protein to aggregate and pathological aggregates can be transmitted between neurones, a process which may explain the pathological spreading of polyQ aggregates. It has been suggested that spreading of aggregated polyQ is mediated by direct cell-to-cell transmission of aggregates, and that this process involves seeded polymerisation of polyQ in a prion-like fashion (Kim et al., 2017; Pearce, Spartz, Hong, Luo, & Kopito, 2015; Pecho-Vrieseling et al., 2014; Ren et al., 2009).

A study by Ren and colleagues showed that fibrillar aggregates of PolyQ peptides were internalised by HEK293 cells, penetrated the cytosolic compartment and became co-sequestered in aggresomes (Ren et al., 2009). The internalised polyglutamine aggregates were able to nucleate the aggregation of soluble, cytoplasmic proteins containing polyQ tracts, with which they shared homologous amyloidogenic sequences (Ren et al., 2009). In an independent study, human stem cell-derived neurones acquired mutant huntingtin when functionally integrated in the neural network of organotypic brain slices of an HD mouse model, suggesting trans-neuronal propagation of mutant huntingtin (Pecho-Vrieseling *et al.*, 2018). Importantly, the mutant huntingtin from organotypic brain slices induced HD-like pathology in human neurones (Pecho-Vrieseling *et al.*, 2018). The prion-like propagation of mutant

huntingtin has also been demonstrated *in vivo*. In the *Drosophila* brain, phagocytic glia cells engulfed neuronal huntingtin aggregates, and these in turn nucleated the conversion of soluble huntingtin to an aggregated state (Pearce *et al.*, 2015). Kim and colleagues employed the *Caenorhabditis elegans* (*C. elegans*) model and showed that mutant huntingtin was transmitted between pharyngeal muscle cells and neighbouring neurons (Kim *et al.*, 2017). Importantly, the transmission of mutant huntingtin was gradually increased with aging of the animal and *C. elegans* with polyQ transmission exhibited degenerative phenotypes (Kim *et al.*, 2017).

1.9.5 Superoxide Dismutase 1 (SOD1) and Transactive response DNA binding Protein 43 (TDP-43)

Frontotemporal dementias (FTDs) and Amyotrophic lateral sclerosis (ALS) share some clinical, neuropathological and genetic features (Ferrari *et al.*, 2011). FTDs encompass six types of dementias which cause degeneration of frontal and temporal lobes (Ferrari *et al.*, 2011). ALS has mainly been described as a neurological disorder that affects the motor system but is now recognised as a multisystem neurodegenerative disease. This is because other than motor areas of the brain undergo degeneration (Ferrari *et al.*, 2011). Aggregated, pathologic TDP-43 protein associated with ubiquitin-positive inclusions is a feature of both FTD and ALS (Neumann *et al.*, 2006). Misfolding of SOD1 protein is implicated in the pathogenesis of both sporadic and familial ALS (Bosco *et al.*, 2010). Mutations in the *SOD1* gene are causative factors of ALS (Rosen *et al.*, 1993).

An increasing body of evidence suggests that SOD1 and TDP-43 propagate and spread in a prion-like fashion (Munch, O'Brien and Bertolotti, 2011; Nonaka *et al.*, 2013; Udan-Johns *et al.*, 2014; Ayers, Fromholt, *et al.*, 2016; Pokrishevsky, Grad and Cashman, 2016; Smethurst *et al.*, 2016; Grad, Pokrishevsky and Cashman, 2017; Healy, 2017). This may in turn explain why the symptoms and the deposition of aggregates in ALS and FTD are progressive. Mutant SOD1 aggregates were shown to exhibit properties reminiscent of prions, as they were internalised by endocytosis by N2a cells and triggered the self-perpetuating aggregation of endogenous SOD1 (Munch, O'Brien and Bertolotti, 2011). It has been reported that intracellular transmission of misfolded SOD1 can occur through the release of naked aggregates by cells, which are taken up by micropinocytosis and can induce seeded aggregation in recipient cells (Grad *et al.*, 2014). Alternatively, misfolded SOD1 transmission between cells can be mediated through the release and uptake of exosomes (Grad *et al.*, 2014).

Structural studies showed that enervating the electrostatic loop in SOD1 protein leads to a “gain-of-interaction”, which in turn mediates the formation of SOD1 amyloid-like filaments and prion-like aggregation (Healy, 2017). Prion-like aggregation of SOD1 was also demonstrated *in vivo*. SOD1 transgenic mice carrying the G85R SOD1 mutation, developed paralysis at six months of age when injected with spinal homogenates from paralysed mutant SOD1 mice (Ayers, Fromholt, *et al.*, 2016b). Notably, G85R SOD1 transgenic mice do not develop ALS symptoms until after twenty months of age. In the aforementioned model system, SOD1 inclusion pathology spread slowly along neuroanatomical pathways, implicating the prion-like propagation of misfolded SOD1 as a potential mechanism for the spreading of ALS (Ayers, Fromholt, *et al.*, 2016b).

TDP-43 has also been shown to propagate and spread via a prion-like mechanism. Pathological aggregates of TDP43 extracted from ALS brain and spinal cord tissue caused the mislocalisation of endogenous TDP-43 from the nucleus to the cytoplasm, where it became insoluble and aggregated via seeded polymerisation (Smethurst *et al.*, 2016). Serial passage of TDP-43 aggregates in cells, led to an increase in aggregated TDP-43 levels, suggesting more efficient propagation and reminiscent of adaptation when prions are passaged to a new host (Smethurst *et al.*, 2016). When insoluble TDP-43 aggregates from ALS brains were introduced into SH-SY5Y cells expressing TDP-43, these aggregates seeded intracellular TDP-43 aggregation in a prion-like manner (Nonaka *et al.*, 2013). A study by Pokrishevsky and colleagues showed that pathological TDP-43 may be involved in ALS pathology by initiating the misfolding and propagation of endogenous SOD1 (Pokrishevsky, Grad and Cashman, 2016).

1.10 Proteopathic strains in neurodegenerative diseases

A growing body of evidence suggests that conformational strains either generated with recombinant proteins or isolated from diseased brains have been described for multiple amyloidogenic proteins including tau, amyloid beta (Aβ), Superoxide Dismutase-1 (SOD1), and alpha synuclein (α-Syn) (Peelaerts et al., 2015; Stöhr et al., 2014; Ren et al., 2009; Guo et al., 2013). Strains can be differentiated by their unique conformations, morphology, toxicity, transmission pattern and neuropathological lesion profiles and may underlie the tremendous heterogeneity of clinicopathological phenotypes within a single neurodegenerative disease such as Alzheimer’s disease.

1.10.1 Alpha synuclein (α-Syn)

Evidence for the existence of α-Syn strains has been shown in a number of studies. Guo and co-workers have demonstrated that two distinct strains of synthetic α-Syn fibrils are remarkably different in terms of their efficiency to cross-seed tau aggregation (Guo *et al.*, 2013). Importantly, the strains also differed in their sensitivity to Proteinase K (PK) digestion as well in their immunoreactivity to the monoclonal antibody (mAb), b9029-03 (Guo *et al.*, 2013). Mutational variants of α-Syn can drastically affect the initial steps of lipid-induced fibril formation, the growth of fibrils as well as their amplification (Flagmeier *et al.*, 2016). In a different study that characterised the effect of familial alpha synuclein mutations on the conformational stability of alpha synuclein fibrils, it was shown that the mutants differentially affected the stabilities of the fibrils without inducing overall fibril structural changes, suggesting that mutant variants of alpha synuclein can affect the kinetics of aggregation and propagation (Xu *et al.*, 2017)**.** Nuclear Magnetic Resonance (NMR) studies of α-Syn A30P and A53T mutations have proposed that polymorphs of the same mutants of α-Syn co-exist and that mutations cause redistribution of the ensemble of conformers of α-Syn fibrils (Bertoncini *et al.*, 2005). Using Atomic Force Microscopy (AFM), a study by Conway et al. demonstrated that A53T mutant α-Syn exists as a mixture of several distinct species including non-fibrillar oligomeric α-Syn, fibrillar and monomeric α-Syn (Conway *et al.*, 2000).

The faithful replication of distinct α-Syn conformers was shown to be analogous to the faithful amplification of prion strains. Prion strains can maintain the conformation of the original seed even after multiple rounds of PMCA (Castilla *et al.*, 2008). *In vivo*, fibrils of alpha synuclein derived from two transgenic mouse strains, each representing a distinct synucleopathy, were amplified by PMCA (Jung *et al.*, 2017). The PMCA gave rise to two different fibril conformers with distinct proteinase K digestion profiles. These findings demonstrate that a trace amount of α-synuclein fibrils in tissue extracts can be amplified without altering the conformation of the original seed (Jung *et al.*, 2017).

Post-translational modifications have been implicated in the diversity of prion strains (Baskakov & Katorcha, 2016; Lawson, Collins, Masters, & Hill, 2005; Wadsworth et al., 1999). Protein phosphorylation is the most abundant post translational modification and abnormal protein phosphorylation is involved in the pathogenesis of neurodegenerative diseases including Parkinson's and Alzheimer's disease (Sato, Kato, & Arawaka, 2013; Gong & Iqbal, 2008). In Parkinson's disease, the main form of α-Syn that is involved in the pathological cascade is phosphorylated α-Syn at serine

129 (pS129 α-Syn). This variant is the main component of pathological lesions and is associated with multiple strain formation *in vivo* (Ma *et al.*, 2016). Experiments conducted by Ma et al. demonstrated that phosphorylation of α-Syn at Serine129 gives rise to a distinct strain of α-Syn. Importantly, wild type α-Syn fibres differed significantly from the phosphorylated fibrils in terms of structure and ability to propagate monomeric, endogenous α-Syn leading to aggregate formation. Treatment of mouse N2a neuroblastoma cells with the two strains showed that the phosphorylated variant exhibited significantly higher cytotoxicity as determined by increased Caspase 3 activation and reactive oxygen species (ROS) production (Ma *et al.*, 2016). In a different study to characterise two α-Syn strains, Luc Bousset and co-workers demonstrated that two α-Syn polymorphs are different in terms of structure, cytotoxicity and propagation properties (Bousset *et al.*, 2013). The two strains were able to imprint their intrinsic architecture to the reporter endogenous α-Syn in N2a cells. This was accompanied by differences in the rates of formation of fibrillary assemblies in the cells. The existence of α-Syn strains that display differential seeding capacities, strain-specific pathology and neurotoxic phenotypes has also been reported by other groups (Peelaerts *et al.*, 2015).

To date, there is no evidence for the existence of α-Syn strains in humans; however, the aforementioned studies provide a molecular basis for the heterogeneity in neuropathological progression in neurodegenerative disorders caused by α-Syn aggregation.

1.10.2 Tau

The heterogeneity in clinicopathological phenotypes of tauopathies may be explained by the existence of tau strains.

An increasing body of evidence suggests that prion-like propagation may underlie tau aggregation and spread. A study by Sanders et al., has demonstrated that different human tauopathies are associated with distinct sets of tau strains (Sanders *et al.*, 2014). The study also showed that inoculation of tau strains (derived from cells transduced with tau fibrils) into transgenic P301S mice induced unique pathological phenotypes. These phenotypes could be maintained through multiple passages in mice, a process reminiscent of the faithful replication of prion strains after several passages *in vivo*. Intracerebral injection of human tauopathy brain lysates induced local tau pathology or pathology that spread along connected brain regions in wild type, non-transgenic mice (Clavaguera *et al.*, 2013). Interestingly, the tau strains

associated with different sporadic human tauopathies gave rise to distinct clinical phenotypes and glial and/or neuronal pathologies in inoculated mice, recapitulating the pathology observed in individual human tauopathies (Clavaguera *et al.*, 2013). For example, the intracerebral injection of Progressive Supranuclear Palsy (PSP) brain homogenates into ALZ17 mice, expressing a wild-type human tau, resulted in the formation of silver-positive astrocytic aggregates that resembled tufted astrocytes, the hallmark lesions of PSP. This is reminiscent of the ability of prion strains to induce pathology in distinct brain areas and to target specific cell types, a phenomenon which underlies selective neuronal vulnerability in prion diseases (see chapter **1.8**).

A different study showed that tau strains maintain their conformation and strain-specific properties in mice (Kaufman *et al.*, 2017). In the same study, formaldehyde-fixed tissue from the hippocampi of mice inoculated with two distinct tau strains, DS9 and DS10, recapitulated the phenotypes of the original strains upon inoculation into cells. The two strains exhibited different inclusion morphologies in cells and gave rise to distinct neuropathological profiles in the brains of inoculated mice. Distinct conformational assemblies of tau may account for some aspects of clinical variation among tauopathies. Another study has demonstrated that tau strains derived from recombinant, human and mouse sources can be discriminated by their seeding profile and inclusion morphology in primary hippocampal neurones (Kaufman *et al.*, 2016). Interestingly, the aforementioned tau strains could also be differentiated *in vivo* following inoculation in transgenic mice. Tau strains differed with respect to their tropism for specific brain regions, rate of spread of tau pathology along neural networks and ability to induce intracellular pathology in distinct cell types (Kaufman *et al.*, 2016).

Conformational differences between tau species can determine the seeding potency of tau aggregates. It has been shown that synthetic tau aggregates exhibit a significantly reduced seeding activity compared to sarkosyl-insoluble Tau from TgP301S Tau mouse brain (Falcon *et al.*, 2015). These findings imply that tau behaves like a prion and that the conformational stability of tau conformers correlates with their seeding activity. A different study has shown that tau oligomers derived from AD human brain induced the aggregation of monomeric, recombinant tau *in vitro* much more rapidly than performed, recombinant tau oligomers (Lasagna-Reeves *et al.*, 2012). Additionally, brain-derived tau dramatically impaird synaptic function compared to oligomers prepared from recombinant tau (Lasagna-Reeves *et al.*, 2012). These findings are reminiscent of what is seen with synthetic and naturally occurring prion

stains. In mice, synthetic prions are thought to be more stable and exhibit longer incubation times than natural prion isolates (Kim et al., 2010). It has been observed that an inverse correlation exists between structural stability and seeding activity of prion strains (Legname *et al.*, 2006).

1.10.3 Amyloid beta (Aβ)

The existence of distinct conformational variants or strains of Aβ, is supported by various lines of evidence (Stöhr et al., 2014; Condello et al., 2018). Work conducted by Jan Stöhr and colleagues showed that synthetic Aβ40 and Aβ42, differed structurally and gave rise to different neuropathological phenotypes in the brains of inoculated transgenic mice (Stohr *et al.*, 2014). Inoculation of mice with synthetic Aβ40 gave rise to amyloid plaques composed of both Aβ40 and Aβ42. Contrary to this observation, intracerebral inoculation of synthetic Aβ42 stimulated the formation of smaller plaques composed predominantly of Aβ42. These findings suggested that in the absence of sodium dodecyl sulphate (SDS), Aβ40 and Aβ42 could be discriminated by differences in biological and physical properties. However, in the presence of SDS, Aβ42 became indistinguishable from Aβ40, with respect to its physical and biological properties. The results suggested that two strains of synthetic Aβ42 were formed: the first strain was formed in the absence of SDS and the second strain in the presence of SDS (Stohr *et al.*, 2014).

To investigate whether distinct Aβ strains exist in AD patients, susceptible, transgenic mice were inoculated with brain homogenates from sporadic or familial (Arctic and Swedish) AD cases (Watts *et al.*, 2014). Mice inoculated with the Arctic AD sample exhibited a distinct disease phenotype that was distinguishable from mice inoculated with the Swedish or sporadic AD samples. This was evident by the differential accumulation of Aβ isoforms and the morphology of cerebrovascular Aβ deposition. Inoculation of transgenic mice with brain samples from patients with two different heritable forms of AD, not only produced two distinct patterns of cerebral Aβ deposition, but these differences were also maintained on serial passage in mice (Watts *et al.*, 2014). Work by Petkova and colleagues showed that fibrils formed from the 40-residue Aβ peptide of Alzheimer's disease display different morphologies with different molecular structures (Petkova *et al.*, 2005). The structure of fibrils was sensitive to subtle differences in fibril growth conditions. The two different fibril structures exhibited markedly different toxicities in neuronal cell cultures, implying that inherent structural differences are responsible for the differential fibril toxicity in

primary hippocampal neurones. In a separate study, the cross-seeding of Aβ 1–40 Wild type (WT) monomers with preformed seeds of mutant Aβ 1–40 peptide gave rise to fibrils with distinct conformations (Spirig *et al.*, 2014). Electron microscopy to examine fibril morphologies, revealed that distinct amyloid beta conformations were propagated over multiple cycles of seeded polymerisation (Spirig *et al.*, 2014). These findings provide evidence for the existence of Aβ strains and at least partly, form the molecular basis for the clinical heterogeneity observed in Alzheimer's disease (see chapter **1.7.3**).

Intracerebral injection of APPPS1 brain extract into young APP23 mice induced Aβ deposition with different morphology, spectral properties and Ab40/42 ratio compared to amyloid beta deposition induced when APP23 brain extract was injected into young APP23 mice (Heilbronner *et al.*, 2013). APPPS1 transgenic mice express a chimeric mouse/human amyloid precursor protein and a mutant human presenilin 1. APP23 transgenic mice carry the Swedish double mutation in APP (K670N/M671L) associated with Alzheimer's disease. These findings reveal that distinct Aβ morphotypes exist and the phenotype of Aβ deposition in these transgenic mice reflected the properties of the original seed in the donor brain extracts. Additionally, their findings further strengthen the concept of templated misfolding of Aβ by a prion-like seeding mechanism.

The existence of distinct Aβ strains may explain the diversity in phenotypes of AD and contribute to our understanding of the difference between slowly progressive (spAD) and rapidly progressive AD (rpAD) (Akiyama et al., 1999; Cohen et al., 2015; Cohen, Appleby, & Safar, 2016). There is no evidence that there are differences in the neuropathology between spAD and rpAD. Additionally, there is no evidence to suggest that there are differences in the morphology and distribution of neurofibrillary tangles (NFTs) and amyloid plaques in the two forms of AD, suggesting that other factors may be responsible for the differences in the two AD sub-types (Cohen, Appleby and Safar, 2016). It was shown that rpAD cases were associated with a unique spectrum of Aβ42 species (Cohen *et al.*, 2015). For example, when compared to spAD, rpAD was associated with Aβ42 conformers that were less stable upon exposure to guanidine hydrochloride (Cohen *et al.*, 2015). The lower stability of these conformers suggests that they might be more susceptible to fragmentation *in vivo*, in contrast to more stable conformers. It is therefore possible that each AD sub type is characterised by a unique spectrum of oligomeric Aβ species and that these structures may govern the toxicity and variable rates of Aβ propagation in the brain, giving rise to different disease manifestations (Cohen, Appleby and Safar, 2016). These findings are consistent with

observations that less stable prion strains fragment more easily and replicate faster, leading to more rapid progression of prion disease (Kim et al., 2011.; Kim et al., 2012).

1.10.4 Superoxide Dismutase 1 (SOD1) and Transactive response DNA binding Protein 43 (TDP-43)

A number of proteins have been implicated in the pathogenesis of ALS, including TDP43 and SOD1. Factors other than mutations in disease-related genes are likely to account for the variability in age of onset, clinicopathological phenotype and disease duration. Evidence for the existence of distinct strains of SOD1 and TDP43 is currently increasing (Bidhendi et al., 2016; Bergh et al., 2015; Smethurst et al., 2016).

A study conducted by Jacob I. Ayers and colleagues showed that motor neuron disease (MND) was accelerated in transgenic mice expressing the G85R variant of SOD1 by injecting spinal cord homogenate from paralysed mutant SOD1 transgenic mice (Ayers, Diamond, *et al.*, 2016b). Additionally, aggregates of misfolded, recombinant WT SOD1 gave rise to MND with distinct inclusion pathology in transgenic mice. This pathology was faithfully transmitted to G85R Tg mice upon successive passages. When slice cultures from G85R Tg mice were exposed to spinal homogenates from patients diagnosed with ALS caused by the A4V mutation in SOD1, the cells developed robust inclusion pathology but spinal homogenates from sALS cases failed to induce misfolding of mutant SOD1 and accompanying pathology in these cultures. Similar findings were reported *in vivo*. Homogenates from paralysed mice expressing the G93A SOD1 variant induced MND in recipient transgenic mice but homogenates from paralysed mice expressing the G37R variant failed to transmit disease in recipient animals, implying that different SOD1 strains with different seeding capacities exist (Ayers *et al.*, 2014). While the first passage of G93A homogenate into G85R mice induced MND in 60% of the animals, second passage of homogenates from G93A → G85R mice back into G85R mice, caused disease in all of the inoculated animals (Ayers *et al.*, 2014). This is reminiscent of prion strain adaptation which occurs when prions gradually adapt to a new host when serially transmitted within the same species following cross-species transmission. The above findings support the existence of SOD1 strains by demonstrating that not any SOD1 conformer can induce the propagation of pathology, given that spinal cord tissues from human sporadic ALS and some mutant SOD1 variants lack the prion-like potential seen with homogenates from SOD1 mutant fALS cases (Ayers, Fromholt, Koch, Debosier, et al., 2014, Ayers et al., 2016a).

In a separate study, seeding of cells with TDP-43 from ALS brain or spinal cord gave rise to distinct morphological inclusions in these cells, recapitulating the morphological diversity of TDP-43 inclusions detected in ALS patient CNS tissue (Smethurst *et al.*, 2016). Bidhendi and colleagues have recently demonstrated that two distinct strains of human mutant SOD1 (hSOD1) aggregates (denoted A and B) can be isolated from transgenic mice (Bidhendi *et al.*, 2016). Inoculation of human SOD1 transgenic mice with these aggregates gave rise to an ALS-like pathology and the two strains could be differentiated by their progression rates, neuraxis distributions, end-stage aggregate levels and histopathology (Bidhendi *et al.*, 2016).

It remains elusive why mutant SOD1 is selectively toxic to motor neurone populations and the existence of different SOD1 conformations may help to address this question. It has been shown that the monoclonal antibody C4F6 specifically reacts with mutant SOD1 and shows remarkable selectivity for disease-affected tissues and cells (Brotherton *et al.*, 2012). Tissue that was not affected by the disease but accumulated high levels of mutant SOD1 such as sensory neurones, showed no immunoreactivity with C4F6. These findings suggest that the antibody specifically recognises a toxic, mutant form of SOD1 that accumulates in pathologically affected tissues in transgenic ALS rodent models and in humans with SOD1 mutations, adding to the evidence that distinct SOD1 species exists, only some of which are toxic and therefore relevant in ALS pathogenesis (Brotherton *et al.*, 2012). A separate study has reported that C4F6 specifically recognises soluble oligomers of mutant SOD1, but not dimers or monomers and that oxidative stress increases the abundance of these oligomers and therefore increases exposure of the disease-specific epitope recognised by C4F6 (Redler *et al.*, 2014).

1.11 Discrimination of prion strains

1.11.1 Discrimination of prion strains *in vitro*

Prion strains can be discriminated by differences in their biochemical characteristics. These include electrophoretic mobility following PK digestion, glycosylation profile, extent of resistance to PK digestion, resistance to denaturation by chaotropic agents and sedimentation rate (Morales et al., 2007; Morales, 2017). Differences in electrophoretic mobility following proteinase K digestion are thought to arise from distinct PrP^{Sc} conformations. Denaturation with guanidine hydrochloride (GdnHCl) has revealed differences in conformational stabilities of different PrP^{Sc} conformers from

synthetic and naturally occurring sources (Legname *et al.*, 2006). In the same study the authors found that less stable prions replicated more rapidly than stable prions and exhibited shorter incubation times when inoculated in mice.

Prion strains exhibit differences in their binding affinity for copper. Experiments by Wadsworth and colleagues suggested that two different human PrP^{Sc} types, seen in clinically distinct subtypes of sporadic CJD gave indistinguishable fragment sizes on a Western blot upon treatment with the metal-ion chelator Ethylenediaminetetraacetic acid (EDTA) (Wadsworth *et al.*, 1999). In contrast, the same treatment did not alter the generation of characteristic cleavage products from PrP^{Sc} types 3 or 4. These findings suggest that the binding of metal ions such as copper, alters the conformation of PrP^{Sc} in a strain-dependent manner and provides a new mechanism for the generation of multiple prion strains.

It has been shown by Eri Saijo et al, that C-terminal conformational differences exist between RML, 22L and Me7 as identified by an indirect enzyme-linked immunosorbent assay (ELISA) using the monoclonal antibody 6H10 (Saijo *et al.*, 2016). The antibody recognised the folded, abnormal conformations of Me7 and 22L but not RML. A plausible explanation for this observation is that for Me7 and 22L, there might be folds that bring components of the 6H10 epitope together in space to form conformations to which 6H10 binds more avidly. Strain-specific antibodies have been developed to discriminate between two strains of sCJD (Polymenidou *et al.*, 2005).

It has recently been demonstrated in prion-susceptible cells, that perturbation of different endocytic pathways affects prion infection is a strain-specific manner, arguing that prion strains rely on different endocytic routes for established prion infection (Fehlinger *et al.*, 2017). For example, perturbation of clathrin-mediated endocytosis significantly enhanced the levels of newly formed PrP^{Sc} following 22L infection but significantly reduced the levels of PrP^{Sc} in RML-infected cells.

Glycosaminoglycans (GAGs) are unbranched polysaccharides that have been implicated in prion disease and sulphation of GAGs is important in determining GAG function (Esko and Selleck, 2002). Heparan Sulphate (HS) has been found associated with prion plaques in human and animal forms of prion disease (Snow, Kisilevsky, Willmer, Prusiner, & DeArmond, 1989; McBride, Wilson, Eikelenboom, Tunstall, & Bruce, 1998). A number of GAGs have been investigated as cofactors in prion conversion and it has been reported that they both enhance or have no effect on the conversion process (Wong et al., 2001; Ben-Zaken et al., 2003). A study by Ellett and colleagues found that two sulphated GAGs, heparin and heparan sulphate, which

differ at levels of sulphation, can change the biochemical properties of PrP^{Sc}, including solubility and protease resistance (Ellett *et al.*, 2015). These findings propose a model whereby differential distribution of GAGs in different cell types or brain regions, contributes to the differential cell and brain tropism of prion strains.

1.11.1.1 Glycosylation

Prion strains can be discriminated by differences in glycosylation. Mature PrP molecules have 2 N-linked glycosylation sites at residues 180 and 196 and can therefore exist as di-, mono- or unglycosylated PrP (Endo *et al.*, 1989). When visualised by Western blot, following PK digestion, molecular weights range from 33KDa for the fully glycosylated human prion species; 29KDa for the mono-glycosylated species and 21KDa for the unglycosylated moiety. The size of the bands reflects the conformation of different strains, whereas band intensity corresponds to the affinity of antibodies to a specific PrP^{Sc} epitope and is representative of the proportions of glycosylation site occupancy. The glycosylation "signature" is dependent on the prion strain (Kuczius, Haist, & Groschup, 1998) but it is also tissue, cell line and brain region specific (Atkinson, 2004; Somerville, 1999).
The strain-specific PrP^{Sc} glycosylation profiles of four mouse-adapted scrapie strains were analysed. The glycosylation profiles of RML and 87V strains significantly differed whereas the glycosylation sites of 22L and Me7 strains overlapped (Vorberg and Priola, 2002). Variant CJD has a glycoform "signature" very similar to BSE but markedly different to other types of CJD (Collinge *et al.*, 1996).

Strain-specific neurotropism is a phenomenon that describes the ability of neuronal cells to distinguish prion strains. Strain-specific neurotropism is therefore governed by features like glycosylation profile of PrP molecules, strain-specific PrP^{Sc} conformational differences, the presence of putative accessory molecules such as lipids or DNA as well as host-encoded proteins such as chaperones. PrP^{c} glycosylation influences both strain-selective neuronal targeting and cross-species susceptibility to prion infection (Priola and Lawson, 2001). Experiments by De Armond et al., showed that PrP^{Sc} deposition was perturbed in Tg mice expressing PrP mutated at one or both glycosylation sites. Mutations that prevented Asn-linked glycosylation resulted in aberrant topologies of PrP^{C} within the CNS and altered PrP^{C} trafficking (DeArmond *et al.*, 1997). A study by Piro et al. has demonstrated that unglycosylated RML and 301C prions are both infectious to wild-type mice and neuropathological analysis revealed that mice inoculated with these two strains maintained the pattern of

PrP^{Sc} deposition and neuronal vacuolation that is characteristic of the aforementioned strains. These results imply that PrP^{Sc} glycosylation is not required or is not the only determinant of strain-specific prion neurotropism (Piro *et al.*, 2009). In addition to these findings, neuroblastoma N2a cells transiently expressing mutated, unglycosylated PrP, could sustain conversion of PrP^{C} to PrP^{Sc} after infection with RML, Me7 or 301V. This indicates that lack of glycosylation per se does not prevent PrP^{C} from being targeted to the cell surface and being converted to PrP^{Sc}. However, it remains to be determined whether characteristics such as pattern of PrP^{Sc} deposition and vacuolation are preserved for each prion strain following the inoculation of mice that express the same, unglycosylated version of PrP^{C} (Korth, Kaneko and Prusiner, 2000).

It has been proposed that specific ratios of di-, to mono-, to unglycosylated PrP^{Sc} molecules can form an ordered oligomer of a specific type which then grows into larger aggregates by reproducing the structure of the original seed. The infectious seed can then determine the glycosylation "signature" of the final oligomer or aggregate (Aguzzi, Heikenwalder and Polymenidou, 2007). While PrP^{C} glycoforms can be individually captured with glycoform –specific mAbs, differentially glycosylated molecules of native PrP^{Sc} could co-immunoprecipitate and the ratio of immunoprecipitated PrP^{Sc} glycoforms from diverse prion strains resembled that observed on denaturing Western blots (Khalili-Shirazi *et al.*, 2005). These findings demonstrate that while there is no intermolecular association between the major PrP glycoforms in native PrP^{C}, glycoforms of PrP^{Sc} are strongly associated together as a complex in a fashion that prevents their differential immunoprecipitation in the native state (Khalili-Shirazi *et al.*, 2005). This is consistent with the notion that complexes of PrP^{Sc} glycoforms are comprised of different proportions of un-, mono- and di-glycosylated PrP^{Sc} and this is characteristic for each prion strain.

1.11.1.2 Resistance to denaturation by chaotropic agents: The Conformation-dependent immunoassay (CDI)

Prion strains can be discriminated by their differential sensitivity to PK digestion and resistance to denaturation by chaotropic agents. Resistance to denaturation by chaotropic agents can determine the conformational stability of a prion strain. The conformation-dependent immunoassay is a sensitive technique that provides a "quantitative" signature of the native conformation of a prion strain based on the degree of resistance to denaturation by guanidinium hydrochloride (GdnHCl) (Safar et al., 1998; Choi, Peden, Gröner, Ironside, & Head, 2010). The assay relies on the effect

of increasing concentrations of GdnHCl, which exposes epitopes in PrP that become hidden during the structural rearrangements that lead to PrP^{Sc} formation. The assay depends on immunodetection with the monoclonal antibody 3F4 and can detect both PK-resistant and PK-sensitive isoforms of PrP. This strain typing technique not only increases our understanding of prion strains but it also establishes that biological properties of prion strains are “enciphered” in the conformation of PrP^{Sc} (Safar *et al.*, 1998). In contrast, the Western Blotting approach is indirect, of relatively low sensitivity and only provides information about PK-resistant PrP isoforms.

Making use of the CDI, Safar et al., provided evidence for different conformations of PrP^{Sc} in eight different prion strains passaged in Syrian hamsters (Safar *et al.*, 1998). Importantly, the strains could be distinguished by CDI but not by Western blotting, as they had similar patterns of protease resistance. Conformational stability was measured by determining the GdnHCl concentration required to denature half of the PrP^{Sc} molecules. When incubation times were plotted as a function of conformational stability, a linear relationship was observed (Legname *et al.*, 2006). It was shown that strains consisting of less stable prions exhibited shorter incubation times, as less stable prions replicate more rapidly and kill the host faster (Legname *et al.*, 2006). For example, the passage of MoSP1 prion strain in FVB mice reduced incubation time, altered the distribution of neuropil vacuolation and drastically reduced the conformational stability of the prions (Legname *et al.*, 2005).

The CDI assay has shown that up to 90% of the PrP^{Sc} present in a sCJD brain is sensitive to proteolytic digestion and would therefore not be resolved by classical procedures such as Western blot (Safar *et al.*, 2005). CDI has also been used to discriminate between sCJD and vCJD, showing that PrP^{Sc} in the most commonly occurring MM1 subtype of sCJD is more resistant to denaturation by GdnHCl than PrP^{Sc} in vCJD (Choi *et al.*, 2010).

1.11.1.3 Resistance to digestion by proteases and differences in sedimentation properties

Even though historically, the molecular diagnosis of prion disease depended on the detection of protease-resistance fragments of PrP^{Sc} following digestion with PK, it is becoming increasingly apparent that a significant fraction of disease-related PrP is sensitive to proteolysis and therefore destroyed during this reaction (Pastrana *et al.*, 2006; Kim *et al.*, 2011; Monaco *et al.*, 2012). Thermolysin, is an extracellular protease that in contrast to Proteinase K, digests PrP^{C} but preserves both PK-sensitive and PK-

resistant isoforms of disease-related PrP. This property of thermolysin has been exploited in the implementation of new methods of prion strain discrimination (Owen *et al.*, 2007a) and prion disease diagnoses (Owen *et al.*, 2007b). There is only a subtle difference in the molecular mass of PK-resistant PrP^{Sc} between ovine BSE and scrapie (Gretzschel et al., 2005; Hill et al., 1998), and such subtle differences are not easily detected by Western blots (Baron, Madec and Calavas, 1999). However, use of thermolysin produced PrP^{Sc} signatures on Western blots that readily distinguished experimental sheep bovine spongiform encephalopathy (BSE) from classical scrapie. In addition to these findings, natural scrapie isolates could be separated into 4 distinct molecular profiles based on deposition and molecular profiles of PrP^{Sc} in defined CNS regions, following digestion with thermolysin (Owen *et al.*, 2007a).

Strain diversity arises from variations in PrP^{Sc} conformations but the physical relationship between the infectious PrP isoform and PrP^{Sc} aggregation state and how this varies between different prion strains remain elusive (Sajnani and Requena, 2012). Using a sedimentation velocity technique and a panel of natural, biologically cloned strains, Tixador et al sought to determine the physical relationship between infectivity and prion protein aggregation state (Tixador *et al.*, 2010). The technique, which allows separation of macromolecular complexes according to size, density and shape, was used to fractionate PrP particles and then characterise the relative levels of infectivity of each fraction using a mouse bioassay. In general, the most infectious component was predominantly associated with slowly sedimenting particles, corresponding to smaller PrP^{Sc} species. Interestingly, the study revealed that for two prion strains, infectivity peaked in a markedly different region of the sedimentation gradient, suggesting that prion infectious particles are subjected to apparent strain-dependent variations which in turn control the biological phenotype and replication dynamics of each strain.

Conformational aspects relating to PrP^{Sc} tertiary structure account for the differential infectivity of some prion strains (Legname et al., 2006, J. Safar et al., 1998) . It has been demonstrated that more dense fractions of PrP^{Sc} aggregates correspond to larger multimers that are PK resistant, whereas intermediate fractions correspond to smaller aggregates that are more sensitive to proteolysis by PK, suggesting that resistance to PK digestion principally depends on PrP^{Sc} quaternary structure i.e size of the polymer complex (Tzaban et al., 2002; Pastrana et al., 2006; Klingeborn, Race, Meade-White, & Chesebro, 2011). Importantly, the Nor98 atypical scrapie prion strain was highly sensitive to PK digestion. Nonetheless, Nor98 also exhibited the highest proportion of faster sedimenting PrP^{Sc} species (PrP^{Sc} assemblies of higher densities)

(Tixador *et al.*, 2010). Therefore, Nor98 findings argue that this strain's high sensitivity to PK digestion is not due to the presence of low size aggregates in this isolate but rather to the strain's tertiary structure, which is unique for each prion strain. These findings argue that PK resistance is associated with the size of PrP aggregates and the tertiary structure of PrP^{Sc}.

Levels of PK-sensitive PrP^{Sc} have been shown to be directly proportional to prion disease incubation time (Safar *et al.*, 1998). However, the Drowsy (DY) prion strain contains a much higher proportion of PK-sensitive PrP^{Sc} than the 263K prion strain, yet it has a significantly longer incubation time (Tanaka *et al.*, 2006). One would therefore expect the PK-sensitive prions in the DY isolate to produce a shorter incubation period. However, it has been shown that the DY prion strain is composed of a higher proportion of large size aggregates which might in turn increase fibre stability and increase incubation time (Tanaka *et al.*, 2006). In agreement with the above findings, studies have shown that smaller sub fibrillary particles of the mammalian prion protein tend to be more fragile, more infectious, and more pathological than larger amyloid fibrils (Silveira *et al.*, 2005).

1.11.2 Discrimination of prion strains *in vivo*

Reliable, *in vivo* methods to discriminate between prion strains are very important, as different species exhibit distinct interspecies transmission properties and different pathogenicity for humans. In support of this statement, vCJD is caused by the transmission of BSE prions to humans. This was evident by the striking similarities in PrP deposition patterns and ratio of glycoforms between BSE- and vCJD-inoculated animals (Will et al., 1996; Lasmézas et al., 2001; Hill et al., 1997b).

In vivo, prion strains can be discriminated by clinical phenotypes, disease incubation times and lesion profiles of affected animals. These phenotypic traits persist upon serial transmission in the same host. Mammalian prion strain diversity was first demonstrated in goats by Pattison and Millson in 1961 (Pattison and Millson, 1961), who observed that there was extremely wide variation in the clinical manifestations of disease in scrapie-affected goats. Depending on the nature of the inoculum, some goats came down with the "scratching syndrome", characterised by areas of broken hair produced by scratching with their horns, while others came down with the "nervous syndrome", characterised by a spectrum of nervous symptoms including hyperexcitability and postural abnormalities. In 1973, Dickinson and colleagues investigated five strains of scrapie, following inoculation in mice (Fraser and Dickinson,

1973). The strains could be distinguished by differences in disease incubation times and histopathological lesion profiles in affected mice. The distribution and intensity of vacuolation was distinct for each prion strain in nine different brain areas.

When passaged under defined conditions of mouse strain, route of inoculation and dose of infectivity, prion strain properties such as incubation period and histopathological lesions are typically stable. Even though the scrapie prion strain 87A was stable when passaged at low dose in C57BL mice, it often suddenly altered its properties during a single passage if high doses are used, always resulting in the same new strain (Bruce and Dickinson, 1987). This novel strain, designated 7D, was characterised by a much shorter incubation period and a markedly different lesion profile than that of 87A (Bruce and Dickinson, 1987). In 87A-infected mice, vacuolation was prominent in the hypothalamus, dorsal medulla and ventral regions of the mesencephalon, leaving all other brain areas unaffected. On the contrary, 7D-infected mice exhibited much more generalised brain pathology. Experiments by Kimberlin and co-workers have shown that the passage of 139A prions through hamsters led to the emergence of a new strain designated 139-H/M (Kimberlin, Cole and Walker, 1987). This new strain produced an incubation period twice as long as that of 139A in affected mice. Work by Bessen and Marsh demonstrated that a source of Transmissible Mink Encephalopathy (TME) resulted in two distinct syndromes, termed hyper (HY) and drowsy (DY), following inoculation in hamsters (Bessen and Marsh, 1992a). The two strains were characterised by marked differences in clinical signs, incubation period, brain titre, brain lesion profile and pathogenicity in mink. For example, the Hyper strain was characterised by clinical signs of hyperaesthesia and cerebellar ataxia whereas the Drowsy strain was characterised by lethargy and absence of hyperexcitability or cerebellar ataxia. Notably, after passage in mink, only the Drowsy strain had retained its pathogenicity whereas Hyper was non-pathogenic in mink.

Neuropathological changes of animal TSEs are defined by grey matter vacuolation of the neuropil, astrogliosis and microglial activation, amyloid deposition and neuronal loss (Jeffrey *et al.*, 2011). There is substantial variation in neuropathological changes induced by different prion strains. For example, many different naturally occurring cases of cattle BSE and experimental SSBP/1 scrapie do not produce significant neuropil and neuronal vacuolation or gliosis (Wells, Wilesmith, & McGill, 1991, Begara-McGorum et al., 2002). It was shown by J Dearmond and colleagues that inoculation of three different strains of mice all of which carry the *Prnp*^{a} gene, with RML, resulted

in different patterns of PrP^{Sc} deposition in each mouse strain (DeArmond *et al.*, 1997). These findings are in agreement with the hypothesis that patterns of PrP^{Sc} accumulation in defined brain regions are not just prion-strain dependent, but they are also heavily influenced by host genetic background. Moreover, modification of PrP^{C} glycosylation by mutagenesis altered the neuroanatomic topology of PrP^{Sc} deposition suggesting that glycosylation can modify the conformation of PrP^{C} and in turn alter its affinity for a particular prion strain (DeArmond *et al.*, 1997). These findings provide an explanation for the selective targeting of neuronal populations in prion diseases.

The mouse-adapted scrapie strains RML, 22L and Me7 can be discriminated by differences in incubation period and histopathological lesion profiles. Strain ME7 was derived from the spleen of scrapie-infected sheep (Zlotnik and Rennie, 1963). RML emerged from a sheep scrapie brain pool which was then passaged to the “Drowsy goat” line (Kimberlin and Walker, 1978). The murine strain Me7 is known to induce severe neuronal loss in the CA1 region of the hippocampus (Cunningham *et al.*, 2003; Jeffrey *et al.*, 2001). It has been shown that 22L mainly targets the cerebellum and RML targets the cortex, hippocampus and brainstem (Karapetyan *et al.*, 2009). In agreement with the fact that 22L targets the cerebellum, Siskova and colleagues demonstrated that for the aforementioned prion strain, even though presynaptic compartments within the hippocampus are more susceptible to chronic neurodegenerative changes than other compartments, in the cerebellum, Purkinje cell dendrites were first to exhibit hallmarks of degeneration (Šišková *et al.*, 2013).

1.11.3 Discrimination of prion strains in cultured cells

Prion strains can be distinguished in cell culture and selective prion susceptibility of cell lines has been reported in a number of studies (Solassol, Crozet, & Lehmann, 2003; Vilette, 2008; Mahal et al., 2007). While some cell lines exhibit broad susceptibility to multiple prion strains, others are susceptible to only one or two strains. The mouse cholinergic septal neuronal cell line SN56 is permissive to the murine strains RML, Me7 and 87V (Baron *et al.*, 2006). The microglial cell line MG20 is susceptible to Me7, RML and the mouse-adapted BSE strain (Iwamaru *et al.*, 2007). Sublines of N2a cells appeared to be susceptible to RML but resisted infection with the Me7 prion strain (Bosque and Prusiner, 2000). Work by Klohn et al., has shown that subcloning of N2a cells can yield both highly RML susceptible and RML resistant subclones (Klohn *et al.*, 2003).

The PC12 rat pheochromocytoma cell line was shown to be much more susceptible to the mouse-adapted scrapie strain 139A than to Me7, yielding significantly higher infectivity titres upon infection with the former prion strain (Rubenstein *et al.*, 1992). Additionally, this cell line was shown to be refractory to infection by the hamster-derived 263K or rat-derived 139R scrapie strains (Rubenstein *et al.*, 1992). In a separate study by Nishida et al., the overexpression of PrP^{C} in the neuroblastoma cell lines GT-1 and N2a, rendered the cells susceptible to the prion strains Chandler, 139A, and 22L but not to 87V and 22A (Nishida *et al.*, 2000). The mouse fibroblast cell line L929 expresses low levels of cellular mouse prion protein, yet it shows broad susceptibility to the strains Me7, 22L and RML but is resistant to infection with the 87V strain (Vorberg *et al.*, 2004).

Mahal and colleagues developed the Cell Panel assay (CPA) which allows discrimination of murine prion strains, based on their ability to infect a panel of cell lines (Mahal et al., 2007, **Figure 1.6**). The CPA has also been used to assess changes in cell tropism of prion strains which can occur when prions are transferred to a different replication environment or in the presence of certain drugs (Mahal et al., 2009; J. Li et al., 2010). The CPA makes use of the Standard Scrapie Cell assay (SCA), a sensitive, accurate and rapid cell-based procedure that employs the highly RML-susceptible N2a-derived PK1 cell line to quantify infectivity based on the immunodetection of PrP^{Sc}-containing cells (Klohn *et al.*, 2003). It was shown that a panel of 4 cell lines (LD9, R33, PK1 and CAD5 cells) show widely different responses to 4 mouse-adapted prion strains (Mahal et al., 2007, **Figure 1.6**). For example, the catecholaminergic neuronal cell line, CAD5, shows broad susceptibility to the prion strains RML, 22L, Me7 and 301C, whereas R33, an N2a-derived cell line, is only susceptible to one of the strains, 22L. All cell lines carry the $Prnp^{a}$ allele and do not show significant differences in the levels of PrP^{C} expression (Mahal *et al.*, 2007).

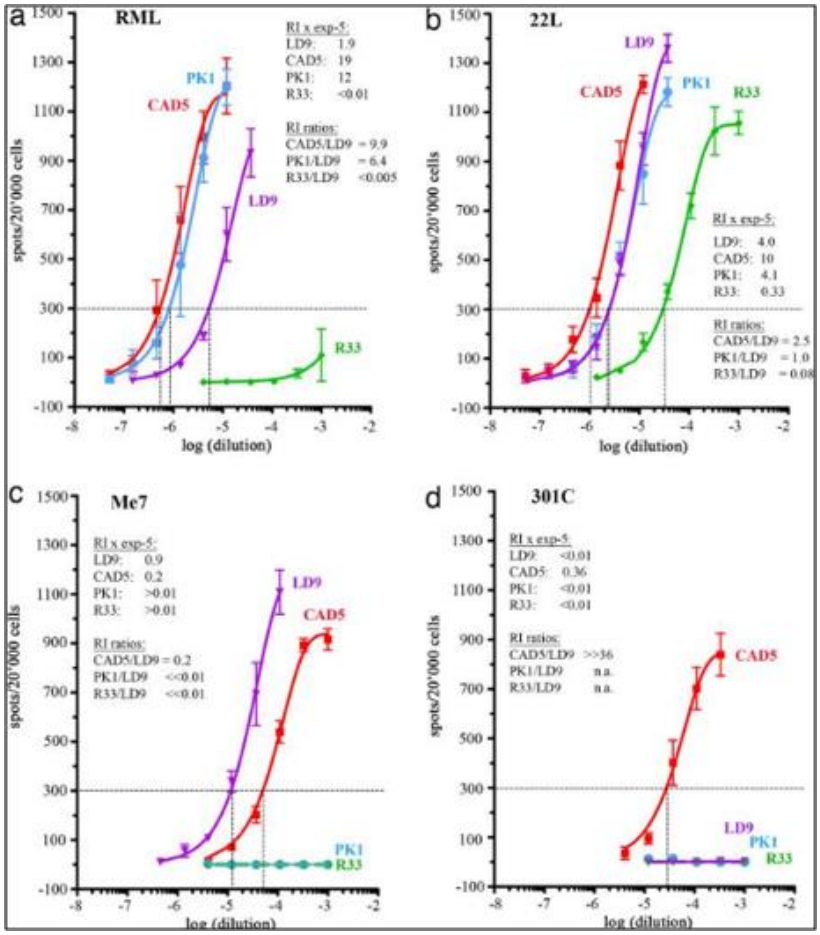

Figure 1.6 Prion strain discrimination in cultured cells: The Cell Panel Assay (C.P.A) (from Mahal et al., 2007) The C.P.A makes use of the Standard Scrapie Cell Assay (SSCA), which quantifies the number of PrP^{Sc}-positive cells after the third passage, following prion infection. Four prion strains (RML, 22L, Me7 and 301C) can be discriminated based on their ability to infect a panel of murine cell lines (CAD5, PK1, LD9, R33). For example, CAD5 cells show broad susceptibility to all four prion strains, R33 is only susceptible to 22L.

A study by James A. Carroll and colleagues demonstrated differential cell tropism of prion strains in the brains of prion-infected mice by showing that different cell types are associated with different prion strains (Carroll *et al.*, 2016). For example, Me7 PrP^{Sc} deposition was prominent in neurones and was not associated with astroglia or oligodendrocytes. On the contrary, 22L PrP^{Sc} deposition was predominantly associated with astroglia with no involvement of neurones. In a separate study, following the infection of primary neuronal cultures with three murine prion strains, it was shown that the neurotoxicity associated with each prion strain was dependent on the neuronal cell type (Hannaoui *et al.*, 2013). For example, the authors observed selective vulnerability of cerebellar cultures to 22L infection, consistent with *in vivo* data (Kim *et al.*, 1987).

The above findings support the notion that susceptibility of a cell line to a specific prion strain cannot be predicted on the basis of its tissue origin or its level of expression of the cellular prion protein alone, pointing towards the involvement of cell line-specific determinants in the ability of these cell lines to propagate prion strains selectively. Interestingly, work by Marbiah et al., has shown that genes that regulate extracellular matrix remodelling and differentiation state, determine susceptibility to prion infection (Marbiah *et al.*, 2014).

1.12 The quasi species model of prions

Prion strains are thought to constitute a dynamic ensemble of diverse molecular assemblies (Collinge & Clarke, 2007; Collinge, 2016, **Figure 1.7**). This phenomenon is analogous to viral quasi species (Domingo, Sheldon and Perales, 2012). The extended definition of viral quasi species, which incorporates general principles of Darwinian evolution is the following: “Viral quasi species are dynamic distributions of non-identical but closely related mutant and recombinant viral genomes subjected to a continuous process of genetic variation, competition and selection, and which act as a unit of selection” (Domingo *et al.*, 2006). In this highly dynamic and mutagenic system, less fit variants are constantly being eliminated. It has long been argued that prion strains can be biologically cloned (Bruce, 1993). This can be achieved by serial passage at limiting dilution of an inoculum such that infection in the next host is established by a single prion. However, it has been observed that some strains are intrinsically unstable and do not “breed true” on passaged in a new host (**Figure 1.7**). Instead, a distinct strain is propagated, and the strain-specific properties are modified by the host in which the isolate was passaged. Such findings have been reported for the hamster Drowsy (DY) strain (Bessen and Marsh, 1994). Additionally, multiple PrP^{Sc} types coexist in the brains of individuals with CJD and are associated with differences in PrP deposition and severity of spongiform changes (Polymenidou et al., 2005; Puoti et al., 1999). Prion isolates show considerable heterogeneity and heat-inactivation studies have demonstrated that thermostable subpopulations exist within a defined strain (Taylor *et al.*, 1998).

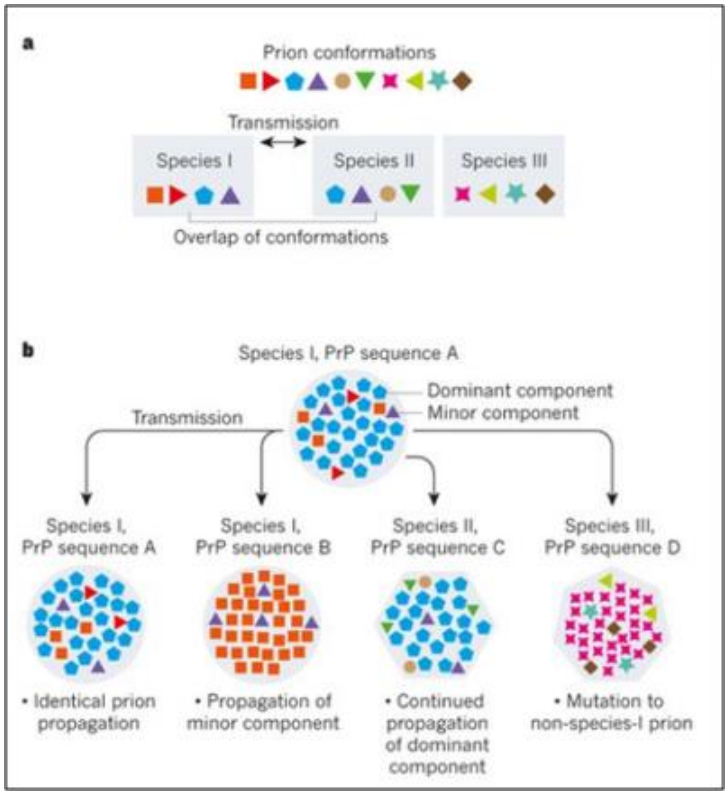

Figure 1.7 Prion strain selection and mutation (from Collinge, 2016) **a.** Transmission barriers can be explained by the degree of overlap between the permissible PrP conformers. Prions can be transmitted between two different species (for example species I and species II) if there is overlap of permissible PrP^{Sc} conformations between the two species involved. **b**. Prion strains are not clonal but constitute an ensemble of PrP^{Sc} conformers. It is possible that strain properties remain unchanged, and the molecular ensemble is maintained during intraspecies transmission (Species I, PrP sequence A). Alternatively, intraspecies transmission of prions from one host to another host that expresses PrP^{C} with a different sequence, might result in the selection and replication of a minor component of the ensemble (Species I, PrP sequence B). Upon transfer to a different species that has a compatible PrP^{C} sequence, strain properties can be maintained, with continued propagation of the dominant component (Species II, PrP sequence C). If there is no compatibility between the permissible PrP conformers between the two species involved, strain mutation results in the generation of a distinct PrP^{Sc} type. Strain mutation provides a mechanism by which transmission barriers are abrogated (Species III, PrP sequence D).

A change in strain properties can also be referred to as “mutation” which can reflect a change in conformation or the biochemical features of the strain but not at the level of protein sequence (Weissmann, 2012). Prion strain mutation does not only occur when prions are transferred between species but also on intraspecies transmission (**Figure 1.7**). A strain with altered characteristics can emerge when the PrP primary sequence of the inoculum differs from that of the recipient host as a result of polymorphism at

codon 129. For example, cases of iatrogenic CJD patients who received human pituitary growth hormone, and were of *PRNP* codon-129 genotype VV or MV, were only associated with a particular subtype of protease-resistant PrP, Type 3, which is characterised by a unique Western blot banding pattern (Collinge *et al.*, 1996). Importantly, prion mutations can also occur on intraspecies transmission where host and donor have identical *Prnp* genes, suggesting that the host genome plays a critical role in influencing prion strain mutation and selection (Lloyd et al., 2004; Asante et al., 2002). It has also been suggested that different cell types within a single host offer different prion replication environments for strain selection. For example, vCJD patients have peripheral pathology and lymphoreticular deposition of PrP^{Sc} while other forms of CJD lack this prominent lymphoreticular phase. In these patients, prion replication in the lymphoreticular system long precedes neurological disease arguing that this long incubation period prior to neuroinvasion is in part, due to the need for selection of a neuroinvasive strain from a pre-existing lymphotropic strain (Collinge and Clarke, 2007). There is indeed evidence for the existence of different PrP^{Sc} types in different peripheral tissues in vCJD, prior to neuroinvasion (Hilton et al., 1998; Hill et al., 1999).

Changes in strain-specific characteristics also occur when prions are transferred from cells to the brain and vice versa (Weissmann *et al.*, 2011). Under a particular selection pressure, such as in the presence of a specific drug, prion populations mutate and evolve, leading to the emergence and selective amplification of drug-resistant variants, while eliminating drug-sensitive variants (Li *et al.*, 2010).

Collectively, these findings can be accommodated within the quasi species model of prions and demonstrate that prion strains are not clonal but instead constitute a dynamic “cloud” of misfolded protein assemblies (**Figure 1.7**). This molecular ensemble is maintained under host selection, consisting of a dominant component, and an array of minor components. Upon transfer to a different replication environment, specific pre-existing variants might be selected and preferentially amplified or might arise as a result of mutation. This in turn leads to the adaptation of a strain to a new host or a new environment (such as replication in the presence of a drug) and enables its survival and spread.

1.13 Prion strain adaptation and transmission barriers

Prion strain adaptation describes the propensity of prions to gradually adapt to a new host, for example when serially transmitted within the same species following interspecies transmission (Baskakov, 2014). This phenomenon leads to the emergence of TSE strains with an expanded host range and increased virulence. When transmitted between species, the transmission efficiency of prions is considerably lower than when transmitted to the same host owing to a species barrier (Pattison, 1966). Inter-species transmission of prions does not usually result in disease, due to incompatibilities in the primary PrP sequence between donor and recipient species (Moore, Vorberg, & Priola, 2005; Hill & Collinge, 2004). However, in some cases, the species barrier can be overcome (Shi *et al.*, 2012). For example, transmission of BSE from cattle to humans led to the emergence of vCJD, the human counterpart of BSE (Andrew F. Hill *et al.*, 1997b). To date, the origin of BSE remains a mystery, but abundant evidence suggests that BSE could have originated from cattle feeding with scrapie-derived material (Wilesmith, Ryan, Hueston, & Hoinville, 1992; Wilesmith, Wells, Cranwell, & Ryan, 1988). It became clear that the degree of amino acid sequence homology between the PrP^{Sc} of the donor and recipient species is not the only parameter that governs transmission barriers. For example, sCJD prions can only be transmitted to transgenic mice that express only human PrP but not to all wild-type mice (Collinge *et al.*, 1995). On the contrary, the transmission of vCJD prions to wild-type mice occurred much more efficiently than vCJD transmission to transgenic mice expressing PrP with characteristics similar to those of BSE prions and in mice expressing human PrP (Collinge *et al.*, 1996). Collectively, these findings are in agreement with the conformational selection model which proposes that the ease of transmission of prions depends on the degree of overlap between the subset of PrP^{Sc} types allowed by PrP^{C} in the host and donor species (Collinge & Clarke, 2007, **Figure 1.7**). Transmission barriers may therefore be explained by the degree of overlap of permissible PrP^{Sc} conformations between the two species involved.

Several examples of prion strain adaptation have been described in experimental models of prion disease. The 263K strain was originally derived from the Drowsy scrapie strain, which was passaged firstly through rats and then several times in hamsters (Kimberlin & Walker, 1977; Walker & Kimberlin, 1978). During the first passage in hamsters, two pools were isolated and following inoculation in mice, two novel strains emerged, 302K and 431K, which were pathogenic to both mice and hamsters. After subsequent passages in hamsters, the hamster-passaged scrapie

from both pools was no longer pathogenic to mice but maintained its pathogenicity for hamsters, demonstrating a gradual change in strain properties that was influenced by the host.

Other studies provided evidence for subclinical prion infection (Race & Chesebro, 1998; Hill et al., 2000; Race, Raines, Raymond, Caughey, & Chesebro, 2001). In subclinical cases of prion infection, prion replication and infectivity are both present, but the host never develops clinical disease on primary passage. For example, inoculation of hamster Sc237 prions into mice does not cause clinical scrapie while PrP^{Sc} deposition was evident in the brain of all inoculated animals (Hill *et al.*, 2000). PrP^{Sc} was readily detectable with a mouse and hamster-specific anti-PrP antibody whereas no PrP^{Sc} could be detected using the hamster specific anti-PrP antibody. Sub-passage from clinically normal mice inoculated with hamster prions resulted in clinical disease in both mice and hamsters, with 100% of the animals succumbing to disease. Importantly, these findings demonstrate that upon passage in mice, novel prion strain(s) were generated that were infectious to both mice and hamsters (Hill *et al.*, 2000). In sharp contrast to the original prion strain, Sc237, the novel strain(s) exhibited an expanded host range. In an independent study, Race and colleagues demonstrated that in mice inoculated with the 263K hamster scrapie, the original hamster scrapie agent persisted without detectable replication of PrP^{Sc} for over 1 year (Race *et al.*, 2001). However, during the second year following post-inoculation, there was both replication of hamster scrapie as well as adaptation of the strain to mice, giving rise to a strain that was virulent to both mice and hamsters.

A change in strain properties can also be referred to as “mutation” which can reflect a change in conformation or the biochemical features of the strain but not at the level of protein sequence (Weissmann, 2012). It has been shown that the host genome plays a crucial role in influencing prion strain mutation and selection. Primary passage of BSE prions in two different inbred lines of mice carrying the same *Prnp* allele, resulted in the emergence of two distinct prion strains, designated MRC1 and MRC2 respectively (Lloyd *et al.*, 2004) . The two strains were markedly different in terms of their glycosylation profile, incubation periods and patterns of PrP immunoreactive deposits and neuronal loss. The strains “bred true” upon subpassage in a single line of inbred mice (SJL), retaining their original characteristics and confirming that two distinct strains had been isolated (Lloyd *et al.*, 2004). Prion strain adaptation and mutation leading to the emergence of novel strains can also arise *de novo* in transgenic mice (Legname *et al.*, 2006). When a transgenic mouse line, Tg9949, was

inoculated with two synthetically-derived prion isolates, MK4977 and MK4985 respectively, the neuropathology was indistinguishable (Legname *et al.*, 2006). However, when the same isolates were used to inoculate FVB and Tg4053 mice, the neuropathologies in FVB and Tg4053 mice inoculated with the MK4977 were markedly different from those found in mice inoculated with the MK4985 isolate. The stark differences in the pattern of vacuolar degeneration, PrP^{Sc} deposition and incubation times in FVB and Tg4053 indicated that MK4977 and MK4985 isolates were distinct.

Adaptation of strains of synthetic origin has been reported in a number of studies. Amyloid fibrils generated *in vitro* from recombinant PrP can initiate prion disease when inoculated in animals such as mice and Syrian hamsters and this phenomenon resembled prion strain adaptation (Makarava et al., 2011; Legname et al., 2004; Makarava et al., 2010; Legname et al., 2005). Preparations of recombinant PrP amyloid fibrils lacked any detectable PrP^{Sc} particles, yet produced transmissible prion diseases when inoculated into wild-type animals (Makarava *et al.*, 2011). When inoculated with recombinant fibrils, only a small fraction of animals developed infectious disease, and two additional serial passages were required for a fully developed clinical disease with a distinct set of symptoms to evolve. The long silent stage to disease that involved two serial passages was accompanied by dramatic changes in neuropathological properties and biochemical features of the PK-resistant material before authentic PrP^{Sc} evolved (Makarava *et al.*, 2011). These findings are consistent with a model whereby prion strain adaptation led to the emergence of a new strain characterised by unique clinical, neuropathological and biochemical features. A new strain originated from a recombinant amyloid structure. A separate study by Legname et al., showed that prion strain adaptation can occur using synthetic mouse prions and that synthetic prions can “encode” strain-specific characteristics (Legname *et al.*, 2005). When inoculated into transgenic Tg9949 mice expressing N-terminally truncated MoPrP (Δ23-88), the mouse synthetic prion strain MoSP1 caused disease after 516 days and 268 days on the first and second passage, respectively. When MoSP1 prions passaged in Tg9949 mice were inoculated into wild-type FVB mice, the incubation time dramatically decreased, and this was accompanied by a dramatic reduction in the conformational stability of the adapted prions. Experiments by Makarava N et al., using a synthetic prion strain, demonstrated that prion strain adaptation can occur upon serial transmission without changing the host species (Makarava *et al.*, 2012). The study provided evidence that PrP^{Sc} properties continued to evolve for as long as four serial passages and the accumulation of PrP^{Sc} in brain regions and peripheral tissues became more rapid and aggressive with serial

transmission. Prion strain adaptation with strains of synthetic origin has also been described by others (Colby et al., 2009; Raymond et al., 2012).

Numerous studies provided evidence for prion strain adaptation in cell culture (Weissmann, 2012; Ghaemmaghami et al., 2011; Li, Browning, Mahal, Oelschlegel, & Weissmann, 2010). As previously mentioned in this section, prions possess the ability to "mutate" despite being devoid of nucleic acid. After repeated passage in mice, the mouse synthetic strain MoSP gradually adopted a shorter incubation time and reduced conformational stability and these changes were accompanied by a structural change (Ghaemmaghami *et al.*, 2011). This was evident by a shift in the molecular mass of the protease-resistant core of MoSP1 from approximately 19 kDa [MoSP1(2)] to 21 kDa [MoSP1(1)]. Challenge of N2a neuroblastoma cells with MoSP1 led to the preferential propagation of MoSP1(1), leading to the disappearance of MoSP1(2) (Ghaemmaghami *et al.*, 2011). Notably, the propagation of MoSP1(1) and MoSP1(2) and therefore their persistence in cells was heavily influenced by the composition of the culture media and the presence of polyamidoamines. These findings are very important as they demonstrate that prions "mutate" via conformational changes, providing a mechanism by which prions evolve and adapt in a particular environment.

Prion strain mutation and adaptation have also been demonstrated in cell-free systems such as Protein Misfolding Cyclic Amplification (PMCA). It has been shown that the hamster-adapted scrapie strain 263K underwent adaptation in an RNA-depleted environment in PMCA, and then readapted to an environment containing RNA (Gonzalez-Montalban *et al.*, 2013). Upon re-adaptation in the presence of RNA, strain 263K gave rise to novel strain, designated $263K^{R+}$. When compared to the original 263K strain, $263K^{R+}$ was characterised by a dramatically lower conformational stability and proteinase K (PK) resistance and by a significantly higher PMCA amplification rate. Further experiments revealed that $263K^{R+}$ was absent in the original 263K brain material but emerged as a result of changes in RNA content (Gonzalez-Montalban *et al.*, 2013). To gain a better understanding of the mechanism of appearance of sporadic prion disease and "spontaneous" protein misfolding, a study has reported spontaneous generation of PrP^{Sc} *in vitro* using PMCA with brain homogenate substrate but in the absence of seeds of *in vivo* generated PrP^{Sc} (Barria *et al.*, 2009). When inoculated in wild-type hamsters, the *de novo* generated PrP^{Sc} prions induced a new disease phenotype with unique clinical, neuropathological and biochemical characteristics.

1.14 Darwinian evolution and selection of prions

Changes in strain properties at the conformational level underlie prion strain adaptation and provide a mechanism by which transmission barriers are overcome (**Figure 1.7**). Prion populations evolve to replicate more rapidly in the new host, which explains the marked reductions in incubation periods after serial transmission within the new host (Bruce & Fraser, 1991; R. H. Kimberlin & Walker, 1977; Hill et al., 2000). Prion populations can acquire mutations when transferred to a different replication environment, such as the transfer of prions from brain to cells (Li et al., 2010; Weissmann et al., 2011). The C.P.A provides a means to examine changes in strain properties that are too subtle to be detected by classical procedures such as Western blotting. As strain properties change, the ability of some prion strains to infect a panel of cell lines, changes (Mahal et al. 2007; J. Li et al., 2010**, Figure 1.6**). Additionally, the extent to which chronic prion infection of PK1 cells is inhibited by swansonine (swa), an inhibitor of a key enzyme in N-linked glycan processing, also reflects changes in the properties of prions (Li *et al.*, 2010). For example, cell-adapted 22L prions, differed from their brain-derived counterparts. In contrast to brain-derived 22L prions, cell-derived 22L prions were unable to infect R33 cells (R33-incompetent) and PK1 cells in the presence of swa, as passage in PK1 cells rendered 22L prions R33-incompetent and swa-sensitive (Li *et al.*, 2010). Importantly, this gradual change in strain properties was reversible, as transfer of the cell-adapted prions back to the brain led to the gradual reacquisition of their original properties and became indistinguishable from the original 22L strain (Li, Mahal, Demczyk, Weissmann, & Florida, 2011; Weissmann et al., 2011).

Importantly, prion strain properties can also change under particular selection pressures, leading to the emergence of mutant variants. It was shown that in some PK1-derived sublines but not in the parental PK1 line, RML prion populations consisting mainly of swa-sensitive variants, contained low levels of swa-resistant variants that were selected for and amplified in the presence of the drug (Oelschlegel and Weissmann, 2013). In a separate study, the introduction of swa in the culture medium led to a sudden decrease in 22L prion propagation in PK1 cells, as the prion population consisted mostly or solely of swa-sensitive variants (Li *et al.*, 2011). However, after a number of successive splits, prion propagation increased, as a swa-resistant prion population emerged, demonstrating adaptation to the new environment (Li *et al.*, 2011). In the presence of swa, pre-existing or newly generated swa-resistant variants with a selective advantage, outcompeted swa-sensitive variants and

dominated the prion population (Li et al., 2010; Weissmann, 2012). Notably, the conformational stability of PrP^{Sc} associated with swa-resistant 22L prions and swa-sensitive 22L prions was shown to be different, suggesting that mutations give rise to conformational changes during prion propagation, and these are responsible for variant-specific properties, such as swa resistance (Mahal *et al.*, 2010).

Acquisition of drug resistance by prions has also been demonstrated by other groups. It was shown that the 2-aminothiozole IND24 prolonged the lives of scrapie-infected mice, but the RML-infected mice treated with IND24 eventually developed neurological dysfunction and died (Berry *et al.*, 2013). The prion strain isolated from IND-24-treated mice, designated RML [IND24], had acquired drug resistance to IND24 and different cell tropism when compared to RML (Berry *et al.*, 2013). The prions remained resistant to high concentrations of IND24 when passaged in CAD5 cells. Importantly, the acquisition of drug resistance was a reversible trait as RML [IND24] prions regained their sensitivity to IND24 in CAD5 cells after a single passage of RML [IND24] in untreated mice (Berry *et al.*, 2013). Similar findings were reported with quinacrine. Continuous administration of quinacrine to RML-infected mice led to a reduction in PrP^{Sc} levels but this reduction was transient and PrP^{Sc} levels were recovered during the course of the treatment (Ghaemmaghami *et al.*, 2009). These findings mirrored *in vitro* data. Upon quinacrine treatment, PrP^{Sc} levels initially decreased in prion-infected neuroblastoma cells but then rapidly recovered after three days of continuous treatment. Continuous administration of quinacrine led to the emergence of a drug-resistant strain *in vitro* and *in vivo,* which was characterised by a lower conformational stability compared to the prions found in brains of untreated mice (Ghaemmaghami *et al.*, 2009).

Prions can also acquire mutations in the absence of selective pressures imposed by drugs. For example, the strain-specific characteristics of the mouse-adapted scrapie strain 79A changed after passage in mice with PrP lacking glycans, but those of Me7 and 301C strains were retained, suggesting that glycosylation modulates prion strain mutation and selection and that strain properties are independent of host PrP glycosylation status for some, but not all TSE strains (Cancellotti *et al.*, 2013). In a similar study, following inoculation of GPI-anchorless mice with three different prion strains, it was shown that for RML and Me7 but not for 22L, prion propagation in these mice had altered their strain properties, and the “mutant” strains were characterised by novel cell tropisms (Mahal *et al.*, 2012). When transferred back to the wild-type brain, Me7 prions recovered their original properties but RML-derived prions did not recover

their original cell tropism even after three passages in wild-type mice and instead gave rise to a novel, stable strain (Mahal *et al.*, 2012). These findings demonstrate that changes in strain properties can be stable, such as in the case of RML, or reversible, such as in the case of Me7. Experiments by Kimberlin and Walker, demonstrated that the transfer of cloned murine 139A prions to hamster and then repeated passages in mouse led to the emergence of a new strain, 139A-H/M (Kimberlin, Cole and Walker, 1987). The emergence of the new strain was attributed to mutation of the 139A agent. When Me7 prions were subjected to the same procedure, they remained unchanged, suggesting that some strains are mutable, while others maintain their original properties on passage to a different host (Kimberlin, Walker and Fraser, 1989). Collectively, these findings demonstrate the plasticity of prion strains, which acquire mutations that in turn enable them to adapt to a particular environment (Mahal *et al.*, 2012).

Changes in strain properties of prions such as the acquisition of drug resistance or changes in cell tropism can be explained by two, not mutually exclusive hypotheses. Variants with altered strain properties can arise by mutation (Li et al., 2010; Collinge, 2016, **Figure 1.7**). In this case, the aforementioned variants were not present in the original population but arose as a result of exposure to a drug or transfer to a new replication environment, such as transfer to a new tissue. An alternative hypothesis is that variants with altered strain properties pre-exist in the prion population and are selected, and preferentially amplified (**Figure 1.7**) under a particular selection regime, such as in the presence of a drug. The latter explanation is consistent with the model that prions form quasi species populations (Collinge and Clarke, 2007). In this case, the mutant variant was present at low levels and in the presence of a selection pressure, for example, the introduction of a drug, this variant was preferentially selected and propagated, becoming the dominant PrP^{Sc} species (Oelschlegel and Weissmann, 2013). It is thought that prions constitute quasi species, with a high mutation rate amongst variants. In this dynamic system, less fit mutants are eliminated, allowing for the selective amplification of variants or sub strains that are better adapted to a particular environment (Collinge & Clarke, 2007; Collinge, 2016). Charles Weissmann and colleagues proposed a model whereby sub-strains within a hypothetical strain A can interconvert readily because they are separated by activation energy barriers that are relatively low (compared to activation energy barriers between strains) and can be overcome in a particular environment (Weissmann, 2012). The transfer of a strain to a new environment such as from cells to the brain, favours the selective amplification of a different sub-strain. With reference to the quasispecies

model of prions, virus and prion populations are similar in that they are both heterogeneous by acquiring mutations and are therefore subject to evolution under a particular selection regime. While in a viral quasispecies mutations occur at the DNA or RNA level, in a prion quasispecies mutations occur at the conformational level of the protein (Li et al., 2010; Weissmann, 2012; Weissmann et al., 2011).

Prion phenomena have also been observed in yeast and filamentous fungi (Wickner, 1994; Maddelein, Dos Reis, Duvezin-Caubet, Coulary-Salin, & Saupe, 2002). It is thought that the induction of the prion state [PSI^{+}] as a result of Sup35 aggregation might be conferring a survival advantage under environmental stress (Tyedmers, Madariaga and Lindquist, 2008). Similar findings were reported for Mod5, a yeast transfer RNA isopentenyltransferase. It was shown that under selective pressure exerted by anti-fungal drugs, the soluble Mod5 switches to an aggregated state allowing yeast cells to develop resistance to antifungal drugs by upregulating ergosterol biosynthesis (Suzuki, Shimazu and Tanaka, 2012).

Yeast prion strains are thought to exist as ensembles of multiple structurally distinct variants, a phenomenon that has also been used to describe mammalian prion strains. It has been reported that Sup35's prion domain, termed NM, can spontaneously form distinct assemblies of infectious amyloid strains (Shorter, 2010). Certain compounds including DAPH-12 and Epigallocatechin gallate (EGCG) selectively inhibit the formation of some yeast prion strains. DAPH-12 induced structural remodelling of Sup35's amyloidogenic core, resulting in morphologically altered aggregates with compromised self-templating activity (Shorter, 2010; Wang et al., 2008). EGCG prevented the reorganisation of oligomers that facilitate the formation of the NM25 strain (Roberts *et al.*, 2009). Additionally, in the presence of EGCG, the yeast prion strain NM4 gave rise to a new strain designated NM4E, which arose as a result of rearrangements in prion folding and was resistant to EGCG (Roberts *et al.*, 2009). This compound could therefore eradicate some strains while facilitating the emergence of new drug-resistant strains.

1.15 Cell models of prion disease

Cell lines permissive to prions have greatly enhanced our knowledge on the molecular and cellular events that control the conversion of PrP^{C} to its abnormal isoform PrP^{Sc} and the cell-to-cell spreading of prions. Additionally, prion cell culture models have shed light on the molecular basis of prion strain-specific replication and on the

mechanisms of neurodegeneration, and have also been used to identify a range of anti-prion molecules.

The uptake of PrP^{Sc} is an early event in prion infection and it is not dependent on the expression of PrP^{C} or on the scrapie strain (Paquet *et al.*, 2007; Greil *et al.*, 2008). Additionally, PrP^{Sc} uptake was observed in nonpermissive cell lines, denoting that uptake is not indicative of a productive prion infection (Paquet *et al.*, 2007; Greil *et al.*, 2008). Pulse-chase experiments in scrapie-infected neuroblastoma cells showed that translocation of PrP^{C} to the plasma membrane precedes the formation of PrP^{Sc} (Caughey and Raymond, 1991). The precise site of prion replication remains elusive but studies in cultured cells showed that PrP^{Sc} is mainly found in vesicles of the endocytic pathway, including early endosomes, recycling endosomes, and lysosomes (Borchelt, Taraboulos and Prusiner, 1992; Marijanovic *et al.*, 2009; Veith *et al.*, 2009). Experiments conducted using cultured cells chronically infected with scrapie showed that PrP^{Sc} synthesis occurs after PrP^{C} transits from the cell surface (Borchelt, Taraboulos and Prusiner, 1992). Importantly, cooling the cultured cells at 18°C, conditions known to inhibit the transport of membrane glycoproteins through the endosomal pathway, reversibly inhibited PrP^{Sc} synthesis, implicating the endocytic pathway in the formation of PrP^{Sc} (Borchelt, Taraboulos and Prusiner, 1992). A study demonstrated that PrP^{C} and PrP^{Sc} co-localise in calveolae-like domains (CLDs) isolated from scrapie-infected neuroblastoma cells (ScN2a) (Vey *et al.*, 1996). Following lysis of ScN2a cells, PrP^{C} and PrP^{Sc} were found concentrated in detergent-insoluble complexes that resembled CLDs. Importantly, the calveolae-specific markers ganglioside GM1 and the GTP-binding protein H-Ras were present in CLDs of ScN2a cells. These findings support the notion that CLDs are likely to be the sub cellular compartment where conversion of PrP^{C} to PrP^{Sc} occurs.

Both lysosomes and autophagosomes have been implicated in the degradation of $PrP^{Sc.}$. In prion-infected cells, trehalose, an activator of autophagy, significantly reduced PrP^{Sc} levels in a dose-and time-dependent manner, and this was achieved through the induction of autophagy (Aguib *et al.*, 2009). In contrast to this finding, the pharmacological inhibition of autophagy neutralised the anti-prion effect of trehalose, providing direct evidence that autophagy is involved in the physiological degradation of cellular PrP^{Sc}. Similar findings were reported by Heiseke et al., who showed that lithium, an activator of autophagy, significantly reduced PrP^{Sc} levels in prion-infected neuronal and non-neuronal cells (Heiseke *et al.*, 2009). In a separate study, the tyrosine kinase inhibitor STI571 was highly effective in the clearance of PrP^{Sc} in prion-infected cells and this effect was mediated through activation of the lysosomal

degradation of PrP^{Sc} (Ertmer *et al.*, 2004). Dendritic cells (DC) of the $CD11c^{+}$ myeloid phenotype can efficiently degrade PrP^{Sc} derived from scrapie-infected hypothalamic neuronal cells (GT1-1 cells) *in vitro* (Luhr *et al.*, 2002). It was later shown that cysteine proteases in $CD11c^{+}$ dendritic cells and scrapie-infected GT1-1 cells mediate the degradation of PrP^{Sc} (Luhr *et al.*, 2004). The degradation of PrP^{Sc} was inhibited by treatment with cysteine protease inhibitors while inhibitors of serine and aspartic proteases and inhibitors of metalloproteases had no effect.

Several groups investigated the cell-to-cell transmission of prions. A study using differentiable SN56 cells demonstrated that PrP^{Sc} associated with microsomes significantly enhanced persistent PrP^{Sc} formation when compared to purified, membrane-free PrP^{Sc}, suggesting that membrane-associated forms of PrP^{Sc} may be the most efficient means of transfer of PrP^{Sc} between cells (Baron *et al.*, 2006). Persistently infected SN56 cells released prions into the cell culture supernatant which in turn, initiated infection in recipient cells. Other studies have also demonstrated that scrapie infectivity is released into the culture medium by scrapie-infected cells thereby initiating prion propagation in recipient cells (Schatzl *et al.*, 1997; Maas *et al.*, 2007). Abundant evidence suggests that the cell-to-cell transmission of prions occurs via exosomes that are released by prion-infected cells. Exosomes are membranous vesicles of endocytic origin secreted upon fusion of multivesicular endosomes with the plasma membrane. Cell supernatant obtained from two prion-infected cell lines and analysed using continuous sucrose density gradient and immunoelectron microscopy, revealed that a fraction of released PrP^{Sc} was associated with membrane vesicles (Fevrier *et al.*, 2004). The morphology and size of these vesicles bearing PrP^{Sc} were reminiscent of exosomes. A different study using prion-infected neuroblastoma cells has shown that PrP^{C} ,PrP^{Sc} and scrapie infectivity co-fractionate with exosomes, suggesting that the exosomal pathway is a potential route exploited by prions in order to be exported and disseminated (Alais *et al.*, 2008). The transfer of PrP^{Sc} via exosomes has also been demonstrated by Vella and colleagues, who showed that N-terminal modification of PrP and selection of distinct PrP glycoforms precede packaging of PrP^{Sc} into exosomes (Vella *et al.*, 2007). In some cell culture models, direct proximity between donor and recipient cells led to a significant increase in infection efficiency, indicating that prion infection depends on cell contact (Kanu *et al.*, 2002). A study by Gousset and colleagues showed that cytoplasmic bridges known as tunnelling nanotubes (TNTs) are involved in the spreading of PrP^{Sc} within neurones in the CNS (Gousset *et al.*, 2009). The authors demonstrated that endogenous PrP^{Sc}

aggregates from prion-infected mouse neuronal CAD cells was transferred to no-infected CAD cells via TNTs. TNTs mediated the transfer of PrP^{Sc} from bone marrow-derived dendritic cells to primary neurons, suggesting that these structures could be involved in the spreading of PrP^{Sc} from the peripheral nervous system (PNS) to the CNS via neuroimmune interactions involving dendritic cells.

Prion-infected cultured cells have been very useful experimental tools to study the cell biology of PrP^{Sc} as well as the mechanisms that control the conversion of PrP^{C} to PrP^{Sc}. Cellular heparan sulphate is a linear polysaccharide consisting of a variably sulphated repeating disaccharide unit (Turnbull, Powell and Guimond, 2001). A large body of evidence has implicated heparan sulphates in the PrP^{C} to PrP^{Sc} conversion process (Wong et al., 2001; Ben-Zaken et al., 2003; Ellett et al., 2015). A study demonstrated that heparan sulphate chains are an essential component of cellular receptors for the internalisation of prions and established prion infection (Horonchik *et al.*, 2005). Mouse neuroblastoma N2a cells, hypothalamic GT1-1 cells and Chinese Hamster Ovary (CHO) cells were able to efficiently internalise purified prion “rods”, but this process was severely compromised by the addition of compounds that inhibit sulphation and by GAG-degrading enzymes. Treatment of prion-infected N2a cells with Heparinase III, which degrades heparan sulphate, led to a drastic reduction in the levels of PrP^{Sc} (Ben-Zaken *et al.*, 2003). Studies have shown that sulphated GAGs including pentosan polysulphate, dextran sulphate and heparin, are potent inhibitors of PrP^{Sc} accumulation in several prion-infected cell lines (Caughey and Raymond, 1993; Gabizon *et al.*, 1993; Birkett *et al.*, 2001). It has been proposed that sulphated glycans competitively inhibit the interaction between endogenous cellular GAGs and PrP^{C} (Gabizon *et al.*, 1993).

Lipid rafts are detergent-resistant microdomains in the plasma membranes of cells that are enriched in sphingolipids and cholesterol (Simons and Ikonen, 1997). In brain and cultured cells, PrP^{C} is incorporated into lipid rafts (Naslavsky *et al.*, 1997; Sunyach *et al.*, 2003; Walmsley, Zeng and Hooper, 2003), as many other GPI-anchored proteins. The accumulation of PrP^{C} and PrP^{Sc} in lipid rafts of prion-infected cells (Vey *et al.*, 1996; Naslavsky *et al.*, 1997), raised the possibility that rafts might be involved in the conversion process. The depletion of cellular cholesterol in scrapie-infected mouse neuroblastoma cells, diminished the formation of PrP^{Sc} and the degradation of PrP^{C}, suggesting that a cholesterol-dependent pathway related to the membranous microdomains where PrP^{C} is found, is involved in the degradation of PrP^{C} and in the formation of PrP^{Sc} (Taraboulos *et al.*, 1995). In an independent study, reducing the

levels of the sphingolipids sphingomyelin (SM) and ganglioside GM1, increased the levels of PrP^{Sc} 3-4-fold in scrapie-infected cells, without altering the production of PrP^{C} (Naslavsky *et al.*, 1999). Incubating the cells with sphingomyelinase which selectively reduces the levels of sphingomyelin, led to an increase in PrP^{Sc} levels. Contrary to these findings, the glycosphingolipid inhibitor 1-phenyl-2-decanoylamino-3-morpholino-1-propanol (PDMP) reduced PrP^{Sc} levels and increased the levels of SM. Therefore, an inverse correlation was observed between SM levels and levels of PrP^{Sc}, whereby decreased SM levels led to enhanced PrP^{Sc} formation in scrapie-infected cells.

1.16 Rationale and Aims: *Towards understanding selective neuronal vulnerability: Establishing an in-vitro model for strain selection*

In neurodegenerative diseases, distinct subpopulations of neurones are targeted, leading to the progressive failure of defined brain regions, a phenomenon known as “selective neuronal vulnerability”. Prion strains cause damage in particular areas of the brain, and this is thought to be associated with distinct clinicopathological phenotypes of prion disease. To date, the molecular mechanisms that link brain tropism of prion strains to diverse clinicopathological phenotypes are unknown.

In contrast to *in vivo* findings, prion toxicity is not readily observed *in vitro*, in most cell lines. However, differences in susceptibility of cell lines to prion strains have been broadly observed. Some cell lines are selectively susceptible to some strains, but not to others, suggesting that susceptibility to a prion strain depends on specific cellular factors. The murine strains Me7 and RML can be discriminated *in vivo* by differences in incubation time and pattern of neuropathology. Intracerebral inoculation of mice with Me7 induced hippocampal neuronal loss whereas RML does not cause degeneration in this brain region. *In vitro*, Me7 and RML can be discriminated by differences in cell tropism. The neuroblastoma cell line PK1 is refractory to Me7 but highly susceptible to RML.

The aim of this PhD project was to isolate a panel of genetically similar cell clones that are differentially susceptible to the prion strains Me7 and RML. Secondly, we investigated whether cells with exclusive susceptibility to any one of the murine prion strains Me7, RML and 22L can be isolated, as these cells will enable the identification of cellular factors that determine susceptibility to distinct prion strains. The final part of this PhD project aimed to examine whether passage of murine prion strains in

susceptible cells alters the biochemical properties and virulence of the prions, respectively.

In this PhD project, I employed single cell cloning, and isolated rare Me7-susceptible cell clones from the Me7-refractory mouse neuroblastoma cell line PK1. Me7-susceptible and Me7-refractory PK1 sublines with equal susceptibility to the prion strains RML and 22L were isolated. Such cell clones provide the means to identify factors associated with susceptibility to Me7. The PK1 cell line has been used extensively in prion research and has been thoroughly characterised by our group to identify genetic factors that confer susceptibility to the mouse prion strain RML, by comparing RML-susceptible and RML-resistant PK1 cell clones (Marbiah et al., 2014).

In the results and discussion chapters, I outline the challenges involved in employing the PME2/PME2-6D8 cell model to identify cells with exclusive susceptibility to a single prion strain. I also employed the murine fibroblast cell line LD9, as an additional cell model, to determine whether cell clones with differential susceptibility to the prion strains Me7 and RML can be isolated. I will outline the development of a high throughput cryopreservation method and the challenges involved in maintaining the susceptibility of cell clones to a specific prion strain.

1.17 Rationale and Aims: *The role of Fkbp proteins in molecular mechanisms of prion propagation*

Human prion diseases can be sporadic, inherited or acquired, but regardless of the aetiology, several genes influence susceptibility, age of onset and duration of disease. While the prion protein gene (*PRNP*) is a major genetic determinant of susceptibility, genome-wide association studies in humans and quantitative trait loci mapping in mice have confirmed that other genes contribute to overall genetic susceptibility.

A microarray gene expression study which correlated the level of mRNA expression, in uninfected brains, from 5 inbred lines of mice, with their respective incubation times identified several potential prion modifier genes including *Fkbp9*. Higher levels of expression of *Fkbp9* correlated with longer incubation times in mice, following prion infection. These findings were validated *in vitro*, using the Scrapie Cell Assay (SCA). Stable knock down (KD) of *Fkbp9* in the mouse neuroblastoma cell line PK1, showed a significant increase prion propagation. Consistent with this observation, overexpression of *Fkbp9* in PK1 cells led to a significant reduction in the number of PrP^{Sc}-positive cells, as quantified using the SCA. A more recent study has shown that

KD of *Fkbp10* in scrapie-infected cells, induced PrP^C degradation, and this subsequently inhibited prion propagation. Fkbp proteins belong in the immunophilin family of proteins and possess peptidylpropyl *cis/trans* isomerase (PPIase) activity which allows them to catalyse the *cis/trans* interconversion of peptide bonds with the amino acid proline (Xaa-Pro). Fkbp proteins also function as chaperones, assisting in protein folding and several lines of evidence suggest that this activity is independent of their PPIase activity.

The aim of this project was to characterise the functional roles of Fkbp family members in prion propagation. In addition to Fkbp9, the project focuses on four genes (*Fkbp1a*, *Fkbp4*, *Fkbp5* and *Fkbp8*) that encode Fkbp12, 52, 51 and 38 proteins respectively. To establish whether Fkbp proteins have a role in prion propagation, I generated a panel of PK1 cell lines by stable gene silencing of *Fkbp* candidate genes and employed the SCA to test whether *Fkbp* KD influences prion propagation. For each *Fkbp* gene, four to eight KD cell lines were generated. For each KD cell line, the level of mRNA expression of *Fkbp* genes relative to control cells was determined, and only cell lines with over 50% reduction in mRNA expression were screened in the SCA. To examine whether an independent gene silencing approach for the examined gene targets recapitulates the results of stable gene silencing, siRNAs were used to transiently knock down *Fkbp* genes in chronically RML-infected PK1 cells (iS7 cells).

For Fkbp9, and other family members that are shown to affect prion propagation, the aim was to conduct further *in vitro* studies to understand the molecular mechanisms by which Fkbp proteins influence prion propagation. The aim was to produce recombinant Fkbp proteins that would have been used in cell-free assays to test whether these proteins affect prion replication and/or modulate the fibrillisation of recombinant PrP^C. Even though I successfully induced the expression of recombinant Fkbp9 and Fkbp52 proteins, no further experiments were carried out for this project.

2 Materials and Methods

2.1 Cell culture

2.1.1 Cell lines used

The N2a subclone N2aPK1 (PK1 for short), is susceptible to the murine prion strain RML and was derived from the N2a parent line (Klohn *et al.*, 2003). The N2a-PK1-S7 cell line was derived from the N2a parent line, is highly susceptible to infection with RML prions, and has been used to generate the chronically infected cell line N2aPK1-IPKS7 (iS7). N2a-R33 cells are also derived from the N2a parent line but the cell line is not susceptible to RML prions (Klohn *et al.*, 2003). The CAD5 cell line is a variant of a CNS catecholaminergic cell line, derived from mouse neuroblastoma tissue (Mahal *et al.*, 2007). LD9 cells were derived from the murine fibroblast cell line L929 (Mahal *et al.*, 2007). The LD9 (3E11)-1E9 cell clone was derived from LD9 cells in two successive subcloning experiments based on its enhanced susceptibility to Me7 when compared to the parental LD9 line.
The primary cell clone for experimental use in this project was the N2a-PK1-PME2 (PME2 for short). The PME2 subclone was isolated in a subcloning experiment conducted by Dr. Peter Kloehn. Following challenge of N2aPK1 clones with Me7, two clones were isolated, designated PME1 and PME2 respectively. The aforementioned cell clones were isolated on the basis of their possible susceptibility to Me7 prions, returning 351 and 378 PrP^{Sc}-positive cells respectively, in the Scrapie Cell Assay (SCA).

The PME2-6D8 subclone was isolated during the subcloning of PME2. This cell clone was susceptible to Me7 in 3 independent SCAs. PME2 (6D8)-X represents subclones isolated during single cell cloning of PME2-6D8.

Most cell lines were cultured in Opti-MEM (Invitrogen) supplemented with 10% (v/v) Heat Inactivated Fetal bovine Serum (FBS, Invitrogen) and 1% (v/v) PenStrep (100 U/ml penicillin, 100 ug/ml streptomycin; Invitrogen) (OFCS). CAD5 cells were cultured in Opti-MEM (Invitrogen) supplemented with 10% (v/v) HyClone Bovine Growth Serum (BGS, GE Healthcare Life Sciences) and 1% (v/v) PenStrep (100 U/ml penicillin, 100 ug/ml streptomycin; Invitrogen) (OBGS). LD9 cells were cultured in Minimum Essential Medium Eagle (MEME, Sigma) supplemented with 10% (v/v) Heat Inactivated Fetal bovine Serum (FBS, Invitrogen) and 1% (v/v) PenStrep (100 U/ml penicillin, 100 ug/ml streptomycin; Invitrogen). Phoenix Ecotropic φ-NX Eco packaging cells (Insight

Biotechnology) were cultured in complete Dulbecco's Modified Eagle Medium (DMEM; Invitrogen) supplemented with 10% (v/v) Heat Inactivated Fetal Bovine Serum (FBS; Invitrogen) and 1% (v/v) PenStrep (100 U/ml penicillin, 100 µg/ml streptomycin; Invitrogen). Cells were cultured at 37°C and 5% CO_2 in a humidified atmosphere in a HERAcell incubator. The culturing conditions of all cell lines are described in **Table 2.1.**

Cell line	Species	Culture conditions	Split method	Split ratio
Fkbp-stably silenced PK1 cell lines	Mouse	OFCS, 37°C 5% CO_2	Pipetting	1:8
N2a-PK1-PME1 (‘PME1’)	Mouse	OFCS, 37°C 5% CO_2	Pipetting	1:6
N2a-PK1-PME2 (‘PME2’)	Mouse	OFCS, 37°C 5% CO_2	Pipetting	1:6
PME2-6D8	Mouse	OFCS, 37°C 5% CO_2	Pipetting	1:6
PME2 (6D8)-X	Mouse	OFCS, 37°C 5% CO2	Pipetting	1:6
N2a-PK1 (‘PK1’)	Mouse	OFCS, 37°C 5% CO_2	Pipetting	1:8
N2a-PK1-S7 (‘S7’)	Mouse	OFCS, 37°C 5% CO_2	Pipetting	1:8
L929-LD9 (‘LD9’)	Mouse	MEME, 37°C 5% CO_2	Requires trypsin	1:12
LD9 (3E11)-1E9	Mouse	MEME, 37°C 5% CO_2	Requires trypsin	1:12
N2a-PK1-R33 (‘R33’)	Mouse	OFCS, 37°C 5% CO_2	Pipetting	1:5
CAD5	Mouse	OBGS, 37°C 5% CO_2	Pipetting	1:7
Phoenix Ecotropic φ-NX Eco packaging cells	Human	DMEM, 37°C 5% CO_2	Pipetting	1:10

Table 2.1 Culturing conditions of cell lines.

2.1.2 Nomenclature of cell clones

Single cell clones were named according to their position in the 96 well plates. For example, the PME2-6D8 clone was derived from the PME2 parental line and was originally found in plate 6, position D8 and the LD9-3E11 sub clone was derived from the LD9 parental line and was originally found in plate 3, position E11.
In the case where cell clones were isolated from an existing cell clone such as PME2-6D8, sister clones were for example designated as PME2 (6D8)-1A12, where 1A12 refers to the position of the PME2-6D8 clone in the 96 well plate.

When cell clones were chronically infected with a mouse-adapted prion strain, the cell clone name was written first, followed by the prion strain, written in square brackets. For example, PME2-1H10 [RML] represents cell clone PME2-1H10 that has been infected with RML prions.

2.1.3 The Scrapie Cell Assay (SCA)

The SCA is a sensitive, accurate and rapid cell-based procedure for quantification of prion infectivity using mouse-adapted prion strains and a panel of recipient murine cell lines mentioned above (Klohn *et al.*, 2003). Multiple splits are used to induce propagation and prion infectivity can be determined through an Enzyme Linked ImmunoSpot Assay (Elispot). The SCA has been fully automated and allows for high throughput determination of infectious titres.
Depending on the assay, cell lines were either exposed to serial dilutions of prion-infected 10% w/v brain homogenate of terminally sick CD-1 mice or to prion-infected or non-infected (mock) cell homogenates for a period of three days. Cell lines were plated out in the appropriate cell density (see **Table 2.2**) in 10-12 wells of 96 well plates (Corning Costar cell culture plates; Sigma Aldrich) 16 hours before exposure to brain or cell homogenates. For *Fkbp*-silenced cell lines, 18 000 cells of each cell line were seeded in 10-12 wells of 96 well plates (Corning Costar cell culture plates; Sigma Aldrich) 24 hours before exposure to RML brain homogenate ($3x10^{-5}$ to $1x10^{-7}$ dilutions in OFCS). During that time the cells were allowed to adhere at normal culture conditions (37°C, 5.0% CO_2). Dilutions of both brain and cell homogenates were made in the normal culture medium for each cell line, as described in **Table 2.1**. For subcloning experiments, the cell clones were split at least twice after isolation, to synchronise cell growth rates, and were seeded at a total volume of 243 µl/well the day before infection. Clones were challenged with 27 µl of brain homogenate. For example, a stock of prion-infected brain homogenate was prepared at $1x10^{-4}$ and 27 µl

of this was added to each well already containing 243 µl of media to make sure that the cells are exposed to a final concentration of $1x10^{-5}$ of prion-infected brain homogenate. For all other assays, the cells were seeded at the appropriate cell density (**Table 2.2**) at a total volume of 200 µl/well the day before infection and infected with 100 µl of brain or cell homogenate. For example, a stock of prion-infected brain or cell homogenate was prepared at 3x (1:5000) and 100 µl of this was added to each well already containing 200 µl of media to make sure that the cells are exposed to a final concentration of 1:5000 of brain or cell homogenate. The infected cells or cell clones were cultured for 3 to 4 weeks. During that period, the cells were split at least twice prior to being assayed for prion infectivity. This was done to ensure that the original inoculum in the supernatant was completely diluted out and that any signal detected originated from PrP^{Sc}-positive cells and was therefore due to *de novo* prion replication. During that time, the cells were split at different ratios, depending on the cell line (**Table 2.2**), then grown to confluence and split again, 3-5 times in succession every 3 or 4 days. Control cells were either treated with normal media or uninfected brain or cell homogenate. The cells were assayed after the second split by the ELISPOT Assay (see **Section 2.1.5**). For most of the assays, including the subcloning experiments, prion infectivity was assayed after the second, third and fourth splits.

Cell line	**Cell density at which the cells were plated out the day before prion infection**	**Split ratio in a 96well format**
PK1	50 000 cells/ml	1/8
PME2-6D8	50 000 cells/ml	1/7
PME2 (6D8)-4H4	50 000 cells/ml	1/7
R33	50 000 cells/ml	1/5
LD9 (3E11)-1E9	10 000 cells/well	1/12
CAD5	50 000 cells/ml	1/7

Table 2.2 Cell densities and split ratios of each cell line/cell clone in the SCA

2.1.4 Generation of chronically infected CAD5 and N2aPK1-PME2 cell clones using the SCEPA (Scrapie Cell Assay in EndPoint Format) Protocol

The SCA can be applied to an endpoint format to increase sensitivity, by performing five to eight rather than three splits because the proportion of infected cells, but not the background, increases continuously with time, once the particles due to the inoculum have been diluted out, resulting in a higher signal-to-noise ratio (Klohn *et al.*, 2003). In the SCEPA protocol, prion-susceptible cells are exposed to a concentration of prions so low that only a few cells per well are infected (Klohn *et al.*, 2003). This does not allow detection by the Elispot assay as the readout is very close to background (5–15 spots/20 000 cells). However, if the prion-challenged cell population is propagated for several generations, uninfected cells gradually become infected by secreted prions, resulting in an increase in the proportion of infected cells. In this project, the SCEPA protocol was used to generate chronically infected cells by challenging susceptible cells with high concentrations of brain homogenate and keeping them in culture for at least six passages.

Heterogeneous populations of CAD5 cells, the PME2 and PME2-6D8 cell clones were seeded in a 96 well format at a cell density of 50 000 cells/ml 24 hours prior to infection. The next day, the medium was removed and replaced with 300 µl of prion inoculum. For RML and Me7, a 10^{-3} dilution of the prion-infected brain homogenate was used for infection whereas for 22L, a 10^{-4} dilution was used for prion infection (**Table 2.3**). The dilutions of prion inocula were made in OFCS medium and OBGS medium for PME2 cells and CAD5 cells respectively. The cells were exposed to the prion-containing inoculum for 4 days, grown to confluence and split 3 times 1:3 every 2 days and three times 1:8 every three days. As a negative control, each cell line was challenged with a 10^{-4} dilution of uninfected CD-1 brain homogenate. With each cell passage, the cells were expanded to several wells of a 96well plate and at the end of the assay, the proportion of prion-infected cells was assessed in the ELISPOT revelation assay (see **Section 2.1.5**).

Once chronically infected cells were generated, 12-24 confluent wells of each of the infected cell populations were pooled together in single 10 cm dishes, respectively. The cells were allowed 3-4 days to grow to confluency and were either plated out at a limiting dilution to isolate single cell clones or assessed directly for the proportion of PrP^{Sc}-positive cells using the SCA.

Cell line	Mouse adapted prion strain used for infection	Dilution factor of prion-infected brain homogenate	Split Ratio
CAD5	RML, 22L and Me7	10^{-3}	1:3 and 1:8
PME1	RML, 22L and Me7	10^{-3} for RML and Me7, 10^{-4} for 22L	1:3 and 1:8
PME2	RML, 22L and Me7	10^{-3} for RML and Me7, 10^{-4} for 22L	1:3 and 1:8
PME2-6D8	Me7	10^{-3}	1:3 and 1:6

Table 2.3 Cell culture conditions for SCEPA

2.1.5 ELISPOT determination of PrP^{Sc}-positive cells

The Elispot protocol assesses the number of PrP^{Sc}-positive cells in a 96-well PVDF membrane plate (Corning) format**.**

For the Elispot Assay, 85 µl of cell suspension or 25 µl of 1/10 diluted cell suspension (used only for chronically infected cells, see **Section 2.1.6**) were transferred to membranes of ELISPOT plates (Multi Screen Immobilon P 96-well Filtration Plates, sterile; Millipore), previously activated with 70% ethanol and washed twice with PBS by suction. For *Fkbp*-silenced cell lines, 25 000 cells were transferred to membranes of ELiSPOT plates. The proportion of PrP^{Sc}-positive cells was identified by an Enzyme-Linked Immunosorbent Assay (ELISA). The cells were resuspended in their normal culture medium and suspended in 100 µl of PBS in each well. Vacuum was applied. After the plates were dried for 1 h at 50°C, Proteinase K (recombinant; Roche; 1:10 000 dilution of 19mg/ml stock) in Lysis buffer (50 mM TrisHCL (pH 8), 150 mM NaCl, 0.5% Sodium Deoxycholate, 0.5% Triton X-100) was added to each well, incubated for 1 h at 37°C, and suctioned off. The wells were washed twice with PBS on vacuum, exposed to 1mM phenylmethylsulfonyl fluoride (PMSF) for 10 minutes at room temperature and suctioned off. Following incubation with 3M guanidinium thiocyanate (GTC,Sigma) in 10 mM Tris HCl (pH8), the wells were washed 7 times with PBS. The wells were exposed to Superblock (ThermoScientific) for 1 h at room temperature and suctioned off. The anti-PrP ICSM18 antibody (D-gen, 0.6µg/ml in 1XTBST/1% milk powder (10X TBST stock was made up of 50 mM Tris, 150 mM NaCl, 0.1% Tween 20)

was added to each well of the plate and incubated for 1 h at room temperature. The supernatant was removed, and the wells were washed 5 times with 1XTBST. The plate was incubated with alkaline phosphatase conjugated anti-IgG1 (Southern Biotechnology Associates; 1:6000 in 1XTBST/1% milk powder) for 1 hour at room temperature and then washed 5 times with TBST. The plates were incubated with alkaline phosphatase conjugate substrate (45 µl/well, prepared as recommended by Biorad) for 30-40 minutes. The plates were then washed twice with water, dried and stored at -20°C. PrP^{Sc}-positive cells were counted using the Bioreader 5000-Eβ (BioSys). Individual wells of a 96 well plate were counted as technical repeats, with the exception of subcloning experiments where one well represented a single clone.

2.1.6 Elispot assay for chronically prion infected cells

In addition to assessing prion propagation after *de novo* prion infection using the SCA, the Elispot assay can also be used to quantify prion propagation in chronically infected cells. A population of chronically infected cells is expected to be uniformly infected, whereas in the SSCA, only a proportion of the cells are expected to have established prion infection. For this reason, chronically infected cells are seeded at a lower cell density on the Elispot plates, to prevent plate reader saturation. Prior to transferring the cells on an Elispot plate, a confluent monolayer of cells was suspended and diluted 1/10 in PBS in a separate 96 well plate. A 25 µl aliquot of the diluted cell suspension was then transferred to the Elispot membrane. The Elispot plate was processed as described above (chapter **2.1.5**).

2.1.7 Trypan Blue (TB) Assay to determine cell number

Because the Scrapie Cell Assay requires determination of the proportion of PrP^{Sc}-positive cells, the total number of cells transferred onto individual wells of the Elispot plate can be estimated using the Trypan Blue Assay. Estimating total cell number is important especially in the case of subcloning experiments, where sister clones of a parental cell line are expected to have variable growth rates. We observed that the standard deviation of TB counts of clones was consistently less than 30% of the mean TB count, suggesting that the variation in doubling rates between clones was acceptable. Additionally, we noticed that in, in many cases, the Elispot readout was higher than the TB readout, giving the false impression than there were more PrP^{Sc}-positive cells than there were cells, which is not possible. For this reason, we concluded that the TB assay is less sensitive than the Elispot assay and only raw data

was taken into account for the preparation of figures and tables. In cases where normalised data was used, this was indicated in the figure legend.

For the TB assays, a confluent monolayer of cells was suspended. For the determination of cell number, a 25 µl aliquot of the 1:10 diluted cell suspension was transferred onto an Elispot plate and vacuum is applied. The plates are dried for at least 1 h at 50°C, until all the wells were dry. Cells seeded on the dried Elispot plates were stained by washing the wells (100 µl/well, a few seconds exposure) with 0.04% Trypan Blue (Sigma) in lysis buffer (50 mM TrisHCL (pH 8), 150 mM NaCl, 0.5% Sodium Deoxycholate, 0.5% Triton X-100). The wells were rinsed twice with PBS under vacuum and dried. Plates were then dried in a hood and read using a Bio-Sys plate reader as described above.

2.1.8 Determining the proportion on PrP^{Sc}-positive cells to the total number of cells

A fixed volume of 85 µl of cell suspension from a suspended, confluent cell monolayer was transferred to the well of an Elispot plate, unless stated otherwise. Certain cell lines are not very susceptible to some prion strains and *de novo* prion infection of cells is not expected to yield a uniformly infected cell population. For this reason, 85µl of an undiluted cell suspension was transferred directly to an Elispot plate. For the determination of cell number, a 25 µl aliquot of the 1:10 diluted cell suspension was transferred to a separate Elispot plate for a TB assay, as stated above. In cases where the number of PrP^{Sc}-positive cells was normalised to the total number of cells in each well, this was indicated in the relevant figure legend. To determine the total number of cells in the well:

(85 µl x 10)/25 =34 as 85 µl of undiluted cell suspension were transferred to an Elispot plate but only 25 µl of 1/10 diluted cell suspension were transferred for a TB assay.

R value gives an estimate of the total number of cells in each well, divided by 10 000 and is given by R= (TB readout x 34)/ 10 000.

To then normalise the number of PrP^{Sc}-positive cells to the total number of cells, the Elispot readout was divided by the R value of each well.

2.1.9 Generation of Stable Gene Silenced N2aPK1 Cells

Confluent φ-NX Eco packaging cells were split 1:5 and transfected the next day with 7 µg pSUPER.retro.puro (pRS) plasmid constructs using Fugene HD (Promega)

transfection reagent. The transfection medium was replaced with fresh DMEM supplemented with 10% (v/v) FBS and 1% Pen/Strep the next day. Moloney murine leukaemia virus (MMLV) pseudotyped retroviral supernatants were collected 48 hours post-transfection and added to 1 × 10^6 N2aPK1 cells in the presence of 8 µg/ml polybrene (Millipore). The OFCS media of N2aPK1 cells was replaced after 6 hours and the cells were placed under puromycin (Sigma) drug selection (4 µg/ml) 48 hours post-infection. Transduced cells were cultured in puromycin selection media for 2 weeks before gene expression analysis for stable knockdown. The cells were maintained in drug selection media.

2.1.10 Transient transcriptional silencing of *Fkbp* genes in RML-chronically infected N2aPK1 cells (iS7 cells)

Confluent iS7 cells in 10 cm dishes were resuspended in fresh OFCS and counted using the Z™ Series Coulter CounterCell and Particle Counter (Beckman Coulter). Readings were taken by mixing 50 µl aliquots of cell suspension into 10 ml 1XPBS in 20 ml plastic cuvettes. An average of 6 readings was taken. The iS7 cell suspension was diluted with OFCS to the required concentration (100 000 cells/ml).

Lyophilized siRNAs were purchased from Integrated DNA Technologies and were reconstituted in RNAse-free duplex buffer. For the preparation of each siRNA treatment, 0.4 µM of reconstituted siRNA and 4.7 µl of the transfection reagent DharmaFECT (0.35DF3) were added to 100 µl serum-free OPTIMEM (Invitrogen), supplemented with 1% Pen/Step (Invitrogen) in a sterile 2 ml screw-top eppendorf tube. Scrambled siRNA (NC1) and a siRNA against PrP^c mRNA were used as a positive control and a negative control respectively. Each solution was mixed, vortexed, centrifuged briefly, and incubated at room temperature for 20 minutes. After the 20-minute period, 2 ml OFCS were added to each siRNA treatment and the tubes were inverted 3-4 times to mix. For the reverse transfections, 150 µl aliquots of each siRNA treatment were transferred to each well of a complete row of a 96-well plate (Corning), using a multichannel pipette. 150 µl iS7 cells (100 000 cells/ml) were then added dropwise to each siRNA mixture already in the well and mixed by circular motion of the pipette tips. The transfected cells were incubated at 37°C and 5% CO_2 for three days. After the three days, the 96 well plates with confluent, transfected iS7 cells were used for automated SCAs and Trypan Blue Assays with the Robot machine.

Briefly, the automated SCAs and TB assays were performed as follows: the supernatant was removed from the wells and replaced with 300µL Serum-free

OPTIMEM. The cells were resuspended. In a new 96-well plate, 270µL 1XPBS were added to each well. 30µL aliquots of the resuspended cells were then diluted into the 270µL PBS (1/10 dilution of the cells). 25µL or 50µL of the diluted cell suspension were transferred to ELISPOT plates. 25µL of the diluted cell suspension were used for the Trypan Blue Assays (described in detail chapter **2.1.7**).

2.2 Quantification of mRNA knockdown

2.2.1 Cell lysis and reverse transcription

Quantitative Reverse Transcription (RT)-PCR was used to determine the level of mRNA expression of candidate *Fkbp* genes in stably silenced PK1 cell lines. 5 000 cells were lysed using TaqMan Gene Expression Cells-to-CT Kit (Ambion, Life Technologies). Briefly, the culture medium was removed from the wells in the 96 well plate and 1X PBS (4°C) was added to each well. After the removal of PBS, the cells were mixed with Lysis solution containing DNase I (1:100 dilution in lysis solution) and the lysis reactions were incubated for five minutes at room temperature. During this step, RNA is released into the lysis solution. Stop solution was added to the lysates to inactivate the lysis reagents. Cell lysates were reverse-transcribed to obtain cDNA using a 20X Reverse Transcription (RT) Enzyme Mix and a 2X RT Buffer. Control no-reverse transcriptase reactions were run in parallel. For each stable cell line, 6 technical qRT PCR reactions were carried out (starting out from 2 biological replicates of cell lysates and 2 biological replicates of RT reactions. Each RT reaction was set up as shown in **Table 2.4.**

Component	Volume (µl)
2X RT Buffer	25
**20X RT Enzyme Mix	2.5
Double Distilled Water	12.5
Cell lysate	10
Final volume of RT reaction	50

Table 2.4 Composition of Reverse Transcription reaction.

**For the No-RT control reaction, RT enzyme mix was replaced with double distilled water.

The RT reaction was run on a PCR Thermal Cycler machine (Bio-Rad) as follows:

Step	Temperature	Duration
Reverse Transcription	37°C	60 min
RT inactivation	95°C	5 min
Hold	4°C	Indefinite

2.2.2 Quantitative Reverse Transcription PCR (qRT-PCR)

The cDNA generated from the reverse transcription was then amplified by qRT-PCR using Fam-labelled TaqMan Gene Expression assays (Life Technologies) in a duplex reaction using Vic-labelled mouse GAPDH (Life Technologies) as an endogenous control on the Applied Biosystems 7500 Fast Real-Time PCR machine. Each qRT-PCR reaction was set up as shown in **Table 2.5**:

Component	Volume (µl)
2X TaqMan Gene Expression Master Mix	10
Fkbp Assay (primers)	1
Mouse GAPDH Assay (TaqMan Life Technologies)	1
Double distilled Water	4
RT reaction (cDNA)	4
Final Volume	20

Table 2.5 Composition of qRT-PCR reaction

The Real Time PCR reaction was carried out as follows:

Step	Temperature	Duration
Uracil DNA glycosylase (UDG) decontamination step	50°C	2 min
Initial denaturation step	95°C	10 min
Cycle of denaturation, annealing, extension (40 cycles)	95°C 60°C	15 sec 1 min

2.3 Preparation of cell lysates and cell homogenates

2.3.1 Preparation of RIPA lysates

Cells were grown to confluence in 10 cm dishes. Cells were washed twice with cold, sterile PBS (Sigma Aldrich). As PK1 cells and PK1-derived cell lines are non-adherent, the pipetteboy speed was lowered for all the washes to avoid detaching cells from the surface of the plate. Residual PBS was removed completely with a P1000 Gilson pipette. For each dish, 1 ml of cold RIPA buffer (50 mM Tris, 150 mM NaCl, 0.5% sodium deoxycholate, 1% Triton (v/v)) was added dropwise to the cells. Prior to lysing the cells, the RIPA buffer was supplemented with benzonase (25-29 U/µl, Merck Millipore) at 2 µl/ml. The cells were incubated in the presence of lysis buffer for 30 minutes in ice water, tilting the dishes every 5 minutes. Using a p1000 Gilson pipette, lysed cells were detached from the surface of the plate and the lysate was collected in an Eppendorf tube. Lysates were centrifuged in a benchtop centrifuge for 10 minutes at 15 000 rpm at 4°C. The pellet was discarded, and the supernatant was transferred to a fresh pre-chilled Eppendorf tube. Lysates were stored at -80°C.

2.3.2 Generation of cell homogenates by ribolysation

2.3.2.1 Non-adherent cells (PK1, PME2)

Table 2.6 provides a description of each cell homogenate. Prion-infected and non-infected cell clones or pools of clones were grown to confluence (90-100% confluent monolayer of cells) in 15 cm tissue culture dishes (Corning). A media change was carried out the day prior to cell homogenisation. For each cell line, the cells in two confluent 15 cm dishes were resuspended in serum-free media (Opti-MEM), Thermofisher) and a total of 20 ml of cell suspension were transferred in a single 50 mL falcon tube. The cells were centrifuged at 500 g for 5 minutes at 4°C. The supernatant was removed, and the cell pellet was re-suspended in 1mL of serum-free media (Opti-MEM) containing Protease Inhibitor Cocktail Mix (100X, Calbiochem) at a 1X final concentration and benzonase (25-29 U/µl, Merck Millipore) at a 4 µl/ml. The resuspended cell pellet was transferred to a skirted 2 mL screw-top Eppendorf tube filled up to approximately 1/3 with Zirconia Ceramic beads. The tubes were transferred to the Ribolyser machine (Precellys 24) and the cells were homogenised at 6500 rpm in two 60 second cycles with 60 seconds resting between the cycles. The cell homogenates were then incubated in ice water for about 5 minutes to allow them to

cool down and for beads to settle at the bottom of the tubes. Homogenates were transferred to clean screw-top Eppendorf tubes and stored at -80°C until needed.

2.3.2.2 Adherent LD9 cells

The ribolysation procedure was the same as the one described above but due to the adherent nature of this cell line, the cells could not be resuspended by pipetting. Instead, the media was removed and the cell monolayer was washed with 20 mL of sterile PBS (Sigma). The cells were incubated in 4.5 ml of Trypsin-EDTA (0.25%, Sigma) for 2 minutes at 37°C. By that time, the cells had detached from the surface of the plate and were re suspended in 10 ml of serum-free Minimum Essential Medium Eagle (Sigma) and then transferred to a 50 ml falcon tube. The rest of the procedure was carried out as outlined above (chapter **2.2.2.1**).

Cell homogenate name	Description
PME2-1H10 [Me7]	Chronically Me7-infected clone derived from single cell cloning of PME2
PME2-1H10 Mock	Non-infected PME2 clone derived from single cell cloning of PME2
iS7 (A6) [RML]	Chronically RML-infected S7 cells
PME2 (6D8) pool [Me7]	Pool of three chronically Me7-infected clones derived from single cell cloning of PME2-6D8
PME2 (6D8) pool [RML]	Pool of three chronically RML-infected clones derived from single cell cloning of PME2-6D8
PME2-6D8 [Me7]	PME2-6D8 cell clone challenged with 10^{-3} dilution of brain Me7 and homogenised after nine passages in cell culture.
PK1 [Me7]	PK1 cells challenged with 10^{-3} dilution of brain Me7 and homogenised after nine passages in cell culture; used as a negative control
LD9 (3E11) pool [Me7]	Pool of five Me7-infected clones derived from single cell cloning of

	LD9-3E11
LD9 (3E11) pool Mock	Pool of two non-infected clones derived from single cell cloning of LD9-3E11

Table 2.6 A description of cell homogenates prepared by ribolysation

2.4 Western blotting

2.4.1 Sample preparation and set up of Proteinase K digestion reactions

2.4.1.1 Cell homogenates

Cell homogenates were prepared as previously described by the method of ribolysation. The total protein concentration in the cell homogenate samples was determined using the bicinchoninic acid assay (BCA assay), as outlined below (chapter **2.4.2**). The appropriate volume was then determined for each homogenate such that 50 µg of total protein for each sample were used for Western blotting. The appropriate volume of cell homogenate was mixed with an equal volume of RIPA buffer (50 mM Tris, 150 mM NaCl, 0.5% sodium deoxycholate, 1% Triton (v/v)) and incubated on ice for 15 minutes. The RIPA buffer was used as a source of detergent to solubilise insoluble protein aggregates. The appropriate volume of PBS was added to each sample to make sure that after the addition of Proteinase K and 4-(2-aminoethyl)benzenesulfonyl fluoride hydrochloride (AEBSF), the total volume of all samples was 100 µl. In non-PK-digested samples, volumes of PK and AEBSF were replaced with PBS. Proteinase K (1 mg/mL, Merck) was diluted 1/10 in PBS to a final concentration of 100 µg/mL and this was used as a stock solution for all subsequent PK digestion reactions (**Table 2.7**). Once the required volume of PK was added to each sample, the samples were incubated at 37°C, 800 rpm on a thermomixer for 30 minutes. After 30 minutes, all samples were placed on ice and the PK digestion reaction was terminated by the addition of AEBSF (stock at 100mM) at a final concentration of 10mM. A total of 100 µl of 2XSDS sample buffer (Invitrogen) containing 4% beta mercapto-ethanol (Sigma) were added to 100 µl of each PK-digested cell homogenate and the samples were boiled for 5 minutes at 100°C on a heat block. Samples were either used for Western blotting straight away or were left to cool down and stored at -80°C. The table shows how the PME2 (6D8) pool [Me7] cell

homogenate was digested with a range of proteinase K concentrations starting from a 100 µg/mL stock solution of PK.

Final concentration of PK in the sample (µg/ml)	Volume of cell homogenate (µl)	Volume of RIPA buffer (µl)	Volume of PBS (µl)	Volume of 100 µg/ml Proteinase K (µl)	Volume of 100mM AEBSF (µl)
0.0	17.2	17.2	65.6	-	-
1.0	17.2	17.2	54.7	0.9	10
3.0	17.2	17.2	52.9	2.7	10
5.5	17.2	17.2	50.7	5.0	10
10	17.2	17.2	46.6	9.0	10
30	17.2	17.2	28.6	27.0	10
55	17.2	17.2	6.10	49.4	10

Table 2.7 Reaction set up of PME2 (6D8) pool [Me7] cell homogenate digested with a range of PK concentrations.

2.4.1.2 Mouse brain homogenates

10% (v/v) RML and Me7 brain homogenates from terminally ill CD-1 mice were used for further processing. Homogenates were diluted 1/10 in non-infected CD-1 homogenate. Samples were treated with 1/100 dilution of benzonase (25-29 U/µl, Merck Millipore) in the presence of Magnesium chloride at a final concentration of 500 µM (stock at 25 mM) and incubated for 10 minutes at 37°C, 800 rpm on a thermomixer. Following benzonase treatment, brain samples were centrifuged at 100 g for 1 minute. The homogenates were digested by adding Proteinase K (Merck, stock at 1 mg/mL) at a final concentration of 40 µg/mL in each sample. The proteinase K digestion reaction was carried out by incubating the samples for 1 hour at 37°C, 800 rpm on a thermomixer. Samples were centrifuged at 16 000 g for 1 minute and the Proteinase K reaction was terminated by the addition of AEBSF at a final concentration of 10mM. PK-treated homogenates were incubated on ice for 10 minutes in the presence of AEBSF. A total of 13.2 µl of 2XSDS sample buffer with 4% beta-mercapto-ethanol were added to 13.2 µl of PK-digested homogenate and boiled

for 5 minutes at 100°C on a heat block. The 1xSDS stock of 1/10 diluted homogenate was made up to 100 µl with 1XSDS sample buffer and stored in aliquots at -80°C. This was used to further dilute the homogenate and use a final 1/100 dilution of homogenate for Western blotting.

2.4.2 Bicinchoninic acid assay (BCA assay) for protein quantification

All cell homogenates that were used for Western clotting and for prion infection of cells during the SCA, were previously quantified for protein content using the BCA assay. As all homogenates were previously prepared in Opti-MEM medium, this was also used to dilute and prepare the bovine serum albumin (BSA) standards. However, as a blank, Opti-MEM medium on its own gave a very high absorbance at 562 nm, making these assay conditions unsuitable for determining the protein concentrations of cell homogenates. Instead, Opti-MEM was diluted 1:50 in RIPA buffer and this was in turn used as a blank and to prepare BSA standards. Cell homogenates were also diluted 1:50 in RIPA buffer and then used for quantification via the BCA (bicinchoninic acid) Assay kit.

2.4.3 Electrophoresis and blotting

For each brain homogenate sample, a final 1/100 diluted homogenate was mixed with 35 µl of 1XSDS sample buffer and all 45 µl were transferred to a 16% Tris/Glycine gel (Thermofisher Scientific) and run alongside SeeBlue Plus 2 ladder (Life Technologies). Electrophoresis was carried out for 80 minutes at 170 V in 1XSDS/tris/glycine running buffer. For each cell homogenate sample, 45 µl (corresponding to 50 µg of protein) were transferred directly onto the gel, without any intermediate dilutions in SDS sample buffer. Empty wells were loaded with 45 µl of 1XSDS sample buffer. The gel was blotted onto polyvinylidene fluoride (PVDF) membrane in 1XTris/glycine blotting buffer at 15 V overnight. The membrane was blocked with 5% milk in PBST (PBS with 0.05% Tween 20 added) for 4 hours and then incubated overnight at 4°C with the ICSM35B (D-Gen Ltd) primary antibody in PBS-T (1:10 000 dilution). Following overnight incubation, the membrane was washed in PBS-T (5x15 minutes) and incubated with the secondary antibody NeutrAvidin-horseradish peroxidase (HRP) (1:7000 in PBS-T) for three hours at 4°C. The membrane was washed again in PBS-T (5x15 minutes), drained and incubated for 3 minutes with 2-3 ml SuperSignal West Pico chemiluminescent substrate (Thermoscientific) for revelation by hand-developing.

2.4.4 Developing

PVDF membranes were placed in a developer cassette between two sheets of clear plastic. In a dark room, a sheet of Kodak Carestream BioMax MR film (Sigma-Aldrich) was put on top of each blot and was exposed for the desired length of time under a red safelight. The film was immersed in Developer solution (Sigma-Aldrich) for approximately 1 min, rinsed with water, immersed in Fixer solution (Sigma-Aldrich) for 1 min, rinsed again, and left to dry for analysis.

2.5 Subcloning and methods of cryopreservation of cell clones

2.5.1 Subcloning

Cells were plated out in limiting dilution (150-300 cells/plate) in 10 cm petri dishes and allowed to grow for a period of 10-12 days. Monoclonal colonies were picked using a p200 pipette and transferred into single wells of a 96 well plate already containing 200 µl of growth medium. To synchronise cell growth rates of individual subclones, cells were split 2-3 times after reaching 80-90% confluence. Cell clones with very fast or very slow growth rates were discarded.

2.5.2 Cryopreservation of subclones

To maintain early characteristics of clones after isolation, two cryopreservation methods were employed.

2.5.2.1 96 well format

Subclones were frozen down in a 96 well format, 2-3 cell passages after they were isolated to preserve early characteristics of clones such as high susceptibility to Me7 or exclusive susceptibility to either RML or 22L. After reaching about 90% confluence, cell clones were re-suspended in 130 µl of culture medium. An equal volume of 16% dimethyl sulfoxide (DMSO) (Sigma) prepared in culture medium was added to each well to give a final concentration of 8% DMSO and was mixed to ensure uniform distribution of the DMSO in cell suspension. For each 96 well plate, the lid was replaced, and the periphery of the plate was sealed with autoclave tape. To provide insulation, plates were wrapped in 5-6 layers of blue roll paper and then placed in Styrofoam boxes. The boxes were placed in a -80°C freezer overnight. After 24 hours, the plates were removed from the Styrofoam boxes, the blue roll was removed, and

the plates were transferred to the vapour phase of liquid nitrogen for long-term storage.

2.5.2.2 Cryovials

Throughout the course of the SCA, replicates of 96 well plates with uninfected subclones were kept in culture and split every 3 or 4 days, after reaching confluence. After analysis of SCA data, desired subclones were expanded sequentially from a single well of a 96 well plate to a 12 well format, to 6 wells and finally to 10 cm petri dishes. After reaching about 90% confluence, cells were cryopreserved in vials with 6% DMSO in culture medium in 500 µl aliquots, and long term stored in the liquid nitrogen.

2.5.3 Resurrection of subclones in a 96 well format

To revive desired subclones in a 96 well format, 96 well plates were placed in a pre-cleaned 37°C water bath, making sure that only the base of each plate is submerged in water. After about 20 minutes, uniform thawing of all wells was achieved, and the cells settled at the bottom of each well. Plates were then cleaned externally with 70% ethanol and placed into a tissue culture Microbiological Safety Cabinet (MSC). The DMSO-containing medium was removed slowly to avoid aspirating any cells. This was then replaced with fresh medium dropwise, using a multichannel pipette, and the cells were placed in a 37°C incubator for 24 hours, after which desired cell clones were split and expanded to more wells of a fresh 96 well plate. Cell clones were split 2-3 times before being used for another assay.

2.6 Immunofluorescence

Chronically prion infected and non-infected control cells were plated into wells of 8 well chamber slides (Thermo Scientific) at a cell density of 50 000 cells/ml. Alternatively, when cell clones were grown in 96 well format, 30-50 µl aliquots of cell suspension from a single confluent well were transferred to a single well of a chamber slide, depending on the cell line. The cells were cultured for 5 to 6 days with a single media change. In some instances, the cells were pre-stained with CellMask Deep Red plasma membrane stain (Thermo Fisher Scientific) prior to fixation. In this case, the culture medium was removed from the chamber slide wells and replaced with 1:1000 diluted CellMask stain in culture medium. The cells were incubated for 10 minutes at

37°C and 5% CO_2 after which the stain was removed, and the cells were washed twice with culture medium. The cells were fixed with 3.7% Formaldehyde in PBS for 11 minutes and washed once with PBS. To remove lipids from the plasma membrane, the cells were incubated for 1 minute with chilled acetone and washed once with PBS. Following treatment with acetone, cells were incubated for 12 minutes with 3.5 M Guanidinium Thiocyanate (GTC) prepared in PBS. The cells were washed at least 5 times with PBS to completely remove GTC before incubation with the primary antibody. Cells were then incubated with the primary antibody 5B2 (SantaCruz Biotechnologies) at 1:500 dilution in a 1:4 dilution of sterile-filtered Superblock (Pierce) solution/PBS (v/v), overnight at 4°C. When dual immunolabelling was carried out, cells were incubated with primary antibodies 5B2 and 6D11 at 1:500 and 1:1000 dilutions respectively. The next day, primary antibodies were removed with a single PBS wash, and the cells were incubated with a 1:10,000 dilution of 4′,6-diamidino-2-phenylindole dihydrochloride (DAPI, 2 mg/ml in DMSO) and the relevant secondary antibodies. When single labelling was carried out with 5B2, the cells were incubated with the secondary antibody AF488 Affinipure goat anti mouse IgG (Jackson Immunoresearch Laboratories) at 1:1000 dilution in the aforementioned dilution of Superblock/PBS. When double labelling was carried out with 5B2 and 6D11, cells were incubated with 1:1000 dilution of secondary antibodies Rhodamine Red-X conjugated minimal X reactive AffiniPure goat anti-mouse IgG1 (Jackson Immunoreserach Laboratories) and AF488 AffiniPure goat anti-mouse IgG2a (Jackson Immunoreserach Laboratories) overnight at 4°C. The next day, cells were washed once with PBS and stored at 4°C in 5% Penicillin/Streptomycin (100X, Thermo Fisher Scientific) in PBS until microscopy. Images were captured and analysed with a Zeiss LSM 710 confocal microscope and Zen imaging software (Carl Zeiss).

2.7 Cloning

2.7.1 Design and Generation of Double -stranded Small Hairpin RNAs (shRNAs)

A total of twenty-eight 19-mer shRNA sequences were designed using Dharmacon's siDESIGN Center tool http://dharmacon.gelifesciences.com/design-center/?redirect=true. The sequences of single-stranded oligonucleotides are shown in **Table 2.8**. The 19-mer shRNAs were selected based on the following parameters: A/U at position 1, no more than 2 T bases at the 3' end, avoiding stretches of 3 A/U and runs of 4 of any base, and at least one shRNA in the untranslated region of each gene.

These were designed to target a 19-base pair (bp) region of the cognate mRNA of each gene including sense and anti-sense strands connected by a 9-nucleotide spacer region (5′-TTCAAGAGA-3′). The pSUPER.retro.puro vector uses the polymerase III H1-RNA gene promoter to drive the expression of a 60-nucleotide, single-stranded RNA molecule which folds into a hairpin structure, using the following sequences: top strand-5′GATCCCC target sequence (sense) TTCAAGAGA target sequence (antisense) TTTTTA 3′ and bottom strand-5′AGCTTAAAAA target sequence (sense) TCTCTTGAA target sequence (antisense) GGG 3′. Post-transcriptional processing of the hairpin structure yields a functional siRNA molecule. Complementary single-stranded oligonucleotides were annealed in annealing buffer (1mM Tris-HCl pH8, 0.1mM EDTA, 5mM NaCl). The annealing reaction was assembled by mixing 1 µl of each oligo (forward and reverse, both at a final concentration of 500 nM) with 48 µl annealing buffer. The mixture was heated to 95°C for 2 minutes and cooled slowly to room temperature. Double stranded ShRNA oligonucleotides were cloned into the pSUPER.retro.puro (pRS) plasmid vector (Oligoengine).

Oligonucleotide name	**Sequence 5'→3'**
Fkbp1a -1F	GATCCCCGCTTGAAGATGGAAAGAAATTCAAGAGATTT CTTTCCATCTTCAA GCTTTTTA
Fkbp1a -1R	AGCTTAAAAAGCTTGAAGATGGAAAGAAATCTCTTGAA TTTCTTTCCATCTT CAAGCGGG
Fkbp1a-2F	GATCCCCAGTGATTTGGTGAGAGAAATTCAAGAGATTT CTCTCACCAAATC ACTTTTTTA
Fkbp1a-2R	AGCTTAAAAAAGTGATTTGGTGAGAGAAATCTCTTGAA TTTCTCTCACCAA ATCACTGGG
Fkbp1a-3F	GATCCCCTGAGGGAGGTCCTGTTAAATTCAAGAGATTT AACAGGACCTCCC TCATTTTTA
Fkbp1a-3R	AGCTTAAAAATGAGGGAGGTCCTGTTAAATCTCTTGAA TTTAACAGGACCT CCCTCAGGG
Fkbp1a-4F	GATCCCCACTGAAAGCCCTACCCAAATTCAAGAGATTT GGGTAGGGCTTT CAGTTTTTTA
Fkbp1a-4R	AGCTTAAAAAACTGAAAGCCCTACCCAAATCTCTTGAA TTTGGGTAGGGCT TTCAGTGGG
Fkbp1a-5F	GATCCCCGTAGTGATTTGGTGAGAGATTCAAGAGATCT CTCACCAAATCA CTACTTTTTA

Fkbp1a-5R	AGCTTAAAAAGTAGTGATTTGGTGAGAGATCTCTTGAA TCTCTCACCAAATC ACTACGGG
Fkbp1a-6F	GATCCCCACTGAAAGCCCTACCCAAATTCAAGAGATTT GGGTAGGGCTTTCA GTTTTTTA
Fkbp1a-6R	AGCTTAAAAAACTGAAAGCCCTACCCAAATCTCTTGAA TTTGGGTAGGGCTTT CAGTGGG
Fkbp1a-7F	GATCCCCGATCTAAGTTTCCAATGAATTCAAGAGATTC ATTGGAAACTTAGAT CTTTTTA
Fkbp1a-7R	AGCTTAAAAAGATCTAAGTTTCCAATGAATCTCTTGAAT TCATTGGAAACTT AGATCGGG
Fkbp1a-8F	GATCCCCGATCCGAGGCTGGGAGGAATTCAAGAGATT CCTCCCAGCCTCGGA TCTTTTTA
Fkbp1a-8R	AGCTTAAAAAGATCCGAGGCTGGGAGGAATCTCTTGA ATTCCTCCCAGCC TCGGATCGGG
Fkbp4-1F	GATCCCCAAGAGAAGGCTGAGGGTGATTCAAGAGATC ACCCTCAGCCTTCTC TTTTTTTA
Fkbp4-1R	AGCTTAAAAAAAGAGAAGGCTGAGGGTGATCTCTTGAA TCACCCTCAGCCT TCTCTTGGG
Fkbp4-2F	GATCCCCAAGCCAGGGTGGAGAAGAATTCAAGAGATT CTTCTCCACCCTGG CTTTTTTTA
Fkbp4-2R	AGCTTAAAAAAAGCCAGGGTGGAGAAGAATCTCTTGAA TTCTTCTCCAC CCTGGCTTGGG
Fkbp4-3F	GATCCCCAGATGAAGGGTGAGCGGAATTCAAGAGATT CCGCTCACCCTTC ATCTTTTTTA
Fkbp4-3R	AGCTTAAAAAAGATGAAGGGTGAGCGGAATCTCTTGAA TTCCGCTCACCCT TCATCTGGG
Fkbp4-4F	GATCCCCAGAGCAACATAGTGAAAGATTCAAGAGATCT TTCACTATGTTGC TCTTTTTTA
Fkbp4-4R	AGCTTAAAAAAGAGCAACATAGTGAAAGATCTCTTGAA TCTTTCACTATG TTGCTCTGGG
Fkbp5-1F	GATCCCCAGAAGGAGCCGCTGGCAAATTCAAGAGATT TGCCAGCGGCTC CTTCTTTTTTA
Fkbp5-1R	AGCTTAAAAAAGAAGGAGCCGCTGGCAAATCTCTTGAA TTTGCCAGCGGCT CCTTCTGGG
Fkbp5-2F	GATCCCCTGGTGAAGATGCAGAGAGATTCAAGAGATC

	TCTCTGCATCTTCA CCATTTTTA
Fkbp5-2R	AGCTTAAAAATGGTGAAGATGCAGAGAGATCTCTTGAA TCTCTCTGCATCTT CACCAGGG
Fkbp5-3F	GATCCCCGAGAAAGGCTTGTACAGAATTCAAGAGATTC TGTACAAGCCTTT CTCTTTTTA
Fkbp5-3R	AGCTTAAAAAGAGAAAGGCTTGTACAGAATCTCTTGAA TTCTGTACAAGCCT TTCTCGGG
Fkbp5-4F	GATCCCCAAACTTGGGCATTGAATTATTCAAGAGATAA TTCAATGCCCAAGT TTTTTTTA
Fkbp5-4R	AGCTTAAAAAAAACTTGGGCATTGAATTATCTCTTGAAT AATTCAATGCCCAA GTTTGGG
Fkbp5-5F	GATCCCCGGACAGTGCCAATGAGAAATTCAAGAGATTT CTCATTGGCACTGT CCTTTTTA
Fkbp5-5R	AGCTTAAAAAGGACAGTGCCAATGAGAAATCTCTTGAA TTTCTCATTGGCACT GTCCGGG
Fkbp5-6F	GATCCCCGGATGTTGTCAGATGGAAATTCAAGAGATTT CCATCTGACAACA TCCTTTTTA
Fkbp5-6R	AGCTTAAAAAGGATGTTGTCAGATGGAAATCTCTTGAA TTTCCATCTGAC AACATCCGGG
Fkbp5-7F	GATCCCCGAAAGACAGAGGAGTATTATTCAAGAGATAA TACTCCTCTGTCTTT CTTTTTA
Fkbp5-7R	AGCTTAAAAAGAAAGACAGAGGAGTATTATCTCTTGAA TAATACTCCTCTG TCTTTCGGG
Fkbp5-8F	GATCCCCTTACAAAGGACAATGACTATTCAAGAGATAG TCATTGTCCTTTGTA ATTTTTA
Fkbp5-8R	AGCTTAAAAATTACAAAGGACAATGACTATCTCTTGAAT AGTCATTGTCCTT TGTAAGGG
Fkbp8-1F	GATCCCCTCTCAAAGCTGGTAAAGAATTCAAGAGATTC TTTACCAGCTTTGAG ATTTTTA
Fkbp8-1R	AGCTTAAAAATCTCAAAGCTGGTAAAGAATCTCTTGAAT TCTTTACCAGCTT TGAGAGGG
Fkbp8-2F	GATCCCCTCAAATAACCCAAGAAGCATTCAAGAGATGC TTCTTGGGTTATTTG ATTTTTA
Fkbp8-2R	AGCTTAAAAATCAAATAACCCAAGAAGCATCTCTTGAAT GCTTCTTGGGTT ATTTGAGGG

Fkbp8-3F	GATCCCCATGCAGAGGAGGAAGATGATTCAAGAGATC ATCTTCCTCCTCTGC ATTTTTTA
Fkbp8-3R	AGCTTAAAAAATGCAGAGGAGGAAGATGATCTCTTGAA TCATCTTCCTCCTC TGCATGGG
Fkbp8-4F	GATCCCCGAGCAAGGATTGAGGGTCATTCAAGAGATG ACCCTCAATCCTTG CTCTTTTTA
Fkbp8-4R	AGCTTAAAAAGAGCAAGGATTGAGGGTCATCTCTTGAA TGACCCTCAATC CTTGCTCGGG
Fkbp8-5F	GATCCCCGGACATGACTTGTGAGGAGTTCAAGAGACT CCTCACAAGTCATG TCCTTTTTA
Fkbp8-5R	AGCTTAAAAAGGACATGACTTGTGAGGAGTCTCTTGAA CTCCTCACAAG TCATGTCCGGG
Fkbp8-6F	GATCCCCGTGAATATAGTGAGGCCATTTCAAGAGAATG GCCTCACTATATTC ACTTTTTA
Fkbp8-6R	AGCTTAAAAAGTGAATATAGTGAGGCCATTCTCTTGAA ATGGCCTCACTATAT TCACGGG
Fkbp8-7F	GATCCCCAGGTCAAGTGTCTGAACAATTCAAGAGATTG TTCAGACACTTGACC TTTTTTA
Fkbp8-7R	AGCTTAAAAAAGGTCAAGTGTCTGAACAATCTCTTGAA TTGTTCAGACACTTG ACCTGGG
Fkbp8-8F	GATCCCCGGTCAAATAACCCAAGAAGTTCAAGAGACTT CTTGGGTTATTTGA CCTTTTTA
Fkbp8-8R	AGCTTAAAAAGGTCAAATAACCCAAGAAGTCTCTTGAA CTTCTTGGGTTA TTTGACCGGG

Table 2.8 shRNA oligonucleotides for cloning into pSUPER.retro.puro *BglII* or *HindIII* restriction site sequence; spacer nucleotides. The suffixes F and R denote forward and reverse shRNAs respectively. These are annealed prior to cloning to produce double stranded shRNAs. For example, oligos Fkbp1a-1F and Fkbp1a-1F are annealed together and represent one shRNA targeting construct for *Fkbp1a*.

2.7.2 Restriction Enzyme Digests

The purified and double digested (with *NcoI* and *XhoI*) pET-23d(+) plasmid was a kind gift from Professor Parmjit Jat. The pRS plasmid DNA (12 µg) was digested with *BglII* and *HindIII* (Roche) restriction enzymes for 3 hours in a 37°C water bath. The restriction enzyme digest was set up as follows: Restriction enzyme buffer B (10X;

Roche) at a 1X final concentration, pRS plasmid vector (12 µg), 2 µl of *HindIII* (Roche) and 2 µl of *BglII* (Roche), made up to 50 µl with double distilled water.
The pMA-RQ-*Fkbp9* construct was double digested as follows: a restriction digest reaction was set up with 3 µg of pMA-RQ-*Fkbp9* plasmid DNA, 2 µl *NcoI* (New England Biolabs; NEB), 2 µl *XhoI* (NEB), 1X NEBuffer 3.1 (NEB) (stock at 10X), and made up to 50 µl with double distilled water. The reaction was incubated for 1.5 hours in a 37°C water bath. The procedure was repeated for the pMA-RQ-*Fkbp4* construct.

For the purpose of diagnostic restriction enzyme digests following colony PCR reactions, a total of 6 restriction digest reactions were set up as follows: 0.5 µl *NcoI* (NEB), 0.5 µl *XhoI* (NEB), 1X NEBuffer 3.1 (NEB), 240 ng of plasmid DNA, made up to 10 µl with double distilled water and incubated for 1 hour in a 37°C water bath. These were carried out to confirm the presence of the 1.7 kb and 1.4 kb DNA fragments (corresponding to *Fkbp9* and *Fkbp4* respectively) in the pET-23d(+) expression vector.

The cleaned *Fkbp9* PCR product was double digested as follows: 3 µg of clean *Fkbp9* DNA, 2 µl *NcoI* (NEB), 2 µl *XhoI* (NEB), and 1X NEB3.1 Enzyme Buffer (NEB), made up to 50 µl with double distilled water. The reaction was incubated for 1.5 hours in a 37°C set water bath.

2.7.3 Agarose Gel Electrophoresis

All agarose gels were made with agarose powder (Invitrogen) in 1X Tris-Borate-EDTA (TBE) buffer (10X TBE buffer stock; 1 M Tris, 0.9 M Boric Acid, 0.01 M EDTA, pH 8.4; Invitrogen). The solution was boiled in a microwave for 1-2 minutes and then cooled for some time before the addition of 2 µl Ethidium Bromide (Sigma Aldrich). In all agarose gels, HyperLadder I (Bioline) was used as a molecular weight marker to resolve products >1.0 kb. DNA fragments on agarose gels were run in gel electrophoresis tanks loaded with 1X TBE buffer. All samples containing DNA were first mixed with 5Xloading dye (Bioline) to a final concentration of 1X prior to electrophoresis. All gels were visualized on a UV Trans-Illuminator Gel Doc imaging system (Biorad).
The 50 µl pRS restriction digest reaction was mixed with 5X loading dye (Bioline) and the mixture was run on a 0.8% (w/v) agarose gel. The double digested pMA-RQ-*Fkbp9* and pMA-RQ-*Fkbp4* DNA constructs were run on a 1% (w/v) agarose gel. Gel electrophoresis was carried out for 2 hours at 120 Volts. After visualisation, the double digested pRS plasmid DNA and the *Fkbp4* and *Fkbp9* gene constructs were excised from the gel with a scalpel for gel purification.

Individual PCR reactions of colony PCR (see section **2.7.11**) were run on a 1% agarose gel and gel electrophoresis was carried out for 20 minutes at a constant voltage of 100 Volts. Positive clones (i.e containing the *Fkbp9* and *Fkbp4* inserts respectively) were identified following gel visualisation to confirm the presence of the insert in each of the positive clones; the colony suspension of each clone in the master plate was used to make up 10 ml overnight cultures containing ampicillin (Sigma) at 50 µg/ml. Plasmid DNA was extracted and purified using the QIAprep Spin Miniprep Kit (Qiagen) according to the manufacturer's protocol. A total of 6 restriction digest reactions were set as described in section **2.7.2**. The reactions were run on a 1% agarose gel and gel electrophoresis was carried out for 1.5 hours 120 Volts. Gel visualization confirmed the presence of 1.7 kb and 1.4 kb fragments (corresponding to the *Fkbp9* and *Fkbp4* genes respectively) in each restriction digest.

Five microliters of the *Fkbp9* PCR product were electrophoresed for 1 hour at 190 Volts on a 1% agarose gel. The presence of a 1.7 kb fragment following gel visualisation confirmed the success of the PCR reaction and the generation of an *Fkbp9* gene fragment lacking the endoplasmic reticulum (ER) signal and ER retention motifs respectively.

2.7.4 Plasmid DNA Isolation

Bacterial cultures in 50 ml falcon tubes were centrifuged at 5000 rpm in a floor centrifuge (Beckman Coulter) and the medium was removed. DNA was extracted using the QIAgen Spin Miniprep Kit according to the manufacturer's protocol. The pelleted bacterial cells were resuspended in 250 µl Buffer P1 and transferred to a microcentrifuge tube. 250 µl buffer P2 was added and mixed thoroughly by inverting the tube 4-6 times to lyse the cells. The lysis reaction was allowed to proceed for 5 minutes before neutralising the reaction with 350 µl Buffer N3. The solution was mixed thoroughly by inverting the tube 4-6 times. The solution was centrifuged for 10 minutes at 13 000 rpm in a bench-top microcentrifuge (Thermo Scientific). The white pellet was discarded, and the supernatant was applied to the QIAprep 2.0 spin column by pipetting. This was centrifuged for one minute and the flow-through was discarded. The QIAprep 2.0 spin column was washed with 750 µl Buffer PE. Centrifugation was carried out for one minute, the flow-through was discarded, and the column was centrifuged for an additional minute to remove residual wash buffer. The QIAprep 2.0 spin column was placed in a clean 1.5mL microcentrifuge tube. For the elution of DNA, 50 µl Buffer EB (10 mM Tris.Cl, pH8.5) were added to the center of each QIAprep 2.0

spin column; the column was let to stand for one minute and then centrifuged for an additional minute.

2.7.5 Transformations

2.7.5.1 DH5α

DH5α bacterial cells were transformed with the shRNA constructs generated for the knock down of candidate *Fkbp* genes. An aliquot of NEB 5-alpha Competent *E. coli* cells (NEB) was used for each ligation reaction and was thawed on ice for 10 minutes. The DNA ligation reaction (10 µl) was added to the cells and mixed by flicking the tube 4-5 times. The mixtures were incubated on ice for one hour. Heat shock was performed at 42°C in a water bath for exactly 30 seconds. The mixtures were then incubated on ice for 5 minutes. A total of 850 µl room temperature SOC medium was transferred to each mixture and these were then incubated in an incubator shaker at 37°C, 250 rpm. The tubes were centrifuged for one minute at 15 000 rpm to remove 750 µl SOC medium and concentrate the cells. Using a pipette, the cell pellets were resuspended in the remaining SOC medium. 100 µl of each transformed cell suspension was transferred onto a 37°C pre-warmed LB agar selection plate (containing ampicillin at 100 µg/ml) and spread using a sterile spreader. The last step was carried out next to a flame. The plates were inverted to prevent condensation (which may contaminate the colonies) and incubated overnight at 37°C to allow for colony formation.

2.7.5.2 BL21 (DE3)

A vial of competent BL21 (DE3) cells (Agilent Technologies) was thawed on ice. The cells were mixed gently with a pipette and an aliquot of 100 µl was transferred to a second pre-chilled microcentrifuge tube on ice. Beta mercapto-ethanol (provided with the kit) at a final concentration of 25 mM was added to each tube containing the competent cells and the tubes were swirled gently. Individual transformation reactions were incubated on ice for 10 minutes and swirled every 2 minutes. 30 ng (2 µl) pET-23d(+)-*Fkbp9* and pET-23d(+)-*Fkbp4* plasmid DNA were added to each tube of competent cells separately. The reactions were incubated on ice for 30 minutes. Each transformation was then heat-pulsed for exactly 45 seconds in a 42°C water bath and the reactions were then incubated on ice for 2 minutes. A total of 900 µl preheated (42°C) SOC medium were added to each transformation reaction and these were

incubated at 37°C for one hour with shaking at 250 rpm. Using a sterile spreader, 100-200 µl aliquots of the reactions containing the transformants were spread onto pre-warmed (37°C) LB agar plates containing carbenicillin at 300 µg/ml. The plates were incubated inverted overnight at 37°C to allow for colony formation.

2.7.6 Ligation Reactions

Ligation reactions of double stranded shRNAs into the pRS plasmid were set up as follows: each reaction was made up of 9 µL ligation mix (1XT4 DNA Ligase reaction buffer (NEB), T4 DNA Ligase enzyme (400 000U/mL; NEB), 6 ng double digested pRS plasmid DNA, and nuclease-free water) and 1 µL of each double stranded oligonucleotide. The reactions were incubated at 16°C overnight on a PCR thermal cycler machine (Biorad). Individual ligation reactions were transformed in competent DH5α *E. coli* cells (New England Biolabs) as described in section **2.7.5.**

Ligation of *Fkbp4* and *Fkbp9* genes into the pET-23d (+) plasmid respectively, were carried out as follows: 100 ng *Fkbp9* insert (generated from the PCR reaction), 100 ng pET-23d (+) plasmid DNA previously digested with *XhoI* and *NcoI*, 1X T4 Ligase Buffer (NEB) (stock at 10X), and 1 µl T4 DNA ligase (NEB). The reaction was made up to a final volume of 10 µl with double distilled water and incubated overnight at 15°C on a PCR Thermal Cycler machine (Biorad). The same reaction set up was used for the ligation of the *Fkbp4* gene into the pET-23d (+) plasmid.

2.7.7 DNA Gel Extraction

Gel purification was carried out using the QIAquick Gel Extraction Kit (Qiagen) according to the manufacturer's protocol. Briefly, the gel slice was weighed in a microcentrifuge tube and three volumes of Buffer QG were added to one volume gel. This was incubated at 50°C on a heat block for 10 minutes until the gel slice was completely dissolved. One gel volume of isopropanol (Fisher Chemicals; >99.5%) was added to the sample and mixed. The mixture was transferred to a 2 ml spin column fitted in a collection tube and centrifuged for one minute. For washing, 750 µl buffer PE was added to the spin column and this was centrifuged for one minute. The flow-through was discarded and the spin column was placed back in the collection tube and centrifuged for an additional minute to remove residual buffer. The column was placed in a clean microcentrifuge tube and for DNA elution, 30 µl of Buffer EB (10 mM Tris.Cl pH 8.5) was added to the centre of the column membrane. The column was left to stand for one minute and then centrifuged for one minute to elute the DNA.

2.7.8 Preparation of LB Broth and LB Agar

Luria Broth (Miller; LB) powder (Sigma) was used for the preparation of 2.5% LB solution. The solution was made by dissolving the powder in double distilled water and autoclaving for 30 minutes in a benchtop autoclave (Prestige Medical).
LB Agar (Miller) powder (Sigma) was used to make LB agar base for the preparation of LB bacterial plates. The solution was made up at 30.5 g/ml, autoclaved as described above, and left to cool to about 50°C prior to the addition of antibiotics for selection. The concentrations of the antibiotics ampicillin and carbenicillin that were used for the preparation of LB solution and LB agar are shown in **Table 2.9**. 20ml of liquid LB agar containing antibiotic were then added to sterile plastic petri dishes.

Antibiotic	Company	Concentration of stock solution	Working concentration
Ampicillin	Sigma	100 mg/ml	100 µg/ml
Carbenicillin	Melford Biolaboratories	60 mg/ml	300 µg/ml
Puromycin	Sigma	4 mg/ml	4 µg/ml

Table 2.9 Antibiotics used for selection

All antibiotic stock solutions were made in double distilled water and filter-sterilised.

2.7.9 DNA Sequencing

DNA sequencing was performed to verify the cloning of the shRNA oligonucleotides into the pRS vector. In a 96 well plate, 15 µl sequencing reactions were set up as follows: 1.7X BetterBuffer (DNA sequencing dilution buffer; Microzone, stock at 5X), 1 µl Big Dye (Applied Biosystems), 0.3 µM pSUPER.retro.puro Forward Primer (**Table 2.10**), 1 M Betaine (Sigma Aldrich), 240 ng of each plasmid DNA, and nuclease-free water to make up the target volume. The sequencing reaction was performed on a PCR Thermal Cycler machine as described below:

Step	Temperature	Duration
Initial denaturation step	96°C	1 min
Cycle (25 cycles)	96°C	10 seconds
	50°C	5 seconds
	60°C	4 minutes
Hold	4°C	Indefinite

The sequenced DNA was precipitated as follows. In each well of the 96 well plate, 50 mM Sodium Acetate (pH 5.2, Sigma), 2 mM EDTA (0.5 M stock solution; Sigma), and 55 µl absolute ethanol (Fisher Scientific) were added. The plate was centrifuged at 100 rpm (maximum speed) for 45 minutes at 4°C. The supernatant was removed by inverting the plate and the plate was spun inverted at 100 g for 1 minute. A total of 150 µl 70% ethanol were added to each well and the plate was spun for 10 minutes at 4 100 rpm (4°C). The supernatant was removed by inverting the plate, which was then spun inverted at 100 g for 1 minute. After the addition of 10µl of hi-di-formamide (Life Technologies) to each well, the plate was vortexed and centrifuged briefly. The DNA was denatured at 95°C for 2 minutes and then re-natured at 4°C for 2 minutes on a PCR Thermal Cycler machine (Biorad). The DNA was then sequenced by the 3730xl DNA Analyzer (AME Bioscience). Analysis of the DNA sequences was performed using the Sequence Scanner v1.0 (Applied Biosystems) software.

DNA sequencing was also performed to confirm that the *Fkbp9* and *Fkbp4* inserts respectively were cloned in the correct orientation and reading frame into the pET-23d(+) vector. The constructs were sequenced using 8 different primers (**Table 2.10**) and therefore 8 individual sequencing reactions were set up. Each sequencing reaction was set up as follows: 1.7Xl Better Buffer, 1µl Big Dye, 0.3 µM of each sequencing primer (stock at 10 µM), 1 M Betaine, and 240 ng plasmid DNA, made up to 15 µl with double distilled water. DNA sequencing, precipitation, and analysis were carried out as described above.

Sequencing Primer name	Sequence 5'→3'
pET_T7F	ATTAATACGACTCACTATAGGGAG
pET_T7R	TGCTAGTTATTGCTCAGCGGTG
Fkbp9_F1seq	TGATGTTCTGCTGGTTGATAT
Fkbp9_R1seq	AATACCCACATAGGTATCGTAG
Fkbp9_F2seq	AATCACACCTTTGATACCTATA
Fkbp9_ R2seq	ATGGATATCAAACACCAGAACT
Fkbp9_F3seq	AAAACGCACCGTTATTATTCC
Fkbp9_R3seq	ATCGATTTCTTCAAACAGGTTC
Fkbp4_F1seq	ATTAATACGACTCACTATAGGGAG
Fkbp4_R1seq	TTCAGATAAACGATGCTATGTT
Fkbp4_F2seq	AAGGCAAATACAAACAGGCACT
Fkbp4_ R2seq	TATCCAGTTCCAGTGCTTTATT
Fkbp4_F3seq	ATTTTCAGAAAGTGCTGCAGC
Fkbp4_R3seq	TATTCCGGTTTGCAGGTAATAT
pRS _Forward	CCCTTGAACGTCCTCGTTCGACC

Table 2.10 DNA sequencing primers

pET_T7F, pET_T7R and pRS_Forward primers were purchased from Sigma Aldrich. All other primers were purchased from Eurofins Genomics.

2.7.10 Polymerase Chain Reaction (PCR)

PCR was performed using the Phusion High-Fidelity PCR kit (Thermo Scientific) to remove both the Endoplasmic Reticulum (ER) signal sequence and the ER retention motif from the *Fkbp9* gene sequence. The modification of the pET-23d (+)-*Fkbp9* cloning strategy aimed to optimise the expression of the recombinant Fkbp9 protein. The PCR reaction was set up as shown in **Table 2.11**. The sequences of the *Fkbp9* primers used to carry out the PCR reaction are shown in **Table 2.12**.

Component	Volume in a 50 µl reaction
Double distilled water	Add to 50 µl
5X Phusion High Fidelity (HF) Buffer	10 µl
10mM dNTPs	1 µl
Primer pETF1_PCR_Fkbp9 (10µM)	1 µl
Primer pETR1_PCR_Fkbp9 (10µM)	1 µl
Template pET-23d (+)-*Fkbp9* plasmid DNA	1 µl (10 ng)
DMSO (100%)	1.5 µl
Phusion DNA Polymerase	0.5 µl

Table 2.11 PCR reaction composition

PCR Primer name	Sequence 5'→3'
Forward Primer pETF1_PCR_Fkbp9	CATCCATGGCTCATCATCATCACCATCATCTGGTTCCG CGTGGTAGCGCAC CGGTTCTGGGTCTGGCAGTTAGC
Reverse Primer pETR1_PCR_Fkbp9	CATCTCGAGTTAGGCCTCTTGATCTTTCAGTTTGAACT CTTC

Table 2.12 PCR forward and reverse primers. Primers were designed and purchased from Eurofins Genomics.

The PCR reaction was carried out as follows:

Step	Temperature	Duration
Initial denaturation step	98° C	30 seconds
Cycle (30 cycles)	98°C 67°C 72°C	10 seconds 30 seconds 1 minute
Final DNA elongation step	72°C	10 minutes
Hold	4°C	Indefinite

The PCR reactions were set up in 0.2 ml PCR tubes. The PCR product was cleaned and concentrated using microCLEAN solution (Microzone). An equal volume of microCLEAN solution was added to the PCR DNA sample. This was mixed by pipetting and left to stand at room temperature for 5 minutes. In a benchtop centrifuge the mixture was spun down at 13 000 rpm for 7 minutes and the supernatant was discarded. The tube containing the PCR DNA was spun down briefly again to remove all the supernatant. The pellet of precipitated DNA was resuspended in 30 µl buffer Tris-EDTA (TE buffer; Sigma). The tube was left to stand for 5 minutes to rehydrate the DNA before quantification using Nanodrop-1000 Spectrophotometer. The cleaned PCR product was restriction digested, purified from agarose gel, and ligated to the pET-23d(+) vector as described above.

2.7.11 Colony PCR-Screening for pET-23d(+) -Fkbp9 and pET-23d(+) Fkbp4 recombinant clones

PCR colony screen was performed to confirm the presence of the *Fkbp9* insert DNA in the pET-23d(+) plasmid construct. Individual bacterial colonies (transformants) were mixed with 100 µl water in a 96 well plate. The PCR mix was made up of 8 µl MegaMix-Blue (Ready to use PCR mix; Microzone) and 0.6 µM of each of forward and reverse pET primers (stock at 10 µM) (see **Table 2.12**). A 1 µl aliquot of each transformant reaction was mixed with 9 µl of the PCR mix in a separate 96 well plate. The colony PCR reaction was run on a PCR Thermal Cycler machine (Bio-Rad) as shown below:

Step	Temperature	Duration
Initial denaturation step	95°C	3 min
Cycle (35 cycles)	94°C 60°C 72°C	30 seconds 30 seconds 2 minutes
Final DNA elongation step	72°C	5 minutes
Hold	4°C	Indefinite

2.7.12 Glycerol Stock Preparation

Glycerol stocks were prepared for both BL21 (DE3) bacterial cells that had been transformed with the pET-23d(+)-*Fkbp9* and pET-23d(+)-*Fkbp4* constructs, respectively. Stocks were prepared using one-day old bacterial cultures stored at 4°C. A 50% Glycerol solution was made up by mixing 25 ml 100% Glycerol (Sigma) with 25 ml double distilled water. This was autoclaved on a bench-top autoclave (Prestige Medical) and filter-sterilized using sterile 22 µm filters (Jet Biofil).

Working by a flame, 500 µl of the bacterial culture were mixed 25% glycerol (stock at 50%) in a 2 ml screw-cap tube and mixed gently. This step was carried out next to a flame to ensure that the glycerol stocks are kept sterile. The glycerol stock tubes were stored at -80°C.

2.8 Inducing the expression of recombinant Fkbp9 and Fkbp52 proteins

A total of four 10 ml BL21 (DE3) cultures expressing the pET-23d(+)-*Fkbp9* and pET-23d(+)-*Fkbp4* constructs respectively, were set up overnight at 30°C, 200 rpm. Carbenicillin was added to the culture medium at a final concentration of 300 µg/ml. The next morning, two more cultures were set up from each overnight culture by inoculating 10 ml LB (Sigma) with 200 µl of the overnight parental culture; one of the cultures was destined for induction with Isopropyl β-D-1-thiogalactopyranoside (IPTG) and the other acted as an uninduced control. The medium was supplemented with carbenicillin at 300 µg/ml and glucose (Sigma) at a final concentration of 1% v/v. The cultures were incubated at 37°C, 250 rpm and the Optical Density at 600 nm was monitored using the Nanodro-1000 Spectrophotometer. The cultures were induced with IPTG (Melford Biolaboratories) at a final concentration of 1 mM at OD_{600}= 0.6-0.7. Following IPTG induction, both the induced and the uninduced control cultures were shifted to 30°C, 200 rpm for 5 hours, then lysed for the protein expression trial.

The protocol was repeated for the induction of expression of the recombinant Fkbp52 protein. However, for this construct, bacterial cultures were incubated at 37°C (not 30°C), following IPTG induction.

The expression trial was carried out as follows: 1 ml from each bacterial culture was transferred to an Eppendorf tube and these were spun down on a benchtop centrifuge for 5 minutes at 15 000 rpm. The LB supernatant was removed, and the bacterial pellet was resuspended in 1X Sodium dodecyl sulphate (SDS) loading buffer. This was

made up by mixing 100µl double distilled water with 100 µl of 2XSDS loading buffer (142 mM TrisHCl, 22.72% v/v glycerol, 4.54% w/v SDS, 0.022% w/v bromophenol blue made up to 100 ml with double distilled water and titrated to pH 6.8 with hydrochloric acid). The lysates were boiled for 10 minutes at 100°C on a heating block. From each SDS sample, 15 µl were loaded in each well of a 10% Tris-Glycine gel (Thermo Fisher Scientific) and run using 1X SDS Tris-Glycine buffer (made up from 10X SDS Tris Glycine Buffer; Invitrogen). Gel electrophoresis was carried out for 1.5 hours at 180 Volts. Induced and uninduced cultures were run in parallel and alongside SeeBlue Plus2 Prestained Standard Protein markers (Invitrogen). The gel was stained for 1 hour in Coomassie Blue solution (50% water, 10% Acetic acid (glacial), 40% Methanol, 3g/L Coomassie Blue R (Sigma Aldrich). The gel was then transferred to Destain solution (50% water, 40% Methanol, 10% Acetic Acid) for 30 minutes and the solution was then replaced every 1 hour for the rest of the day to allow for the detection of recombinant proteins. The gel was then scanned using a Scanner machine (Cannon).

2.9 Statistical analysis

Statistical analysis and graphs were generated in Microsoft Excel. Statistical significance was determined by the one-way analysis of variance (ANOVA) test and the student's t-test, using the GraphPad Instat software. All results, except in the case of subclones where n=1, are reported as averages, with error bars representing standard deviation (SD). In cases where error bars represent standard error of the mean (SEM), this is indicated in the figure legend. Blots showing PrP^{Sc} from cell homogenates digestedwith different concentrations of Proteinase K, were quantified using the ImageJ software (Wayne Rasband, version 1.47).

3 Results (Towards understanding Selective Neuronal Vulnerability: Establishing an *in vitro* model for strain selection)

3.1 Isolation of prion strain-selective cells and evidence for a novel cell model of prion strain adaptation.

3.1.1 Rationale

In neurodegenerative diseases, selective subpopulations of neurones are targeted, leading to the progressive failure of defined brain regions, a phenomenon known as selective neuronal vulnerability. In prion diseases, selective neuronal vulnerability is linked to degeneration of particular brain areas in a strain-dependent manner. For example, intracerebral inoculation of mice with the murine strain Me7 induces hippocampal neuronal loss whereas RML does not cause degeneration in this brain region (Jeffrey et al. 2001; Karapetyan et al. 2009). Additionally, the murine strain 22L targets the cerebellum, as this brain region is the first to exhibit hallmarks of neurodegeneration following inoculation with 22L (Šišková *et al.*, 2013). The mechanisms which underlie brain tropism of prion strains are poorly understood.
It has long been assumed that by targeting distinct brain regions, prion strains give rise to different disease phenotypes. However, no direct evidence exists to support this hypothesis, making it difficult to understand selective neuronal vulnerability using *in vivo* models. This is because the molecular mechanisms that link brain tropism of prion strains to diverse clinicopathological phenotypes are unknown.

Although prion toxicity is not readily observed in most cell lines, differences in their tropism to mouse-adapted prion strains has been broadly observed (Mahal et al., 2007, Rubenstein et al., 1992, Vorberg, Raines, Story, & Priola, 2004, Vilette, 2008). It has also been shown that in diseased mouse brains, distinct prion strains accumulate in different cell types. For example, Me7 PrP^{Sc} deposition was prominent in neurones and was not associated with astroglia or oligodendrocytes (Carroll *et al.*, 2016). On the contrary, 22L PrP^{Sc} deposition was predominantly associated with astroglia (Carroll et al., 2016). These findings suggest that susceptibility of a cell line to a specific prion strain cannot be predicted based on its tissue origin or its level of expression of the cellular prion protein alone, pointing towards the involvement of cell-specific determinants in the ability of these cell lines to propagate prion strains selectively.

The above findings raise the question of how a cell model must look like to help us understand the molecular underpinning of selective neuronal vulnerability? To address this question, we aimed to develop a suitable cell model that would comprise of a panel of cognate (genetically similar) cell clones that are differentially susceptible to the prion strains Me7 and RML. We next investigated whether cells with exclusive susceptibility to any one of the murine prion strains Me7, RML and 22L can be isolated. Single cell cloning generates genetically similar cell clones that are nonetheless highly heterogeneous with regards to their susceptibility to a specific prion strain (Klöhn et al. 2003; Mahal et al. 2007). While PK1 cells readily propagate RML, they are refractory to Me7. However, as presented in this work, serial single cell cloning leads to the isolation of rare PK1 cell clones that are susceptible to Me7 (**Figure 3.1**). This approach makes it possible to isolate and compare cell clones that are susceptible or refractory to Me7 and/or RML, and in turn, identify genetic or epigenetic factors that account for the ability of a cell line to propagate these strains. Understanding the mechanisms that underlie cell tropism of Me7 and RML, may lay the foundation to understand brain tropism of these mouse-adapted prion strains.

The pedigree of cell clones that have been derived in this PhD, is shown below (**Figure 3.1**). The PME2 subclone (**see Section 3.1.2**), is a PK1-derived subclone with low susceptibility to Me7, that was used as the parental line for downstream subcloning experiments to derive highly Me7-susceptible cells.

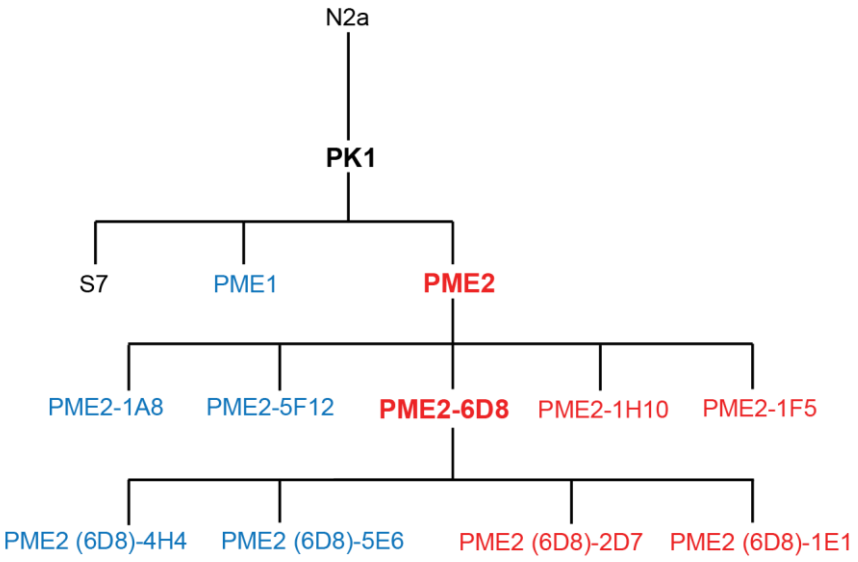

Figure 3.1 Lineage of Me7 susceptible and resistant cell clones isolated from parental N2a cells (black: resistant; red: susceptible; blue: revertant resistant).

3.1.2 Isolation of PME1 and PME2, two rare N2aPK1 cell clones permissive to Me7

It has previously been shown by others that the N2a subclone, N2a-PK1 (PK1 for short), is refractory to Me7 but highly susceptible to the murine prion strains RML and 22L (Mahal et al., 2007, Klohn, Stoltze, Flechsig, Enari, & Weissmann, 2003). The strategy of subcloning has been employed successfully in the past, to isolate highly prion-susceptible cell clones (Mahal et al., 2007, Klohn, Stoltze, Flechsig, Enari, & Weissmann, 2003, Bosque and Prusiner 2000). This is because subclones of a heterogeneous pool of cells greatly vary in their susceptibility to a prion strain. For example, the PK1 cell line is highly heterogeneous in regard to its susceptibility to RML and 22L prions, which enables the isolation of sister clones that are highly susceptible to RML but not to 22L and vice versa (Mahal *et al.*, 2007).

To confirm that N2a cells are refractory to Me7, we conducted a single cell cloning experiment, and challenged a total of 672 PK1 clones with a $2x10^{-6}$ dilution of Me7 brain homogenate. While the vast majority of clones (97.3%) were refractory to Me7, 3 clones were identified, that produced over 300 PrP^{Sc}-positive cells/well, raising the possibility that rare PK1 cell clones are susceptible to Me7 (**Table 3.1**). Two of these clones with spot numbers of 351 and 378, were designated PME1 and PME2 respectively (**Table 3.1**). These were isolated and cryopreserved on the basis of their potential susceptibility to Me7.

PK1 subclone	Spot number with $2x10^{-6}$ Me7
PME2	**378**
PME1	**351**
1A1	327
4G2	261
5H5	166
1A5	157
6C2	154
5D10	9
1F12	5
2D8	4
4F1	3

Table 3.1 Rare N2a clones are putatively permissive to Me7 prions. A total of 672 single PK1 cell clones were isolated and challenged with a $2x10^{-6}$ dilution of Me7 brain homogenate and prion propagation was assessed using the Scrapie Cell Assay (SCA). The clones are

ranked according to their susceptibility to Me7. The table shows data for 11 representative clones. *(Data from Dr. Peter Kloehn).*

To first test whether PME1 and PME2 retained their initial susceptibility to Me7, the two cell clones were revived from liquid nitrogen and rechallenged with Me7 at concentrations increasing from 10^{-4} to 10^{-9} dilutions of homogenate. The Me7-refractory cell line, S7, is derived from PK1 cells and is highly susceptible to RML. This was used as a negative control for infection with Me7. The three cell lines PME1, PME2 and S7 were also challenged with RML and 22L. A persistent or chronic state of prion infection is characterised by continuous propagation of PrP^{Sc} that holds pace with cell division (Vorberg, Raines and Priola, 2004). In acute prion infection, prion replication proceeds at a rate lower than that of cell division and infectivity is halved with each cell division, leading to a diluting-out of prions (Weissmann, 2004).

All three cell lines were highly susceptible to RML as evident by the increase in the number of PrP^{Sc}-positive cells between subsequent cell splits (**Figure 3.2**). An increase in prion propagation between two cell passages was observed for 22L-challenged PME2 and S7 cells, but not for PME1 cells (**Figure 3.2**). When challenged with Me7, there was a noticeable decrease in spot number after one cell passage for all cell lines, indicating that none of the cell lines are able to maintain prion infection. When challenged with Me7, the spot number of Me7-refractory S7 cells dropped to zero by passage 4, indicating that prions cannot be detected after four passages. (**Figure 3.2**). Contrary to this data, PME2 showed a slower slope factor, which suggests that this clone may propagate Me7 prions at a slow rate.

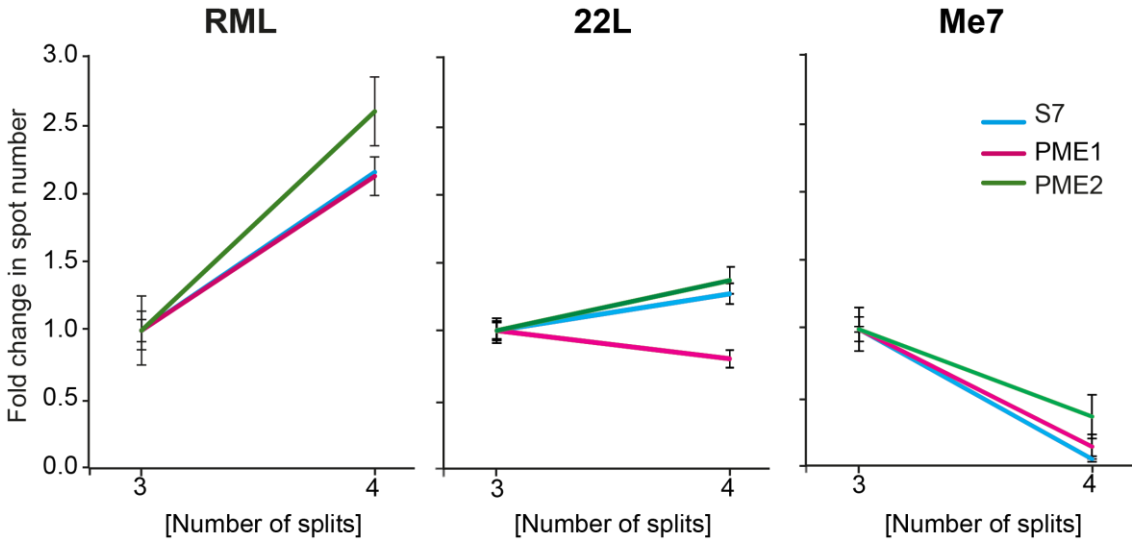

Figure 3.2 Changes in spot number after infection of three cell lines with three mouse-adapted prion strains. PME1, PME2 and S7 cells were challenged with 22L and RML brain homogenates at a $1x10^{-5}$ dilution, and with Me7 homogenate at a $1x10^{-4}$ dilution. Elispot assays were carried out at cell passages 3 and 4. The fold change in spot number between successive passages was calculated by dividing the spot numbers of Split 4 by the spot numbers of Split 3 for each prion-infected cell line. For each cell line, 12 wells of a 96 well plate were challenged with each dilution of homogenate. The line graphs show the mean fold change± standard deviation for each prion-infected cell line. The figure shows the results of one experiment.

Since PME2 showed a significantly higher spot number when compared to S7, we next asked whether subcloning of PME2 cells after an initial challenge with Me7 may result in persistently infected cells. We therefore challenged the parental lines, PME1 and PME2 with Me7, 22L and RML brain homogenates, isolated single cell clones and determined the number of PrP^{Sc}-positive cells by Elispot Assay.

After seven passages in cell culture, PME1 and PME2 cells challenged with the all three mouse-adapted prion strains were plated out at limiting dilution and single cell clones were isolated. For all three prion strains, a higher number of PME2 prion-susceptible sibling clones was isolated when compared to PME1 sibling clones (**Figure 3.3**).

For Me7-infected PME2 cells, 14% of sibling clones consisted of over 100 PrP^{Sc}-positive cells and 4% consisted of over 300 PrP^{Sc}-positive cells (**Figure 3.3**). In contrast to this observation, only one PME1 cell clone with 77 PrP^{Sc}-positive cells could be isolated, corresponding to 0.3% of all the Me7-infected PME1 cell clones, while the remaining PME1 clones consisted of less than 15 PrP^{Sc}-positive cells (**Figure 3.3**).

From the above experiments, we concluded that, it was possible to isolate chronically Me7-infected PME2 sibling clones (**Figure 3.3**). Collectively, these findings justified the use of PME2 cells in downstream experiments to isolate Me7-susceptible cells.

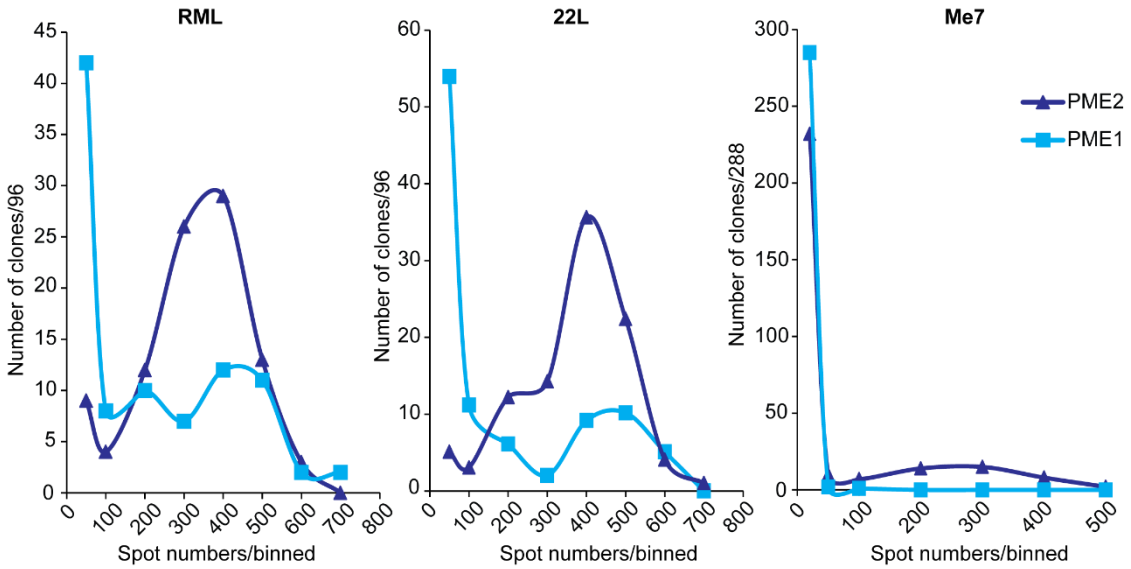

Figure 3.3 Population distribution of PME1 and PME2 sublines following infection of the parental cell populations with 22L, RML and Me7 Cultures of PME1 and PME2 cells were challenged with 22L, RML and Me7 brain homogenates, at a $1x10^{-3}$ dilution for RML and Me7 and $1x10^{-4}$ dilution for 22L. After 7 passages, each prion-infected cell population was plated out at limiting dilution and single cell PME1 and PME2 clones were isolated 12 days later. The number of PrP^{Sc} positive cells of each subclone was determined in an Elispot assay. A total of 288 PME1 and 288 PME2 Me7-infected clones were isolated. A total of 96 22L and 96 RML-infected clones were isolated. The x-axis represents spot numbers of individual clones, pooled into bins of 100. The first two bins are 0-50 and 50-100. A spot count below 50 is considered background.

3.1.3 Single cell cloning of PME2, a clone with marginal susceptibility to Me7, enriches for cell clones that are highly susceptible to Me7

Isolation of persistently Me7-infected PME2 subclones, encouraged us to conduct larger scale subcloning experiments. We hypothesised that single cell cloning of PME2, a cell line with low susceptibility to Me7, will bring forth clones with greatly enhanced susceptibility to Me7. Additionally, sister clones derived from the same parental line are genetically similar, thereby reducing differences in gene expression unrelated to the phenotype that the cell clone is being selected for.

The parental PME2 cells were plated out at limiting dilution and single cell clones were isolated after 12 days. In this subcloning experiment, a total of 960 clones were isolated and challenged with Me7 brain homogenate at a $1x10^{-5}$ dilution. The number of PrP^{Sc}-positive cells for each clone was determined after passage 3 and 5 (**Table 3.2**).

3.1.3.1 The PME2 subclone, PME2-6D8, is susceptible to Me7

The initial Me7 susceptibility screen was conducted without technical repeats, given the high number of clones screened. To confirm the data of this initial screen, the six most Me7-susceptible PME2 clones that emerged from the subcloning of PME2, including PME2-6D8, were rechallenged with the same Me7 brain homogenate dilution ($1x10^{-5}$), 10 passages after isolation (**Figure 3.4 A**).

Surprisingly, PME2-6D8 was the only clone that was susceptible to Me7 after re-infection, as evident by the high number of PrP^{Sc}-positive cells, while other Me7-susceptible clones were refractory (**Figure 3.4 A**). For this reason, we subcloned PME2-6D8 cells in the final subcloning experiment, which led to a marked increase in the number of highly Me7-susceptible PME2-6D8 cell clones (**Table 3.2, Figure 3.5**)

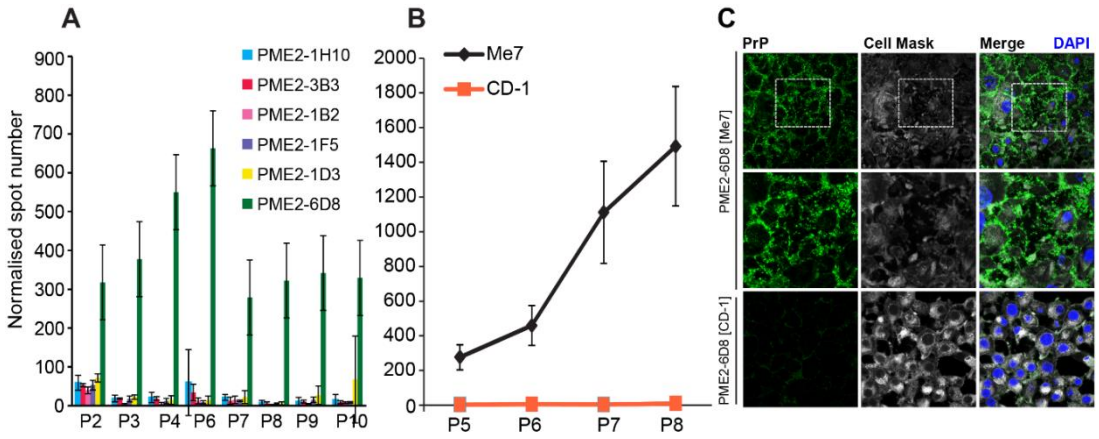

Figure 3.4 The PME2-6D8 clone maintains a persistent state of infection when challenged with Me7. A. Upon identification of Me7-susceptible PME2 clones, their non-infected counterparts were expanded from the master plates to 4 wells/cell clone and re-challenged with Me7 brain homogenate at a $1x10^{-5}$ dilution (n=4). All six clones had been in culture for 10 passages before being re-infected with Me7. The bar graph shows the number of PrP^{Sc}-positive cells from each clone from passage 2 to passage 10. The number of PrP^{Sc}-positive cells determined in Elispot assay was normalised to the total number of cells determined in a Trypan Blue assay for all clones. Bars represent mean values of normalised spot numbers ± standard deviation. **B.** PME2-6D8 cells were challenged with Me7 at a $1x10^{-3}$ dilution or with non-infected CD-1 homogenate at a $1x10^{-4}$ dilution and split according to the

SCEPA protocol (see Materials and Methods). Elispot assays were performed after the 5th, 6th, 7th and 8th passage, and values normalised to the total number of cells. Data points show mean values of normalised spot numbers ± standard deviation. **C.** Immunofluorescence was carried out 9 passages after the PME2-6D8 cells were challenged with a $1x10^{-3}$ dilution of Me7. PME2-6D8 cells were allowed to grow for 7 days on chamber slides before being stained with Cell Mask and fixed with 3.7% formaldehyde (FA). The cells were immunostained with the anti-PrP antibody 5B2, after treatment with acetone and 3.5M guanidinium thiocyanate (GTC). PME2-6D8 cells challenged with non-infected CD-1 brain homogenate at a $1x10^{-4}$ dilution were also stained with 5B2 as a negative control. Disease-associated PrP deposits are shown in green.

To generate chronically Me7-infected cells for confocal microscopy, the PME2-6D8 clone was challenged with a $1x10^{-3}$ dilution of Me7 and split 5 times before being assessed for prion propagation in an Elispot assay. There was a 5-fold increase in the number of PrP^{Sc}-positive cells between passages 5 and 8, indicating that PME2-6D8 maintained a persistently-infected state upon challenge with a high concentration of Me7 homogenate (**Figure 3.4 B**). These findings were also confirmed by immunofluorescence. Immunostaining of Me7-challenged PME2-6D8 cells with the anti-PrP antibody 5B2 revealed extracellular deposits of disease-associated PrP (PrP^{d}) in these cells, 10 passages after challenge with Me7 brain homogenate (**Figure 3.4 C**). PrP^{d} comprises of PK-resistant PrP as well as PK-sensitive forms of disease-related PrP (Safar et al., 1998), whereas PrP^{Sc} is defined biochemically as PK-resistant PrP.

3.1.3.2 Single cell cloning of PME2-6D8 generates cell clones highly susceptible to Me7

So far, I have shown that PME2-6D8 emerged during the subcloning of PME2. The susceptibility of the aforementioned clone to Me7 was confirmed by re-challenge of PME2-6D8 cells with the same concentration of Me7 homogenate. We hypothesized that single cell cloning of PME2-6D8 will increase the number of subclones that are susceptible to Me7. In the final round of subcloning, a total of 472 PME2-6D8 cell clones were isolated.

In each subcloning round, the percentage of Me7-susceptible cells increased by 6-fold and 20-fold, respectively. Initially, the cell clones PME1 and PME2 were classified as "weakly Me7-suscepible" with 351 and 378 PrP^{Sc}-positive cells respectively, however, in the second round of subcloning, 2% of PME2 sibling clones with PrP^{Sc}-positive cells between 600 and 2000 were isolated (**Figure 3.5 B**). This indicates that subcloning not only increased the proportion of Me7-susceptible cells but also the overall

susceptibility of clones to this strain as evident by the sharp increase in the number of PrP^{Sc}-positive cells per clone (**Table 3.2, Figure 3.5 B, C, E**).

***PME2 subclone* (Generation 1)**	***P3 Me7***	***P5 Me7***	***FD between P3 and P5***
1H10	88	2235	25
1F5	92	2206	24
1B2	59	1748	30
3B3	58	1788	31
6D8	98	1356	14
2G6	49	1229	25
2E9	20	1287	64
1A8	7	10	1
5F12	13	11	1
PME2 parental cell line	41±13	137±91	3
***PME2 (6D8) subclone* (Generation 2)**	***P3 Me7***	***P5 Me7***	***FD between P3 and P5***
4F11	2079	3191	2
2C6	1863	3169	2
5B9	2178	3152	1
5B1	1618	3147	2
5F1	2131	3142	1
1G1	1844	3121	2
5E1	1997	3103	2
5C5	2030	3071	2
5E6	17	3	0.2
4H4	35	8	0.2

Table 3.2 Susceptibilities of PME2 and PME2-6D8 sibling clones to Me7 over the course of two cell passages. PME2 (Generation 1) and PME2-6D8 (Generation 2) clones isolated during the subcloning of PME2 and PME2-6D8, respectively, were challenged with a $1x10^{-5}$ dilution of Me7 brain homogenate. After reaching confluence, cell clones at passage 3 (P3) and 5 (P5) were seeded for an Elispot Assay to determine the number of PrP^{Sc}-positive cells for each cell clone. As a comparison, the number of PrP^{Sc}-positive cells for the Me7-infected PME2 parental line was also determined. For this cell line, spot numbers represent average of 12 wells ± Standard Deviation. Susceptible clones are shown in light blue colour, refractory clones are shown in darker blue colour; FD= fold difference; this was calculated by dividing spot numbers of passage 5 cells by spot numbers of passage 3 cells for all the cell clones.

A significant increase in the number of PrP^{Sc}-positive cells was observed in the second subcloning experiment, even though the majority of PME2 sibling clones were refractory to Me7 as they did not exceed a threshold value of more than 100 PrP^{Sc}-positive cells per clone which explains the low correlation coefficient in scatter plot 1 (**Figure 3.5 B, D**). Further subcloning of PME2-6D8 (**Figure 3.5 B**, Experiment 3), a clone with high susceptibility to Me7, substantially increased the permissiveness of PME2-6D8 sibling clones to Me7 (**Figure 3.5 D, Table 3.2**). The success of serial subcloning strategy is best represented by **Figure 3.5 E.** The histogram shows a dramatic shift from a cell clone population consisting mostly of Me7-refractory cell clones to a cell clone population that was dominated by highly Me7-susceptible cell clones. Serial single cell cloning led to the isolation of highly Me7-susceptible PME2 and PME2-6D8 cells from a clone with low susceptibility to Me7, PME2 (**Table 3.2**, **Figure 3.5**).

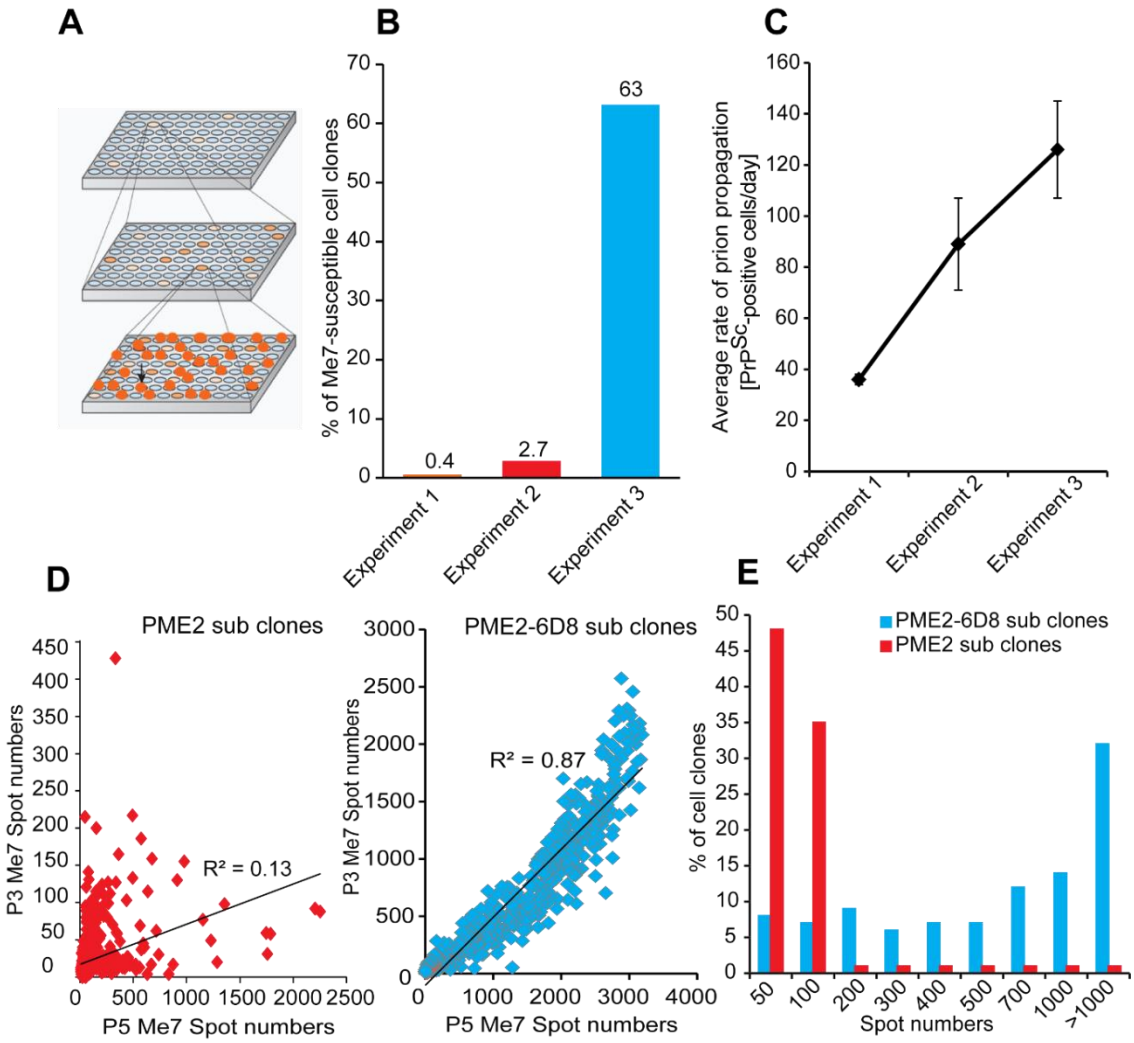

Figure 3.5 Enrichment of Me7-susceptible cells by single cell cloning A. Schematic representation of a serial subcloning strategy to obtain N2a-PK1 cell clones that are highly susceptible to Me7. A bulk culture of N2a-PK1 cells was the starting cell line. **B. Increase in the percentage of Me7-susceptible cell clones.** The bar graph represents the percentage of Me7-positive cell clones isolated from three subsequent subcloning experiments. Cell clones were challenged with a $2x10^{-6}$ dilution of Me7 brain homogenate in the first experiment and with a $1x10^{-5}$ dilution of Me7 brain homogenate in the last two experiments. In each experiment, cell clones at passages 3 and 5 were assessed for the number of PrP^{Sc}-positive cells. In experiment 1, 3 out of a total of 672 clones produced over 300 PrP^{Sc}-positive cells, in experiment 2, 26 out of 960 clones produced over 500 PrP^{Sc}-positive cells and in experiment 3, 298 out of 472 clones produced over 1000 PrP^{Sc}-positive cells (based on passage 5 data). **C. Increase of prion propagation rates.** For each subcloning experiment, the average rate of prion propagation was calculated for 5 representative clones. The rate of prion propagation was defined as the number of PrP^{Sc}-positive cells divided by the number of days between prion infection and Elispot assay. Points represent the average rate of prion propagation for 5 cell clones± Standard deviation. **D. Correlation between passage 3 and passage 5 spot**

numbers of Me7-infected PME2 and PME2-6D8 cell clones respectively. For experiments 2 and 3, the number of PrP^{Sc}-positive cells at passage 3, was plotted against the number of PrP^{Sc}-positive cells at passage 5, for each cell clone. Each scattergram includes a line of best fit and a correlation coefficient (R^2) **E.** PME2 and PME2-6D8 clones were challenged with a $1x10^{-5}$ dilution of Me7 brain homogenate. A total of 960 PME2 clones and a total of 472 PME2-6D8 clones were isolated. The figure shows the distribution of passage 5 PME2 clones (red bars) and PME2-6D8 clones (blue bars) in each spot number bin. The frequency of cell clones in each bin is expressed as a percentage of the total number of clones isolated in each experiment. A spot count below 50 is considered background.

We showed that it is possible to isolate both Me7-susceptible and Me7-refractory PME2 and PME2-6D8 clones (**Table 3.2, Figure 3.5 E**). Given their differential response to Me7, we asked whether PME2-6D8 clones are also differentially susceptible to the murine strains RML and 22L. To address this question, we challenged all 472 PME2-6D8 clones with 22L and RML brain homogenates at dilutions of $1x10^{-6}$ and $1x10^{-5}$, respectively. The number of PrP^{Sc}-positive cells for each clone was determined in Elispot assays on passage 3 and passage 5 (**Table 3.3**). While PME2-6D8 clones with differential susceptibility to Me7 could be isolated, all cell clones showed a similar response to 22L and RML (**Table 3.3**). Whereas it was not possible to isolate 22L-exclusive (22L+/RML-/Me7-) or RML-exclusive clones (RML+/22L-/Me7-) from the PME2-6D8 parental clone, single cell cloning of PME2 yielded rare variant sibling clones with exclusive susceptibility to either 22L or RML, and the results are summarised in supplementary chapter **3.1.8**. These clones will enable us to identify differentially expressed genes with a role in strain-specific prion propagation. To maintain strain-specific prion susceptibility of sibling clones, we sought to develop a high-throughput cryopreservation method in a 96 well format, which is outlined in detail in supplementary chapter **3.1.7**.

Me7-refractory PME2 (6D8) subclone	*P5 Me7*	*P5 22L*	*P5 RML*
5E6	3	3038	2881
4C7	4	3151	2910
4D4	5	3170	2937
4C12	6	2786	2724
5G5	6	2949	2851
5E2	7	2935	2656
4H4	8	2723	2675
Me7-susceptible PME2 (6D8) subclone	***P5 Me7***	***P5 22L***	***P5 RML***
4F11	3191	2849	2883
2C6	3169	2858	2763
5B9	3152	2898	2824
5B1	3147	2772	3064
5F1	3142	2420	2368
1G1	3121	2602	2293
5E1	3103	2576	2840

Table 3.3 Genetically similar PME2-6D8 cell clones are very different with regards to their susceptibility to Me7 but are equally susceptible to 22L and RML. PME2-6D8 clones were challenged with a $1x10^{-5}$ dilution of Me7 and RML brain homogenates respectively, and with a $1x10^{-6}$ dilution of 22L brain homogenate. The table shows the number of PrP^{Sc}-positive cells of passage 5 (P5) cell clones as determined by an Elispot assay, after challenge of the clones with the three prion strains.

Results so far have shown that several PME2 and PME2-6D8 clones maintained a persistent state of infection when challenged with a $1x10^{-5}$ dilution of Me7 brain homogenate (**Figure 3.5**, **Tables 3.2**, **3.3**, **Figure 3.6 B**). This was evident by the high number of PrP^{Sc}-positive cells in each clone, which remained steady throughout the course of the assay, even after several passages in cell culture (**Tables 3.2**, **3.3**, **Figure 3.6 B**).

To analyse Me7-infected cell clones using confocal microscopy, the Me7-infected PME2 cell clones were treated with acetone and guanidinium thiocyanate (GTC), prior to immunolabelling, according to established protocols (Marbiah *et al.*, 2014). Immunofluorescence analysis revealed PrP^{d} deposits at the basement membrane

level and extracellular matrix (ECM) of Me7-infected PME2 cells, a phenotype that was not present in uninfected cells (**Figure 3.6Ai, ii**).

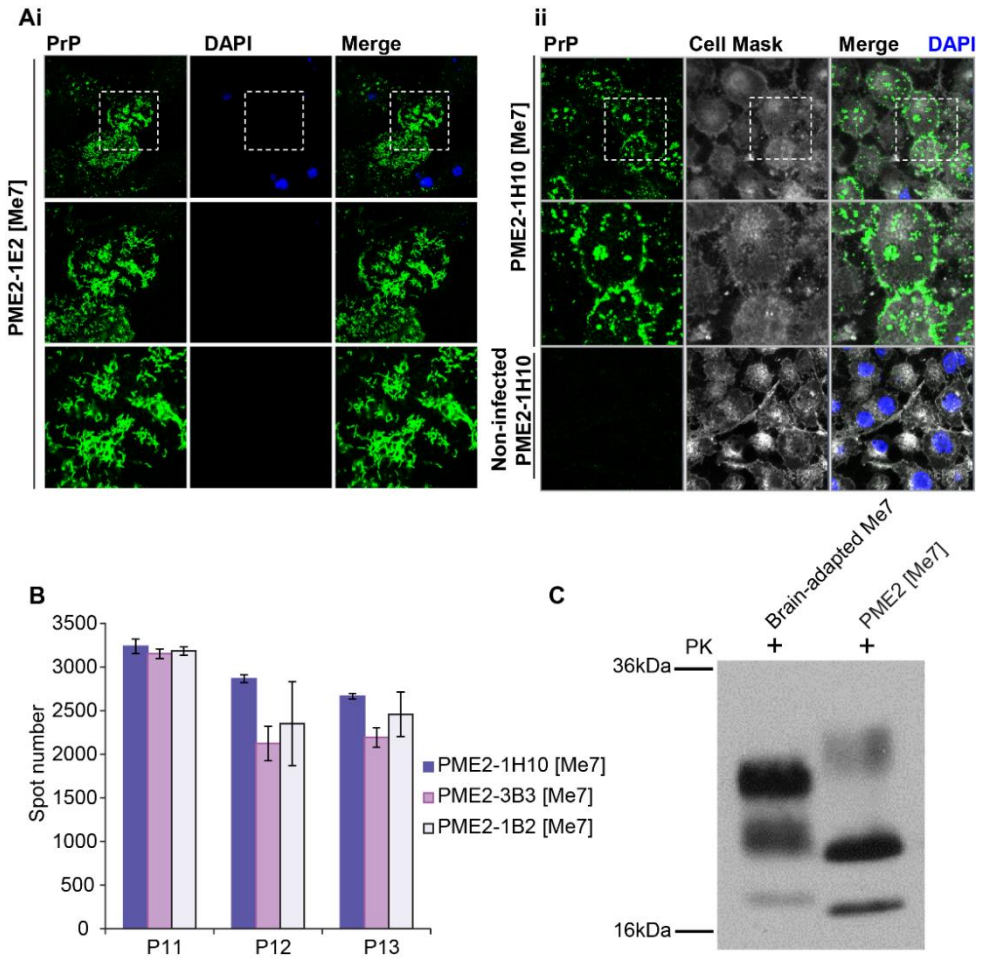

Figure 3.6 Persistently Me7-infected PME2 clones deposit disease-associated PrP (PrP^d) with altered biochemical properties Ai, ii Eleven passages after challenge of cells with a $1x10^{-5}$ dilution of Me7 brain homogenate, two PME2 clones were plated out on wells of a chamber slide and were kept in culture for a period of 6 days before fixation with 3.7% formaldehyde (FA). The cells were immunolabelled with the anti-PrP antibody 5B2, after treatment with acetone and 3.5 M guanidinium thiocyanate. For some clones (Aii), the cells were first stained with Cell Mask prior to fixation with FA. Extracellular matrix deposits of disease-associated PrP (PrP^d) are shown in green colour, in the Me7-infected PME2 cells. A non-infected PME2 clone was also stained with 5B2 and used as a negative control **B. Quantification of PrP^{Sc}-positive cells for three persistently Me7-infected PME2 clones over the course of three cell passages.** The number of PrP^{Sc}-positive cells for three PME2 cell clones was determined, 11, 12 and 13 passages after challenge with a $1x10^{-5}$ dilution of Me7 brain homogenate. Bars represent mean of 6 wells ±SD. The figure represents the results of one experiment. **C. Western blot analysis of brain-adapted Me7 and PME2 cell-adapted Me7.** PK-digested, 100-fold diluted Me7 brain homogenate was run alongside PK-digested, Me7-infected PME2 cell homogenate. Proteinase K (PK) treatment and preparation of cell

homogenates are described in detail in Materials and Methods. The Western blot is representative of three independent experiments.

It has previously been shown that changes in the biochemical characteristics of PrP^{Sc} occur when a prion strain is transferred from brain to cells (Arjona et al. 2004; Arima et al. 2005). A drastic change in electrophoretic mobility and glycosylation pattern was noted when brain-adapted Me7 was passaged in permissive PME2 cells (**Figure 3.6 C**). While brain-adapted Me7 is characterised by a dominant di-glycosylated PrP^{Sc} band, PME2 cell-adapted Me7 is characterised by a dominant mono-glycosylated PrP^{Sc} band (**Figure 3.6 C**).

In summary, we have shown that serial single cell cloning led to the isolation of cell clones that are highly heterogeneous with regards to their susceptibility to Me7. By starting off with a weakly Me7-susceptible cell clone, PME2, single cell cloning generated a large number of clones with high susceptibility to Me7. Western blot analysis of brain-adapted Me7 and cell-adapted Me7 from persistently infected PME2 cells, revealed differences in the biochemical characteristics of PrP^{Sc}.

3.1.4 A novel cell model of prion strain adaptation: Brain-adapted Me7 prions and cell-adapted Me7 prions can be discriminated by striking differences in cell tropism

I have shown in **Section 3.1.3**, that the passage of brain-adapted Me7 in PME2 cells leads to a drastic change in glycosylation pattern and electrophoretic mobility (**Figure 3.6 C**). We assumed that the change in biochemical characteristics that occurred upon transfer of Me7 to PME2 cells, might be the result of strain adaptation.

Prion strain adaptation is the propensity of prions to overcome transmission barriers and gradually adapt upon transfer to a new host environment. This phenomenon leads to the emergence of Transmissible Spongiform Encephalopathy (TSE) strains with an expanded host range and increased virulence. It has been proposed that BSE resulted from interspecies transmission of sheep scrapie to cattle via contaminated food additives (Wilesmith, Ryan, Hueston, & Hoinville, 1992, Wilesmith, Wells, Cranwell, & Ryan, 1988). During cattle-to-cattle passages, adaptation of sheep scrapie led to the emergence of BSE which is also transmissible to humans, giving rise to variant CJD. Prion strain adaptation has also been demonstrated in mice. Primary passage of BSE prions to two different lines of inbred mice (both carrying the *Prnp*^{a} allele) resulted in the emergence of two distinct PrP^{Sc} subtypes with distinct pattern of PrP-

immunoreactive deposits and neuronal loss, highlighting the importance of the host genome in modulating prion strain selection and “mutation” (Lloyd *et al.*, 2004). In the context of prions, “mutation” refers to heritable changes in biochemical properties or conformation of PrP^{Sc}.

Recent evidence shows that prions are subject to “mutation” and selective amplification, thereby showing hallmarks of Darwinian evolution, despite their lack of nucleic acids (Li *et al.*, 2010). It has been reported that under a particular selection regime, such as in the presence of a drug, prions acquire drug resistance, leading to the emergence of drug resistant variants which gradually replace drug sensitive variants and dominate the prion population (Oelschlegel & Weissmann, 2013; Ghaemmaghami et al., 2009).

It was shown that strain-specific properties are retained when prions are transferred from brain to cells and back to brain (Arjona et al., 2004, Arima et al., 2005). However, classical approaches such as Western blot cannot always be used to determine changes in the properties of prions while in cell culture. For example, when two mouse-passaged CJD strains characterised by different disease incubation times and lesion profiles were propagated in the murine hypothalamic neuronal cell line, GT-1, the PrP^{Sc} banding and glycosylation patterns of the two strains were indistinguishable (Arjona *et al.*, 2004). Mahal and colleagues developed a cell-based assay, the Cell Panel Assay (CPA), and showed that a panel of murine cell lines propagate prion strains selectively (Mahal *et al.*, 2007). While certain cell lines show broad susceptibility different prion strains, other cell lines are permissive to only one strain. They showed that changes in strain properties, for example when prions are transferred from the brain to cells, can lead to changes in cell tropism. For example, the transfer of 22L prions from mouse brain to PK1 cells, led to a change in 22L strain properties (Li *et al.*, 2010). In contrast to brain-adapted 22L prions, cell-adapted 22L prions had lost their ability to infect the N2a-derived cell line, R33 (Li *et al.*, 2010).

To examine whether cell-adapted Me7 is different from brain-adapted Me7, we challenged Me7-refractory PK1 cells with homogenates from chronically Me7-infected PME2 cells. As PK1 cells are refractory to brain-adapted Me7, we expected that they would also be refractory to cell-adapted Me7, unless the strain properties of brain-adapted Me7 changed during passage in PME2 cells.

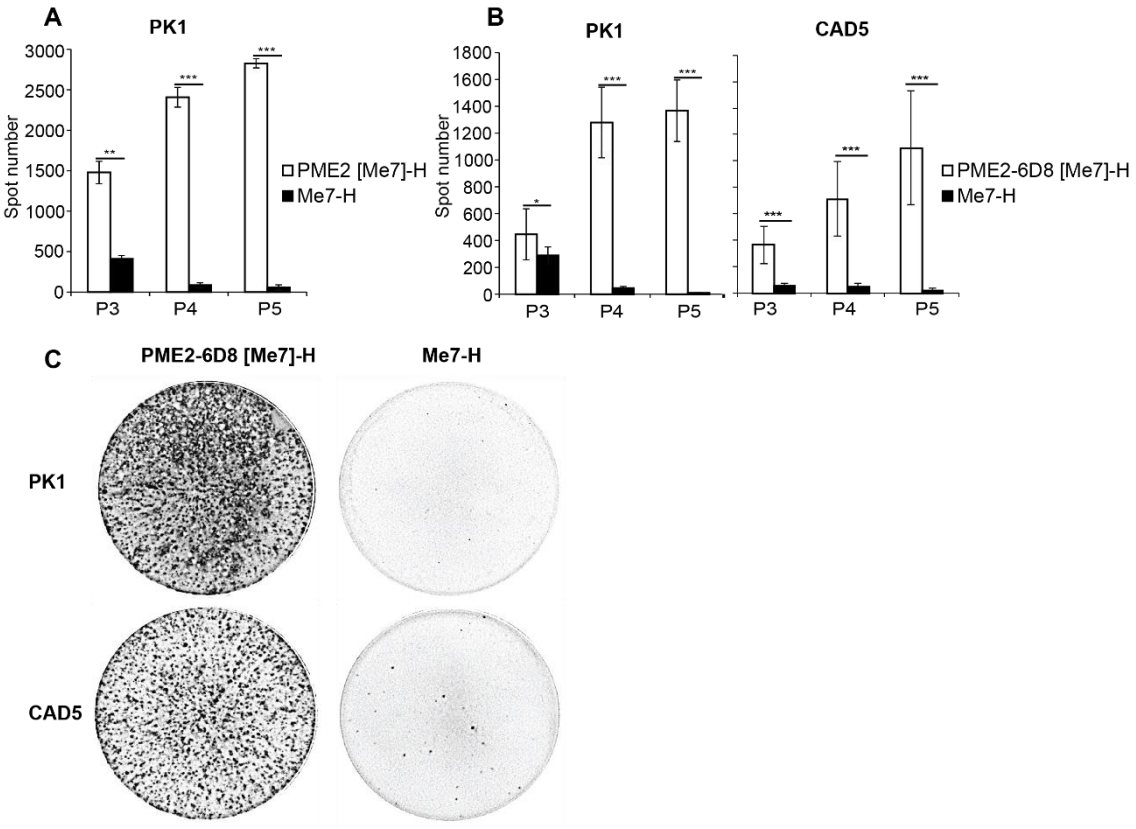

Figure 3.7 Prion strain adaptation in cell culture: PK1 cells and CAD5 propagate cell- but not brain-adapted Me7 A. PK1 cells were challenged with Me7 brain (**Me7-H**) and Me7-infected cell homogenate (**PME2 [Me7]-H)** at 1x10^{-4} and 1/500 dilutions respectively. The Me7-infected cell homogenate was derived from a single PME2 cell clone isolated in the first subcloning experiment. Following prion infection, the number of PrP^{Sc}-positive cells was determined in Elispot assays at the 3rd, 4th and 5th cell passage. Twelve wells of a 96 well plate were challenged with each homogenate. Bars represent mean of spot numbers ±Standard Deviation. Statistical significance was calculated using Student's t-test, ***p<0.001*, ****p<0.0001.* **B.** PK1 cells were challenged with Me7 brain and Me7-infected cell homogenates (**PME2-6D8 [Me7]-H)** at 1x10^{-4} and 1/500 dilutions respectively. CAD5 cells were challenged with Me7 brain and Me7 cell homogenates at 1x10^{-5} and 1/5000 dilutions respectively. The Me7-infected cell homogenate was derived from a pool of three PME2-6D8 cell clones, isolated in the second subcloning experiment. Elispot assays were performed at the 3rd, 4th and 5th passage. Twelve wells of a 96 well plate were challenged with each homogenate. Bars represent mean of spot numbers ±Standard Deviation. Statistical significance was calculated using Student's t-test, **p<0.05*, ****p<0.0001.* **C.** Representative wells of an Elispot plate showing PrP^{Sc}-positive PK1 and CAD5 cells as black spots after challenge with Me7-infected cell homogenate (left wells). No PrP^{Sc}-positive cells are seen when PK1 cells are challenged with Me7 brain homogenate (top right well). Very few PrP^{Sc}-positive cells are detectable when CAD5 cells are challenged with Me7 brain homogenate (bottom right well).

Strikingly, PK1 cells were highly susceptible to cell-adapted Me7 from chronically Me7-infected PME2 cells, but refractory to Me7, suggesting that passage in PME2 cells changed the strain properties of brain-adapted Me7 (**Figure 3.7**). Notably, the relatively high spot number observed after infection of PK1 cells with Me7 at passage 3, was due to residual brain homogenate which was also detected with the pan anti-PrP antibody used, and not due to bona-fide infection of cells (**Figure 3.7 A, B**). However, spot numbers dropped significantly at passage 4 and 5, confirming that PK1 cells do not propagate Me7 brain homogenate (**Figure 3.7**). The steady increase in the number of PrP^{Sc}-positive PK1 cells challenged with cell-adapted Me7 prions from passage 3 to 5, is indicative of prion propagation, irrespective of the source of cell-adapted Me7 (PME2 or PME2-6D8 cells) (**Figure 3.7**).

To corroborate this result, we challenged the CNS catecholaminergic cell line CAD5, with Me7 and homogenates from chronically Me7-infected PME2 cells.

Similarly, CAD5 cells were refractory to brain-adapted Me7 prions and highly permissive to cell-adapted Me7 prions, as indicated by the steady increase in the number of PrP^{Sc}-positive cells from passage 3 to 5.

Figure 3.7 C shows representative wells of an Elispot plate that are saturated with PrP^{Sc}-positive cells when PK1 cells and CAD5 cells are challenged with PME2 Me7 cell-adapted prions. When challenged with brain-adapted Me7, PK1 cells were negative, while CAD5 cells were weakly positive (**Figure 3.7 C**). Contrary to their differential response to brain and cell-adapted Me7, PK1 and CAD5 cells were equally susceptible to brain and cell-adapted RML, suggesting either that the strain properties of RML remained unchanged during passage in PME2 cells or that brain and cell-adapted RML show a similar cell tropism in this cell model (**Figure 3.8**).

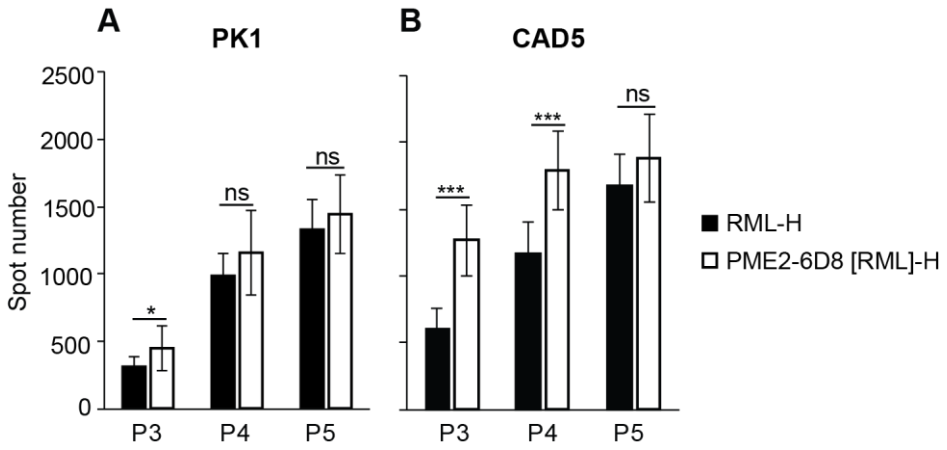

Figure 3.8 PK1 and CAD5 cells are equally susceptible to brain and cell-adapted RML PK1 cells were challenged with RML brain (**RML-H**) and RML-infected cell homogenate (**PME2-6D8 [RML]-H**) at $1x10^{-6}$ and 1/500 dilutions respectively. The number of PrP^{Sc}-positive cells was determined in Elispot assays at the 3rd, 4th and 5th passage. Twelve wells of a 96 well plate were challenged with each homogenate. Bars represent mean of spot numbers ±Standard Deviation. Statistical significance was calculated using Student's t-test, **p<0.05, ns= not significant*. **B.** CAD5 cells were challenged with RML brain and RML-infected cell homogenate at $1x10^{-6}$ and 1/500 dilutions respectively. Elispot assays were carried out after the 3rd, 4th and 5th passage. Twelve wells of a 96 well plate were challenged with each homogenate. Bars represent mean of spot numbers ±Standard Deviation. Statistical significance was calculated using Student's t-test, ****p<0.0001.*

During subcloning of PME2 and PME2-6D8, several clones that were refractory to Me7 were isolated (**Tables 3.2, 3.3**). An Me7-refratory cell clone, designated PME2 (6D8)-4H4 (**Figure 3.1**, **Table 3.3**), and the Me7-susceptible PME2-6D8 clone (See chapter **3.1.3.1**), were both challenged with brain and PME2 cell-adapted Me7 (**Figure 3.9**). As expected, PME2-6D8 cells were permissive to brain-adapted Me7, with over 600 PrP^{Sc}-positive cells, as determined by an Elispot assay at passage 5 (**Figure 3.9**). In contrast, PrP^{Sc}-positive cells could not be detected following challenge of PME2 (6D8)-4H4 clone with brain-adapted Me7 (**Figure 3.9 B**, bottom right well), confirming that this cell clone is refractory to brain-adapted Me7. The relatively high number of PrP^{Sc}-positive cells in the PME2 (6D8)-4H4 cell clone at passage 3 simply reflects immunoreactivity from residual inoculum in the culture medium, which was diluted out completely by passage 5. However, the Me7-refractory PME2 (6D8)-4H4 appeared to be highly susceptible to cell-adapted Me7, suggesting that the novel cell-adapted Me7 prions can be propagated by all PME2 cell clones regardless of whether they are susceptible or refractory to brain-adapted Me7 (**Figure 3.9**).

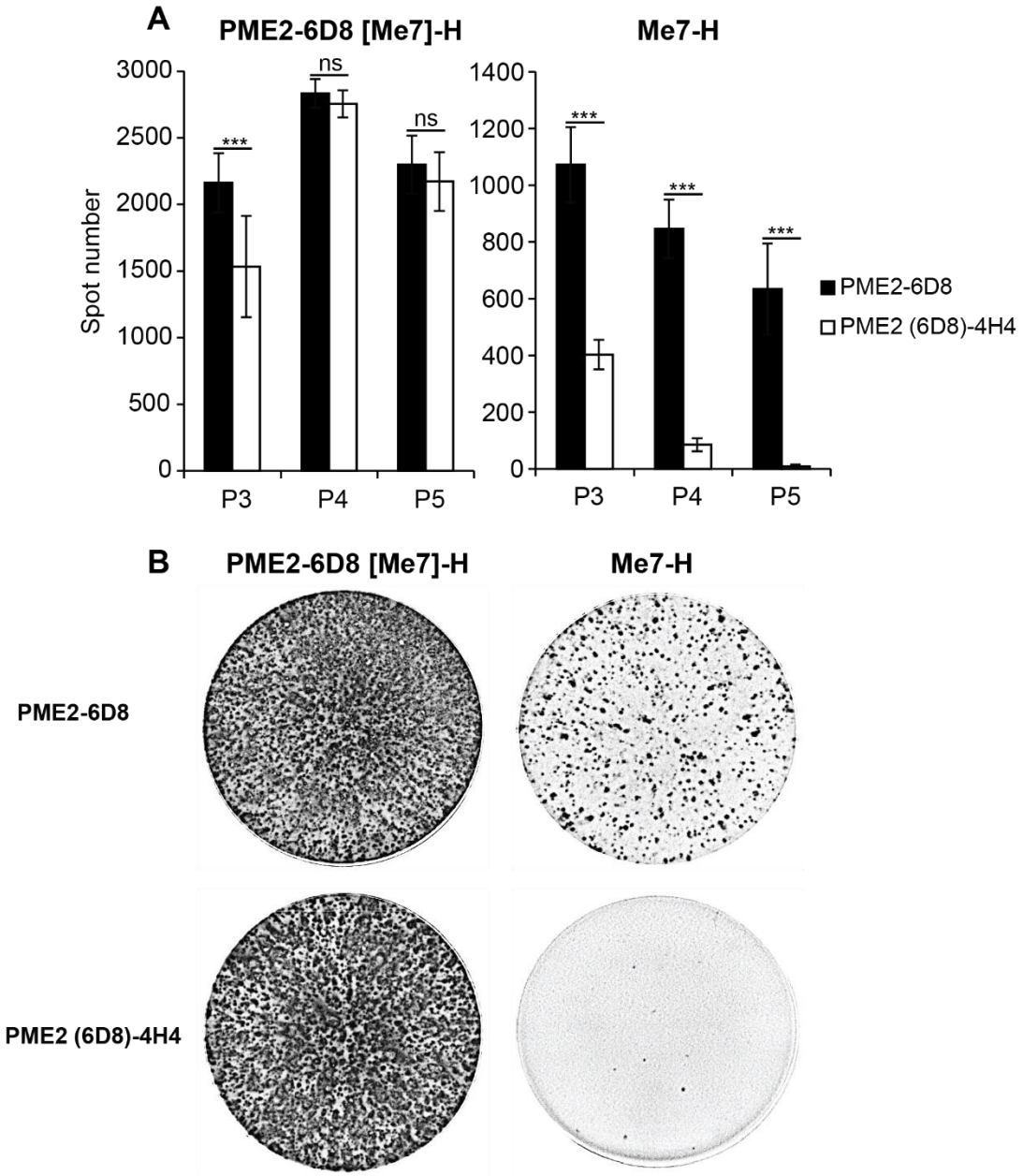

Figure 3.9 The resistant PME2 (6D8)-4H4 clone is highly susceptible to cell-adapted Me7 A. The PME2 (6D8)-4H4 cell clone and the PME2-6D8 clone were challenged with Me7 brain (**Me7-H**) and Me7-infected cell homogenate (**PME2-6D8 [Me7]-H**) at a $1x10^{-4}$ and 1/5000 dilutions respectively. The number of PrP^{Sc}-positive cells for each clone was assessed in Elispot assays at the 3rd, 4th and 5th passage. Twelve wells of a 96 well plate were challenged with each homogenate. Bars represent mean of spot numbers ±Standard Deviation. Statistical significance was calculated using Student's t-test, for PME2-6D8 [Me7]-H; ****p<0.0005*, *ns=not significant*, for Me7-H; ****p<0.0001* **B.** Representative wells of an Elispot plate are saturated with PrP^{Sc}-positive cells following challenge of PME2-6D8 and PME2 (6D8)-4H4 cell clones with Me7-infected cell homogenate (left wells). Susceptibility of the PME2-6D8 clone to Me7 brain homogenate is represented by the high number of PrP^{Sc}-positive cells (top right well).

This phenotype is absent when the PME2 (6D8)-4H4 clone is challenged with the Me7 brain homogenate (bottom right well).

Experiments conducted so far have shown that, upon passage in PME2 cells, the strain properties of Me7 changed (**Figures 3.6 C**, **3.7**, and **3.9**). When compared to Me7, cell-adapted Me7 was characterised by different electrophoretic mobility and glycosylation pattern (**Figure 3.6 C**). Additionally, Me7 and cell-adapted Me7 could be discriminated by marked differences in cell tropism. While Me7 was only propagated by Me7-susceptible PME2 cell clones, cell-adapted Me7 was propagated by PK1, CAD5, as well as Me7-refractory PME2 clones.

3.1.5 Cell-adapted Me7 and Cell-adapted RML are two distinct prion strains

3.1.5.1 Cell-adapted RML and Cell-adapted Me7 can be discriminated by differences in their sensitivity to Proteinase K digestion

In section **3.1.4**, we showed that passage of Me7 in PME2 cells, evoked a change in strain properties, rendering cell-adapted Me7 and RML indistinguishable in their tropism to PK1 and CAD5 (**Figures 3.7, 3.8**). Even though PK1 and CAD5 cells are refractory to Me7, these cell lines were equally susceptible to cell-adapted Me7 (**Figure 3.7**). A plausible explanation for the similarities in cell tropism between RML and cell-adapted Me7, is that cell-adapted Me7 is an “RML-like” conformational variant.

In vivo, Me7 and RML can be discriminated by distinct incubation times and patterns of neuropathology (Karapetyan *et al.*, 2009). Additionally, the two strains were shown to exhibit differences in their conformation (Legname et al., 2006, Thackray, Hopkins, Klein, & Bujdoso, 2007) and glycosylation profiles (Thackray et al. 2007; Wenborn et al. 2015).

Since cell-adapted Me7 is propagated by PK1 cells, we asked whether Me7 has become more “RML-like”, upon passage in PME2 cells. To address this question, we employed a classical, strain-typing approach. Resistance to protease digestion is used to characterise prion strains (Kuczius and Groschup 1999; Safar et al. 1998; J Safar, Cohen, and Prusiner 2000; Morales 2017).

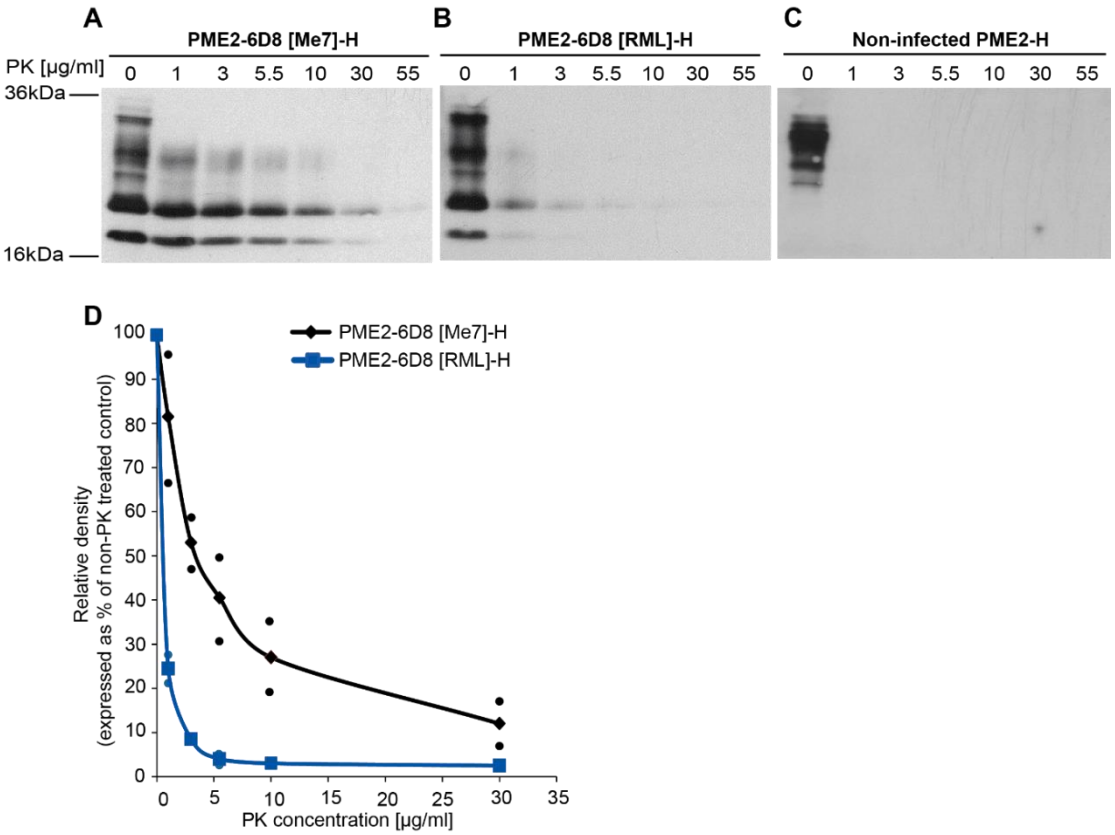

Figure 3.10 Cell-adapted Me7 and cell-adapted RML prions are markedly different in their sensitivity to Proteinase K digestion A, B, C. A pool of three Me7- and RML-infected PME2-6D8 clones were used to generate homogenates by ribolysation. Me7 and RML-infected cell homogenates as well as a non-infected PME2 homogenate were all digested with Proteinase K (PK) at concentrations from 1 to 55 µg/ml and run on SDS-PAGE. PrP was detected with ICSM35b (1:10 000). The Western blots are representative of three independent experiments. **D.** ImageJ was used to quantify the PrP signal in the Me7-infected and RML-infected cell homogenates, respectively. For each PK-digested sample, the PrP^{Sc} signal is expressed as a percentage of the PrP signal in the undigested cell homogenate. For each PK-treated sample, two readings (represented by circles) were taken. Points on the line represent the average of the two readings.

Me7 and RML infected PME2 cell homogenates were treated with Proteinase K at concentrations from 1 to 55 µg/ml. Results demonstrated that PME2 cell-adapted Me7 was significantly more resistant to proteolysis by PK when compared to PME2 cell-adapted RML (**Figure 3.10 A, B, D**). At the lowest PK concentration used, 1µg/ml, a remarkable 75% of cell-adapted RML PrP^{Sc} was digested whereas at the same PK concentration, only 12% ± 20% of cell-adapted Me7 PrP^{Sc} was degraded (**Figure 3.10 A, B, D**). At 3 µg/ml PK, over 50% of cell-adapted Me7 PrP^{Sc} signal was retained whereas at the same PK concentration, less than 10% of cell-adapted RML PrP^{Sc} signal was detectable (**Figure 3.10 A, B, D**). The non-infected PME2 clone was used

to determine the PK concentration at which cellular PrP (PrP^{c}) is completely digested, ensuring that any signal detected in the prion-infected homogenates originates from PrP^{Sc} and not from PrP^{c}. As the PrP signal in the non-infected PME2 homogenate disappeared completely at 1 µg/ml PK (**Figure 3.10 C**), this confirmed that any signal detected in the prion-infected cell homogenates treated with PK concentrations of 1 µg/ml and higher, originates solely from PrP^{Sc}.

In conclusion, cell-adapted Me7 and cell-adapted RML are very different with regards to their sensitivity to PK digestion, demonstrating that Me7 did not "mutate" to an "RML-like" variant upon passage in PME2 cells. It has been reported that differential sensitivity to PK digestion reflects conformational differences possibly stemming from aggregate size and stability (Saverioni *et al.*, 2013).

3.1.5.2 ***Supplementary*: Cell-adapted Me7 and cell-adapted RML can be discriminated by differences in LD9 cell tropism**

We have previously shown that cell-adapted Me7 and cell-adapted RML are differentially sensitive to PK digestion despite being indistinguishable in their tropism to PK1 and CAD5 cells. We asked whether cell-adapted Me7 and cell-adapted RML can be discriminated by their tropism to a different cell line.

It has been shown by Mahal and colleagues that the murine fibroblast cell line LD9 exhibits equal susceptibility to Me7 and RML (Mahal *et al.*, 2007). Experiments conducted in this project showed that LD9 was only weakly susceptible to RML and its susceptibility to RML did not increase even after a round of subcloning (**Table 3.4, Figure 3.14**). After two rounds of subcloning, we derived the LD9 (3E11)-1E9 clone with significantly enhanced susceptibility to Me7 but with low susceptibility to RML (**Figures 3.13 A**). Therefore, in our hands, Me7 and RML could be discriminated by differences in LD9 cell tropism (**Figure 3.11 A, Table 3.4**). To determine whether cell-adapted Me7 and cell-adapted RML can also be discriminated by differences in LD9 cell tropism, we challenged the LD9 (3E11)-1E9 subclone with Me7- and RML-infected cell homogenates and prion propagation was assessed in Elispot assays at passages 3, 4 and 5.

Figure 3.11 shows that cell-adapted Me7 and cell-adapted RML can be discriminated by differences in LD9 cell tropism. Importantly, LD9 cells were significantly more susceptible to cell-adapted Me7 compared to cell-adapted RML, reminiscent of their differential susceptibility to Me7 and RML prion strains respectively (**Figure 3.11**). These findings indicated that the changes in Me7 strain properties that occurred upon

passage in PME2 cells, did not significantly change the susceptibility of LD9 cells to cell-adapted Me7. This might be explained by the fact that, upon passage of Me7 in PME2 cells, some strain-specific properties of Me7 associated with LD9 cell tropism, are retained.

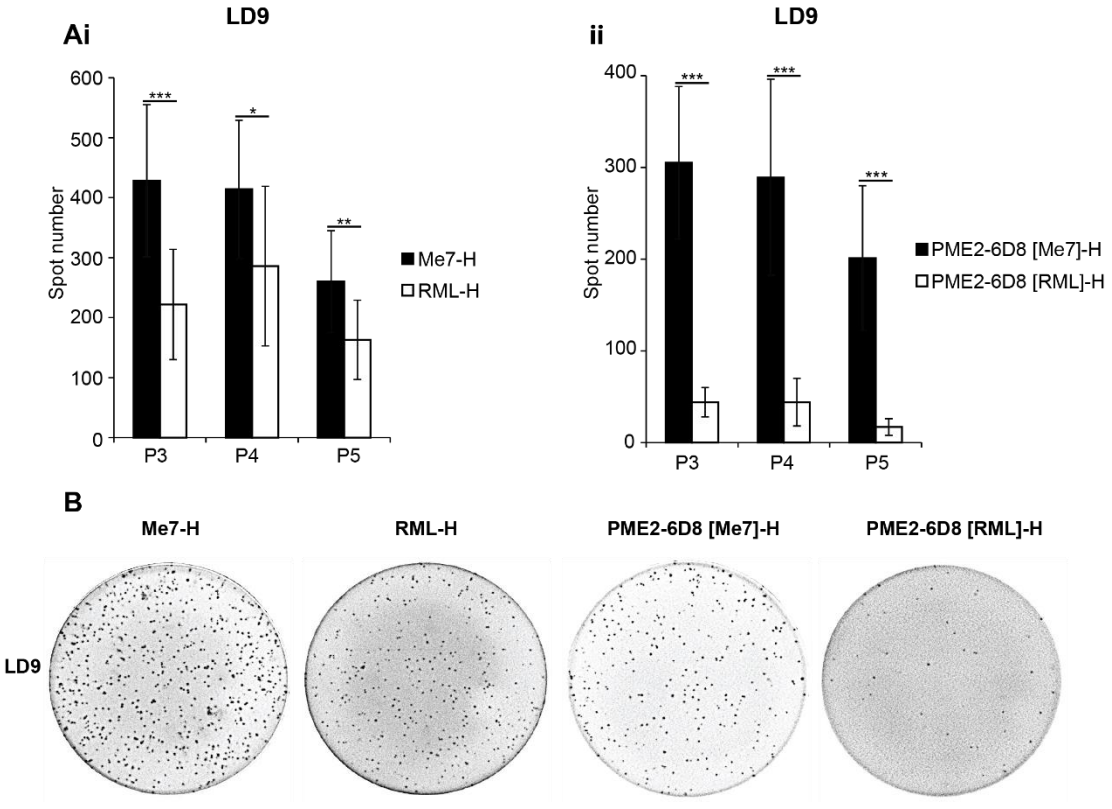

Figure 3.11 Susceptibility of LD9 cells to brain and cell-adapted RML and Me7 prions respectively A. LD9 (3E11)-1E9 cells were challenged with prion-infected brain and cell homogenates. Cells were infected with Me7 (**Me7-H**) and RML (**RML-H**) brain homogenates at a $1x10^{-5}$ dilution and with Me7 (**PME2-6D8 [Me7]-H**) and RML-infected cell homogenates (**PME2-6D8 [RML]-H**) at 1/500 dilution. The number of PrP^{Sc}-positive cells was determined in Elispot assays at the 3rd, 4th and 5th passage. Graph **Ai** shows the response of LD9 (3E11)-1E9 cells with brain-adapted Me7 and RML prions, respectively. Graph **Aii** shows the response of LD9 (3E11)-1E9 cells with cell-adapted Me7 and cell-adapted RML, respectively. Twelve wells of a 96 well plate were challenged with each homogenate. Bars represent mean of spot numbers ±Standard Deviation. Statistical significance was calculated using Student's t-test. Graph **A**i; *$p<0.05$, **$p<0.005$, ***$p<0.0005$. Graph **Aii**; ***$p<0.0001$. **B.** Representative wells of an Elispot plate showing PrP^{Sc}-positive LD9 (3E11)-1E9 cells as black spots following challenge with prion-infected brain (Me7-H, RML-H) and cell (PME2-6D8 [Me7]-H, PME2-6D8 [RML]-H) homogenates.

3.1.5.3 ***Supplementary***: Double labelling with two anti-PrP antibodies does not discriminate between cell-adapted Me7 and cell-adapted RML

To date, the development of prion strain-specific antibodies has been hampered by the fact that PrP^{Sc} has the same primary sequence as PrP^{C}. Additionally, PrP^{Sc}-speficic epitopes are often hidden by PrP^{Sc}'s tightly packed multimeric nature, its glycosylation and GPI anchoring. It has been shown by Eri Saijo et al, that C-terminal conformational differences exist between RML, 22L and Me7 as identified by an indirect enzyme-linked immunosorbent assay (ELISA) using the monoclonal antibody 6H10 (Saijo *et al.*, 2016). The authors have shown that the antibody recognizes the folded, abnormal conformations of Me7 and 22L but not RML. Strain-specific differences in immunoreactivity between two strains of Transmissible Mink Encephalopathy have also been reported (R A Bessen and Marsh, 1992a).

We have shown above that cell-adapted Me7 and cell-adapted RML can be discriminated by differences in their sensitivity to PK digestion as well as differences in LD9 cell tropism. We next asked whether the two cell-adapted strains can also be discriminated by differences in immunoreactivity with two different anti-PrP antibodies, 5B2 and 6D11.

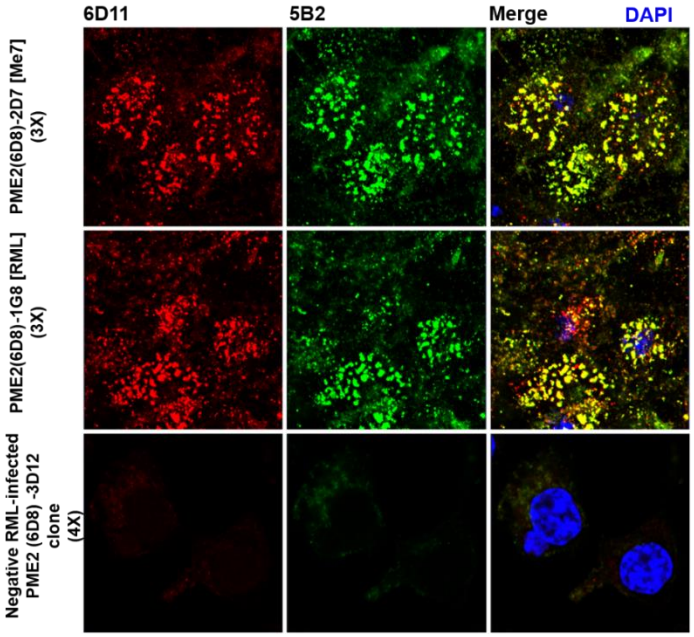

Figure 3.12 Dual labelling with two anti-PrP antibodies does not discriminate between cell-adapted Me7 and cell-adapted RML. Me7-infected and RML-infected PME2-6D8 clones were plated out on chamber slides and the cells were kept in culture for a period of 6 days before fixation with 3.7% Formaldehyde (FA). Dual labelling of the cells with anti-PrP antibodies

5B2 (1:500 dilution) and 6D11 (1:1000 dilution) was carried out after treatment with acetone and 3.5M Guanidinium thiocyanate. The top panel shows an Me7-infected PME2-6D8 clone and the middle panel shows an RML-infected PME2-6D8 clone. The bottom panel shows a PME2-6D8 clone that has been infected with RML but was designated refractory to this strain. The number of PrP^{Sc}-positive cells for this clone was less than 10 and it was therefore used as a negative control for immunostaining.

Antibodies 5B2 and 6D11 recognise the N-terminus and core amino acid residues of PrP respectively. One RML-infected and one Me7-infected PME2-6D8 cell clone were used in this experiment. The two clones were plated out on chamber slides and were allowed to grow for a period of six days before fixation with formaldehyde. As a negative control for immunostaining, a negative, RML-infected PME2-6D8 clone was used. With less than 10 PrP^{Sc}-positive cells, this clone was designated as RML-negative in the SCA, justifying its use as a negative control.
Extracellular PrP^{d} immunoreactive deposits were detected by both antibodies in both the Me7 and RML-infected cell clones, in contrast to the negative clone in which this phenotype was absent (**Figure 3.12**). No phenotypic difference between the two prion strains could be detected based on their immunoreactivity to 5B2 and 6D11, most likely because the aforementioned antibodies are not prion-strain specific (**Figure 3.12**).

3.1.6 ***Supplementary:*** Cell lines other than PK1, as *in vitro* models for prion strain selection

3.1.6.1 LD9 cells

In Sections 3.1.2 and 3.1.3 we showed successful isolation of highly Me7-susceptible clones, derived from the Me7-refractory cell clone PK1. These genetically similar clones only differed in their susceptibility to Me7 and were equally susceptible to RML and 22L. By analysing the transcriptome of such clones, it is possible to identify genetic and epigenetic factors that account for susceptibility to Me7.
To validate genetic/epigenetic factors that account for Me7 susceptibility, gene signatures associated with Me7 susceptibility in one cell line, must overlap with gene signatures associated with Me7 susceptibility in at least one other cell line. This approach requires the identification of Me7-susceptible and Me7-refractory sublines of a cell line other than the PME2. The murine fibroblast cell line LD9 was shown to exhibit equal susceptibility to Me7 and RML (Mahal *et al.*, 2007). Experiments

conducted in this project showed that LD9 was only weakly susceptible to RML, in contrast to published data and its susceptibility to RML did not increase after a round of subcloning (**Table 3.4, Figure 3.14**). However, LD9 susceptibility to Me7 was greatly enhanced by serial single cell cloning (**Figure 3.13, Table 3.4**).

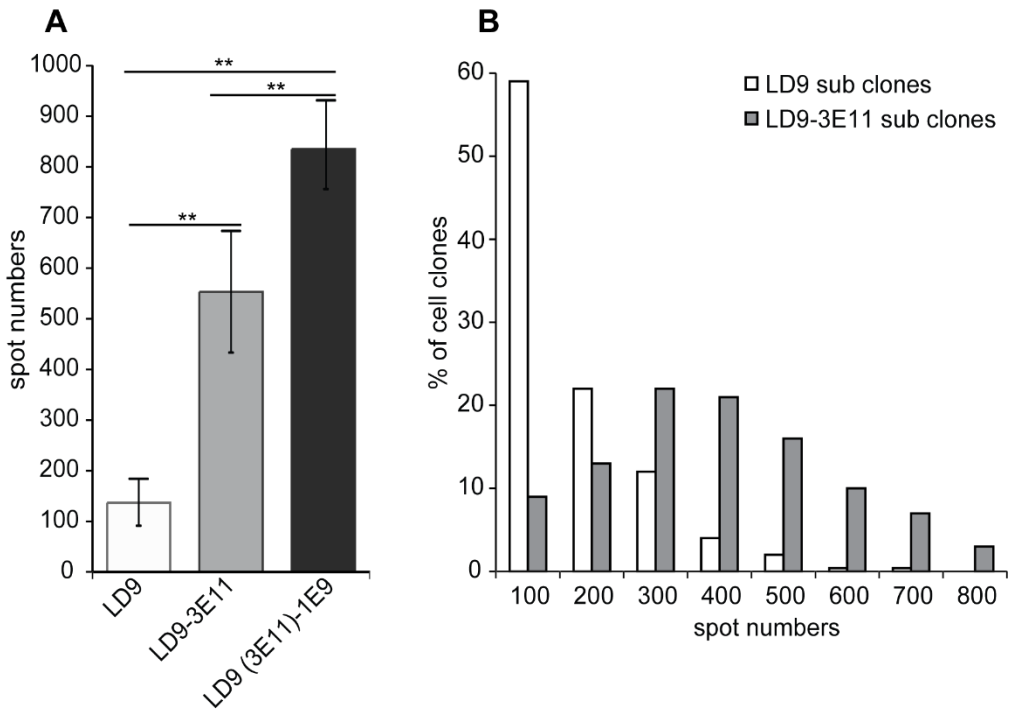

Figure 3.13 Isolation of LD9 clones highly susceptible to Me7 by serial single cell cloning A. LD9 cells were used for the isolation of LD9-3E11, which was in turn used to derive LD9 (3E11)-1E9. The parental line, LD9, as well as LD9-3E11 and LD9 (3E11)-1E9, were challenged with a $1x10^{-5}$ dilution of Me7 brain homogenate and the number of PrP^{Sc}-positive cells was determined in an Elispot assay at cell passage 7. Six wells of a 96 well plate were challenged with a $1x10^{-5}$ dilution of Me7 brain homogenate. Bars represent mean of spot numbers ±Standard Deviation. Statistical significance was calculated using one-way ANOVA, ***p<0.001*. Results are representative of two experiments. **B.** LD9 and LD9-3E11 cell clones were challenged with a $1x10^{-5}$ dilution of Me7 brain homogenate and the number of PrP^{Sc}-positive cells for each clone was determined in an Elispot assay at passage 4. A total of 468 LD9 subclones and 180 LD9-3E11 subclones were isolated in the two experiments, respectively. Spot numbers for the clones isolated in the two sub cloning experiments were binned. The frequency of cell clones in each bin is expressed as a percentage of the total number of clones isolated in each experiment. The x-axis represents spot numbers of individual clones, pooled into bins of 100.

The clones with highest susceptibility to Me7, LD9-3E11 and LD9 (3E11)-1E9, were isolated in two successive single cell cloning experiments respectively. The parental line LD9 was used to derive LD9-3E11 which was in turn used to derive LD9 (3E11)-1E9. LD9-3E11 was subcloned based on its susceptibility to Me7 as determined by an Elispot assay on passage 3 cells (**Table 3.4**).

In two successive single cell cloning experiments, the average number of PrP^{Sc}-positive cells increased from 137 for LD9 cells, to 553 and 835 for LD9-3E11 and LD9 (3E11)-1E9 cell clones respectively, reflecting an increase in susceptibility to Me7 (**Figure 3.13 A**).

The histogram in **Figure 3.13 B** demonstrates that, in two rounds of subcloning, there was a shift from a cell population consisting mostly of cells with low susceptibility to Me7 to a cell population of clones with greatly enhanced susceptibility to Me7 (**Figure 3.13 B**). This is illustrated in **Figure 3.13 B**, which shows that bins with higher spot numbers were more densely populated by LD9-3E11 than by LD9 cell clones.

LD9 subclone	**P3**		**P4**	
	Me7	**RML**	**Me7**	**RML**
5G6	760	267	638	173
3E11	855	146	622	72
5C4	634	133	576	119
5D3	438	21	507	9
3D6	721	138	469	58
1B8	1037	151	464	56
LD9 parental line (n=12)	210±67	83±44	137±64	37±19
LD9-311 subclone	**Me7**			
	P3		**P4**	
1E9	725		735	
2E4	533		725	
2D4	693		709	
1G5	462		707	
2C2	725		703	
1A11	597		691	

Table 3.4 Susceptibilities of representative LD9 and LD9-3E11 clones to Me7 and RML. LD9 and LD9-3E11 clones were challenged with a $1x10^{-5}$ dilution of Me7 brain homogenate. LD9 clones were also challenged with a $1x10^{-5}$ dilution of RML brain homogenate. The number

of PrP^{Sc}-positive cells for each cell clone was determined in Elispot assays at passages 3 (P3) and 4 (P4). The table shows spot numbers for six representative LD9 and six representative LD9-3E11 subclones. As a comparison, the number of PrP^{Sc}-positive cells for the Me7-infected and RML-infected LD9 parental line was also determined. For this cell line, spot numbers represent average of 12 wells ± Standard Deviation.

For LD9-3E11 clones, a steady increase in the number of PrP^{Sc}-positive cells was observed between passages 3 and 4 (**Table 3.4**). Contrary to this observation, for the majority of Me7-infected LD9 clones, the number of PrP^{Sc}-positive cells dropped by passage 4 (**Table 3.4)**. These findings suggest that serial subcloning of LD9 cells led to an overall increase in the number of Me7-susceptible clones and also increased the number of clones that can sustain an infected state.

As mentioned in chapter **3.1.5.2**, the LD9 cell line exhibits low susceptibility to RML and single cell cloning did not enhance the susceptibility of sibling clones to RML (**Table 3.4**, **Figure 3.14**). Notably, 93% of RML-challenged LD9 clones consisted of less than 100 PrP^{Sc}-positive cells and no RML-infected clone with a spot number over 300 could be isolated. As shown in **Figure 3.14**, bins with spot numbers over 400 were exclusively occupied by Me7-challenged cell clones.

In conclusion, serial subcloning increased the number of Me7-susceptible LD9 clones. In contrast to PME2-6D8 clones that maintained a persistently-infected state after challenge with Me7 (**Tables 3.2**, **3.3**), spot numbers of Me7-challenged LD9-3E11 clones were considerably lower (less than 750 spots at P4), questioning the usefulness of LD9 cells as a robust, *in vitro* model for the identification of factors that account for Me7 susceptibility.

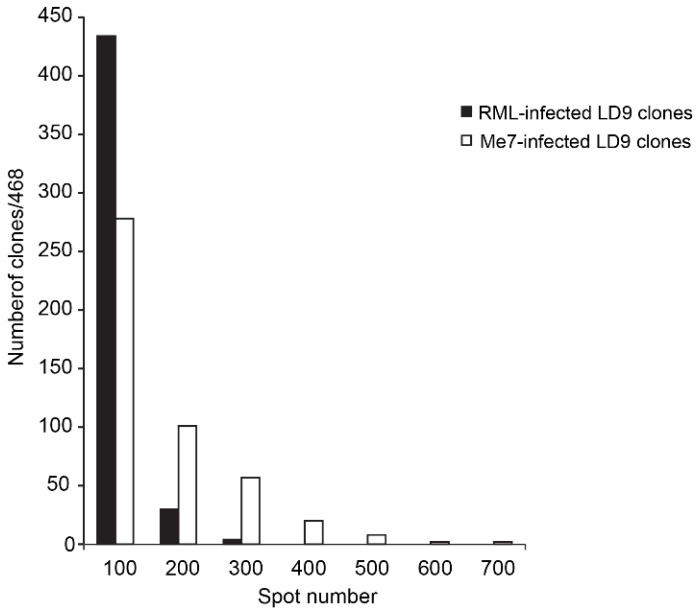

Figure 3.14 Susceptibility of LD9 clones to RML and Me7 A total of 468 LD9 clones were challenged with a $1x10^{-5}$ dilution of RML and Me7 brain homogenates respectively, and the number of PrP^{Sc}-positive cells was assessed in an Elispot assay at passage 4. Spot numbers of Me7- and RML-infected clones were pooled into bins of 100 spots.

3.1.6.2 CAD5 cells

The murine CNS catecholaminergic cell line CAD5, was shown by others to be susceptible to Me7 (Mahal *et al.*, 2007), making it a potentially attractive *in vitro* model for the identification of factors associated with Me7 susceptibility. In our hands, CAD5 cells did not appear to be susceptible to Me7, returning a mean of only 24 spots at passage 7, following challenge with the highest homogenate concentration ($1x10^{-3}$). In contrast, when challenged with 22L and RML, CAD5 spot numbers were 447 and 312 respectively (**Figure 3.15 A**).

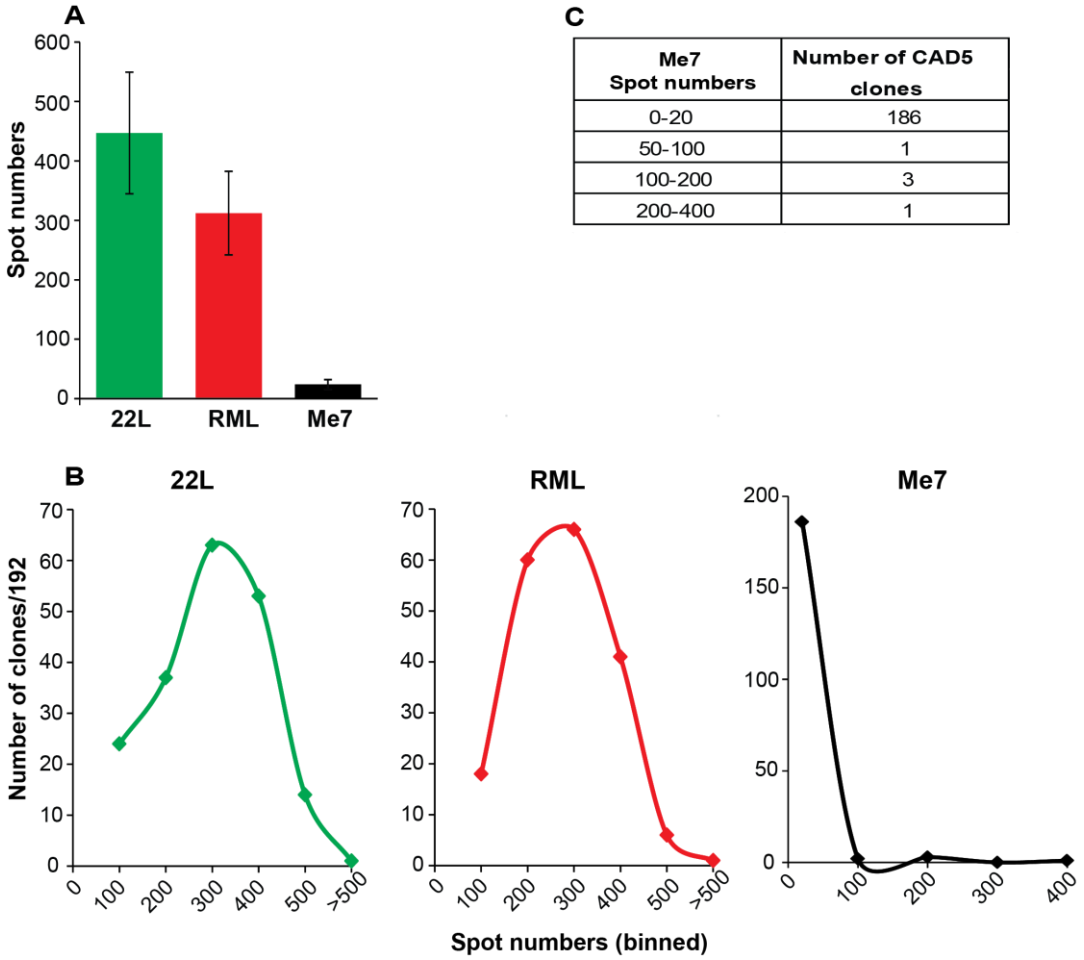

Figure 3.15 Heterogeneous pools of CAD5 cells and CAD5 sublines are highly susceptible to RML and 22L but not to Me7 A. Heterogeneous pools of CAD5 cells were challenged with 22L, RML and Me7 brain homogenates at a $1x10^{-3}$ dilution. At passage 7, the number of PrP^{Sc}-positive cells was determined in an Elispot assay. Twenty-four wells of a 96 well plate were challenged with each brain homogenate. Bars show mean of spot numbers ± standard deviation. Results represent one experiment. **B.** At passage 7, prion-infected CAD5 cells were plated out at limiting dilution and single cell clones were isolated 11 days later. A total of 192 single cell clones were isolated for each prion strain and the number of PrP^{Sc}-positive cells for each clone was determined in an Elispot assay at passage 3. The histograms show the distribution of CAD5 clones in each spot number bin for 22L-, RML-, and Me7-challenged CAD5 cell clones. The x-axis represents spot numbers of individual clones, pooled into bins of 100. For Me7-infected clones, the first bin is 0-50. **C.** The table shows the number of Me7-infected CAD5 clones in each spot number bin.

To determine whether chronically prion-infected CAD5 sublines can be isolated, CAD5 cells were challenged with 22L, RML and Me7 brain homogenates at a $1x10^{-3}$ dilution and single cell clones were isolated 11 days later. The susceptibilities of CAD5 sibling clones to the aforementioned prion strains reflected the susceptibility of the parental

CAD5 cell line to the three strains (**Figure 3.15**). Overall, CAD5 sibling clones exhibited the highest susceptibility to 22L, with 35% of the 22L-challenged clones giving spot numbers between 400 and 500. For RML-infected clones, 25% of the clones gave spot numbers between 400 and 500. In contrast to these observations, only 0.5% of the Me7-infected CAD5 clones with spot numbers between 300 and 400 could be isolated.

Morphologically, CAD5 cells grew in clamps. This phenotype imposed challenges during single cell cloning as a significant proportion of clones detached from the plate surface and were therefore lost. Additionally, these clones in suspension could have potentially "contaminated" the homogeneous cell population of a clone straight after its isolation. Their poorly adherent nature rendered CAD5 cells unsuitable for immunofluorescence studies as all the processing steps led to a significant loss of cells.

The low susceptibility of CAD5 cells to Me7 and the very low frequency at which Me7-susceptible CAD5 clones occurred, led us to the conclusion that this cell line is not a suitable model to study Me7 prion strain selection.

3.1.7 ***Supplementary:*** Development of a cryopreservation method to maintain early characteristics of subclones with high susceptibility to Me7

To retain the early characteristics of PME2 and PME2-6D8 subclones with regards to their susceptibility to Me7 prion infection and to therefore validate initial findings, we sought to develop and optimise a high throughput cryopreservation method. We have previously shown that rechallenge of originally Me7-susceptible cell clones with Me7 after few passages in cell culture, resulted in complete loss of susceptibility in 5 out of 6 clones even in the absence of an intermediate freeze-thaw cycle (**Figure 3.4 A**).
Cryopreservation in a 96 well format, allowed for increased throughput, however this method appeared to be problematic especially upon resurrection of cell clones from the vapour phase of Liquid nitrogen. It appeared to be very challenging to define the precise amount of time required to achieve simultaneous thawing for all the cell clones. Wells on the inside of a 96 well plate almost always took longer to thaw whereas the ones at the periphery of the plate were the fastest to thaw. Additionally, the removal of the DMSO-containing medium with a multichannel pipette sometimes resulted in cell aspiration by disturbing the monolayer of cells at the base of the well.

Cell stress following resurrection was an apparent phenotype and for some cell clones, none of the cells were viable.

To determine which is the best approach to preserve susceptibility of cell clones to Me7, we employed two different cryopreservation methods. Cryopreservation in a 96 well format allowed for preservation of low passage cell clones. On the other hand, cryopreservation in vials required that all uninfected clones remained in culture until the end of the SCA, at which point Me7-susceptible clones could be identified. Once Me7-susceptible clones were identified, these were expanded from single wells of a 96 well plate to 10cm dishes and were frozen down in vials using conventional methods. Even though the latter method circumvented freezing down in 96 well plates, it involved the cryopreservation of cell clones at a higher passage number.

A selected cohort of 22 Me7-susceptible PME2 clones was resurrected from the vapour phase of liquid nitrogen in a 96 well format and challenged with a $1x10^{-5}$ dilution of Me7 homogenate and an Elispot assay was carried out at passage 3. A drastic reduction in spot numbers was observed for all 22 Me7-challenged cell clones (**Figure 3.16 A**). A greater than 10-fold decrease in the number of PrP^{Sc}-positive cells was noted for 77% of cell clones (**Figure 3.16 A**).

In an independent experiment, 9 high passage number Me7-susceptible PME2-6D8 clones were resurrected from vials and challenged with $1x10^{-5}$ dilution of Me7 homogenate. An Elispot assay was carried out at passage 3. Consistent with data of cryopreservation of cells in a 96 well format, there was an overall reduction in the spot number of all Me7-challenged PME2-6D8 clones (**Figure 3.16 B**). However, this reduction was not as pronounced as that observed for cells that had been cryopreserved in a 96 well format. For 78% of Me7-challenged PME2-6D8 clones, a 3-fold or less decrease in spot numbers was observed when comparing the response of clones before and after cryopreservation (**Figure 3.16 B**).

Importantly, some PME2 and PME2-6D8 cell clones retained their susceptibility to Me7 after a single freeze-thaw cycle, regardless of the method of cryopreservation used, suggesting that the ability to maintain susceptibility to Me7 is also cell clone-specific (**Figure 3.16 C**).

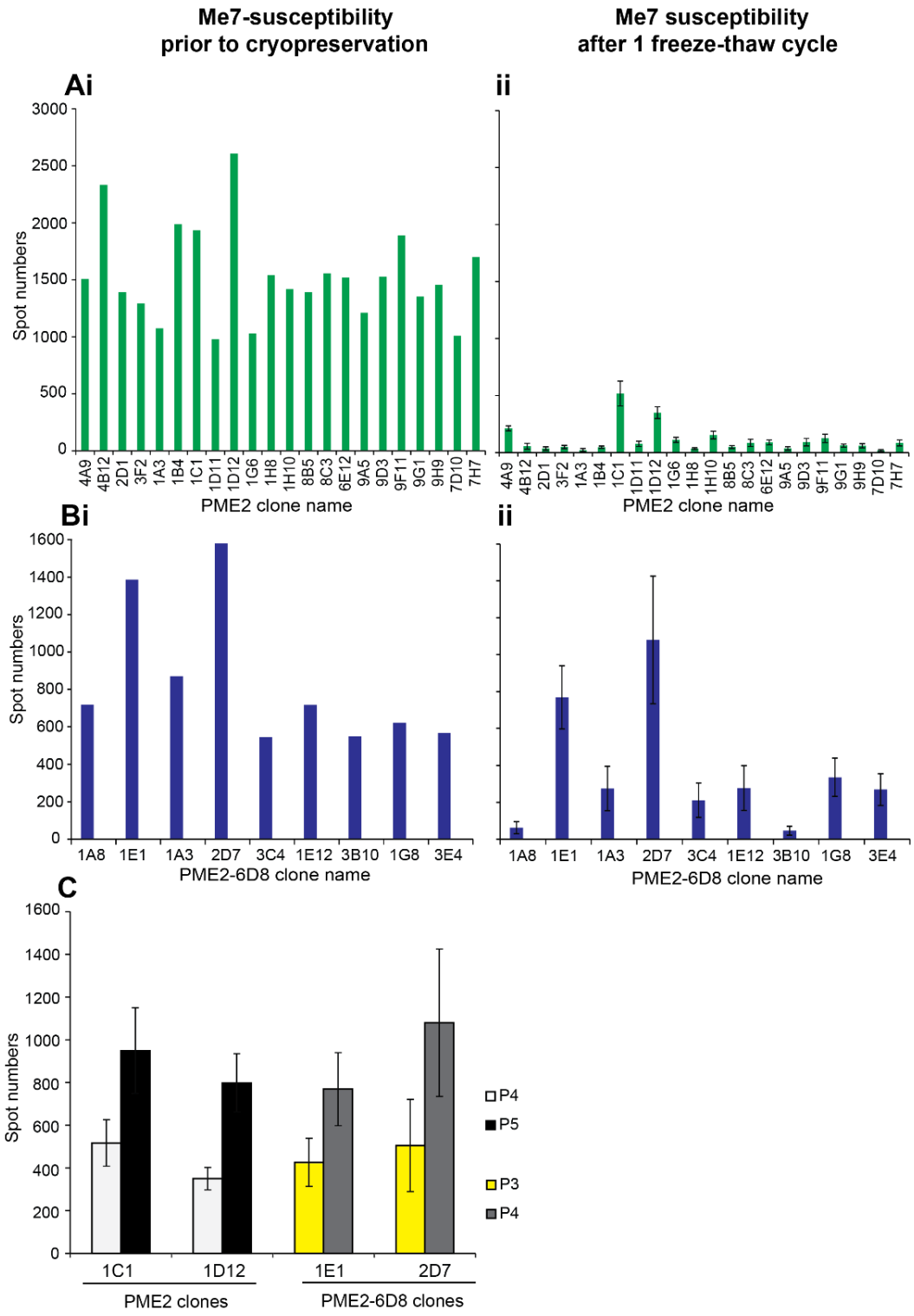

Figure 3.16 The ability to maintain susceptibility to Me7 is cell clone-specific and depends on the method of cryopreservation A. Ai. A total of 864 PME2 clones were challenged with a $1x10^{-5}$ dilution of Me7 brain homogenate. An Elispot assay was carried out at passage 3 and Me7-susceptible clones were identified based on the number of PrP^{Sc}-positive cells per clone. **Aii**. Replicates of PME2 clones were cryopreserved in a 96 well format and transferred to the vapour phase of liquid nitrogen for long-term storage. Upon resurrection, 22

Me7-susceptible cell clones were split, expanded to 4 wells per clone and re-challenged with the same concentration of Me7 homogenate. An Elispot assay was carried out at passage 3 and the number of PrP^{Sc}-positive cells per clone are shown in Graph **Aii.** Bars represent average of four wells per clone ±Standard deviation **B. Bi**. A total of 192 PME2-6D8 clones were challenged with $1x10^{-5}$ dilution of Me7 and an Elispot assay was carried out at passage 3 to identify Me7-susceptible cell clones. **Bii**. Replicates of non-infected PME2-6D8 cell clones were kept in separate 96 well plates in culture, throughout the experiment. Me7-susceptible clones were identified, expanded from a single well of a 96 well plate and cryopreserved in vials and stored in liquid nitrogen. Nine Me7-susceptible clones were revived and challenged with the same dilution of Me7 homogenate. The number of PrP^{Sc}-positive cells per clone was determined in an Elispot assay after passage 3. Bars represent average of twelve wells per clone ±Standard deviation. **C.** Two clones from each cryopreservation/thawing experiment, maintained their susceptibility to Me7 after a single freeze/thaw cycle. Upon resurrection, the two PME2 and PME2-6D8 clones were challenged with Me7 brain homogenate at a $1x10^{-5}$ dilution and the number of PrP^{Sc}-positive cells per clone was determined at passage 4 (P4) and 5 (P5) for the PME2 clones and at passage 3 (P3) and 4 (P4) for the PME2-6D8 clones. Bars represent average spot numbers of 4 wells for PME2 clones, and average spot numbers of 12 wells for PME2-6D8 clones ±Standard deviation.

3.1.8 ***Supplementary:*** Rare variant PME2 subclones selectively propagate distinct prion strains

Even though all PME2-6D8 clones were equally susceptible to RML and 22L (**Table 3.3**), we noticed that the response of individual PME2 subclones to RML and 22L varied. During the subcloning of PME2, we identified 11 variants that propagated RML or 22L selectively (**Table 3.5**). Rare variant PME2 cell clones that are exclusively susceptible to either RML or 22L (**Table 3.5**) provide a useful *in vitro* model to identify potential gene signatures associated with susceptibility to RML and 22L respectively. A study by Marbiah et al., compared the transcriptome of prion-resistant and prion-susceptible PK1 subclones and showed that genes that regulate extracellular matrix remodelling and differentiation state, influence susceptibility to prion infection (Marbiah *et al.*, 2014).

22L-preferring subclones comprised 0.5% of the cell clone population whereas RML-preferring subclones comprised 0.6% of the cell clone population (**Table 3.5**). Each clone was assigned a selectivity score (SS) where SS= RML_{spots} **/** (RML_{spots} +$22L_{spots}$), which is a relative measure of the susceptibility of a cell clone to any two prion strains (**Table 3.5**). The Selectivity Score was used to assess whether a particular cell clone

is equally susceptible to both 22L and RML (SS of approximately 0.5), is susceptible to RML but not to 22L (SS of approximately 0.9-1) or susceptible to 22L but not RML (SS of approximately 0.1).

22L preferring					
PME2 subclone	**RML**	**22L**	**Me7**	**SS**	**22L FD**
10G10	385	2114	17	0.15	5
2H11	148	1727	16	0.08	12
5C11	555	2176	11	0.20	4
9F8	299	1761	7	0.15	6
5A4	516	2580	5	0.17	5
RML preferring					
PME2 subclone	**RML**	**22L**	**Me7**	**SS**	**RML FD**
10A12	1978	10	12	0.99	198
10F5	2003	29	17	0.99	69
10D10	1730	33	18	0.98	52
8G2	2174	60	23	0.97	36
10D7	1918	69	4	0.97	28
10D1	2076	85	14	0.96	24

Table 3.5 PME2 sibling clones show very different relative susceptibilities to RML and 22L. PME2 clones were challenged with a $1x10^{-5}$ dilution of RML and Me7 brain homogenates respectively, and with a $1x10^{-6}$ dilution of 22L homogenate. An Elispot Assay was carried out at passage 3 to determine the number of PrP^{Sc}-positive cells for each cell clone, for each prion strain. SS=Selectivity Score, FD=Fold difference. 22L FD was calculated by dividing 22L spot numbers by RML spot numbers for each clone. RML FD was calculated by dividing RML spot numbers by 22L spot numbers for each clone.

Following single cell cloning of PME2, 960 subclones were challenged with a $1x10^{-5}$ dilution of RML and Me7 respectively, and $1x10^{-6}$ dilution of 22L. The number of PrP^{Sc}-positive cells for each clone was assessed in an Elispot assay at passage 3. Susceptibilities of all clones to one prion strain were plotted against their susceptibilities to another prion strain (**Figure 3.17**).

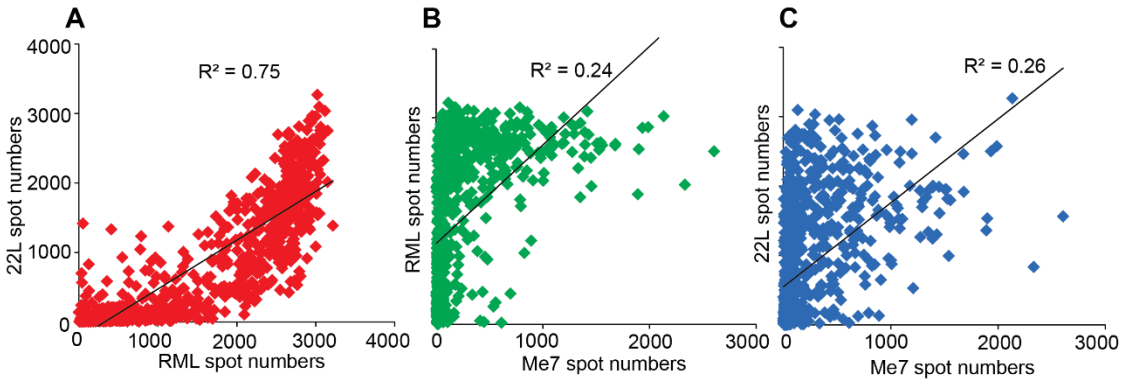

Figure 3.17 Correlating susceptibilities of PME2 clones to three mouse-adapted prion strains A, B, C Following challenge with a $1x10^{-5}$ dilution of RML and Me7 respectively, and a $1x10^{-6}$ dilution of 22L, the number of PrP^{Sc}-positive cells for each PME2 cell clone was assessed in an Elispot assay. For all the prion-infected clones, spot numbers of one prion strain were plotted against spot numbers of another prion strain. The line of best fit and correlation coefficients are shown for each scattergram. For each clone, n=1, and scatter plots represent one single cell cloning experiment.

As expected, a strong correlation was observed between RML-and 22L-susceptible PME2 clones (R^2=0.75) **(Figure 3.17 A**). The majority of PME2 subclones were highly susceptible to both RML and 22L, consistent with the high susceptibility of the parental PK1 cell line to the aforementioned prion strains. In contrast to these observations, there was little correlation between the spot numbers of clones to either RML or 22L and their spot numbers to Me7 (R^2=0.24 and R^2= 0.26 respectively) (**Figure 3.17 B, C**). This was not surprising, given the fact that the majority of PME2 clones were refractory to Me7 but susceptible to both RML and 22L.

Overall, Me7-susceptible clones occurred at a lower frequency compared to RML and 22L-susceptible clones (**Figure 3.17**). In the final subcloning experiment (See **Section 3.1.3**), 63% of the PME2-6D8 clones were susceptible to Me7 and 100% of the clones were susceptible to both RML and 22L. These findings suggest that the probability of isolating an Me7-susceptible clone that is refractory to both or either RML and 22L is negligible. However, PME2-6D8 sublines that are differentially susceptible to Me7 but equally susceptible to RML and 22L, can be used to identify cell-specific factors that account for susceptibility to Me7 (**Section 3.1.3.2, Table 3.3**).

4 Results (The role of Fkbp proteins in molecular mechanisms of prion propagation)

4.1 Determining mRNA knock down in *Fkbp* stably silenced N2aPK1 cell lines

A microarray gene expression study identified *Fkbp9* as a prion modifier gene (Brown *et al.*, 2014). Additionally, knock down (KD) of *Fkbp10* in scrapie-infected cells had an inhibitory effect on prion propagation (Stocki *et al.*, 2016). Given the role of Fkbp proteins in prion propagation, and their well-established role in neurodegeneration, the aim of this project was to study the role of Fkbp9 as well as other Fkbp proteins on prion propagation. This was done by stable gene silencing of *Fkbp* candidate genes in the RML-susceptible mouse neuroblastoma cell line N2aPK1 (PK1).

The aim was to generate at least 2 cell lines with a stable KD of *Fkbp* genes by at least 50% to ensure reproducible results and to reduce the possibility of false positive results due to off-target effects. This approach was previously employed by others to identify genes that affect prion propagation (Brown *et al.*, 2014). To determine whether *Fkbp* gene KD results in an increase or decrease in prion propagation, the number of PrP^{Sc}-positive cells of the non-targeting GFP control cell line was compared to the number of PrP^{Sc}-positive cells of the *Fkbp*-silenced cell lines.

Quantitative Reverse Transcription Polymerase Chain Reaction (qRT-PCR) was used to quantify the level of mRNA knock down of the target gene in each cell line (**Table 4.1**). Four candidate *Fkbp* genes were targeted by generating a total of 28 stably silenced cell lines. All 4 genes were well expressed in N2aPK1 cells, rendering them suitable for a knock down approach. The mean mRNA knock down of cell lines tested in the SCA was 57% for *Fkbp1a*, 71% for *Fkbp4*, 68% for *Fkbp5* and 66% for *Fkbp8*. mRNA expression levels of *Fkbp* genes were normalised to *GAPDH* expression in all the cell lines, and measured relative to the control cell line GFPsh1.

Gene	Cell line	% mRNA KD
Fkbp1a **(12)**	Fkbp1a-sh1	61
	Fkbp1a-sh2	53
	Fkbp1a-sh3	66
	Fkbp1a-sh4	38
	Fkbp1a-sh5	61
	Fkbp1a-sh6	45
	Fkbp1a-sh7	58
	Fkbp1a-sh8	0
Fkbp4 **(52)**	Fkbp4-sh1	61
	Fkbp4-sh2	56
	Fkbp4-sh3	82
	Fkbp4-sh4	85
Fkbp5 **(51)**	Fkbp5-sh1	80
	Fkbp5-sh2	54
	Fkbp5-sh3	44
	Fkbp5-sh4	26
	Fkbp5-sh5	70
	Fkbp5-sh6	77
	Fkbp5-sh7	85
	Fkbp5-sh8	26
Fkbp8 **(38)**	Fkbp8-sh1	21
	Fkbp8-sh2	9
	Fkbp8-sh3	73
	Fkbp8-sh4	65
	Fkbp8-sh5	66
	Fkbp8-sh6	50
	Fkbp8-sh7	78
	Fkbp8-sh8	39

Table 4.1 Percentage level of mRNA knock down following transcriptional silencing of *Fkbp* gene targets (*Fkbp1a, Fkbp4, Fkbp5, Fkbp8*) in N2aPK1cells. To determine the percentage of knock down (KD), mRNA expression levels were measured using qRT-PCR, normalised to *GAPDH* and relative to the control cell line (*GFP*-sh1). The protein name corresponding to each *Fkbp* gene is shown in brackets.

4.2 Scrapie Cell Assay (SCA) of *Fkbp* silenced N2aPK1 cell lines

To determine the effect of target gene knock down on prion propagation, each cell line with a knock down of at least 50% was challenged with the RML prion strain and prion propagation was assessed in three independent SCAs. Normalised spot numbers from the average of three independent SCAs are shown in **Figure 4.1**.
The growth rate and differentiation status of N2aPK1 cells are factors that can affect the final number of PrP^{S}-positive cells at the end of the assay. The SCA output was controlled by plating a defined number of cells per well (25 000) onto the ELISPOT plate for final counting.

A significant reduction in the number of PrP^{Sc} positive cells ($p<0.005$) was observed for three out of six *Fkbp1a* knock-down cell lines (Fkbp1a-sh2, Fkbp1a-sh5 and Fkbp1ash-6), whereas *Fkbp1a* gene silencing in cell lines Fkbp1a-sh1, Fkbp1a-sh3 and Fkbp1a-sh7 had no effect on the number of PrP^{Sc}-positive cells (**Figure 4.1**). Therefore, for cell lines Fkbp1a-sh1, Fkbp1a-sh3 and Fkbp1a-sh7, the low levels of *Fkbp1a* mRNA expression did not lead to a corresponding reduction in the number of PrP^{Sc}-positive cells (**Table 4.1, Figure 4.1**).

Three out of four *Fkbp4* cell lines, two out of five *Fkbp5* cell lines and four out of five *Fkbp8* cell lines showed a significant reduction of the number of PrP^{Sc}-positive cells ($p < 0.005$, **Figure 4.1**).

For *Fkbp5*, 2 cell lines gave a significant reduction in the number of PrP^{Sc} positive cells ($p<0.005$**, Figure 4.1**). These two cell lines (Fkbp5-sh6 and Fkbp5-sh7) had a mean level of mRNA knock down of 81% (**Table 4.1**). The 80% level of *Fkbp5* mRNA knock down in cell line Fkbp5-sh1 did not generate a corresponding reduction in the number of PrP^{Sc}-positive cells, as reported by the SCA (**Table 4.1**, **Figure 4.1**). This might be due to an off-target effect of Fkbp5-sh1. An off-target effect occurs when an shRNA down regulates unintended targets by having partial sequence complementarity with other gene targets. The less pronounced effect of *Fkbp5* knock down in spot number makes the data for *Fkbp5* inconclusive.

Knock down of *Fkbp8* in N2aPK1 cells caused highly significant reductions ($p<0.005$) in spot number in 4 out of the 5 cell lines screened in the SCA (**Figure 4.1**). Even though *Fkbp8* mRNA levels were reduced by 73% in the Fkbp8-sh3 cell line (**Table 4.1**), there was no corresponding reduction in the number of PrP^{Sc}-positive cells when compared to the control GFP-sh1 cell line (**Figure 4.1**).

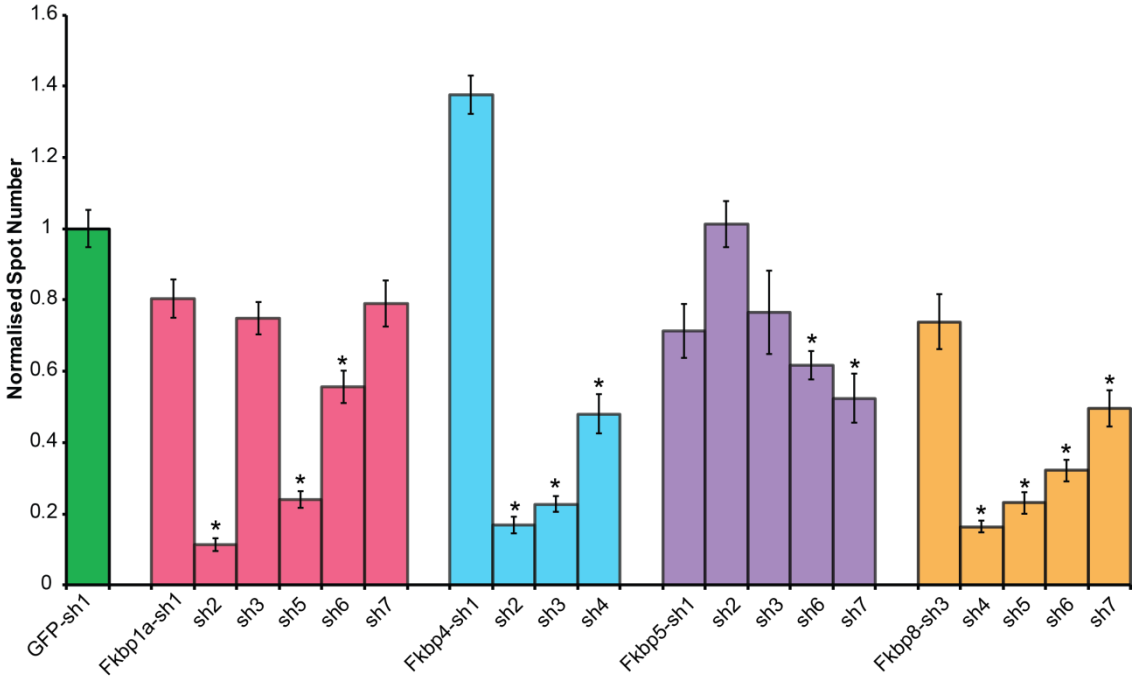

Figure 4.1 Quantification of the number of PrP^{Sc}-positive cells following stable transcriptional silencing of *Fkbp* genes in PK1 cells. Stable gene silenced (shRNA) N2aPK1 cell lines together with a control cell line (*GFP* shRNA), were infected with a $1x10^{-5}$ dilution of RML brain homogenate and the number of PrP^{Sc}-positive cells was determined in an Elispot assay after 3 cell passages. Average PrP^{Sc} spot numbers from three independent assays are shown normalised to the control cell line (green bar) ± standard error of the mean (sem). *P<0.005. For each cell line, data from three independent SCAs (10 wells per assay) were normalised to the spot number obtained from the control cell line (GFP-sh1) for statistical analysis using a *t*-test.

4.3 Transient transcriptional silencing of *Fkbp* genes in RML-chronically infected N2aPK1 cells

To examine whether an independent gene silencing approach for the examined gene targets recapitulates the results of stable silencing, custom made siRNAs, ordered from IDT, were used to transiently knock down *Fkbp* genes in N2aPK1 cells, chronically infected with RML (iS7 cells) (Klohn *et al.*, 2003). In contrast to *de novo* infected PK1 cells, in iS7 cells, prion infection is established. This means that *Fkbp* gene silencing in iS7 cells will not detect gene effects that modify early events such as uptake of prion infectivity.

According to the manufacturer, at least one of the first three siRNAs, selected with a proprietary algorithm of the manufacturer, yields a 70% or lower knock down. Transient knock-down of *Prnp* served as a control. Four siRNAs were sourced for

each *Fkbp* gene. Knock down of a target gene lasts for at least 3 days. These siRNAs remain to be characterised to determine the level of mRNA knock down in each case. SiRNAs targeting *Fkbp9* and *Fkbp10,* which have previously been implicated in prion propagation, were also tested. Transient silencing of the target *Fkbp* genes was carried out by reverse transfection and the number of PrP^{Sc}-positive cells was then determined by the SCA.

Surprisingly, none of the siRNAs against the specified *Fkbp* genes reduced the number of PrP^{Sc} positive iS7 cells (**Table 4.2**). Previous findings have reported that *Fkbp9* stably silenced cell lines of N_2aPK1 cells show a significant increase in the number of PrP^{Sc} positive cells (Brown *et al.*, 2014). Conversely, in the same study, stable *Fkbp9* overexpression in these cells significantly reduced the number of PrP^{Sc} positive cells. A study by Stocki and colleagues has found that transient silencing of *Fkbp10* in N2a cells induced a significant reduction in PrP^{Sc} levels in these cells (Stocki *et al.*, 2016).

A scrambled siRNA as well as an siRNA directed against *Prnp* were used as positive and negative controls respectively. The fact that none of the Fkbp siRNAs “cured” the cells from RML infection whereas stable knock down of some of these genes in *de novo* infected PK1 cells significantly reduced PrP^{Sc} spot number, may imply that Fkbp proteins do not affect PrP conversion. Instead, the specified *Fkbp* genes may be acting upstream of prion propagation, for example on the uptake of infectivity. If this is the case, this will not be reported by the SCA in transient *Fkbp* knock down in chronically infected cells.

The effect of *Fkbp* siRNA treatment on mRNA and/or protein levels has not yet been determined, which complicates the interpretation of results of the aforementioned assay.

Target	Fold Change	SEM	T-test (corrected)
Prnp	0.41	0.07	1.98E-12
***Fkbp1a* (12)**			
siFkbp1a.1	0.93	0.04	1.80
siFkbp1a.2	1.13	0.04	0.23
siFkbp1a.3	0.87	0.05	0.21
siFkbp1a.4	0.94	0.08	3.33
***Fkbp4* (52)**			
siFkbp4.1	0.93	0.06	3.78
siFkbp4.2	0.73	0.11	0.05
siFkbp4.3	1.00	0.11	8.82
siFkbp4.4	1.17	0.05	0.38
***Fkbp5* (51)**			
siFkbp5.1	1.13	0.06	1.17
siFkbp5.2	1.03	0.06	6.30
siFkbp5.3	1.17	0.04	0.33
siFkbp5.4	1.13	0.03	1.26
***Fkbp8* (38)**			
siFkbp8.1	1.01	0.05	8.19
siFkbp8.2	1.00	0.05	8.64
siFkbp8.3	1.06	0.06	4.32
siFkbp8.4	1.04	0.07	5.85
***Fkbp9* (63)**			
siFkbp9.1	1.03	0.03	4.32
siFkbp9.2	1.01	0.04	8.10
siFkbp9.3	0.99	0.07	7.65
siFkbp9.4	1.29	0.06	0.30

Table 4.2 Fold change in the number of PrP^{Sc}-positive cells following transient transcriptional silencing of *Fkbp* genes on prion propagation in iS7 cells. PrP^{Sc}-positive cells were normalised to total cell numbers (from Trypan Blue Assays). Fold change in the number of PrP^{Sc}-positive spots was calculated relative to the number of spots of the negative control Dicer Substrate siRNA (N.C1) ± sem. Statistical significant difference was calculated using t-test.

4.4 Expression of Recombinant Fkbp9 and Fkbp52 proteins

Optimisation of expression and cloning strategies was employed to successfully induce the expression of recombinant proteins Fkbp9 and Fkbp52 (encoded by the *Fkbp4* gene). Fkbp9 has previously been shown to influence prion propagation (Brown *et al.*, 2014). For *Fkbp4*, three out of four stably silenced cell lines showed a significant reduction in the number of PrP^{Sc}-positive cells. The original aim of the project was to express and purify the aforementioned proteins and then use the recombinant proteins in cell-free assays. The two aims were to: 1. Test for the ability of recombinant Fkbp proteins to modulate the fibrillisation of recombinant PrP^{c}. 2. Employ Protein Misfolding Cyclic Amplification (PMCA), to determine whether recombinant Fkbp proteins affect prion propagation in a cell-free system. PMCA is an *in vitro* technique that mimics prion replication with a similar efficiency to the *in vivo* process (Saborio, Permanne and Soto, 2001). Shortly after optimising the expression of recombinant Fkbp proteins, this project was terminated.

Recombinant proteins Fkbp9 and Fkbp52 were expressed in bacterial cells, following transformation of the cells with the pET-23d(+) -*Fkbp9* and pET-23d(+)-*Fkbp4* plasmid DNA constructs. Protein expression was induced with IPTG. Prior to lysis of bacterial cells for the detection of the recombinant proteins (Fkbp9 and Fkbp52), uninduced bacterial cultures were diluted with LB and OD_{600} readings were taken using Nanodrop Spectrophotometer1000. This was done to ensure that IPTG-induced and uninduced cultures have approximately the same density of bacterial cells. Gel electrophoresis was carried out using bacterial lysates from IPTG-induced and uninduced (control) bacterial cultures.

The recombinant Fkbp9 protein (with a molecular weight of 63kDa) lacking both its ER signal sequence and ER retention motifs was detected adjacent to the molecular weight marker of 64kDa (**Figure 4.2**). This thick band was absent in the uninduced culture, indicating that the BL21 (DE3) bacterial cells have successfully expressed the recombinant protein upon induction with IPTG.

The prominent protein band between the 64kDa and 50kDa molecular weight markers in the IPTG-induced cultures corresponds to the recombinant Fkbp52 protein (**Figure 4.3**). The Fkbp52 protein band was absent from the uninduced bacterial cultures.

The presence of thin bands of the same molecular weight as the recombinant proteins in the uninduced cultures represents the expression of bacterial proteins.

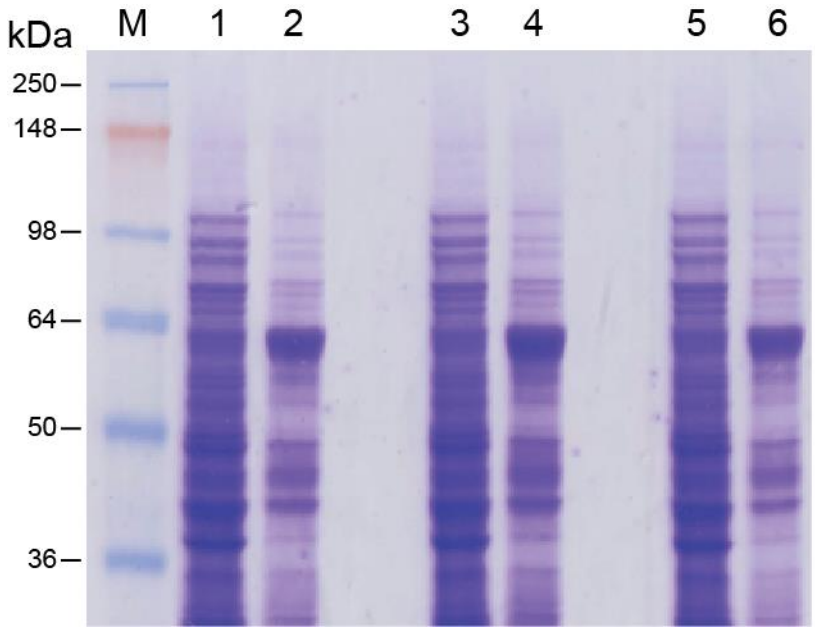

Figure 4.2 Expression of recombinant Fkbp9 protein. Protein separation was carried out using SDS-PAGE gel electrophoresis. The loaded proteins were visualised by Coomassie Blue staining of the gel. BL21(DE3) bacterial lysates from uninduced (lanes 1, 3, 5) and IPTG-induced (lanes 2, 4, 6) cultures were electrophoresed. Molecular-weight markers (M) are indicated to the left. Results are representative of three independent experiments.

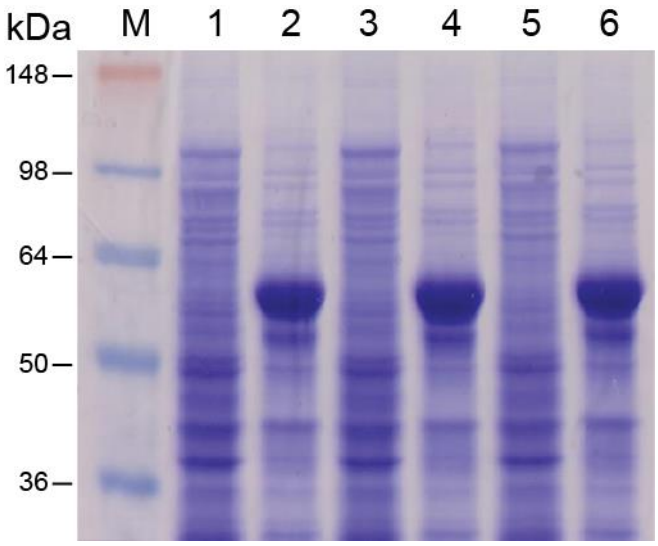

Figure 4.3 Expression of recombinant Fkbp52 protein. Protein separation was carried out using SDS-PAGE gel electrophoresis. The loaded proteins were visualised by Coomassie Blue staining of the gel. BL21(DE3) bacterial lysates from uninduced (lanes 1, 3, 5) and IPTG-induced (lanes 2, 4, 6) cultures were electrophoresed. Molecular-weight markers (M) are indicated to the left. Results are representative of three independent experiments.

5 Discussion

5.1 Towards understanding Selective Neuronal Vulnerability: Establishing an *in vitro* model for strain selection

In this PhD project, I employed single cell cloning and successfully isolated highly Me7-susceptible PK1 sublines from the Me7-refractory neuroblastoma cell line PK1. The first PK1-derived subclone, PME2, was marginally susceptible to Me7 and was used as the progenitor line to derive highly Me7-susceptible cells. Initially, Me7-susceptible PME2 clones were identified at a frequency of only $4x10^{-3}$. In two successive subcloning rounds, the percentage of Me7-susceptible cells increased by 6-fold and 20-fold, respectively, and by the third and final round of subcloning, 63% of cell clones were highly susceptible to Me7. PME2 and PME2-6D8 cell clones challenged with Me7 brain homogenate maintained a persistent state of infection and deposited PrP^{Sc} at the extracellular matrix. Eleven passages after challenge with Me7, susceptible cell clones consisted of over 2000 PrP^{Sc}-positive cells, as quantified using the Scrapie Cell Assay (SCA). Since Me7-susceptible and Me7-refractory PME2-derived cell clones are genetically similar, such cell clones will be instrumental to identify genetic factors that confer susceptibility to Me7.

One of the hypotheses we wanted to test was whether PK1-derived subclones with exclusive susceptibility to any one of the murine prion strain Me7, RML and 22L can be isolated. The isolation of such clones enables us to identify differentially expressed genes with a role in strain-specific propagation. While I identified a panel of cell clones that were susceptible and refractory to Me7, all these clones were highly susceptible to both RML and 22L. In the main body of the Discussion, I outline the challenges involved in identifying subclones with exclusive susceptibility to a single prion strain, using the PME2/PME2-6D8 cell model.

In the second part of the project, I investigated whether passage of the Me7 strain in cells results in faithful propagation or adaptive changes, commonly known as strain adaptation. It has been established that prion strain properties change when prions are transferred from brain to cultured cells, and changes in cell tropism may underlie changes in strain properties (Li *et al.*, 2010). Strikingly, Me7-refractory PK1 cells were found to be highly susceptible when challenged with cell-adapted Me7 prions (PME2-6D8 [Me7]-H), suggesting that a single passage in PME2 cells changed the strain properties of brain-adapted Me7. Importantly, Me7-susceptible and Me7-refractory PME2-6D8 clones with equal susceptibility to the murine strains RML and 22L can be used to identify cellular factors that underlie Me7 strain adaptation. We also employed

Western blot analysis to compare the biochemical characteristics of PrP^{Sc} from brain- and cell-adapted Me7. Cell-adapted Me7 from persistently-infected PME2 cells showed a different electrophoretic mobility and glycosylation pattern when compared to brain-adapted Me7.

The changes that occurred when Me7 was passaged in PME2 cells, rendered cell-adapted Me7 and RML indistinguishable in their tropism to PK1 cells. We therefore tested whether cell-adapted Me7 has adopted an "RML-like" conformation. To address this, we compared the PK resistance of cell-adapted Me7 and RML. Results showed that cell-adapted Me7 and cell-adapted RML were markedly different in their sensitivity to PK digestion, demonstrating that Me7 did not "mutate" to an RML-like variant upon passage in PME2 cells and that cell-adapted Me7 and cell-adapted RML are two different prion strains.

5.1.1 Project background

In neurodegenerative diseases, distinct neuronal populations undergo decline and eventually cell death, and this phenomenon is referred to as selective neuronal vulnerability (SNV). In prion diseases, SNV is associated with degeneration of distinct brain areas in a prion strain-dependent manner. By targeting different brain areas, prion strains are thought to be associated with distinct clinical and neuropathological phenotypes. However, the molecular mechanisms underlying SNV and linking brain tropism of prion strains to diverse clinicopathological phenotypes are unknown. In contrast to *in vivo* findings, prion toxicity is not readily observed *in vitro*, as prions are innocuous to most cell lines. However, differences in the susceptibility of cell lines to prion strains have been broadly observed (Rubenstein *et al.*, 1992; Vorberg *et al.*, 2004; Mahal *et al.*, 2007). Given that subclones of a heterogeneous pool of cells greatly vary in their susceptibility to a prion strain, the strategy of single cell cloning has been used successfully in the past to isolate highly prion-susceptible cell clones (Bosque and Prusiner, 2000; Klohn *et al.*, 2003; Mahal *et al.*, 2007). The existence of cell lines and sibling cell clones that propagate prion strains selectively, suggests that susceptibility to a prion strain depends on specific cellular factors.

Selective neuronal vulnerability is a feature of all neurodegenerative diseases. The selective loss of dopaminergic neurons in the substantia nigra pars compacta underlies SNV in Parkinson's disease and accounts for the major clinicopathological manifestations of the disease (Surmeier, Obeso and Halliday, 2017). ALS leads to the selective degeneration of upper and lower motor neurones whereas Huntington's

disease is characterised by severe atrophy of the brain's corpus striatum (Kiernan *et al.*, 2011; Mealer *et al.*, 2014). A growing body of evidence suggests that SNV in neurodegenerative diseases is governed by cellular factors that are either expressed or not expressed in vulnerable neurons (Guzman et al., 2010; Brockington et al., 2013; Comley et al., 2015; Subramaniam et al., 2011). Gene expression analysis of susceptible and resistant motor neurons in ALS revealed that resistant motor neurons exhibited reduced AMPA-mediated inward calcium current and a higher GABA-mediated inhibitory chloride current, than vulnerable spinal motor neurons, suggesting that enhanced susceptibility to excitotoxicity mediated partly through reduced GABAergic transmission renders spinal motor neurones vulnerable to degeneration (Brockington *et al.*, 2013). In agreement with these findings, Gabra1, which encodes a subunit of GABA receptors, is preferentially expressed in oculomotor motor neurons in symptomatic SOD1 transgenic mice and in end-stage ALS patients, conferring resistance to these neurones (Comley *et al.*, 2015).

In prion diseases, selective neuronal vulnerability is linked to damage in particular brain areas in a strain-dependent manner. For example, intracerebral inoculation of mice with the murine strain Me7 induces hippocampal neuronal loss whereas RML does not cause degeneration in this brain region (Jeffrey, Martin, Barr, Chong, & Fraser, 2001; Karapetyan et al., 2009). The murine strain 22L targets the cerebellum, as this brain region is the first to exhibit hallmarks of neurodegeneration following inoculation with 22L (Šišková *et al.*, 2013). Also, 22L was shown to be more toxic to cerebellar primary neurons when compared to striatal and cortical primary neurons (Hannaoui *et al.*, 2013). Different types of human prion disease are associated with degeneration in specific brain regions (Wadsworth and Collinge, 2007). For example, GSS targets the cerebellum whereas FFI causes thalamic degeneration. Atypical forms of human prion disease provide further evidence that prion strains underlie selective vulnerability in prion disease. For example, atypical forms of FFI present with cerebellar ataxia but no insomnia (Taniwaki *et al.*, 2000). VCJD, which is caused by the BSE strain, is atypical both in its clinical features and electroencephalogram (Collinge *et al.*, 1996). Additionally, all forms of vCJD are characterised by peripheral pathology and lymphoreticular deposition of PrP^{Sc}, which precede neuroinvasion, in contrast to other forms of CJD.

5.1.2 PME2 and PME2-6D8 clones as *in vitro* cell models for the identification of factors that influence prion strain selection

What governs brain tropism of prion strains, and in turn, SNV in prion diseases? Cell lines that propagate prion strains selectively might shed light on this question. Prion strains can be distinguished in cell culture and selective prion susceptibility of cell lines has been reported in a number of studies (Solassol, Crozet, & Lehmann, 2003; Vilette, 2008; Vorberg et al., 2004; Mahal et al., 2007). While some cell lines exhibit broad susceptibility to multiple prion strains, others are susceptible to only one or two strains. In this PhD project I isolated several highly Me7-susceptible PME2 and PME2-6D8 subclones from the Me7-refractory cell line, PK1. Despite being differentially susceptible to Me7, these cell clones were indistinguishable in their susceptibility to the murine strains RML and 22L. PME2-6D8 clones with the highest susceptibility to Me7 gave spot numbers above 2000 whereas Me7-refractory cell clones gave spot numbers below 10. Similar studies showed that cell clones isolated from a single cell line are highly heterogeneous in their susceptibility to prions. Subcloning of N2a cells can yield both highly RML susceptible and RML-resistant subclones (Bosque and Prusiner, 2000; Klohn *et al.*, 2003). Comparative studies between cognate Me7-susceptible and Me7-resistant PME2/PME2-6D8 cell clones can potentially identify specific cellular factors that govern Me7 cell tropism.

Initially, the cell clones PME1 and PME2 were classified as marginally Me7-susceptible with 351 and 387 PrP^{Sc}-positive cells respectively, however, in the second round of subcloning, 2% of PME2 sibling clones with PrP^{Sc}-positive cells between 600 and 2000 were isolated. Notably, single cell cloning of the Me7-susceptible PME2-6D8 clone led to a marked increase in the number of Me7-susceptible cells but also raised the overall susceptibility of clones to this strain as evident by the sharp increase in the number of PrP^{Sc}-positive cells per clone. In the final round of subcloning, 63% of PME2-6D8 clones consisted of over 1000 PrP^{Sc}-positive cells, as quantified by the SCA. Additionally, while being differentially susceptible to Me7, all PME2-6D8 clones were equally susceptible to RML and 22L.These results showed that single cell cloning of a highly Me7-susceptible progenitor line, enriched for sibling cell clones that are susceptible to Me7, pointing towards the involvement of specific host factors in the ability of these cell clones to propagate Me7.

Our findings showed that the Me7 revertant-resistant PK1-derived cell clone PME1 was weakly susceptible to Me7 when it was first isolated, but subsequently lost its susceptibility to the aforementioned murine strain. When challenged with Me7 brain

homogenate, no prion propagation was detectable in PME1 cells as infectivity was diluted out completely by passage 4. This was also the case for the Me7-refractory S7 cell line, which was used as a negative control for infection with Me7. In contrast to these findings, for Me7-challenged PME2 cells, a smaller fold decrease in the number of PrP^{Sc}-positive cells was observed between passages 3 and 4, reflecting prion propagation in these cells, albeit to a small extent. In agreement with the above findings, following single cell cloning of PME2 cells challenged with a $1x10^{-3}$ dilution of Me7 brain homogenate, 14% of sibling clones consisted of over 100 PrP^{Sc}-positive cells and 4% of clones consisted of over 300 PrP^{Sc}-positive cells. Contrary to these results, no Me7-infected sibling clones could be isolated during the subcloning of Me7-challenged PME1 cells, with PME1 cell clones giving less than 15 spots, which is what is usually observed for non-infected control cells. These findings demonstrate that, in contrast to PME2 cells, the Me7-resistant revertant cell line PME1 does not express factors that confer susceptibility to Me7. This explains why no Me7-infected PME1 cell clone could be isolated.

Mahal and colleagues developed the Cell Panel assay (C.P.A), and showed that a panel of murine cell lines, all of which carry the *Prnp*^{a} allele, and express similar levels of PrP^{C}, propagate prion strains selectively (Mahal *et al.*, 2007). The catecholaminergic neuronal cell line CAD5 shows broad susceptibility to the prion strains RML, 22L, Me7 and 301C, whereas R33, an N2a-derived cell line, is only susceptible to 22L. The fibroblast cell line L929, expresses low levels of cellular mouse prion protein, yet, is susceptible to infection with mouse-adapted scrapie strains Me7, 22L and RML but not with 87V (Vorberg *et al.*, 2004). The preference of prion strains for specific cell types has also been demonstrated *in vivo*. In diseased mouse brains, Me7 PrP^{Sc} deposition was prominent in neurones and was not associated with astroglia or oligodendrocytes (Carroll *et al.*, 2016). On the contrary, 22L PrP^{Sc} predominantly accumulated in astroglia with no involvement of neurones. These findings suggest that cell tropism of prion strains cannot be predicated on the basis of a cell line's tissue origin or its level of expression of PrP^{C} alone, pointing towards the involvement of cell-specific determinants in the ability of these cell lines to propagate prion strains selectively.

Collectively, such findings bear resemblance to the differential brain tropism of prion strains and suggest that prion strains show a distinct tropism for different types of neurons, which in turn, contributes to a strain-specific lesion profile. Experiments by Kim et al., showed that, following cerebellar injection of 22L prions, vacuolation was

limited to the cerebellum whereas injection in the cerebral cortex and other brain areas resulted in vacuolation in all brain regions examined (Kim *et al.*, 1987). Additionally, stereotaxic injection of the 139A strain in the striatum resulted in a shorter incubation than the other strains injected in the same brain region. Consistent with this finding, the neurotoxic effect of 139A in striatal primary neurones was higher than that of 22L (Hannaoui *et al.*, 2013).

How can we make use of Me7-susceptible and Me7-refractory PME2 cell clones to unravel the mechanisms that underlie susceptibility to Me7? The C.P.A established that the expression of specific cellular factors govern susceptibility to a prion strain, yet it is not an ideal cell model to be used for the identification of these factors, as the cell lines used in the C.P.A are genetically highly diverse. Fibroblast (LD9) and neuronal cell lines (PK1, CAD5) are genetically very different. This makes it very challenging to compare the transcriptomes of these cells and identify factors that account for prion strain selectivity, as inherent genetic differences will dilute out potentially important gene signatures that are exclusively associated with prion strain selection. The PME2/PME2-6D8 cell model provides a means to identify factors that determine susceptibility to a prion strain, as subclones derived from a single cell line are genetically similar and only differ in their susceptibility to a single prion strain. This will reduce gene expression differences unrelated to the phenotype that the cell clone is being selected for. By employing single cell cloning, previous work in our lab showed that it is possible to carry out comparative studies using RML-susceptible and RML-resistant PK1 sublines (Marbiah *et al.*, 2014). Transcriptome analysis of these sublines led to the identification of genes associated with susceptibility to the murine strain RML. These genes control remodelling of the extracellular matrix and the differentiation state of cells. Given that PME2/PME2-6D8 cell clones are genetically similar and assuming that all cell clones carry the same PrP amino acid sequence and express the same or similar levels of PrP^C, all cell clones should have been able to propagate Me7, however, they do not. Similarly, some PME2 clones propagated 22L but not RML and vice versa. These findings show that the primary sequence of PrP^C is not the only determinant of prion susceptibility, pointing towards the involvement of cell-specific determinants in the ability of these cell clones to propagate prion strains selectively.

To take this project further, we asked whether it was possible to isolate PK1-derived cell clones that are exclusively susceptible to Me7 and refractory to both RML and 22L. Comparative studies between these “Me7-exclusive” sub lines (Me7+/RML-/22L-)

and sublines resistant to all three murine strains (Me7-/RML-/22L-), can lead to the identification of gene signatures associated with susceptibility to Me7. Likewise, “22L-exclusive” (Me7-/RML-/22L+) and “RML-exclusive” (Me7-/RML+/22L-) subclones express host factors that confer susceptibility to 22L and RML, respectively. We estimated the probability of isolating cell clones that are exclusively susceptible to each one of the three murine strains RML, 22L and Me7 from the frequency of isolating cells that are susceptible and refractory to a particular prion strain. During the second round of subcloning, the probability of isolating an RML-exclusive or 22L-exclusive cell clone from PME2 cells was only 6/1000 and 5/1000, respectively. Hence, the probability of isolating an Me7-exclusive cell clone (Me7+/RML-/22L-) was 3/1000 000, due to the low frequency of isolating double-negative RML-/22L- clones. During the subcloning of PME2, RML-susceptible, 22L-susceptible and Me7-susceptible cell clones occurred at a frequency of 960/1000, 950/1000 and 30/1000 respectively. However, during the final round of subcloning, 100% of PME2-6D8 clones were highly susceptible to both RML and 22L whereas 63% were susceptible to Me7. It was therefore impossible to isolate Me7-exclusive clones, due to the exceptionally high susceptibility of PME2-6D8 clones to RML and 22L (2000-3000 spots as quantified by the SCA) and due to the consistently lower frequency at which Me7-susceptible clones occurred. Even though Me7-exclusive sub clones could not be isolated, several Me7-susceptible (Me7+/RML+/22L+) and Me7-refractory (Me7-/RML+/22L+) clones with equal susceptibility to RML and 22L were isolated. Such genetically similar cell clones will be instrumental to identify genetic or epigenetic factors that confer susceptibility to Me7.

Given the exceptionally high susceptibility of PME2-6D8 clones to both RML and 22L, it was not possible to isolate 22L-exclusive and RML-exclusive PME2-6D8 clones. Contrary to this observation, single cell cloning of PME2 gave rise to sibling clones with differential susceptibility to 22L and RML, enabling the isolation of clones highly susceptible to RML and resistant to 22L prions, and vice versa. The isolation of clones differentially susceptible to Me7 and clones exclusively susceptible to RML or 22L suggests that different host factors govern susceptibility of a cell line to each prion strain. To assess the susceptibility of individual cell clones to RML and 22L, each PME2 cell clone was assigned a Selectivity Score (SS), where SS= RML_{spots}/(RML_{spots}/$22L_{spots}$). Selectivity score is a relative measure of the susceptibility of a cell clone to any two strains; in this case to RML and 22L. While the majority of PME2 clones were equally susceptible to RML and 22L with a SS of approximately 0.5, 5/1000 and 6/1000 of clones were designated “22L-preferring” and “RML-preferring”,

respectively. We noticed that all “22L-preferring” subclones were also marginally susceptible to RML, yielding spot numbers between 140 and 500 when challenged with RML. This limits the use of such clones for the identification of factors that underlie exclusive susceptibility to 22L. Also, due to time constraints, it was not possible to obtain confirmatory data for 22L-preferring and RML-preferring clones. Previous work in our lab has shown that cryopreservation of CAD5 sibling clones caused some subclones to lose their exclusive susceptibility to 22L or RML and become susceptible to both prion strains (West, 2016). Due to the limitations of the PME2/PME2-6D8 cell model, a cell line other than PK1 could be used to derive sibling clones exclusively susceptible to a prion strain.

What factors are expressed in Me7-permissive PME2 and PME2-6D8 clones, which confer susceptibility to Me7? It is possible that specific proteins act as cofactors for prion conversion and these might be cell-type specific. It was hypothesised that a molecular factor, designated protein X acts as a chaperone protein and binds to cellular PrP, forming a complex. PrP^{Sc} then binds to PrP^{C} resulting in a ternary complex during the conversion process (Kaneko et al., 1997; Telling et al., 1995). In an *in vitro* system, cell lysate-containing PrP^{C} was incubated with partially purified mouse PrP^{Sc} and prion propagation yielded newly formed PrP^{Sc} (Saborío *et al.*, 1999). Importantly, no conversion was observed under the same conditions using purified proteins in the absence of cell lysate, providing evidence that cell-specific factors in the cell lysate are required for the conversion of PrP^{C} to PrP^{Sc}. In the same study, the amount of PrP^{Sc} produced during incubation with Me7 PrP^{Sc} was greater compared to the one with 139A PrP^{Sc}. This could mean that the 139A PrP^{Sc} product was more sensitive to PK digestion compared to Me7 PrP^{Sc}, and therefore less of the former was detectable on a Western blot. Alternatively, host factors in the cell lysate generated from CHO cells may specifically favour the conversion of the Me7 prion strain, and to a lesser extent the conversion of 139A (Saborío *et al.*, 1999). A study by Leucht et al., showed that ablation of the high-affinity laminin receptor, LRP/LR, prevented PrP^{Sc} propagation in scrapie-infected neuronal cells (Leucht *et al.*, 2003).

Several PrP ligands have been proposed to influence the conversion of PrP^{C} to PrP^{Sc}, including sulphated glycosaminoglycans (GAGs). GAGs are unbranched polysaccharides that have been implicated in prion disease and sulphation of GAGs is important in determining GAG function (Esko and Selleck, 2002). Heparan Sulphate (HS) has been found associated with prion plaques in human and animal forms of prion disease (Snow, Kisilevsky, Willmer, Prusiner, & DeArmond, 1989; McBride,

Wilson, Eikelenboom, Tunstall, & Bruce, 1998). A number of GAGs have been investigated as cofactors in prion conversion and it has been reported that they both enhance or have no effect on the conversion process (Caughey, Brown, Raymond, Katzenstein, & Thresher, 1994; Wong et al., 2001; Ben-Zaken et al., 2003). Transcriptional silencing of *Papss2*, an enzyme involved in the sulphation of lipids, proteins and carbohydrates that was expressed in RML-resistant revertant PK1 sublines, led to undersulphation of heparan sulphate, increased PrP^{C} deposition at the ECM and also increased prion replication rates (Marbiah *et al.*, 2014). A study by Ellett and colleagues found that two sulphated GAGs, heparin and heparan sulfate, which differ at levels of sulphation, can change the biochemical properties of PrP^{Sc}, including solubility and protease resistance (Ellett *et al.*, 2015). These findings propose a model whereby differential distribution of GAGs in different cell types or brain regions, may contribute to the differential cell and brain tropism of prion strains.

The capacity of PrP^{C} to assume a particular conformation and the conformation of PrP within a fibril may be influenced by the extent and nature of its glycosylation (Hecker *et al.*, 1992; DeArmond *et al.*, 1997). Additionally, glycosylation may differ in individual cell lines or brain regions (Beringue et al., 2003; DeArmond et al., 1999). Prion strains are characterised by different glycosylation "signatures" (Khalili-Shirazi *et al.*, 2005; Lawson *et al.*, 2005) but glycosylation does not always determine strain specific properties. For example, the glycosylation profiles of RML and 87V strains were significantly different whereas the glycosylation sites of 22L and Me7 strains overlapped despite the fact that *in vivo*, the latter strains are characterised by different incubation times and patterns of neuropathology (Vorberg and Priola, 2002). Studies demonstrating that the glycosylation profile of PrP^{Sc} associated with specific strains can vary depending on the brain region or organ of prion replication, argue against a pivotal role of glycosylation in governing strain-specific cell and brain tropism (Rubenstein et al., 1991; Meeker, Sersen, & Carp, 1997).

A recent study by Fehlinger and colleagues demonstrated that two prion strains, 22L and RML, employ different endocytic pathways for established infection (Fehlinger *et al.*, 2017). Perturbation of clathrin-mediated endocytosis by knocking down a gene that encodes for the expression of the clathrin heavy chain, significantly enhanced the levels of newly formed PrP^{Sc} following 22L infection, but significantly reduced the levels of PrP^{Sc} in RML-infected cells.

Collectively, these findings provide mechanistic insights into the differential susceptibility of PME2 and PME2-6D8 clones to Me7, RML and 22L.

5.1.3 A novel cell model of prion strain adaptation

Changes in prion replication environment such as the transfer of prions from brain to cultured cells may lead to changes in strain properties (Li *et al.*, 2010; Weissmann *et al.*, 2011). We asked whether the passage of Me7 in PME2 and PME2-6D8 sublines resulted in faithful replication or strain adaptation. We first employed Western blotting, following Proteinase K digestion, to compare brain-adapted Me7 with cell-adapted Me7 derived from chronically Me7-infected PME2 and PME2-6D8 sublines. A significant change in electrophoretic mobility and glycosylation profile was noted when brain-adapted Me7 was passaged in permissive PME2 cells. While brain-adapted Me7 was characterised by a dominant di-glycosylated PrP^{Sc} band, PME2 cell-adapted Me7 was characterised by a dominant mono-glycosylated PrP^{Sc} band. These findings are consistent with previous studies which showed that the biochemical characteristics of PrP^{Sc} were altered upon passage of prions from brain to cells (Arjona *et al.*, 2004; Arima *et al.*, 2005). However, these and other studies (Li *et al.*, 2010) reported that, despite changes in the biochemical features of PrP^{Sc}, strain-specific phenotypes are retained when prions are transferred from brain to cultured cells and back to the brain. For example, when two mouse-passaged CJD strains characterised by different disease incubation times and lesion profiles were propagated in the murine hypothalamic cell line GT-1, the PrP^{Sc} banding and glycosylation patterns of the two strains were indistinguishable and markedly different from brain-derived PrP^{Sc} (Arjona *et al.*, 2004). Additionally, the two mouse-passaged CJD strains that were indistinguishable by their brain PrP^{Sc}-banding patterns on Western blots, continued to produce their distinct phenotypes in mice when transferred from cultured cells back to the brain. These findings suggest that changes in biochemical features of PrP^{Sc} do not always reflect changes in strain-specific properties. Additionally, classical procedures such as Western blotting, can not always discriminate between prion strains or detect changes in the properties of prion strains when prions are transferred from brain to cultured cells. Therefore, we employed an approach other than western blotting, to determine whether a change in strain properties had occurred upon passage of brain-adapted Me7 in PME2 cells.

Mahal and colleagues developed the Cell Panel Assay (C.P.A) and showed that four murine strains can be discriminated based on their ability to infect a panel of cell lines (Mahal *et al.*, 2007). Using this assay, they demonstrated that when prion strain properties change, for example when prions are transferred from brain to cells, this may lead to changes in cell tropism (Li *et al.*, 2010). We made use of this finding and challenged Me7-refractory PK1 cells with homogenates from chronically Me7-infected

PME2 cells. As PK1 cells are refractory to Me7, we expected that they would also be refractory to cell-adapted Me7, unless the strain properties of brain-adapted Me7 changed during passage in PME2 cells. Notably, Me7-refractory PK1 cells were highly susceptible to cell-adapted Me7 from chronically Me7-infected PME2 cells, denoting that the transfer of brain Me7 to PME2 cells evoked a change in strain properties. To validate these findings, we challenged the Me7-refractory CNS catecholaminergic neuronal cell line CAD5, with Me7 and homogenates from chronically Me7-infected PME2 cells. In agreement with PK1 findings, CAD5 cells were refractory to brain-adapted Me7 prions and highly susceptible to cell-adapted Me7. Similar findings were reported by Li et al., who showed that the passage of brain 22L prions in PK1 cells led to changes in cell tropism (Li *et al.*, 2010). In contrast to brain-adapted 22L prions, cell-derived 22L prions were unable to infect the neuroblastoma-derived cell line R33.

Albeit lacking nucleic acid, prion strains are subject to “mutations”. A change in prion strain properties can also be referred to as “mutation”, and mutations reflect changes in conformation or the biochemical features of the strain, but not at the level of protein sequence (Kimberlin, Cole and Walker, 1987; Li *et al.*, 2010; Weissmann, 2012). In this PhD project, I have shown that brain Me7 properties were altered upon passage in PME2 cells and cell-adapted Me7 was now characterised by novel cell tropisms. Changes in strain properties at the conformational level underlie prion strain adaptation and provide a mechanism by which transmission barriers are overcome. Prion strain adaptation describes the propensity of prions to gradually adapt to a new host, for example when serially transmitted within the same species following inter-species transmission (Hill et al., 2000; Kimberlin & Walker, 1977; Walker & Kimberlin, 1978; Baskakov, 2014). This phenomenon leads to the emergence of TSE strains with an expanded host range and increased virulence. When transmitted between species, the transmission efficiency of prions is considerably lower than when transmitted to the same host owing to a species barrier (Pattison, 1966). Inter-species transmission of prions does not usually result in disease, due to incompatibilities in the primary PrP sequence between donor and recipient species (Moore, Vorberg, & Priola, 2005; Hill & Collinge, 2004). However, in some cases, the species barrier can be overcome (Shi *et al.*, 2012). In our PME2/PME2-6D8 cell model, the transmission barrier to Me7 infection was overcome by strain adaptation in permissive PME2 cells. As a result of these adaptive changes, cell-adapted Me7 could infect PK1 cells, CAD5 cells, as well as PME2 sublines, regardless of whether these were permissive or refractory to brain-adapted Me7. In contrast to these observations, brain-adapted Me7, could only infect Me7-susceptible PME2 sublines. These findings are reminiscent of the *in vivo*

manifestations of strain adaptation, including an expanded host range. For example, it has been proposed that BSE resulted from interspecies transmission of sheep scrapie to cattle via contaminated food additives (Wilesmith *et al.*, 1988, 1992). During cattle-to-cattle passages, adaptation of sheep scrapie was suggested to lead to the emergence of BSE which is also transmissible to humans, giving rise to variant CJD. Experiments by Hill and colleagues showed that while primary passage of hamster prions in mice led to PrP^{Sc} deposition but did not cause clinical scrapie, sub-passage from clinically normal mice inoculated with hamster prions resulted in clinical disease in both mice and hamsters, with 100% of the animals succumbing to disease (Hill *et al.*, 2000). Importantly, these findings demonstrated that upon passage in mice, novel prion strain(s) were generated that were infectious to both mice and hamsters (Hill *et al.*, 2000). An expanded host range as a result of strain adaptation has also been reported by others (Race, Raines, Raymond, Caughey, & Chesebro, 2001; Bartz, Bessen, McKenzie, Marsh, & Aiken, 2000; Bartz, Marsh, McKenzie, & Aiken, 1998).

We noticed that, while 2.7% of PME2 cell clones were designated “Me7-susceptible” with spot numbers over 500, the high susceptibility of these clones to Me7 was only evident at cell passage 5 of the SCA (**Table 3.2**). Usually, the susceptibility of a cell line to prions is evident at passage 3 of the SCA. However, at passage 3, 80% of these Me7-susceptible cell clones consisted of less than 100 spots and some clones even consisted of less than 20 spots, which is usually observed for non-infected control cells. After 2 cell passages, there was an unexcepted, sharp increase in spot numbers of Me7-challenged PME2 clones. For some cell clones, the number of PrP^{Sc}-positive cells increased by 60-fold between passages 3 and 5 (**Table 3.2**). Upon sub-passage of cell-adapted Me7 from Me7-susceptible PME2 sublines, recipient cell lines (including PK1 cells and Me7-resistant PME2 cell clones) were highly susceptible to cell-adapted Me7 and this was evident at passage 3. These results bear resemblance to *in vivo* findings. The interspecies transmission of Transmissible Mink encephalopathy (TME) in hamsters resulted in long incubation periods prior to the development of clinical disease (Bartz *et al.*, 2000). Sub-passage of the hamster-passaged TME strain in hamsters led to a significant reduction in incubation times. In an independent study, Race and colleagues demonstrated that in mice inoculated with the 263K hamster scrapie, the original hamster scrapie agent persisted without detectable replication of PrP^{Sc} for over 1 year (Race *et al.*, 2001). However, during the second year following post-inoculation, there was both replication of hamster scrapie as well as adaptation of the strain to mice, giving rise to a strain that was virulent to both mice and hamsters. Similarly, it is possible that infectivity persisted in Me7-

challenged PME2 cells with little or no prion propagation, but adaptation of brain Me7 led to efficient prion propagation in these cells.

I have shown that Me7-susceptible PME2/PME2-6D8 cell clones do not faithfully propagate brain Me7 but instead adapt the Me7 strain and propagate the resulting cell-adapted Me7. Importantly, only a small number of PME2 clones were susceptible to Me7 but the number of susceptible sublines increased by 20-fold during the subcloning of PME2-6D8. The identification of genetically similar cell clones that differ in their ability to adapt the murine strain Me7, suggests that host genetic and epigenetic factors influence prion strain properties and govern prion strain adaptation. *In vivo* studies have established that host genetic background influences prion strain selection and mutation. The primary passage of BSE prions to two inbred lines of mice, that share the same PrP amino acid sequence, led to the emergence of two distinct prion strains (Lloyd *et al.*, 2004). The two strains were characterised by different incubation times, different glycosylation profiles, and different pattern of PrP immunoreactive deposits and neuronal loss. In an independent study, the passage of BSE in transgenic mice expressing human PrP methionine 129 (129MM Tg35), produced a vCJD-like phenotype in some mice, but also a molecular phenotype that was indistinguishable from that of sporadic CJD with PrP^{Sc} type 2 (Asante *et al.*, 2002). Despite having the same *Prnp* genotype, the genetic background of individual 129MM Tg35 mice was different, suggesting that host genome is crucial in determining prion strain mutation and selection.

Coding polymorphisms of PrP such as that at PrP residue 129 that results in the presence of either methionine or valine, has a strong effect on susceptibility and strain selection (Wadsworth *et al.*, 2004; Collinge et al., 1991; Mead et al., 2009; Palmer, Dryden, Hughes, & Collinge, 1991; Lee et al., 2001; Mead et al., 2003) . The challenge of transgenic mice with BSE and vCJD resulted in the propagation of distinct molecular and neuropathological phenotypes dependent on host PrP residue 129 (Wadsworth *et al.*, 2004). Challenge of transgenic mice expressing human PrP Met^{129} (129MM Tg35 and 129MM Tg45 mice) with BSE and vCJD prions resulted in propagation of type 4 PrP^{Sc}, and this was accompanied by the presence of florid PrP plaques, the key neuropathological hallmark of vCJD. In contrast to these findings, challenge of transgenic mice expressing human PrP Val^{129} (129VV Tg152 mice) with vCJD prions was characterised by a considerable transmission barrier to infection as only 50% of inoculated animals were infected. vCJD-inoculated 129VV Tg152 mice propagated Type 5 PrP^{Sc}. This and other studies provide abundant evidence for the powerful effect

of residue 129 on prion strain selection (Collinge, Sidle, Meads, Ironside, & Hill, 1996; Collinge, 1999), which is likely to be exerted by its effect on the conformation of PrP^{Sc}. Such findings, relate to the conformational selection model which suggests that only a subset of permissible PrP conformers that can propagate in a host, are compatible with the host's PrP^{C} sequence (Collinge and Clarke, 2007). It will therefore be necessary to sequence the *Prnp* gene of PME2 and PME2-6D8 clones to exclude the possibility that changes in PrP^{C} primary sequence account for the ability of some of these clones to propagate Me7.

Several studies have shown that prion strain mutations occur under particular selection pressures, leading to the emergence of mutant variants. The acquisition of drug resistance by prions has been described by several groups (Ghaemmaghami *et al.*, 2009; Li *et al.*, 2010; Berry *et al.*, 2013; Oelschlegel and Weissmann, 2013). For example, the introduction of the drug swainsonine (swa) in the culture medium led to a sudden decrease in 22L prion propagation in PK1 cells, as the prion population consisted mostly or solely of swa-sensitive variants. However, after a number of successive splits, prion propagation increased, as a swa-resistant prion population emerged, demonstrating adaptation to the new environment (Li *et al.*, 2011). In the presence of swa, pre-existing or newly generated swa-resistant variants with a selective advantage, outcompeted swa-sensitive variants and dominated the prion population (Li et al., 2010; Weissmann, 2012). Similar findings were reported *in vivo*. The 2-aminothiozole IND24 prolonged the lives of scrapie-infected mice, but the RML-infected mice treated with IND24 eventually developed neurological dysfunction and died (Berry *et al.*, 2013). Importantly, a mutant, drug-resistant strain emerged in IND-24-treated mice. When compared to RML, the drug resistant variant, RML [IND24], was characterised by a different cell tropism. In the PME2/PME2-6D8 cell model, strain adaptation of Me7 occurred in the absence of selective pressures. When transferred from the mouse brain to permissive PME2 cells, "cell-adapted Me7" prions presumably arising as a result of mutation, were preferentially amplified and outcompeted their "brain-adapted Me7" prions.

Our results are consistent with previous findings and demonstrate that, albeit devoid of a nucleic acid genome, prions are subject to mutations and show hallmarks of Darwinian evolution (Li *et al.*, 2010). Upon transfer to a different replication environment, cloned prion populations can become heterogeneous by acquiring mutations, and mutant variants with a selective advantage are preferentially amplified. This in turn leads to the adaptation of a strain to a new host or a new environment

(such as replication in the presence of a drug or transfer of prions between different tissues) and enables its survival and spread. According to this explanation, Me7 exists as a molecular clone and strain mutation generated a distinct PrP^{Sc} type with different strain properties, that was not present in the original brain Me7 homogenate but emerged upon passage of Me7 in PME2 cells. Importantly, the majority of PME2 cell clones were refractory to Me7, but a second round of subcloning markedly increased the number of Me7-susceptible cell clones, suggesting that strain mutation is governed by cellular factors that are expressed in some PME2 clones but not in others.

An alternative explanation for the changes in Me7 strain properties is that cell-adapted Me7 is a conformational variant that was present in the Me7 brain homogenate and was preferentially selected and amplified upon passage in PME2 cells. This explanation is consistent with the quasi species model of prions. This model proposes that prion strains are not clonal, but rather exist as an ensemble or “cloud” of quasi species (Collinge and Clarke, 2007). This highly dynamic and mutagenic system consists of a major component and a multiplicity of variants present at low levels. Upon transfer to a different replication environment, a particular variant or “sub-strain” is selected and preferentially amplified, becoming the dominant PrP^{Sc} type. With reference to the quasi species model of prions, virus and prion populations are similar in that they are both heterogeneous by acquiring mutations and are therefore subject to evolution under a particular selection regime (Collinge and Clarke, 2007; Domingo, Sheldon and Perales, 2012). While in a viral quasi species mutations occur at the DNA or RNA level, in a prion quasi species mutations occur at the conformational level of the protein (Li et al., 2010; Weissmann, 2012; Weissmann et al., 2011). According to this model, it is possible that the cell-adapted Me7 variant pre-existed in the Me7 strain or arose as a result of mutation and was preferentially selected and amplified upon transfer to PME2 cell clones. In agreement with the notion that prions constitute quasi species, Li and colleagues showed that swa-resistant variants pre-existed in the cell-adapted 22L prion population prior to exposure to swainsonine (Li *et al.*, 2010). Subsequently, the swa-resistant variants with a selective advantage outcompeted their swa-sensitive counterparts.

Cell-adapted and brain-adapted Me7 were characterised by different cell tropisms. In contrast to these findings, brain- and cell-adapted RML were indistinguishable in their tropism to PK1 and CAD5 cells. This suggests either that the strain properties of RML remained unchanged during passage in PME2 cells, or that brain- and cell-adapted RML show a similar cell tropism in the PK1/CAD5 cell model. We employed another

cell line to test whether brain-adapted RML and cell-adapted RML can be discriminated by differences in cell tropism. Even though previous studies reported that the murine fibroblast cell line LD9 is equally susceptible to RML and Me7 (Mahal *et al.*, 2007), in our hands, LD9 cells were weakly susceptible to RML. The LD9 (3E11)-1E9 sub clone is an LD9-derived subclone and was isolated based on its enhanced susceptibility to Me7 when compared to the parental LD9 line. LD9 (3E11)-1E9 cells were challenged with brain-adapted RML and PME2 cell-adapted RML to determine whether LD9 cell tropism of RML has changed upon passage of the strain in PME2 cells. The susceptibility of LD9 (3E11)-1E9 cells to cell-adapted RML was lower than their susceptibility to brain-adapted RML, however, the difference in LD9 susceptibility to cell- and brain-adapted RML was not as pronounced as the difference in PK1 and CAD5 susceptibility to cell- and brain-adapted Me7, respectively. Additionally, LD9 cells are considerably less susceptible to RML than they are to Me7, limiting their robustness as a cell model to report changes in RML cell tropism. It was therefore uncertain whether the strain properties of RML changed upon passage in PME2 cells. In agreement with these findings, *in vivo* studies have shown that while some strains are mutable (acquire mutations), others are stable and retain their original properties when the replication environment changes (Mahal *et al.*, 2012; Cancellotti *et al.*, 2013).

5.1.4 Cell-adapted Me7 and cell-adapted RML are markedly different in their sensitivity to Proteinase K digestion

I have shown that passage of Me7 in PME2 cells, altered prion strain properties, rendering cell-adapted Me7 and RML indistinguishable in their tropism to PK1 and CAD5 cells. Even though PK1 and CAD5 cells are refractory to Me7, these cell lines were equally susceptible to cell-adapted Me7. A plausible explanation for the similarities in cell tropism between RML and cell-adapted Me7, is that cell-adapted Me7 is an “RML-like” conformational variant.

The murine strains Me7 and RML can be discriminated *in vivo* by distinct incubation times and patterns of neuropathology (Karapetyan *et al.*, 2009). *In vitro*, the two strains can be discriminated by differences in conformation (Legname *et al.*, 2006; Thackray *et al.*, 2007), glycosylation profile (Wenborn et al., 2015; Thackray et al., 2007) and cell tropism (Mahal *et al.*, 2007). Work in this project has shown that PK1 cells were equally susceptible to RML and PME2 cell-adapted Me7. We therefore asked whether Me7 has become more “RML-like”, upon passage in PME2 cells. To address this

question, we employed a classical strain typing approach. Resistance to protease digestion has been extensively used to characterise prion strains (Kuczius and Groschup 1999; Safar et al. 1998; Safar, Cohen, and Prusiner 2000; Morales 2017). We treated Me7- and RML-infected PME2 cell homogenates with Proteinase K (PK) at concentrations from 1 to 55µg/mL. Western blot results demonstrated that cell-adapted Me7 and cell-adapted RML were markedly different in their sensitivity to Proteinase K digestion. Cell-adapted Me7 was significantly more resistant to proteolysis by PK when compared to cell-adapted RML. At the lowest PK concentration used, 1µg/mL, a remarkable 75% of cell-adapted RML PrP^{Sc} was digested whereas at the same PK concentration, only 12% ± 20% of cell-adapted Me7 PrP^{Sc} was degraded. The large difference in protease resistance between cell-adapted Me7 and cell-adapted RML demonstrated that Me7 did not "mutate" to an "RML-like" variant upon passage in PME2 cells and that cell-adapted Me7 and cell-adapted RML are two different prion strains.

In agreement with our findings, Kuczius and Groschup showed that brain-adapted Me7 PrP^{Sc} was significantly more resistant to proteolytic digestion by PK when compared to RML PrP^{Sc} (Kuczius and Groschup, 1999). The authors showed that after 6 hours of exposure to 50µg/mL PK, 84% of RML PrP^{Sc} was degraded whereas only 17% of Me7 PrP^{Sc} was digested. The significantly higher sensitivity of RML PrP^{Sc} to PK digestion when compared to Me7, has also been reported by others (Thackray *et al.*, 2007; Karapetyan *et al.*, 2009). Thackray et al., showed that the protease resistant core, PrP 27-30, of RML was more sensitive to PK digestion following exposure to either GdnHCl or Sarkosyl (Thackray *et al.*, 2007). Since the PrP amino acid sequence of RML and Me7 was the same, differential sensitivity to PK digestion indicates differences in the conformations of the two strains. Work by Safar et al., showed that prion strains can be discriminated by different levels of PK-sensitive PrP^{Sc} and variation in incubation times is related to the relative protease sensitivity of PrP^{Sc} in each strain (Safar *et al.*, 1998). These findings are important as they indicate that the degree of resistance to proteolytic digestion provides useful information regarding the conformation of PrP^{Sc} and strain-specific biological properties of PrP^{Sc} are contained within the conformation of PrP^{Sc}.

I have shown that cell-adapted Me7 and cell-adapted RML are differentially sensitive to PK digestion despite being indistinguishable in their tropism to PK1 and CAD5 cells. Cell-adapted Me7 was significantly more resistant to proteolysis when compared to cell-adapted RML. Importantly, our results are consistent with previous studies which

showed that brain-adapted Me7 is more resistant to proteolytic digestion by PK than brain-adapted RML. These findings indicate that the changes that occurred to Me7 upon passage in PME2 cells are unlikely to have altered the overall conformation of the strain. Alternatively, changes in the conformation of Me7 might be too subtle to lead to detectable changes in sensitivity to protease digestion. It is also possible that changes in glycosylation or another post-translation modification underlie the changes in prion strain properties that occurred when Me7 was passaged in PME2 cells.

5.1.5 Cell lines other than PK1, as *in vitro* models for prion strain selection

5.1.5.1LD9

To validate genetic or epigenetic factors that govern susceptibility to Me7, gene signatures associated with Me7 susceptibility in one cell line must overlap with gene signatures associated with Me7 susceptibility in at least one other cell line. So far, I have described the isolation of cognate Me7-susceptible and Me7-refractory sublines from the Me7-refractory cell line PK1. During the final round of subcloning, PME2-6D8 clones were differentially susceptible to Me7, however all cell clones were equally susceptible to the murine strains RML and 22L. These genetically similar cell clones are potentially useful *in vitro* tools for comparative studies to identify factors that determine susceptibility to Me7.

Mahal and colleagues showed that the murine fibroblast cell line LD9 is broadly susceptible to the murine strains Me7, RML and 22L (Mahal *et al.*, 2007). While it was reported that LD9 cells exhibit equal susceptibility to Me7 and RML, experiments conducted in this project showed that LD9 cells were only weakly susceptible to RML and their susceptibility to RML did not increase after a round of subcloning. Importantly, LD9 susceptibility to Me7 increased significantly after two rounds of single cell cloning. There was a 6-fold increase in spot numbers of the Me7-challenged LD9 (3E11)-1E9 cell clone when compared to the Me7-challenged LD9 parental line. For LD9 (3E11) clones, there was a steady increase in the number of PrP^{Sc}-positive cells between passages 3 and 4. Contrary to this observation, for the majority of Me7-infected LD9 clones, the number of PrP^{Sc}-positive cells dropped by passage 4. These findings suggest that serial subcloning of LD9 cells led to an overall increase in the number of Me7-susceptible cell clones and also increased the number of clones that can sustain an infected state.

Given that 93% of RML-challenged LD9 clones consisted of less than 100 PrP^{Sc}-positive cells and that no RML-infected clone with a spot number over 300 could be isolated, we did not screen for RML-susceptible cell clones in the final subcloning experiment. LD9 sublines that are exclusively susceptible to Me7 (Me7+/RML-) and Me7-revertant cell lines (Me7-/RML-) would have served as *in vitro* tools for the identification of factors that confer susceptibility to Me7. Even through Me7+/RML- LD9 cell clones were isolated, susceptibility to Me7 was not very high (around 500 spots as quantified by the SCA), but repeated rounds of subcloning can yield clones with high susceptibility to Me7 but refractory to RML. The isolation of clones susceptible to both Me7 and RML (Me7+/RML+) and clones exclusively susceptible to RML (Me7-/RML+) was not be possible because LD9 clones with the highest susceptibility to Me7 were only weakly susceptible to RML, making it impossible to isolate a clone that is highly susceptible to both prion strains. Additionally, it is highly unlikely to encounter a clone susceptible to RML but refractory to Me7, given the very low susceptibility of LD9 cells to RML.

Notably, even though single cell cloning increased the number of Me7-susceptible LD9 and LD9-3E11 clones, all clones consisted of less than 800 PrP^{Sc}-positive cells and there was no significant increase in the number of PrP^{Sc}-positive cells between passages 3 and 4, if any. In contrast to these findings, Me7-susceptible PME2-6D8 cell clones consisted of around 2000 and 3000 PrP^{Sc}-positive cells at passages 3 and 5 respectively, suggesting that for these clones, high susceptibility to Me7 was maintained over several passages.

Trypsynisation was required to passage LD9 cells in petri dishes to maintain the cells in culture. However, we avoided the use of trypsin to passage prion-infected cells in a 96 well format during the SCA, as trypsin can cause the internalisation of surface proteins such as PrP, and may in turn interfere with prion propagation (Caughey *et al.*, 1988). The adherent nature of LD9 cells made it harder to passage these cells by hand in a 96 well format throughout the course of the SCA. Since these experiments were carried out semi-manually, using a liquidator, and not automated robot processing, this limited the number of cell clones that could be screened at once.

The consistently lower susceptibility of LD9 subclones to Me7 when compared to PME2-6D8 clones, and the technical difficulties involved in screening large LD9 cell clone cohorts led us to drop LD9 cells as a model to identify factors for strain-specific prion propagation.

Mahal et al characterised response indexes (RI) for the prion strains tested, and this was equivalent to the reciprocal of the homogenate concentration required to yield 300 spots on an Elispot of 20 000 cells (Mahal *et al.*, 2007). The authors showed that the RIs of LD9 and PK1 cells for the murine strain 22L were similar. We could have exploited the high susceptibility of LD9 cells to 22L and challenged the LD9 and LD9-3E11 subclones with 22L homogenate to identify clones with high susceptibility to both Me7 and 22L (Me7+/22L+) as well as clones exclusively susceptible to 22L and refractory to Me7 (Me7-/22L+). Me7-susceptible and Me7-refractory clones with equal susceptibility to 22L would have occurred at a high frequency, given that the parental LD9 line is highly susceptible to 22L and the susceptibility of sibling clones to Me7 is greatly enhanced by single cell cloning.

5.1.5.2 CAD5

The catecholaminergic neuronal cell line CAD5 is susceptible to the murine strains RML and 22L (Mahal *et al.*, 2007). Even though previous studies reported that CAD5 cells are slightly more susceptible to RML than 22L (Mahal *et al.*, 2007), in our hands susceptibility to 22L was slightly higher.

Originally, we employed CAD5 cells to study phenotypic differences between the three strains RML, Me7 and 22L by comparing RML-, Me7- and 22L-infected CAD5 cell clones using immunofluorescence. We challenged heterogeneous pools of CAD5 cells with 22L, RML and Me7 brain homogenates at a $1x10^{-3}$ dilution and after 7 passages, we plated out prion-infected cells at a limiting dilution for the isolation of single cell clones. Overall, CAD5 sibling clones exhibited the highest susceptibility to 22L, consistent with the high susceptibility of the parental line to 22L. While 35% of 22L-challenged CAD5 clones yielded between 400 and 500 spots, 25% of RML-challenged CAD5 cells yielded between 400 and 500 spots. Previous work in our lab demonstrated that it is possible to isolate rare variant CAD5 subclones with exclusive susceptibility to either RML or 22L (West, 2016). Additionally, it was shown that exclusive susceptibility to RML was maintained over several passages and was therefore more stable than exclusive susceptibility to 22L. Our experimental design did not allow us to screen CAD5 clones for susceptibility to all three prion strains, as single cell cloning was carried out after prion infection.

Only one out of 191 Me7-infected clones yielded between 300 and 400 spots, corresponding to 0.5% of the cell clones. Even though Mahal and colleagues reported that CAD5 cells are susceptible to Me7 (Mahal *et al.*, 2007), heterogeneous CAD5

pools yielded less than 30 spots following challenge with a $1x10^{-3}$ dilution of Me7 homogenate. This explains why 97% of CAD5 sibling clones consisted of less than 20 PrP^{Sc}-positive cells.

Our findings showed that Me7-susceptible CAD5 clones occurred at a very low frequency and their spot numbers were lower than those of 22L-susceptible and RML-susceptible CAD5 clones. Additionally, CAD5 cells were characterised by a clumpy morphology. This rendered the cells unsuitable for immunofluorescence studies as the multiple processing steps led to a significant loss of cells. The clumpy morphology of CAD5 cells caused sibling clones to detach from the plate surface, potentially "contaminating" the homogeneous cell populations of clones straight after isolation. Based on our findings, we concluded that CAD5 cells are not a suitable model to study factors contributing to Me7 susceptibility. However, this cell line might prove useful for the identification of factors that underlie susceptibility to RML and 22L.

5.1.6 Future work

Future studies will aim to determine cellular factors that underlie susceptibility to Me7. Using the PME2/PME2-6D8 cell model, comparative studies between Me7-susceptible and Me7-refractory subclones that are nonetheless equally susceptible to the murine strains 22L and RML, will reveal gene signatures associated with susceptibility to Me7. Previous work in our lab has identified gene signatures associated with susceptibility to RML. This was done by comparing the transcriptomes of RML-susceptible PK1 subclones and RML-revertant subclones that had lost their susceptibility to RML. The differentially expressed genes between revertant and susceptible clones, controlled remodelling of the extracellular matrix and differentiation state of cells. Microarray data of differentially expressed genes was verified by gene silencing of distinct cell candidates. For example, transcriptional silencing of *Papss2*, an enzyme involved in the sulphation of lipids, proteins and carbohydrates that was expressed in RML-resistant revertant PK1 sublines, led to undersulphation of heparan sulphate, increased PrP^{C} deposition at the ECM and also increased prion replication rates (Marbiah *et al.*, 2014). Notably, a transition from a resistant to a susceptible phenotype could also be recapitulated by single knockdown of other genes including fibronectin 1 (*Fn1*), integrin α8 (*Itga8*) and chromogranin A (*Chga*). A study by Fehlinger et. al, showed that the disruption of clathrin-mediated endocytosis by knocking down a gene that encodes for the expression of the clathrin heavy chain, significantly enhanced the

levels of newly formed PrP^{Sc} following 22L infection, but significantly reduced the levels of PrP^{Sc} in RML-infected cells (Fehlinger *et al.*, 2017).

Using a similar approach to the one employed by Marbiah et. al, comparative studies between Me7-susceptible (Me7+/RML+/22L+) and Me7-resistant (Me7-/RML+/22L+) PME2-6D8 clones can reveal potential genes associated with susceptibility to Me7. Microarray data will be verified by transcriptional gene silencing or overexpression of candidate genes. For example, silencing of gene X in Me7-refractory cell clones may render the clones susceptible to Me7. The identification of genes associated with susceptibility to Me7 and/or RML, may lay the foundation to understand the more complex mechanisms that underlie SNV.

A different cell model will be required to identify genes with a role in 22L and RML propagation. PK1-derived subclones are highly susceptible to both RML and 22L and repeated subcloning enhances susceptibility to both strains, making it extremely unlikely to isolate an RML-exclusive (RML+/22L-) or 22L-exclusive cell clones (22L+/RML-). 22L- and RML-preferring PME2 sibling clones could be used for the identification of factors that confer susceptibility to 22L and RML respectively. However, this cell model has limitations. 22L- and RML-exclusive PME2 clones occurred at a very low frequency and we lack confirmatory data regarding the exclusive susceptibilities of these clones to RML and 22L, respectively. Previous work in our lab has shown that cryopreservation may cause 22L- or RML-preferring sub clones to lose their strain selectivity (West, 2016). This means that sibling clones may lose their exclusive susceptibility to RML or 22L and become susceptible to both strains, following cryopreservation. Additionally, we showed that while 22L-preferring clones can be isolated, these clones still propagate RML, albeit to a smaller extent than they propagate 22L. This may limit the usefulness of these clones if they are used to identify genes that account for exclusive susceptibility to 22L.

In the second part of the project, I showed that PME2 and PME2-6D8 sibling clones did not faithfully replicate brain-adapted Me7 and instead altered the strain properties, leading to profound changes in Me7 cell tropism. Importantly, some cell clones lacked the ability to adapt the Me7 strain, yielding less than 10 spots in the SCA. In contrast, susceptible cell clones yielded between 2000 and 3000 spots. These cell clones can serve as *in vitro* tools for the identification of host factors that underlie Me7 strain adaptation.

To determine whether the passage of Me7 in PME2 cells has altered strain-specific biological characteristics *in vivo*, mice will be inoculated with homogenates from Me7-

infected PME2 cell clones. If changes in strain properties have led to changes in biological characteristics of Me7, cell-adapted Me7 might be characterised by a neuropathological lesion profile that is distinct to that of brain-adapted Me7. However, studies have shown that strain specificity is retrained when prions are transferred from brain to cultured cells and back to the brain. Work by Li et. al, has shown that the passage of brain-adapted 22L prions in PK1 cells, changed the cell tropism of 22L and its resistance to swainsonine (Li *et al.*, 2010). However, after intracerebral inoculation in mice, cell-adapted 22L became indistinguishable to the original brain-adapted 22L strain. Cell-derived 22L prions regained their original cell tropism and were characterised by a lesion profile that was identical to that of brain-adapted 22L. Similar findings were reported by others. When a prion strain was passaged in cultured cells, this led to changes in the biochemical characteristics of PrP^{Sc} (electrophoretic mobility and glycosylation profile), but when prions were transferred from cultured cells back to the mouse brain, the biological characteristics of the strain were retained (Arjona *et al.*, 2004; Arima *et al.*, 2005). This was evident by the fact that incubation times, clinical signs and neuropathological profiles were the same whether mice were inoculated with prion-infected brain homogenates or cultured cell lysates.

5.1.7 Conclusions

I have shown here that serial single cell cloning has enabled us to isolate highly Me7-susceptible sibling clones from the Me7-refractory neuroblastoma cell line PK1. PK1 was used as the progenitor line to derive the marginally Me7-susceptible cell clone PME2, which was in turn used to derive highly Me7-susceptible cell clones. Me7-susceptible and Me7-refractory PME2-6D8 cell clones were indistinguishable in their susceptibility to the murine prion strains RML and 22L, rendering them valuable *in vitro* tools for future studies to determine factors that underlie susceptibility to Me7. Even though the original aim of this project was to isolate Me7-exclusive cell clones (Me7+/RML-/22L-), refractory to both RML and 22L, we estimated that the probability of isolating such a clone was 3/1000 000, due to the low frequency of isolating double negative RML-/22L- clones. We also employed a different cell model, the murine fibroblast cell line LD9, to isolate Me7-exclusive sublines. The susceptibility of LD9 cells to Me7 but not to RML was substantially improved by single cell cloning, making it possible to identify Me-susceptible cell clones that are resistant to RML. Such cell clones could be compared to Me7- and RML-double negative cell clones (Me7-/RML-) and determine factors that account for Me7 susceptibility.

In the second part of this project, I showed that the passage of brain-adapted Me7 in permissive PME2 cells led to adaptive changes, commonly known as prion strain adaptation. It has previously been reported that the biochemical characteristics of PrP^{Sc} can change when a strain is transferred from the brain to cultured cells, but strain-specific biological characteristics were retained when the prion strain was transferred from cells back to the mouse brain. However, others have shown that strain properties change when prions are transferred from brain to cells. We showed that cell-adapted Me7 prions acquire different cell tropism, when compared to brain-adapted Me7, suggesting that a single cell passage in PME2 cells changed the properties of Me7. Me7-susceptible and Me7-refractory PME2-6D8 subclones are instrumental for the identification of cellular factors that underlie Me7 strain adaptation.

Strain adaptation of Me7 in PME2 cells rendered cell-adapted Me7 and RML indistinguishable in their tropism to PK1 and CAD5 cells. PK1 and CAD5 cells are refractory to Me7 but were equally susceptible to cell-adapted Me7. To determine whether cell-adapted Me7 is an “RML-like” conformational variant, we compared cell-adapted Me7 and cell-adapted RML with regards to their resistance to proteolytic digestion by increasing concentrations of Proteinase K (PK). Results showed that cell-adapted Me7 was considerably more resistant to proteolytic digestion when compared to cell-adapted RML, demonstrating that cell-adapted Me7 is not an “RML-like” variant, and that cell-adapted Me7 and cell-adapted RML are two different prion strains.

5.2 The role of Fkbp proteins in molecular mechanisms of prion propagation

The objective of this project was to investigate whether Fkbp family members have a role in prion propagation. The first part of the project aimed to identify Fkbp proteins that affect prion propagation. The second part of the project aimed to determine whether the perturbation of prion propagation by Fkbp proteins is due to their direct interaction with PrP^{c}.

In addition to *Fkbp9*, which has already been identified as a candidate modifier gene (Brown *et al.*, 2014), the study focused on four genes, *Fkbp1a, Fkbp4, Fkbp5* and *Fkbp8*, which encode Fkbp12, Fkbp52, Fkbp51 and Fkbp38 proteins respectively. To establish whether these Fkbp proteins have a role in prion propagation, stable gene-silenced prion-susceptible neuroblastoma cell lines (N2aPK1) cell lines were generated using retroviral infection with shRNA constructs. To exclude siRNA off-

target effects I generated at least 2 cell lines with a >50% knock down of the target gene relative to controls as determined by real time RT-PCR. A total of 20 cell lines were then tested for prion propagation using the SCA.

Stable *Fkbp* knock-down cells showed that *Fkbp1a*, *Fkbp4* and *Fkbp8* might have a role in prion propagation as the number of PrP^{Sc}-positive cells was significantly reduced in these cells. To complement these data, transient transcriptional silencing of the same *Fkbp* genes was also carried out in RML-chronically infected N2aPK1 (iS7) cells. Unexpectedly, transient transcriptional silencing of the same *Fkbp* genes had no effect on PrP^{Sc} levels, as determined by a separate SCA, making it difficult to draw definite conclusions about the role of Fkbp proteins in prion replication.

Recombinant Fkbp9 and Fkbp52 (*Fkbp4*) proteins were successfully expressed to test their effect on PrP fibrillisation and amplification using Thioflavin T incorporation and PMCA assays respectively.

In general, the levels of target gene knock down did not correlate linearly with a reduction in the number of PrP^{Sc}-positive cells in the SCA for all the genes. Silencing of *Fkbp1a* (Fkbp1a-sh1, sh3 and sh7 cell lines) showed a good level of knock down (mean of 62%), however, this did not correlate with a reduction in PrP^{Sc} –positive cells in the SCA. Conversely, for cell lines Fkbp1a sh2, sh5 and sh6 (with a mean level of knock down of 53%), a significant reduction in spot number was observed. This can indicate that silencing of Fkbp12 has an inhibitory effect on prion propagation. In a similar fashion that Fkbp12 enhances alpha synuclein fibrillisation (Gerard et al., 2008; Gerard et al., 2006; Deleersnijder et al., 2011), it might also facilitate the conversion of PrP^{c} to PrP^{Sc}. The fact that for cell lines Fkbp1a-sh1, sh3 and sh7, the level of gene knock down did not correlate with a reduction in the number of PrP^{Sc}-positive cells, might suggest that the aforementioned shRNAs had off-target effects. An off-target effect occurs when an shRNA down regulates unintended targets by having partial sequence complementarity with other gene targets. Measurable phenotypes arising from off-target effects are one of the disadvantages of stable transcriptional silencing (Jackson and Linsley, 2010). Stable integration of an shRNA construct into the genome may have a number of unpredictable effects on the cell such as the induction of an unspecific immune response or an effect on growth. Although these responses may not relate at all to target gene knock down, they may lead to measurable phenotypes in the transduced cells such as reduction in PrP^{Sc} levels. Sometimes these false-positive results complicate the interpretation of SCA data.

For Fkbp52, only Fkbp4-sh1 significantly increased PrP^{Sc} levels whereas all other cell lines significantly reduced the number of PrP^{Sc} positive cells, pointing towards an off-target effect for the Fkbp4-sh1 construct. The apparent reduction in PrP^{Sc} in the remaining *Fkbp4*-silenced cell lines may imply that *Fkbp4* plays a role in prion propagation. An overexpressing cell line for this gene could shed light to this question. Importantly, Fkbp52 was shown to induce the aggregation of tauF4, leading to the stabilisation and oligomerisation of aggregation-prone forms of tau (Kamah *et al.*, 2016). Also, down regulation of Fkbp52 in a cell culture model for synucleopathy, reduced alpha synuclein aggregation and concomitant neuronal death (Gerard *et al.*, 2010). In contrast to its effect on tau and α-synuclein, a study showed that the overexpression of Fkbp52 in Aβ-transgenic Drosophila, prolonged the lifespan of the flies and supressed the rough-eye phenotype associated with Aβ42 toxicity (Sanokawa-Akakura *et al.*, 2010). The involvement of Fkbp52 in neurodegeneration, in combination with the SCA data suggests that Fkbp52 may also have a role in prion propagation.

For Fkbp51, there was no convincing evidence that down regulation of its expression had an effect on prion propagation. Although a very good level of *Fkbp5* mRNA knock down (mean of 81%) was achieved in cell lines sh1, sh6 and sh7, reduction in PrP^{Sc} levels in these cell lines was not as pronounced as that observed in *Fkbp1a*, *Fkbp4* and *Fkbp8* stably silenced cell lines. On average, the highest level of gene knock down was observed in *Fkbp5*-silenced cell lines but this did not lead to a corresponding reduction in the number of PrP^{Sc}-positive cells, making it rather unlikely that the Fkbp51 immunophilin plays a critical role, if any at all, in prion propagation.

Interestingly, knock down of the non-canonical immunophilin Fkbp38 in N2aPK1 cells, significantly reduced the level of PrP^{Sc}-positive cells in 4 out of the 5 stably silenced cell lines screened in the SCA. The predominantly mitochondrial Fkbp38, is unlikely to directly interact with the GPI-anchored, trans-membrane PrP^{c}. Nonetheless, it may hinder prion propagation via an indirect mechanism that does not involve physical interaction with either PrP^{c} or PrP^{Sc}.

Transcriptional silencing of endogenous *Fkbp10* was recently shown to reduce PrP^{Sc} levels of prion-infected N2a cells (Stocki *et al.*, 2016). Conversely, *Fkbp9* knock down in N2aPK1 cells significantly increased the number of PrP^{Sc} -positive cells as determined by the SCA (Brown *et al.*, 2014). In agreement with this finding, a microarray gene expression study showed that mice expressing higher levels of the *Fkbp9* gene exhibited longer incubation periods following RML infection (Grizenkova *et*

al., 2012). The opposing effects of Fkbp10 and Fkbp9 on prion propagation complicate the association between Fkbp proteins and prion propagation as one might have expected these two homologous, ER resident proteins to behave in a similar manner. In this project, I showed that transient silencing of *Fkbp9* and *Fkbp10* in iS7 cells had no effect on the number of PrP^{Sc}-positive cells. Since iS7 cells are chronically RML-infected, it may not be possible to further increase prion propagation rates in these cells by knocking down *Fkbp9*. This might explain why transient transcriptional silencing of *Fkbp9* in iS7 cells had no effect on prion propagation. Additionally, the levels of reduction in mRNA expression associated with each siRNA have not yet been determined. It is therefore plausible that some siRNAs caused only a marginal reduction in the mRNA expression levels of *Fkbp* genes, making it impossible to determine whether a specified *Fkbp* gene affects prion propagation.

While stable gene silencing of genes like *Fkbp4*, *Fkbp8* and *Fkbp9* (Brown *et al.*, 2014) had an effect on prion propagation, transient silencing of the same *Fkbp* genes had no effect on PrP^{Sc} levels in chronically infected cells. There are, however limitations associated with the transient transcriptional silencing assay. The disagreement between stable and transient KD data can reflect differences between the two cell systems and assays. Stable gene silencing was carried out on uninfected PK1 cells which were subsequently challenged with RML. Stable KD ensures gene silencing throughout the duration of the assay. This means that any detectable differences in the number of PrP^{Sc}-positive cells can be the result of *Fkbp* gene effects that alter early events such as infectivity uptake and propagation and later events such as PrP^{Sc} accumulation, clearance and cell-to-cell spread. In the case of transient transcriptional silencing, the effect of gene silencing on infectivity uptake cannot be monitored, as RML infection in these cells is already established. Chronically infected cells are typically used for cell curing assays to test the potency of various anti-prion pharmacological compounds (Nicoll *et al.*, 2010).

The fact that the siRNAs had no effect on prion propagation whereas stable knock down of some of these *Fkbp* genes in *de novo* infected PK1 cells significantly reduced PrP^{Sc} spot number may imply that some Fkbp proteins do not act to abrogate established RML infection. Instead, the specified Fkbp genes may be acting upstream of prion propagation, for example, on the uptake of infectivity. If this is the case, this will not be reported by the SCA in transient *Fkbp* knock down in chronically infected cells.

The duration of silencing by the specified siRNAs is an important parameter to consider when evaluating the success of transient *Fkbp* silencing. For example, the short duration of gene silencing by a specified siRNA could impede its ability to modify cellular behaviour if the target gene is not silenced a sufficient amount of time. This would be particularly obvious if the target protein has a long half-life within the cell. This means that knocking down its corresponding mRNA will not result in an immediate decrease in protein levels if mRNA levels can be restored before a considerable amount of protein has been broken down (Bartlett and Davis, 2006). For *siPrnp*, it has been established that day 4 post-treatment gives the maximum level of PrP^{c} mRNA knock down (unpublished data). However, this has not been determined for any of the siRNAs against *Fkbp* genes.

The complex phenotypes associated with prion diseases are likely to be the result of multiple genes and cellular pathways. In this project, we have only studied the effect of *Fkbp* gene silencing on RML prion propagation. By challenging PK1 cell lines with another prion strain such as the murine strain 22L, it is possible to identify prion strain-specific modifiers.

Changes in PrP^{Sc} levels detected in the SCA may be attributable to changes in the uptake of prion infectivity, conversion or clearance. To determine whether Fkbp proteins that report in the SCA influence prion propagation directly, the original aim of the project was to carry out *in vitro* experiments measuring PrP fibrillisation and PrP^{Sc} amplification. PMCA has been shown to generate infectivity and also allows the indefinite amplification of PrP with strain-specific biochemical and biological properties of the original molecules (Saborio, Permanne and Soto, 2001; Castilla *et al.*, 2008). The main objective of the second part of the project was to determine whether a direct encounter of an Fkbp protein with PrP abrogates or enhances conversion, by adding recombinant Fkbp proteins in PMCA reactions.

The second part of the project focused on the expression of recombinant Fkbp9 and Fkbp52 proteins to examine whether they directly interact with PrP^{c}, and in doing so, perturb prion propagation.

To successfully induce the expression of recombinant Fkbp9 and Fkbp52 proteins in *E. coli* cells, two parameters had to be adjusted:

1. Ampicillin was replaced with carbenicillin and its concentration in growth medium was raised to 300 µg/ml .

2. The cloning strategy for the Fkbp9 expression construct had to be modified such that both the ER signal sequence and ER retention motif were removed on either side of the *Fkbp9* gene via PCR.

In the absence of selective pressure, plasmids can be lost at low frequency while they are randomly distributed during bacterial cell division (Rosano and Ceccarelli, 2014). A higher concentration of antibiotics in the culture medium allows plasmids (encoding the gene of interest and the gene conferring antibiotic resistance) to be retained by the bacterial cells, thus minimising the problem of plasmid loss. Additionally, carbenicillin (an ampicillin analogue) is more stable at lower pH and higher temperatures (Baneyx, 1999).

In some cases, removal of a signal peptide or retention motif can increase the expression and stability of recombinant proteins. In the case of *Fkbp9*, the gene sequence was changed without changing the functional domain of the protein. For the ER resident protein Fkbp9, this modification proved to be beneficial, as the protein containing both its ER signal sequence and retention motif could not be expressed in *E. coli* cells (Gopal and Kumar, 2013).

For tau, APP and alpha synuclein, colocalisation and/or physical binding with Fkbp proteins has been established (Giustiniani et al., 2015; Blair et al., 2015b; Kamah et al., 2016; Liu et al., 2006; Gerard et al., 2010). For this reason, cell-free systems have been exploited to gain further understanding about this interaction and its relevance in Alzheimer's and Parkinson's disease respectively. The only instance when immunophilins have been directly linked to PrP^{c} processing is in the case of cyclophilins and PrP^{c} (Cohen and Taraboulos, 2003). Cyclophilins are peptidylpropyl *cis/trans* isomerases and like Fkbp proteins, act by accelerating the isomerisation of X-Proline bonds, a rate-limiting step in the folding of many proteins (Wang and Heitman, 2005). Cyclosporin A (CsA) treatment in CHO-M and N2a cells expressing wild-type PrP caused the accumulation of protease-resistant PrP in aggresomes. Additionally, disease-linked PrP proline mutants (P102L and P105L) mimicked the CsA-induced PrP species that accumulate in aggresomes. These findings indicate that cyclophilins are directly involved in the processing and/or folding of PrP^{c} (Cohen and Taraboulos, 2003).

Fkbp proteins have been implicated in prion propagation *in vitro* (Brown *et al.*, 2014; Stocki *et al.*, 2016) (as already demonstrated for *Fkbp9* and *Fkbp10*), but it has not yet been established whether this is due to a direct interaction with PrP^{c} and/or PrP^{Sc}.

Immunofluorescence can be employed in an attempt to answer the question of whether these proteins do indeed colocalise and/or interact with PrP. The subcellular localisation of Fkbp proteins is diverse and dynamic. Fkbp12 and Fkbp52 are primarily cytosolic and are involved in the stabilization of ryanodine receptors and potentiation of glucocorticoid receptor signalling respectively (Hausch, 2015; Snyder et al., 1998). Fkbp9 and Fkbp65 (encoded by *Fkbp10*) are ER resident proteins (Schwarze et al., 2013; Shadidy et al., 1999) whereas Fkbp38 has a predominantly mitochondrial localisation (Shirane and Nakayama, 2003). The Fkbp52 homologue, Fkbp51, exhibits dynamic nuclear-mitochondrial shuttling (Gallo *et al.*, 2011). Even though most PrP^{C} molecules are localised on the cell surface via a glycophosphatidylinositol (GPI) anchor (Stahl *et al.*, 1987), the pathway for the biosynthesis of PrP^{C} involves transit through the ER and Golgi compartments before delivery to the cell surface (Westergard, Christensen and Harris, 2007). Evidence showed that some PrP^{C} is transferred to clathrin-coated pits where it undergoes constitutive endocytosis and recycling (Shyng, Heuser and Harris, 1994; Naslavsky *et al.*, 1997). The precise site of prion replication has not yet been established. However, studies provided evidence that the endocytic pathway and caveolae-like domains may be sites of conversion of PrP^{C} to PrP^{Sc} (Borchelt, Taraboulos and Prusiner, 1992; Vey *et al.*, 1996). Importantly, a number of proteins that interact directly with PrP^{C}, are localised in the cytoplasm, including synapsin 1b (Spielhaupter and Schätzl, 2001), which is localised in synaptic vesicles, and heat shock protein 60 (HSP60) (Edenhofer *et al.*, 1996). It is possible that PrP^{C} interacts directly with Fkbp proteins such as Fkbp9 during post-translational processing in the ER. Alternatively, Fkbp proteins might affect prion replication via a mechanism that does not involve direct interaction with PrP^{C}.

In conclusion, SCA data from *Fkbp* stably silenced N2aPK1 cell lines showed that *Fkbp1a*, *Fkbp4* and *Fkbp8* might have a role in prion propagation. However, phenotypes arising from off-target effects and the fact that some cell lines with a good level of knock down of the target gene had no apparent effect on PrP^{Sc} levels in the SCA, makes it difficult to draw an accurate and definite conclusion about the involvement Fkbp proteins in prion propagation. To confirm that mRNA KD of target *Fkbp* genes leads to a corresponding reduction in Fkbp protein levels in PK1 stably silenced cell lines, it might be necessary to quantify Fkbp protein levels following gene silencing.

Transient transcriptional silencing of the same *Fkbp* genes had no effect on PrP^{Sc} levels, as determined by a separate SCA. Therefore, this data is not in agreement with

SCA data from stably *Fkbp* silenced cell lines. Surprisingly, even though stable gene silencing of *Fkbp9* in PK1 cells significantly increased prion propagation following challenge of the cells with RML (Brown *et al.*, 2014), experiments conducted in this project showed that transient KD of *Fkbp9* in iS7 cells did not affect the number of PrP^{Sc}-positive cells (as quantified using the SCA). It is possible that some Fkbp proteins act upstream of prion propagation e.g on the uptake of infectivity; an effect that cannot be reported by transient transcriptional silencing in cells with established prion infection.

PrP fibrillisation and PMCA experiments using recombinant wild-type and mutant Fkbp proteins may shed light on the mechanism by which proteins such as Fkbp9 affect prion propagation.

Bibliography

Aguib, Y. et al. (2009) ‘Autophagy induction by trehalose counteracts cellular prion infection’, Autophagy, 5(3), pp. 361–369. doi: 10.4161/auto.5.3.7662.

Aguzzi, A., Heikenwalder, M. and Polymenidou, M. (2007) ‘Insights into prion strains and neurotoxicity’, Nature Reviews Molecular Cell Biology, 8(7), pp. 552–561. doi: 10.1038/nrm2204.

Aguzzi, A., Montrasio, F. and Kaeser, P. S. (2001) ‘Prions: Health scare and biological challenge’, Nature Reviews Molecular Cell Biology, 2(2), pp. 118–126. doi: 10.1038/35052063.

Ahmed, Z. et al. (2014) ‘A novel in vivo model of tau propagation with rapid and progressive neurofibrillary tangle pathology: The pattern of spread is determined by connectivity, not proximity’, Acta Neuropathologica. Springer, 127(5), pp. 667–683. doi: 10.1007/s00401-014-1254-6.

Akhtar, S. et al. (2013) ‘Sod1 Deficiency Reduces Incubation Time in Mouse Models of Prion Disease’, PLoS ONE, 8(1), p. e54454. doi: 10.1371/journal.pone.0054454.
Akiyama, H. et al. (1999) ‘Occurrence of the diffuse amyloid β-protein (Aβ) deposits with numerous Aβ-containing glial cells in the cerebral cortex of patients with Alzheimer’s disease’, Glia. Wiley-Blackwell, 25(4), pp. 324–331.

Alais, S. et al. (2008) ‘Mouse neuroblastoma cells release prion infectivity associated with exosomal vesicles’, Biology of the Cell, 100(10), pp. 603–618. doi: 10.1042/BC20080025.

Alper, T. et al. (1967) ‘Does the agent of scrapie replicate without nucleic acid?’, Nature, 214(5090), pp. 764–766. doi: 10.1038/214764a0.

Alper, T., Haig, D. A. and Clarke, M. C. (1966) ‘The exceptionally small size of the scrapie agent’, Biochemical and Biophysical Research Communications, 22(3), pp. 278–284. doi: 10.1016/0006-291X(66)90478-5.

Altmeppen, H. C. et al. (2011) ‘Lack of a-disintegrin-and-metalloproteinase ADAM10 leads to intracellular accumulation and loss of shedding of the cellular prion protein in vivo’, Molecular Neurodegeneration, 6(1), p. 36. doi: 10.1186/1750-1326-6-36.

Altmeppen, H. C. et al. (2015) ‘The sheddase ADAM10 is a potent modulator of prion disease’, eLife, 2015(4), pp. 1–50. doi: 10.7554/eLife.04260.

Ansari, H., Greco, G. and Luban, J. (2002) ‘Cyclophilin A peptidyl-prolyl isomerase activity promotes ZPR1 nuclear export.’, Molecular and cellular biology, 22(20), pp. 6993–7003.

Arima, K. et al. (2005) ‘Biological and Biochemical Characteristics of Prion Strains Conserved in Persistently Infected Cell Cultures’, Journal of Virology. American Society for Microbiology, 79(11), pp. 7104–7112. doi: 10.1128/JVI.79.11.7104-7112.2005.

Arjona, A. et al. (2004) ‘Two Creutzfeldt-Jakob disease agents reproduce prion protein-independent identities in cell cultures’, Proceedings of the National Academy of Sciences, 101(23), pp. 8768–8773. doi: 10.1073/pnas.0400158101.

Asante, E. A. et al. (2002) ‘BSE prions propagate as either variant CJD-like or sporadic CJD-like prion strains in transgenic mice expressing human prion protein’, EMBO Journal, 21(23), pp.

Atkinson, P. H. (2004) ‘Glycosylation of prion strains in transmissible spongiform encephalopathies’, Australian Veterinary Journal, pp. 292–299. doi: 10.1111/j.1751-0813.2004.tb12709.x.

Ayers, J. I. et al. (2014) ‘Experimental transmissibility of mutant SOD1 motor neuron disease’, Acta Neuropathologica, 128(6), pp. 791–803. doi: 10.1007/s00401-014-1342-7.

Ayers, J. I., Diamond, J., et al. (2016a) ‘Distinct conformers of transmissible misfolded SOD1 distinguish human SOD1-FALS from other forms of familial and sporadic ALS’, Acta Neuropathologica, 132(6), pp. 827–840. doi: 10.1007/s00401-016-1623-4.

Ayers, J. I., Fromholt, S. E., et al. (2016b) ‘Prion-like propagation of mutant SOD1 misfolding and motor neuron disease spread along neuroanatomical pathways’, Acta Neuropathologica, 131(1), pp. 103–114. doi: 10.1007/s00401-015-1514-0.

Baiamonte, B. A. et al. (2013) ‘Attenuation of Rhes Activity Significantly Delays the Appearance of Behavioral Symptoms in a Mouse Model of Huntington’s Disease’, PLoS ONE. Edited by S. L. Sensi, 8(1), p. e53606. doi: 10.1371/journal.pone.0053606.

Banci, L. et al. (2008) ‘SOD1 and amyotrophic lateral sclerosis: Mutations and oligomerization’, PLoS ONE, 3(2), p. e1677. doi: 10.1371/journal.pone.0001677.

Baneyx, F. (1999) ‘Recombinant protein expression in Escherichia coli’, Current Opinion in Biotechnology, 10(5), pp. 411–421. doi: 10.1016/S0958-1669(99)00003-8.

Barik, S. (2006) ‘Immunophilins: for the love of proteins.’, Cellular and molecular life sciences: CMLS, 63(24), pp. 2889–900. doi: 10.1007/s00018-006-6215-3.

Baron, G. S. and Caughey, B. (2003) ‘Effect of glycosylphosphatidylinositol anchor-dependent and -independent prion protein association with model raft membranes on conversion to the protease-resistant isoform’, Journal of Biological Chemistry, 278(17), pp. 14883–14892. doi: 10.1074/jbc.M210840200.

Baron, G. S. et al. (2006) ‘Mouse-Adapted Scrapie Infection of SN56 Cells: Greater Efficiency with Microsome-Associated versus Purified PrP-res’, Journal of Virology, 80(5), pp. 2106–2117. doi: 10.1128/JVI.80.5.2106-2117.2006.

Baron, T. G. M., Madec, J. Y. and Calavas, D. (1999) ‘Similar signature of the prion protein in natural sheep scrapie and bovine spongiform encephalopathy-linked diseases’, Journal of Clinical Microbiology. American Society for Microbiology, 37(11), pp. 3701–3704.

Barria, M. A. et al. (2009) ‘De novo generation of infectious prions in vitro produces a new disease phenotype’, PLoS Pathogens. Edited by D. Westaway. Public Library of Science, 5(5), p. e1000421. doi: 10.1371/journal.ppat.1000421.

Bartlett, D. W. and Davis, M. E. (2006) 'Insights into the kinetics of siRNA-mediated gene silencing from live-cell and live-animal bioluminescent imaging', Nucleic Acids Research, 34(1), pp. 322–333. doi: 10.1093/nar/gkj439.

Bartz, J. C. et al. (1998) 'The host range of chronic wasting disease is altered on passage in ferrets', Virology, 251(2), pp. 297–301. doi: 10.1006/viro.1998.9427.

Bartz, J. C. et al. (2000) 'Adaptation and Selection of Prion Protein Strain Conformations following Interspecies Transmission of Transmissible Mink Encephalopathy', Journal of Virology, 74(12), pp. 5542–5547. doi: 10.1128/JVI.74.12.5542-5547.2000.

Baskakov, I. V. (2014) 'The many shades of prion strain adaptation', Prion. Taylor & Francis, 8(2), p. 169. doi: 10.4161/pri.27836.

Baskakov, I. V. and Katorcha, E. (2016) 'Multifaceted role of sialylation in prion diseases', Frontiers in Neuroscience, 10(AUG), p. 358. doi: 10.3389/fnins.2016.00358.

Basler, K. et al. (1986) 'Scrapie and cellular PrP isoforms are encoded by the same chromosomal gene', Cell, 46(3), pp. 417–428. doi: 10.1016/0092-8674(86)90662-8.

Begara-McGorum, I. et al. (2002) 'Vacuolar lesion profile in sheep scrapie: Factors influencing its variation and relationship to disease-specific PrP accumulation', Journal of Comparative Pathology. W.B. Saunders, 127(1), pp. 59–68. doi: 10.1053/jcpa.2002.0558.

Beitz, J. M. (2014) 'Parkinson's disease: a review', Frontiers in Bioscience, 6(3), pp. 65–74.

Bellinger, F. P. et al. (2008) 'Association of selenoprotein P with Alzheimer's pathology in human cortex', Journal of Alzheimer's Disease, 15(3), pp. 465–472. doi: 10.3233/JAD-2008-15313.

Benn, C. L. et al. (2008) 'Huntingtin Modulates Transcription, Occupies Gene Promoters In Vivo, and Binds Directly to DNA in a Polyglutamine-Dependent Manner', Journal of Neuroscience, 28(42), pp. 10720–10733. doi: 10.1523/JNEUROSCI.2126-08.2008.

Benson, D. F., Davis, R. J. and Snyder, B. D. (1988) 'Posterior cortical atrophy.', Archives of neurology, 45(7), pp. 789–93. doi: 10.1001/archneur.1988.00520310107024.

Ben-Zaken, O. et al. (2003) 'Cellular heparan sulfate participates in the metabolism of prions', Journal of Biological Chemistry, 278(41), pp. 40041–40049. doi: 10.1074/jbc.M301152200.

Bergh, J. et al. (2015) 'Structural and kinetic analysis of protein-aggregate strains in vivo using binary epitope mapping', Proceedings of the National Academy of Sciences, 112(14), pp. 4489–4494. doi: 10.1073/pnas.1419228112.

Beringue, V. et al. (2003) 'Regional heterogeneity of cellular prion protein isoforms in the mouse brain', Brain, 126(9), pp. 2065–2073. doi: 10.1093/brain/awg205.

Berry, D. B. et al. (2013) ‘Drug resistance confounding prion therapeutics’, Proceedings of the National Academy of Sciences, 110(44), pp. E4160–E4169. doi: 10.1073/pnas.1317164110.

Bertoncini, C. W. et al. (2005) ‘Familial mutants of α-synuclein with increased neurotoxicity have a destabilized conformation’, Journal of Biological Chemistry. American Society for Biochemistry and Molecular Biology, 280(35), pp. 30649–30652. doi: 10.1074/jbc.C500288200.

Bessen, R. A. and Marsh, R. F. (1992a) ‘Biochemical and physical properties of the prion protein from two strains of the transmissible mink encephalopathy agent’, J Virol, 66(4), pp. 2096–2101.

Bessen, R. A. and Marsh, R. F. (1992b) ‘Identification of two biologically distinct strains of transmissible mink encephalopathy in hamsters’, Journal of General Virology, 73(2), pp. 329–334. doi: 10.1099/0022-1317-73-2-329.

Bessen, R. A. and Marsh, R. F. (1994) ‘Distinct PrP properties suggest the molecular basis of strain variation in Transmissible Mink [Review]’, Journal of Virology, 68(12), pp. 7859–7868.

Bird, T. D. et al. (1983) ‘Alzheimer’s disease: Choline acetyltransferase activity in brain tissue from clinical and pathological subgroups’, Annals of Neurology, 14(3), pp. 284–293. doi: 10.1002/ana.410140306.

Birkett, C. R. et al. (2001) ‘Scrapie strains maintain biological phenotypes on propagation in a cell line in culture’, EMBO Journal, 20(13), pp. 3351–3358. doi: 10.1093/emboj/20.13.3351.

Bishop, M. T., Will, R. G. and Manson, J. C. (2010) ‘Defining sporadic Creutzfeldt-Jakob disease strains and their transmission properties’, Proceedings of the National Academy of Sciences, 107(26), pp. 12005–12010. doi: 10.1073/pnas.1004688107.

Blair, L. J. (2015a) ‘Age-associated increases in FKBP51 facilitate tau neurotoxicity.’, Dissertation Abstracts International: Section B: The Sciences and Engineering, 75(11–B(E)).

Blair, L. J. et al. (2013) ‘Accelerated neurodegeneration through chaperone-mediated oligomerization of tau.’, The Journal of clinical investigation. American Society for Clinical Investigation, 123(10), pp. 4158–69. doi: 10.1172/JCI69003.

Blair, L. J. et al. (2015b) ‘The emerging role of peptidyl-prolyl isomerase chaperones in tau oligomerization, amyloid processing, and Alzheimer’s disease.’, Journal of neurochemistry, 133(1), pp. 1–13. doi: 10.1111/jnc.13033.

Borchelt, D. R., Taraboulos, A. and Prusiner, S. B. (1992) ‘Evidence for synthesis of scrapie prion proteins in the endocytic pathway’, Journal of Biological Chemistry, 267(23), pp. 16188–16199.

Bosco, D. A. et al. (2010) ‘Wild-type and mutant SOD1 share an aberrant conformation and a common pathogenic pathway in ALS’, Nature Neuroscience, 13(11), pp. 1396–1403. doi: 10.1038/nn.2660.

Bosque, P. J. and Prusiner, S. B. (2000) ‘Cultured cell sublines highly susceptible to prion infection.’, Journal of virology. American Society for Microbiology, 74(9), pp. 4377–4386. doi: 10.1128/JVI.74.9.4377-4386.2000.

Bousset, L. et al. (2013) ‘Structural and functional characterization of two alpha-synuclein strains’, Nature Communications, 4. doi: 10.1038/ncomms3575.

Braak, H. and Braak, E. (1991) ‘Neuropathological stageing of Alzheimer-related changes’, Acta Neuropathologica, 82(4), pp. 239–259. doi: 10.1007/BF00308809.

Braak, H. et al. (2003) ‘Staging of brain pathology related to sporadic Parkinson’s disease’, Neurobiology of Aging, 24(2), pp. 197–211. doi: 10.1016/S0197-4580(02)00065-9.

Brice , A. (2005) ‘Genetics of Parkinson’s disease: LRRK2 on the rise’, Brain, 128(12), pp. 2760-2. doi: 10.1093/brain/awh676.

Brockington, A. et al. (2013) ‘Unravelling the enigma of selective vulnerability in neurodegeneration: Motor neurons resistant to degeneration in ALS show distinct gene expression characteristics and decreased susceptibility to excitotoxicity’, Acta Neuropathologica. Springer-Verlag, 125(1), pp. 95–109. doi: 10.1007/s00401-012-1058-5.

Brotherton, T. E. et al. (2012) ‘Localization of a toxic form of superoxide dismutase 1 protein to pathologically affected tissues in familial ALS’, Proceedings of the National Academy of Sciences. National Academy of Sciences, 109(14), pp. 5505–5510. doi: 10.1073/pnas.1115009109.

Brown, C. A. et al. (2014) ‘In vitro screen of prion disease susceptibility genes using the scrapie cell assay’, Human molecular genetics, 23(19), pp. 5102–5108. doi: 10.1093/hmg/ddu233.

Brown, D. R. (2005) Neurodegeneration and Prion Disease | Springer. Springer Science and Business Media.

Brown, E. J. et al. (1994) ‘A mammalian protein targeted by G1-arresting rapamycin-receptor complex.’, Nature, 369(6483), pp. 756–8. doi: 10.1038/369756a0.

Brown, P. et al. (1984) ‘Creutzfeldt-Jakob disease of long duration: Clinicopathological characteristics, transmissibility, and differential diagnosis’, Annals of Neurology. Wiley Subscription Services, Inc., A Wiley Company, 16(3), pp. 295–304. doi: 10.1002/ana.410160305.

Brown, P., Preece, M. A. and Will, R. G. (1992) ‘“Friendly fire” in medicine: hormones, homografts, and Creutzfeldt-Jakob disease’, The Lancet, 340(8810), pp. 24–27. doi: 10.1016/0140-6736(92)92431-E.

Bruce, M. E. (1993) ‘Scrapie strain variation and mutation’, British Medical Bulletin, 49(4), pp. 822–838. doi: 10.1093/oxfordjournals.bmb.a072649.

Bruce, M. E. and Dickinson, A. G. (1987) ‘Biological evidence that scrapie agent has an independent genome’, Journal of General Virology, 68(1), pp. 79–89. doi: 10.1099/0022-1317-68-1-79.

Bruce, M. E. and Fraser, H. (1991) ‘Scrapie strain variation and its implications.’, Curr Top Microbiol Immunol, 172, pp. 125–138. doi: 10.1007/978-3-642-76540-7_8.

Büeler, H. et al. (1993) ‘Mice devoid of PrP are resistant to scrapie’, Cell, 73(7), pp. 1339–1347. doi: 10.1016/0092-8674(93)90360-3.

Burchell, V. S. et al. (2013) ‘The Parkinson’s disease-linked proteins Fbxo7 and Parkin interact to mediate mitophagy’, Nature Neuroscience, 16(9), pp. 1257-65. Doi: 10.1038/nn.3489.

Cameron, A. M. et al. (1997) ‘FKBP12 binds the inositol 1,4,5-trisphosphate receptor at leucine-proline (1400-1401) and anchors calcineurin to this FK506-like domain.’, The Journal of biological chemistry, 272(44), pp. 27582–8.

Cancellotti, E. et al. (2013) ‘Post-translational changes to PrP alter transmissible spongiform encephalopathy strain properties’, EMBO Journal. Nature Publishing Group, 32(5), pp. 756–769. doi: 10.1038/emboj.2013.6.

Cao, W. and Konsolaki, M. (2011) ‘FKBP immunophilins and Alzheimer’s disease: a chaperoned affair.’, Journal of biosciences, 36(3), pp. 493–8.

Cappai, R. et al. (1999) ‘Familial prion disease mutation alters the secondary structure of recombinant mouse prion protein: Implications for the mechanism of prion formation’, Biochemistry, 38(11), pp. 3280–3284. doi: 10.1021/bi982328z.

Carp, R. I., Meeker, H. and Sersen, E. (1997) ‘Scrapie strains retain their distinctive characteristics following passages of homogenates from different brain regions and spleen’, Journal of General Virology, 78(1), pp. 283–290. doi: 10.1099/0022-1317-78-1-283.

Carroll, J. A. et al. (2016) ‘Prion Strain Differences in Accumulation of PrPSc on Neurons and Glia Are Associated with Similar Expression Profiles of Neuroinflammatory Genes: Comparison of Three Prion Strains’, PLoS Pathogens, 12(4), pp. 1–26. doi: 10.1371/journal.ppat.1005551.

Castellani, R. J. et al. (2004) ‘Sensitivity of 14-3-3 protein test varies in subtypes of sporadic Creutzfeldt-Jakob disease’, Neurology, 63(3), pp. 436–442. doi: 10.1212/01.WNL.0000135153.96325.3B.

Castilla, J. et al. (2008) ‘Cell-free propagation of prion strains’, EMBO Journal. European Molecular Biology Organization, 27(19), pp. 2557–2566. doi: 10.1038/emboj.2008.181.

Caughey, B. and Raymond, G. J. (1991) ‘The scrapie-associated form of PrP is made from a cell surface precursor that is both protease- and phospholipase-sensitive’, Journal of Biological Chemistry, 266(27), pp. 18217–18223.

Caughey, B. and Raymond, G. J. (1993) ‘Sulfated polyanion inhibition of scrapie-associated PrP accumulation in cultured cells’, Journal of virology, 67(2), pp. 643–650.

Caughey, B. et al. (1988) ‘In vitro expression in eukaryotic cells of a prion protein gene cloned from scrapie-infected mouse brain.’, Proc Natl Acad Sci U S A, 85(13), pp. 4657–4661. doi: 10.1073/pnas.85.13.4657.

Caughey, B. et al. (1994) ‘Binding of the protease-sensitive form of PrP (prion protein) to sulfated glycosaminoglycan and congo red [corrected’, Journal of virology, 68(4), pp. 2135–2141.

Cauwenberghe, C. et al. (2016) ‘The genetic landscape of Alzheimer’s disease: clinical implications and perspectives’, Genetics in Medicine, 18(5), pp. 421-30. Doi: 10.1038/gim.2015.117.

Chambraud, B. et al. (2007) ‘The immunophilin FKBP52 specifically binds to tubulin and prevents microtubule formation.’, FASEB journal: official publication of the Federation of American Societies for Experimental Biology, 21(11), pp. 2787–97. doi: 10.1096/fj.06-7667com.

Chambraud, B. et al. (2010) ‘A role for FKBP52 in Tau protein function.’, Proceedings of the National Academy of Sciences of the United States of America, 107(6), pp. 2658–63. doi: 10.1073/pnas.0914957107.

Chan, C. S. et al. (2007) ‘“Rejuvenation” protects neurons in mouse models of Parkinson’s disease’, Nature. Nature Publishing Group, 447(7148), pp. 1081–1086. doi: 10.1038/nature05865.

Chang, Q. and Martin, L. J. (2009) ‘Glycinergic innervation of motoneurons is deficient in amyotrophic lateral sclerosis mice: A quantitative confocal analysis’, American Journal of Pathology, 174(2), pp. 574–585. doi: 10.2353/ajpath.2009.080557.

Chang, Q. and Martin, L. J. (2011) ‘Glycine Receptor Channels in Spinal Motoneurons Are Abnormal in a Transgenic Mouse Model of Amyotrophic Lateral Sclerosis’, Journal of Neuroscience, 31(8), pp. 2815–2827. doi: 10.1523/JNEUROSCI.2475-10.2011.

Cheng, C. et al. (2013) ‘Genetics of amyotrophic lateral sclerosis: an update’, Molecular Neurodegeneration, 8:28. Doi: 10.1186/1750-1326-8-28.

Cheung-Flynn, J. et al. (2005) ‘Physiological Role for the Cochaperone FKBP52 in Androgen Receptor Signaling’, Molecular Endocrinology, 19(6), pp. 1654–1666. doi: 10.1210/me.2005-0071.

Chiang, M.-C. et al. (2007) ‘Systematic uncovering of multiple pathways underlying the pathology of Huntington disease by an acid-cleavable isotope-coded affinity tag approach.’, Molecular & cellular proteomics: MCP, 6(5), pp. 781–97. doi: 10.1074/mcp.M600356-MCP200.

Choi, W.-S. et al. (2008) ‘Mitochondrial complex I inhibition is not required for dopaminergic neuron death induced by rotenone, MPP+, or paraquat’, Proceedings of the National Academy of Sciences, 105(39), pp. 15136–15141. doi: 10.1073/pnas.0807581105.

Choi, Y. P. et al. (2010) ‘Distinct Stability States of Disease-Associated Human Prion Protein Identified by Conformation-Dependent Immunoassay’, Journal of Virology. American Society for Microbiology, 84(22), pp. 12030–12038. doi: 10.1128/JVI.01057-10.

Clavaguera, F. et al. (2009) ‘Transmission and spreading of tauopathy in transgenic mouse brain’, Nature Cell Biology, 11(7), pp. 909–913. doi: 10.1038/ncb1901.

Clavaguera, F. et al. (2013) ‘Brain homogenates from human tauopathies induce tau inclusions in mouse brain’, Proceedings of the National Academy of Sciences. National Academy of Sciences, 110(23), pp. 9535–9540. doi: 10.1073/pnas.1301175110.

Cohen, E. and Taraboulos, A. (2003) ‘Scrapie-like prion protein accumulates in aggresomes of cyclosporin A-treated cells’, EMBO Journal, 22(3), pp. 404–417. doi: 10.1093/emboj/cdg045.

Cohen, M. L. et al. (2015) ‘Rapidly progressive Alzheimer’s disease features distinct structures of amyloid-β’, Brain, 138(4), pp. 1009–1022. doi: 10.1093/brain/awv006.

Cohen, M., Appleby, B. and Safar, J. G. (2016) ‘Distinct prion-like strains of amyloid beta implicated in phenotypic diversity of Alzheimer’s disease’, Prion. Taylor & Francis, 10(1), pp. 9–17. doi: 10.1080/19336896.2015.1123371.

Colby, D. W. et al. (2009) ‘Design and construction of diverse mammalian prion strains’, Proceedings of the National Academy of Sciences. National Academy of Sciences, 106(48), pp. 20417–20422. doi: 10.1073/pnas.0910350106.

Collinge, J. (1999) ‘Variant Creutzfeldt-Jakob disease’, Lancet, 354(9175), pp. 317–323. doi: 10.1016/S0140-6736(99)05128-4.

Collinge, J. (2001) ‘Prion Diseases of Humans and Animals: Their Causes and Molecular Basis’, Annual Review of Neuroscience, 24(1), pp. 519–550. doi: 10.1146/annurev.neuro.24.1.519.

Collinge, J. (2005) ‘Molecular neurology of prion disease.’, Journal of neurology, neurosurgery, and psychiatry, 76(7), pp. 906–19. doi: 10.1136/jnnp.2004.048660.

Collinge, J. (2016) ‘Mammalian prions and their wider relevance in neurodegenerative diseases’, Nature, 539(7628), pp. 217–226. doi: 10.1038/nature20415.

Collinge, J. and Clarke, A. R. (2007) ‘A general model of prion strains and their pathogenicity’, Science, 318(5852), pp. 930–936. doi: 10.1126/science.1138718.

Collinge, J. et al. (1990) ‘Prion dementia without characteristic pathology’, The Lancet. Elsevier, 336(8706), pp. 7–9. doi: 10.1016/0140-6736(90)91518-F.

Collinge, J. et al. (1992) ‘Inherited prion disease with 144 base pair gene insertion: 2. Clinical and pathological features’, Brain, 115(3), pp. 687–710. doi: 10.1093/brain/115.3.687.

Collinge, J. et al. (1995) ‘Unaltered susceptibility to BSE in transgenic mice expressing human prion protein’, Nature, 378(6559), pp. 779–783. doi: 10.1038/378779a0.

Collinge, J. et al. (1996) ‘Molecular analysis of prion strain variation and the aetiology of “new variant” CJD’, Nature, 383(6602), pp. 685–690. doi: 10.1038/383685a0.

Collinge, J., Palmer, M. S. and Dryden, A. J. (1991) ‘Genetic predisposition to iatrogenic Creutzfeldt-Jakob disease’, The Lancet. Elsevier, 337(8755), pp. 1441–1442. doi: 10.1016/0140-6736(91)93128-V.

Collins, S. J. et al. (2006) ‘Determinants of diagnostic investigation sensitivities across the clinical spectrum of sporadic Creutzfeldt-Jakob disease’, Brain, 129(9), pp. 2278–2287. doi: 10.1093/brain/awl159.

Comley, L. et al. (2015) ‘Motor neurons with differential vulnerability to degeneration show distinct protein signatures in health and ALS’, Neuroscience, 291, pp. 216–229. doi: 10.1016/j.neuroscience.2015.02.013.

Condello, C. et al. (2018) ‘Structural heterogeneity and intersubject variability of Aβ in familial and sporadic Alzheimer’s disease’, Proceedings of the National Academy of Sciences, 115(4), p. 201714966. doi: 10.1073/pnas.1714966115.

Conway, K. A. et al. (2000) ‘Acceleration of oligomerization, not fibrillization, is a shared property of both alpha -synuclein mutations linked to early-onset Parkinson’s disease: Implications for pathogenesis and therapy’, Proceedings of the National Academy of Sciences, 97(2), pp. 571–576. doi: 10.1073/pnas.97.2.571.

Cunningham, C. et al. (2003) ‘Synaptic changes characterize early behavioural signs in the ME7 model of murine prion disease’, European Journal of Neuroscience, 17(10), pp. 2147–2155. doi: 10.1046/j.1460-9568.2003.02662.x.

Dauer, W. and Przedborski, S. (2003) ‘Parkinson’s disease: Mechanisms and models’, Neuron, 39(6), pp. 889–909. doi: 10.1016/S0896-6273(03)00568-3.

De Souza, L. C. et al. (2011) ‘Similar amyloid-β burden in posterior cortical atrophy and Alzheimer’s disease’, Brain, 134(7), pp. 2036–2043. doi: 10.1093/brain/awr130.

De Strooper, B. (2007) ‘Loss-of-function presenilin mutations in Alzheimer’s disease. Talking point on the role of presenilin mutations in Alzheimer’s disease’, EMBO reports, 8(2), pp. 141-146. Doi: 10.1038/sj.embor.7400897.

DeArmond, S. J. et al. (1997) ‘Selective neuronal targeting in prion disease’, Neuron. Cell Press, 19(6), pp. 1337–1348. doi: 10.1016/S0896-6273(00)80424-9.

DeArmond, S. J. et al. (1999) ‘PrPc glycoform heterogeneity as a function of brain region: implications for selective targeting of neurons by prion strains.’, Journal of neuropathology and experimental neurology, 58(9), pp. 1000–1009. doi: 10.1097/00005072-199909000-00010.

Deleersnijder, A. et al. (2011) ‘Comparative analysis of different peptidyl-prolyl isomerases reveals FK506-binding protein 12 as the most potent enhancer of alpha-synuclein aggregation.’, The Journal of biological chemistry, 286(30), pp. 26687–701. doi: 10.1074/jbc.M110.182303.

Delgado-Camprubi, M. et al. (2017) ‘Deficiency of Parkinson’s disease-related gene Fbxo7 is associated with impaired mitochondrial metabolism by PARP activation’, Cell Death and Differentiation. Nature Publishing Group, 24(1), pp. 120–131. doi: 10.1038/cdd.2016.104.

Desplats, P. et al. (2009) ‘Inclusion formation and neuronal cell death through neuron-to-neuron transmission of α-synuclein’, Proceedings of the National Academy of Sciences, 106(31), pp. 13010–13015. doi: 10.1073/pnas.0903691106.

Di Fonzo, A. et al. (2009) 'FBXO7 mutations cause autosomal recessive, early-onset parkinsonian-pyramidal syndrome', Neurology, 72(3), pp. 240-5. Doi: 10.1212/01.wnl.0000338144.10967.2b.

Dickinson, A. G. et al. (1972) 'Competition between different scrapie agents in mice', Nature New Biology, 237(77), pp. 244–245. doi: 10.1038/newbio237244a0.dis.2007.02.011.

Domingo, E. et al. (2006) 'Viruses as quasispecies: Biological implications', Current Topics in Microbiology and Immunology, 299, pp. 51–82. doi: 10.1007/3-540-26397-7_3.

Domingo, E., Sheldon, J. and Perales, C. (2012) 'Viral Quasispecies Evolution', Microbiology and Molecular Biology Reviews. American Society for Microbiology, 76(2), pp. 159–216. doi: 10.1128/MMBR.05023-11.

Du, X. et al. (2014) 'Inhibitory act of selenoprotein P on Cu+/Cu2+-induced tau aggregation and neurotoxicity', Inorganic Chemistry, 53(20), pp. 11221–11230. doi: 10.1021/ic501788v.

Edenhofer, F. et al. (1996) 'Prion protein PrPc interacts with molecular chaperones of the Hsp60 family.', Journal of virology. American Society for Microbiology (ASM), 70(7), pp. 4724–4728.

Eichner, T. et al. (2011) 'Conformational Conversion during Amyloid Formation at Atomic Resolution', Molecular Cell, 41(2), pp. 161–172. doi: 10.1016/j.molcel.2010.11.028.

Eisele, Y. S. et al. (2009) 'Induction of cerebral -amyloidosis: Intracerebral versus systemic Aβ inoculation', Proceedings of the National Academy of Sciences, 106(31), pp. 12926–12931. doi: 10.1073/pnas.0903200106.

Eisele, Y. S. et al. (2010) 'Peripherally applied Aβ-containing inoculates induce cerebral β-amyloidosis', Science, 330(6006), pp. 980–982. doi: 10.1126/science.1194516.

Eisenberg, D. and Jucker, M. (2012) 'The amyloid state of proteins in human diseases', Cell. Elsevier, 148(6), pp. 1188–1203. doi: 10.1016/j.cell.2012.02.022.

Ekhtiari Bidhendi, E. et al. (2016) 'Two superoxide dismutase prion strains transmit amyotrophic lateral sclerosis-like disease', Journal of Clinical Investigation, 126(6), pp. 2249–2253. doi: 10.1172/JCI84360.

Ellett, L. J. et al. (2015) 'Glycosaminoglycan sulfation determines the biochemical properties of prion protein aggregates', Glycobiology, 25(7), pp. 745–755. doi: 10.1093/glycob/cwv014.

Endo, T. et al. (1989) 'Diversity of Oligosaccharide Structures Linked to Asparagines of the Scrapie Prion Protein', Biochemistry. American Chemical Society, 28(21), pp. 8380–8388. doi: 10.1021/bi00447a017.

Erlejman, A. G. et al. (2014) 'NF-κB transcriptional activity is modulated by FK506-binding proteins FKBP51 and FKBP52: a role for peptidyl-prolyl isomerase activity.', The Journal of biological chemistry, 289(38), pp. 26263–76. doi: 10.1074/jbc.M114.582882.

Ertmer, A. et al. (2004) ‘The Tyrosine Kinase Inhibitor STI571 Induces Cellular Clearance of PrPSc in Prion-infected Cells’, Journal of Biological Chemistry, 279(40), pp. 41918–41927. doi: 10.1074/jbc.M405652200.

Esko, J. D. and Selleck, S. B. (2002) ‘Order Out of Chaos: Assembly of Ligand Binding Sites in Heparan Sulfate’, Annual Review of Biochemistry, 71(1), pp. 435–471. doi: 10.1146/annurev.biochem.71.110601.135458.

Falcon, B. et al. (2015) ‘Conformation determines the seeding potencies of native and recombinant Tau aggregates’, Journal of Biological Chemistry, 290(2), pp. 1049–1065. doi: 10.1074/jbc.M114.589309.

Fehlinger, A. et al. (2017) ‘Prion strains depend on different endocytic routes for productive infection’, Scientific Reports, 7(1), pp. 1–15. doi: 10.1038/s41598-017-07260-2.

Ferrari, R. et al. (2011) ‘FTD and ALS: A Tale of Two Diseases’, Current Alzheimer Research, 8(3), pp. 273–294. doi: 10.2174/156720511795563700.

Fevrier, B. et al. (2004) ‘Cells release prions in association with exosomes’, Proceedings of the National Academy of Sciences, 101(26), pp. 9683–9688. doi: 10.1073/pnas.0308413101.

Fischer, S., Michnick, S. and Karplus, M. (1993) ‘A Mechanism for Rotamase Catalysis by the FK506 Binding Protein (FKBP)’, Biochemistry. American Chemical Society, 32(50), pp. 13830–13837. doi: 10.1021/bi00213a011.

Flagmeier, P. et al. (2016) ‘Mutations associated with familial Parkinson’s disease alter the initiation and amplification steps of α-synuclein aggregation’, Proceedings of the National Academy of Sciences. National Academy of Sciences, 113(37), pp. 10328–10333. doi: 10.1073/pnas.1604645113.

Fraser, H. (1993) ‘Diversity in the neuropathology of scrapie-like diseases in animals’, British Medical Bulletin, 49(4), pp. 792–809. doi: 10.1093/oxfordjournals.bmb.a072647.

Fraser, H. and Dickinson, A. G. (1973) ‘Scrapie in mice. Agent-strain differences in the distribution and intensity of grey matter vacuolation’, Journal of Comparative Pathology, 83(1), pp. 29–40. doi: 10.1016/0021-9975(73)90024-8.

Fraser, H. and Dickinson, A. G. (1978) ‘Studies of the lymphoreticular system in the pathogenesis of scrapie: The role of spleen and thymus’, Journal of Comparative Pathology, 88(4), pp. 563–573. doi: 10.1016/0021-9975(78)90010-5.

Freixes, M. et al. (2004) ‘Clusterin solubility and aggregation in Creutzfeldt-Jakob disease’, Acta Neuropathologica. Springer-Verlag, 108(4), pp. 295–301. doi: 10.1007/s00401-004-0891-6.

Fritschi, S. K. et al. (2014) ‘Highly potent soluble amyloid-β seeds in human Alzheimer brain but not cerebrospinal fluid’, Brain, 137(11), pp. 2909–2915. doi: 10.1093/brain/awu255.

Frontzek, K. et al. (2016) ‘Amyloid-β pathology and cerebral amyloid angiopathy are frequent in iatrogenic Creutzfeldt-Jakob disease after dural grafting’, Swiss medical weekly, 146, p. w14287. doi: 10.4414/smw.2016.14287.

Frost, B. and Diamond, M. I. (2010) ‘Prion-like mechanisms in neurodegenerative diseases’, Nature Reviews Neuroscience, 11(3), pp. 155–159. doi: 10.1038/nrn2786.

Fu, Y. et al. (2017) ‘A toxic mutant huntingtin species is resistant to selective autophagy’, Nature Chemical Biology, 13(11), pp. 1152–1154. doi: 10.1038/nchembio.2461.

Fusco, D. et al. (2010) ‘The RET51/FKBP52 complex and its involvement in Parkinson disease.’, Human molecular genetics. Oxford University Press, 19(14), pp. 2804–16. doi: 10.1093/hmg/ddq181.

Gabizon, R. et al. (1993) ‘Heparin-like molecules bind differentially to prion-proteins and change their intracellular metabolic fate’, Journal of Cellular Physiology, 157(2), pp. 319–325. doi: 10.1002/jcp.1041570215.

Gaburjakova, M. et al. (2001) ‘FKBP12 binding modulates ryanodine receptor channel gating.’, The Journal of biological chemistry, 276(20), pp. 16931–5. doi: 10.1074/jbc.M100856200.

Galat, A. (2003) ‘Peptidylprolyl Cis / Trans Isomerases (Immunophilins): Biological Diversity - Targets - Functions’, Current Topics in Medicinal Chemistry, 3(12), pp. 1315–1347. doi: 10.2174/1568026033451862.

Gallo, L. I. et al. (2011) ‘The 90-kDa heat-shock protein (Hsp90)-binding immunophilin FKBP51 is a mitochondrial protein that translocates to the nucleus to protect cells against oxidative stress.’, The Journal of biological chemistry, 286(34), pp. 30152–60. doi: 10.1074/jbc.M111.256610.

Gambetti, P. et al. (1995) ‘Fatal familial insomnia and familial Creutzfeldt-Jakob disease: clinical, pathological and molecular features.’, Brain pathology (Zurich, Switzerland), 5(1), pp. 43–51. doi: 10.1111/j.1750-3639.1995.tb00576.x.

Gambetti, P. et al. (2003) ‘Sporadic and familial CJD: Classification and characterisation’, British Medical Bulletin, 66, pp. 213–239. doi: 10.1093/bmb/66.1.213.

Gandhi, S. et al. (2009) ‘PINK1-Associated Parkinson’s Disease Is Caused by Neuronal Vulnerability to Calcium-Induced Cell Death’, Molecular Cell, 33(5), pp. 627–638. doi: 10.1016/j.molcel.2009.02.013.

Gerald, A. H et al. (1991) ‘Bovine Spongiform Encephalopathy: A neuropathological perspective’, Brain Pathology, 1: 69-78.

Gerard, M. et al. (2006) ‘The aggregation of alpha-synuclein is stimulated by FK506 binding proteins as shown by fluorescence correlation spectroscopy.’, FASEB journal: official publication of the Federation of American Societies for Experimental Biology, 20(3), pp. 524–6. doi: 10.1096/fj.05-5126fje.

Gerard, M. et al. (2008) ‘FK506 binding protein 12 differentially accelerates fibril formation of wild type alpha-synuclein and its clinical mutants A30P or A53T.’, Journal of neurochemistry, 106(1), pp. 121–33. doi: 10.1111/j.1471-4159.2008.05342.x.

Gerard, M. et al. (2010) ‘Inhibition of FK506 binding proteins reduces alpha-synuclein aggregation and Parkinson’s disease-like pathology.’, The Journal of neuroscience: the official journal of the Society for Neuroscience, 30(7), pp. 2454–63. doi: 10.1523/JNEUROSCI.5983-09.2010.

Ghaemmaghami, S. et al. (2009) ‘Continuous quinacrine treatment results in the formation of drug-resistant prions’, PLoS Pathogens. Edited by N. Mabbott, 5(11), p. e1000673. doi: 10.1371/journal.ppat.1000673.

Ghaemmaghami, S. et al. (2011) ‘Conformational transformation and selection of synthetic prion strains’, Journal of Molecular Biology, 413(3), pp. 527–542. doi: 10.1016/j.jmb.2011.07.021.

Ghiglieri, V. and Calabresi, P. (2013) ‘Rhes, a key element of selective neuronal vulnerability in Huntington’s disease: A striatal-specific license to kill during energy metabolism failure’, Movement Disorders, 28(6), pp. 735–735. doi: 10.1002/mds.25476.

Giustiniani, J. et al. (2012) ‘Decrease of the immunophilin FKBP52 accumulation in human brains of Alzheimer’s disease and FTDP-17.’, Journal of Alzheimer’s disease: JAD, 29(2), pp. 471–83. doi: 10.3233/JAD-2011-111895.

Giustiniani, J. et al. (2015) ‘The FK506-binding protein FKBP52 in vitro induces aggregation of truncated Tau forms with prion-like behavior.’, FASEB journal: official publication of the Federation of American Societies for Experimental Biology, 29(8), pp. 3171–81. doi: 10.1096/fj.14-268243.

Goedert, M., Clavaguera, F. and Tolnay, M. (2010) ‘The propagation of prion-like protein inclusions in neurodegenerative diseases’, Trends in Neurosciences, 33(7), pp. 317–325. doi: 10.1016/j.tins.2010.04.003.

Gomori, A. J. et al. (1973) ‘The Ataxic form of Creutzfeldt-Jakob Disease’, Archives of Neurology. American Medical Association, 29(5), pp. 318–323. doi: 10.1001/archneur.1973.00490290058006.

Gong, C.-X. and Iqbal, K. (2008) ‘Hyperphosphorylation of Microtubule-Associated Protein Tau: A Promising Therapeutic Target for Alzheimer Disease’, Current Medicinal Chemistry, 15(23), pp. 2321–2328. doi: 10.2174/092986708785909111.

Gonzalez-Montalban, N. et al. (2013) ‘Changes in prion replication environment cause prion strain mutation’, FASEB Journal, 27(9), pp. 3702–3710. doi: 10.1096/fj.13-230466.

Gopal, G. J. and Kumar, A. (2013) ‘Strategies for the production of recombinant protein in escherichia coli’, Protein Journal, 32(6), pp. 419–425. doi: 10.1007/s10930-013-9502-5.

Gorno-Tempini, M. L. et al. (2008) ‘The logopenic/phonological variant of primary progressive aphasia’, Neurology, 71(16), pp. 1227–1234. doi: 10.1212/01.wnl.0000320506.79811.da.

Gousset, K. et al. (2009) ‘Prions hijack tunnelling nanotubes for intercellular spread’, Nature Cell Biology, 11(3), pp. 328–336. doi: 10.1038/ncb1841.

Grad, L. I. et al. (2014) ‘Intercellular propagated misfolding of wild-type Cu/Zn superoxide dismutase occurs via exosome-dependent and -independent mechanisms’, Proceedings of the National Academy of Sciences. National Academy of Sciences, 111(9), pp. 3620–3625. doi: 10.1073/pnas.1312245111.

Grad, L. I., Pokrishevsky, E. and Cashman, N. R. (2017) 'Intercellular prion-like conversion and transmission of Cu/Zn superoxide dismutase (SOD1) in cell culture', in Methods in Molecular Biology, pp. 357–367. doi: 10.1007/978-1-4939-7244-9_24.

Greil, C. S. et al. (2008) 'Acute cellular uptake of abnormal prion protein is cell type and scrapie-strain independent', Virology, 379(2), pp. 284–293. doi: 10.1016/j.virol.2008.07.006.

Gretzschel, A. et al. (2005) 'Strain typing of German transmissible spongiform encephalopathies field cases in small ruminants by biochemical methods', Journal of Veterinary Medicine Series B: Infectious Diseases and Veterinary Public Health, 52(2), pp. 55–63. doi: 10.1111/j.1439-0450.2005.00827.x.

Griffith, J. S. (1967) 'Nature of the scrapie agent: Self-replication and scrapie', Nature, 215(5105), pp. 1043–1044. doi: 10.1038/2151043a0.

Grizenkova, J. et al. (2010) 'The retinoic acid receptor beta (Rarb) region of Mmu14 is associated with prion disease incubation time in mouse', PLoS ONE, 5(12), p. e15019. doi: 10.1371/journal.pone.0015019.

Grizenkova, J. et al. (2012) 'Overexpression of the Hspa13 (Stch) gene reduces prion disease incubation time in mice', Proceedings of the National Academy of Sciences. National Academy of Sciences, 109(34), pp. 13722–13727. doi: 10.1073/pnas.1208917109.

Grizenkova, J. et al. (2014) 'Microglial Cx3cr1 knockout reduces prion disease incubation time in mice', BMC Neuroscience, 15, p. 44. doi: 10.1186/1471-2202-15-44.

Gu, M. et al. (1997) 'Mitochondrial respiratory chain function in multiple system atrophy', Movement Disorders, 12(3), pp. 418–422. doi: 10.1002/mds.870120323.

Guo, J. L. et al. (2013) 'XDistinct α-synuclein strains differentially promote tau inclusions in neurons', Cell. Elsevier Inc., 154(1), pp. 103–117. doi: 10.1016/j.cell.2013.05.057.

Guo, J. L. et al. (2016) 'Unique pathological tau conformers from Alzheimer's brains transmit tau pathology in nontransgenic mice', The Journal of Experimental Medicine. The Rockefeller University Press, 213(12), pp. 2635–2654. doi: 10.1084/jem.20160833.

Guy, N. C. et al. (2015) 'Functions of the Hsp90-binding FKBP immunophilins', Sub-cellular biochemistry, 78, pp. 35–68. doi: 10.1007/978-3-319-11731-7_2.

Guzman, J. N. et al. (2010) 'Oxidant stress evoked by pacemaking in dopaminergic neurons is attenuated by DJ-1', Nature. Nature Publishing Group, 468(7324), pp. 696–700. doi: 10.1038/nature09536.

Hamaguchi, T. et al. (2016) 'Significant association of cadaveric dura mater grafting with subpial Aβ deposition and meningeal amyloid angiopathy', Acta Neuropathologica. Springer Berlin Heidelberg, 132(2), pp. 313–315. doi: 10.1007/s00401-016-1588-3.

Hannaoui, S. et al. (2013) ‘Prion Propagation and Toxicity Occur In Vitro with Two-Phase Kinetics Specific to Strain and Neuronal Type’, Journal of Virology, 87(5), pp. 2535–2548. doi: 10.1128/JVI.03082-12.

Hansen, C. et al. (2011) ‘α-Synuclein propagates from mouse brain to grafted dopaminergic neurons and seeds aggregation in cultured human cells’, Journal of Clinical Investigation. American Society for Clinical Investigation, 121(2), pp. 715–725. doi: 10.1172/JCI43366.

Harrar, Y., Bellini, C. and Faure, J. D. (2001) ‘FKBPs: at the crossroads of folding and transduction.’, Trends in plant science, 6(9), pp. 426–31.

Harris, D. A. (2003) ‘Trafficking, turnover and membrane topology of PrP’, British Medical Bulletin. Oxford University Press, 66(1), pp. 71–85. doi: 10.1093/bmb/66.1.71.

Harris, H. and Rubinsztein, D. C. (2012) ‘Control of autophagy as a therapy for neurodegenerative disease’, Nature Reviews Neurology, 8(2), pp. 108–117. doi: 10.1038/nrneurol.2011.200.

Hausch, F. (2015) ‘FKBPs and their role in neuronal signaling.’, Biochimica et biophysica acta, 1850(10), pp. 2035–40. doi: 10.1016/j.bbagen.2015.01.012.

Healy, E. F. (2017) ‘A prion-like mechanism for the propagated misfolding of SOD1 from in silico modeling of solvated near-native conformers’, PLoS ONE. Edited by E. A. Permyakov. Public Library of Science, 12(5), p. e0177284. doi: 10.1371/journal.pone.0177284.

Hecker, R. et al. (1992) ‘Replication of distinct scrapie prion isolates is region specific in brains of transgenic mice and hamsters’, Genes and Development. Cold Spring Harbor Laboratory Press, 6(7), pp. 1213–1228. doi: 10.1101/gad.6.7.1213.

Heilbronner, G. et al. (2013) ‘Seeded strain-like transmission of β-amyloid morphotypes in APP transgenic mice’, EMBO Reports, 14(11), pp. 1017–1022. doi: 10.1038/embor.2013.137.

Heiseke, A. et al. (2009) ‘Lithium induces clearance of protease resistant prion protein in prion-infected cells by induction of autophagy’, Journal of Neurochemistry, 109(1), pp. 25–34. doi: 10.1111/j.1471-4159.2009.05906.x.

Helekar, S. A. et al. (1994) ‘Prolyl isomerase requirement for the expression of functional homo-oligomeric ligand-gated ion channels.’, Neuron, 12(1), pp. 179–89.

Hill, A. F. and Collinge, J. (2004) ‘Prion Strains and Species Barriers’, Prions, 58(12), pp. 33–49. doi: 10.1159/.

Hill, A. F. et al. (1997a) ‘Diagnosis of new variant Creutzfeldt-Jakob disease by tonsil biopsy’, Lancet, 349(9045), pp. 99–100. doi: 10.1016/S0140-6736(97)24002-X.

Hill, A. F. et al. (1997b) ‘The same prion strain causes vCJD and BSE’, Nature. Nature Publishing Group, 389(6650), pp. 448–450. doi: 10.1038/38925.

Hill, A. F. et al. (1998) ‘Molecular screening of sheep for bovine spongiform encephalopathy’, Neurosci Lett, 255(3), pp. 159–162. doi: S0304394098007368 [pii].

Hill, A. F. et al. (1999) ‘Investigation of variant Creutzfeldt-Jakob disease and other human prion diseases with tonsil biopsy samples’, Lancet, 353(9148), pp. 183–189. doi: 10.1016/S0140-6736(98)12075-5.

Hill, A. F. et al. (2000) ‘Species-barrier-independent prion replication in apparently resistant species’, Proc. Natl. Acad. Sci. USA, 97(18), pp. 10248–10253.

Hill, A. F. et al. (2003) ‘Molecular classification of sporadic Creutzfeldt-Jakob disease’, Brain. Oxford University Press, 126(6), pp. 1333–1346. doi: 10.1093/brain/awg125.

Hilton, D. A. et al. (1998) ‘Prion immunoreactivity in appendix before clinical onset of variant Creutzfeldt-lakob disease’, Lancet. Elsevier, 352(9129), pp. 703–704. doi: 10.1016/S0140-6736(98)24035-9.

Hof, P. R. and Morrison, J. H. (2004) ‘The aging brain: Morphomolecular senescence of cortical circuits’, Trends in Neurosciences, 27(10), pp. 607–613. doi: 10.1016/j.tins.2004.07.013.

Horonchik, L. et al. (2005) ‘Heparan sulfate is a cellular receptor for purified infectious prions’, Journal of Biological Chemistry. American Society for Biochemistry and Molecular Biology, 280(17), pp. 17062–17067. doi: 10.1074/jbc.M500122200.

Hsiao, K. et al. (1989) ‘Linkage of a prion protein missense variant to Gerstmann-Sträussler syndrome.’, Nature, 338(6213), pp. 342–5. doi: 10.1038/338342a0.

Iba, M. et al. (2013) ‘Synthetic Tau Fibrils Mediate Transmission of Neurofibrillary Tangles in a Transgenic Mouse Model of Alzheimer’s-Like Tauopathy’, Journal of Neuroscience, 33(3), pp. 1024–1037. doi: 10.1523/JNEUROSCI.2642-12.2013.

Ikura, T. and Ito, N. (2013) ‘Peptidyl-prolyl isomerase activity of FK506 binding protein 12 prevents tau peptide from aggregating.’, Protein engineering, design & selection: PEDS, 26(9), pp. 539–46. doi: 10.1093/protein/gzt033.

Inouye, H. et al. (2000) ‘Structural changes in a hydrophobic domain of the prion protein induced by hydration and by Ala → Val and Pro → Leu substitutions’, Journal of Molecular Biology, 300(5), pp. 1283–1296. doi: 10.1006/jmbi.2000.3926.

Ironside, J. W. and Head, M. W. (2004) ‘Neuropathology and molecular biology of variant Creutzfeldt-Jakob disease’, Current Topics in Microbiology and Immunology, 284: 133-59.

Israelson, A. et al. (2010) ‘Misfolded mutant SOD1 directly inhibits VDAC1 conductance in a mouse model of inherited ALS’, Neuron, 67(4), pp. 575–587. doi: 10.1016/j.neuron.2010.07.019.

Iwamaru, Y. et al. (2007) ‘Microglial Cell Line Established from Prion Protein-Overexpressing Mice Is Susceptible to Various Murine Prion Strains’, Journal of Virology. American Society for Microbiology, 81(3), pp. 1524–1527. doi: 10.1128/JVI.01379-06.

J, H. A. and C. (2003) ‘Subclinical prion infection in humans and animals’, Br Med Bull, 66(12), pp. 161–170. doi: 10.1093/bmb/66.1.161.

Jackson, A. L. and Linsley, P. S. (2010) ‘Recognizing and avoiding siRNA off-target effects for target identification and therapeutic application’, Nature Reviews Drug Discovery, 9(1), pp. 57–67. doi: 10.1038/nrd3010.

Jackson, S. J. et al. (2016) ‘Short Fibrils Constitute the Major Species of Seed-Competent Tau in the Brains of Mice Transgenic for Human P301S Tau’, Journal of Neuroscience. Society for Neuroscience, 36(3), pp. 762–772. doi: 10.1523/JNEUROSCI.3542-15.2016.

Jagust, W. (2018) ‘Following the pathway to Alzheimer’s disease’, Nature Neuroscience. Nature Publishing Group, 21(3), pp. 306–308. doi: 10.1038/s41593-018-0085-5.

Jaunmuktane, Z. et al. (2015) ‘Evidence for human transmission of amyloid-β pathology and cerebral amyloid angiopathy’, Nature, 525(7568), pp. 247–250. doi: 10.1038/nature15369.

Jayaraman, T. et al. (1992) ‘FK506 binding protein associated with the calcium release channel (ryanodine receptor).’, The Journal of biological chemistry, 267(14), pp. 9474–7.

Jeffrey, M. and Wells, G. A. (1988) ‘Spongiform encephalopathy in a nyala (Tragelaphus angasi)’, Veterinary Pathology, 25(5), pp. 398-9.

Jeffrey, M. et al. (2001) ‘Onset of accumulation of PrPresin murine ME7 scrapie in relation to pathological and PrP immunohistochemical changes’, Journal of Comparative Pathology, 124(1), pp. 20–28. doi: 10.1053/jcpa.2000.0423.

Jeffrey, M. et al. (2011) ‘Cellular and sub-cellular pathology of animal prion diseases: Relationship between morphological changes, accumulation of abnormal prion protein and clinical disease’, Acta Neuropathologica. Springer-Verlag, 121(1), pp. 113–134. doi: 10.1007/s00401-010-0700-3.

Jimenez-Sanchez, M. et al. (2012) ‘Autophagy and polyglutamine diseases’, Progress in Neurobiology. Elsevier, 97(2), pp. 67–82. doi: 10.1016/j.pneurobio.2011.08.013.

Jung, B. C. et al. (2017) ‘Amplification of distinct α-synuclein fibril conformers through protein misfolding cyclic amplification’, Experimental and Molecular Medicine, 49(4), pp. 1–8. doi: 10.1038/emm.2017.1.

Kalia, L. V. and Lang, A. E. (2015) ‘Parkinson’s disease’, The Lancet. Elsevier, 386(9996), pp. 896–912. doi: 10.1016/S0140-6736(14)61393-3.

Kamah, A. et al. (2016) ‘Isomerization and Oligomerization of Truncated and Mutated Tau Forms by FKBP52 are Independent Processes.’, Journal of molecular biology, 428(6), pp. 1080–90. doi: 10.1016/j.jmb.2016.02.015.

Kane, M. D. et al. (2000) ‘Evidence for seeding of beta -amyloid by intracerebral infusion of Alzheimer brain extracts in beta -amyloid precursor protein-transgenic mice.’, The Journal of neuroscience : the official journal of the Society for Neuroscience, 20(10), pp. 3606–11. doi: 20/10/3606 [pii].

Kaneko, K. et al. (1997) ‘Evidence for protein X binding to a discontinuous epitope on the cellular prion protein during scrapie prion propagation’, Proceedings of the National

Academy of Sciences. National Academy of Sciences, 94(19), pp. 10069–10074. doi: 10.1073/pnas.94.19.10069.

Kaneko, K. et al. (2000) 'A synthetic peptide initiates Gerstmann-Straussler-Scheinker (GSS) disease in transgenic mice', Journal of Molecular Biology, 295(4), pp. 997–1007. doi: 10.1006/jmbi.1999.3386.

Kang, C. B. et al. (2008) 'FKBP family proteins: Immunophilins with versatile biological functions', NeuroSignals, 16(4), pp. 318–325. doi: 10.1159/000123041.

Kang, S. et al. (2012) 'CaV1.3-selective L-type calcium channel antagonists as potential new therapeutics for Parkinson's disease', Nature Communications, 3(1), p. 1146. doi: 10.1038/ncomms2149.

Kanu, N. et al. (2002) 'Transfer of scrapie prion infectivity by cell contact in culture', Current Biology, 12(7), pp. 523–530. doi: 10.1016/S0960-9822(02)00722-4.

Karapetyan, Y. E. et al. (2009) 'Prion strain discrimination based on rapid in vivo amplification and analysis by the cell panel assay', PLoS ONE. Edited by S. Koutsopoulos, 4(5), p. e5730. doi: 10.1371/journal.pone.0005730.

Kaufman, S. K. et al. (2016) 'Tau Prion Strains Dictate Patterns of Cell Pathology, Progression Rate, and Regional Vulnerability In Vivo', Neuron. Elsevier Inc., 92(4), pp. 796–812. doi: 10.1016/j.neuron.2016.09.055.

Kaufman, S. K. et al. (2017) 'Characterization of tau prion seeding activity and strains from formaldehyde-fixed tissue', Acta neuropathologica communications. BioMed Central, 5(1), p. 41. doi: 10.1186/s40478-017-0442-8.

Keeney, P. M. (2006) 'Parkinson's Disease Brain Mitochondrial Complex I Has Oxidatively Damaged Subunits and Is Functionally Impaired and Misassembled', Journal of Neuroscience, 26(19), pp. 5256–5264. doi: 10.1523/JNEUROSCI.0984-06.2006.

Kempster, S. et al. (2004) 'Clusterin shortens the incubation and alters the histopathology of bovine spongiform encephalopathy in mice', NeuroReport, 15(11), pp. 1735–1738. doi: 10.1097/01.wnr.0000134990.97051.22.

Khalili-Shirazi, A. et al. (2005) 'PrP glycoforms are associated in a strain-specific ratio in native PrPSc', Journal of General Virology. Microbiology Society, 86(9), pp. 2635–2644. doi: 10.1099/vir.0.80375-0.

Kiefhaber, T. et al. (1990) 'Folding of ribonuclease T1. 1. Existence of multiple unfolded states created by proline isomerization.', Biochemistry, 29(12), pp. 3053–61.

Kiernan, M. C. et al. (2011) 'Amyotrophic lateral sclerosis', The Lancet. Elsevier, 377(9769), pp. 942–955. doi: 10.1016/S0140-6736(10)61156-7.

Kim, C. et al. (2011) 'Protease-sensitive conformers in broad spectrum of distinct prpscstructures in sporadic creutzfeldt-jakob disease are indicator of progression rate', PLoS Pathogens. Edited by D. Westaway. Public Library of Science, 7(9), p. e1002242. doi: 10.1371/journal.ppat.1002242.

Kim, C. et al. (2012) 'Small Protease Sensitive Oligomers of PrPScin Distinct Human Prions Determine Conversion Rate of PrPC', PLoS Pathogens. Edited by S.

Supattapone. Public Library of Science, 8(8), p. e1002835. doi: 10.1371/journal.ppat.1002835.

Kim, D.-K. et al. (2017) 'Cell-to-cell Transmission of Polyglutamine Aggregates in C. elegans', Experimental Neurobiology. Korean Society for Brain and Neural Science, 26(6), p. 321. doi: 10.5607/en.2017.26.6.321.

Kim, J. Il et al. (2010) 'Mammalian prions generated from bacterially expressed prion protein in the absence of any mammalian cofactors', Journal of Biological Chemistry, 285(19), pp. 14083–14087. doi: 10.1074/jbc.C110.113464.

Kim, Y. S. et al. (1987) 'Incubation periods and survival times for mice injected stereotaxically with three scrapie strains in different brain regions', Journal of General Virology, 68(3), pp. 695–702. doi: 10.1099/0022-1317-68-3-695.

Kimberlin, R. H. and Walker, C. A. (1977) 'Characteristics of a short incubation model of scrapie in the golden hamster', Journal of General Virology, 34(2), pp. 295–304. doi: 10.1099/0022-1317-34-2-295.

Kimberlin, R. H. and Walker, C. A. (1978) 'Evidence that the transmission of one source of scrapie agent to hamsters involves separation of agent strains from a mixture', Journal of General Virology, 39(3), pp. 487–496. doi: 10.1099/0022-1317-39-3-487.

Kimberlin, R. H. and Walker, C. A. (1985) 'Competition between strains of scrapie depends on the blocking agent being infectious', Intervirology, 23(2), pp. 74–81. doi: 10.1159/000149588.

Kimberlin, R. H., Cole, S. and Walker, C. A. (1987) 'Temporary and permanent modifications to a single strain of mouse scrapie on transmission to rats and hamsters', Journal of General Virology. Microbiology Society, 68(7), pp. 1875–1881. doi: 10.1099/0022-1317-68-7-1875.

Kimberlin, R. H., Walker, C. A. and Fraser, H. (1989) 'The genomic identity of different strains of mouse scrapie is expressed in hamsters and preserved on reisolation in mice', Journal of General Virology, 70(8), pp. 2017–2025. doi: 10.1099/0022-1317-70-8-2017.

King, C. Y. and Diaz-Avalos, R. (2004) 'Protein-only transmission of three yeast prion strains', Nature. Nature Publishing Group, 428(6980), pp. 319–323. doi: 10.1038/nature02391.

Klein, C. and Westenberg, A. (2012) 'Genetics of Parkinson's disease', Cold Spring Harbor Perspectives in Medicine, 2(1): a008888. Doi: 10.1101/cshperspect.a008888.

Klingeborn, M. et al. (2011) 'Lower specific infectivity of protease-resistant prion protein generated in cell-free reactions', Proceedings of the National Academy of Sciences. National Academy of Sciences, 108(48), pp. E1244–E1253. doi: 10.1073/pnas.1111255108.

Klohn, P.-C. et al. (2003) 'A quantitative, highly sensitive cell-based infectivity assay for mouse scrapie prions', Proceedings of the National Academy of Sciences, 100(20), pp. 11666–11671. doi: 10.1073/pnas.1834432100.

Kordower, J. H. et al. (2008) ‘Lewy body-like pathology in long-term embryonic nigral transplants in Parkinson’s disease’, Nature Medicine, 14(5), pp. 504–506. doi: 10.1038/nm1747.

Korth, C., Kaneko, K. and Prusiner, S. B. (2000) ‘Expression of unglycosylated mutated prion protein facilitates PrPSc formation in neuroblastoma cells infected with different prion strains’, Journal of General Virology, 81(10), pp. 2555–2563. doi: 10.1099/0022-1317-81-10-2555.

Kovacs, G. G. (2015) ‘Invited review: Neuropathology of tauopathies: Principles and practice’, Neuropathology and Applied Neurobiology, 41(1), pp. 3–23. doi: 10.1111/nan.12208.

Kovacs, G. G. et al. (2000) ‘Clinicopathological phenotype of codon 129 valine homozygote sporadic Creutzfeldt-Jakob disease’, Neuropathology and Applied Neurobiology, 26(5), pp. 463–472. doi: 10.1046/j.1365-2990.2000.00279.x.

Kovacs, G. G. et al. (2016) ‘Dura mater is a potential source of Aβ seeds’, Acta Neuropathologica, 131(6), pp. 911–923. doi: 10.1007/s00401-016-1565-x.

Kraus, A. et al. (2015) ‘Prion protein prolines 102 and 105 and the surrounding lysine cluster impede amyloid formation’, Journal of Biological Chemistry, 290(35), pp. 21510–21522. doi: 10.1074/jbc.M115.665844.

Kraus, A. et al. (2017) ‘PrP P102L and Nearby Lysine Mutations Promote Spontaneous In Vitro Formation of Transmissible Prions’, Journal of Virology. American Society for Microbiology, 91(21), pp. e01276-17. doi: 10.1128/JVI.01276-17.

Kuczius, T. and Groschup, M. H. (1999) ‘Differences in proteinase K resistance and neuronal deposition of abnormal prion proteins characterize bovine spongiform encephalopathy (BSE) and scrapie strains’, Molecular medicine. The Feinstein Institute for Medical Research, 5(6), pp. 406–418. doi: 0144 [pii].

Kuczius, T., Haist, I. and Groschup, M. H. (1998) ‘Molecular analysis of bovine spongiform encephalopathy and scrapie strain variation.’, J Infect Dis, 178(3), pp. 693–699.

Laplante, M. and Sabatini, D. M. (2012) ‘mTOR signaling in growth control and disease.’, Cell, 149(2), pp. 274–93. doi: 10.1016/j.cell.2012.03.017.

Lasagna-Reeves, C. A. et al. (2012) ‘Alzheimer brain-derived tau oligomers propagate pathology from endogenous tau’, Scientific Reports. Nature Publishing Group, 2(1), p. 700. doi: 10.1038/srep00700.

Lasmezas, C. I. et al. (2001) ‘Adaptation of the bovine spongiform encephalopathy agent to primates and comparison with Creutzfeldt- Jakob disease: Implications for human health’, Proceedings of the National Academy of Sciences. National Academy of Sciences, 98(7), pp. 4142–4147. doi: 10.1073/pnas.041490898.

Lawson, V. A. et al. (2005) ‘Prion protein glycosylation’, Journal of Neurochemistry, 93(4), pp. 793–801. doi: 10.1111/j.1471-4159.2005.03104.x.

Lee, H. et al. (2001) ‘Increased Susceptibility to Kuru of Carriers of the PRNP 129 Methionine/Methionine Genotype’, The Journal of Infectious Diseases, 183(2), pp. 192–196. doi: 10.1086/317935.

Legname, G. et al. (2005) ‘Strain-specified characteristics of mouse synthetic prions’, Proceedings of the National Academy of Sciences. National Academy of Sciences, 102(6), pp. 2168–2173. doi: 10.1073/pnas.0409079102.

Legname, G. et al. (2006) ‘Continuum of prion protein structures enciphers a multitude of prion isolate-specified phenotypes’, Proceedings of the National Academy of Sciences. National Academy of Sciences, 103(50), pp. 19105–19110. doi: 10.1073/pnas.0608970103.

Lehmann, M. et al. (2013) ‘Diverging patterns of amyloid deposition and hypometabolism in clinical variants of probable Alzheimer’s disease’, Brain, 136(3), pp. 844–858. doi: 10.1093/brain/aws327.

Lehmann, M. et al. (2013) ‘Intrinsic connectivity networks in healthy subjects explain clinical variability in Alzheimer’s disease’, Proceedings of the National Academy of Sciences. National Academy of Sciences, 110(28), pp. 11606–11611. doi: 10.1073/pnas.1221536110.

LeMasson, G., Przedborski, S. and Abbott, L. F. (2014) ‘A Computational Model of Motor Neuron Degeneration’, Neuron, 83(4), pp. 975–988. doi: 10.1016/j.neuron.2014.07.001.

Leucht, C. et al. (2003) ‘The 37 kDa/67 kDa laminin receptor is required for PrPSc propagation in scrapie-infected neuronal cells’, EMBO Reports. European Molecular Biology Organization, 4(3), pp. 290–295. doi: 10.1038/sj.embor.embor768.

Lewis, P. A. et al. (2006) ‘Removal of the glycosylphosphatidylinositol anchor from PrPSc by cathepsin D does not reduce prion infectivity’, Biochemical Journal. Portland Press Ltd, 395(2), pp. 443–448. doi: 10.1042/BJ20051677.

Li, J. et al. (2010) ‘Darwinian evolution of prions in cell culture’, Science, 327(5967), pp. 869–872. doi: 10.1126/science.1183218.

Li, J. et al. (2011) ‘Mutability of prions’, EMBO Reports. Nature Publishing Group, 12(12), pp. 1243–1250. doi: 10.1038/embor.2011.191.

Li, J. Y. et al. (2008) ‘Lewy bodies in grafted neurons in subjects with Parkinson’s disease suggest host-to-graft disease propagation’, Nature Medicine, 14(5), pp. 501–503. doi: 10.1038/nm1746.

Li, S.-H. et al. (1993) ‘Huntington’s disease gene (IT15) is widely expressed in human and rat tissues’, Neuron, 11(5), pp. 985–993. doi: 10.1016/0896-6273(93)90127-D.

Limatola, C. and Ransohoff, R. M. (2014) ‘Modulating neurotoxicity through CX3CL1/CX3CR1 signaling’, Frontiers in Cellular Neuroscience, 8, p. 229. doi: 10.3389/fncel.2014.00229.

Liou, Y.-C. et al. (2003) ‘Role of the prolyl isomerase Pin1 in protecting against age-dependent neurodegeneration.’, Nature, 424(6948), pp. 556–61. doi: 10.1038/nature01832.

Liu, F.-L. et al. (2006) ‘The intracellular domain of amyloid precursor protein interacts with FKBP12.’, Biochemical and biophysical research communications, 350(2), pp. 472–7. doi: 10.1016/j.bbrc.2006.09.073.

Liu, F.-L., Liu, T.-Y. and Kung, F.-L. (2014) ‘FKBP12 regulates the localization and processing of amyloid precursor protein in human cell lines.’, Journal of biosciences, 39(1), pp. 85–95.

Lloyd, S. E. et al. (2001) ‘Identification of multiple quantitative trait loci linked to prion disease incubation period in mice.’, Proceedings of the National Academy of Sciences of the United States of America, 98(11), pp. 6279–83. doi: 10.1073/pnas.101130398.

Lloyd, S. E. et al. (2002) ‘Identification of genetic loci affecting mouse-adapted bovine spongiform encephalopathy incubation time in mice.’, Neurogenetics, 4(2), pp. 77–81.

Lloyd, S. E. et al. (2004) ‘Characterization of two distinct prion strains derived from bovine spongiform encephalopathy transmissions to inbred mice’, Journal of General Virology, 85(8), pp. 2471–2478. doi: 10.1099/vir.0.79889-0.

Lloyd, S. E. et al. (2010) ‘A Copine family member, Cpne8, is a candidate quantitative trait gene for prion disease incubation time in mouse’, Neurogenetics, 11(2), pp. 185–191. doi: 10.1007/s10048-009-0219-8.

Lloyd, S. E., Maytham, E. G., et al. (2009) ‘HECTD2 is associated with susceptibility to mouse and human prion disease’, PLoS Genetics, 5(2), p. e1000383. doi: 10.1371/journal.pgen.1000383.

Lloyd, S. E., Mead, S. and Collinge, J. (2013) ‘Genetics of prion diseases’, Current Opinion in Genetics and Development, 23(3), pp. 345–351. doi: 10.1016/j.gde.2013.02.012.

Lloyd, S. E., Rossor, M., et al. (2009) ‘HECTD2, a candidate susceptibility gene for Alzheimer’s disease on 10q’, BMC Medical Genetics, 10, p. 90. doi: 10.1186/1471-2350-10-90.

Lu, B. and Palacino, J. (2013) ‘A novel human embryonic stem cell-derived Huntington’s disease neuronal model exhibits mutant huntingtin (mHTT) aggregates and soluble mHTT-dependent neurodegeneration’, FASEB Journal, 27(5), pp. 1820–1829. doi: 10.1096/fj.12-219220.

Lu, P. J. et al. (1999) ‘The prolyl isomerase Pin1 restores the function of Alzheimer-associated phosphorylated tau protein.’, Nature, 399(6738), pp. 784–8. doi: 10.1038/21650.

Lugaresi, E. et al. (1986) ‘Fatal Familial Insomnia and Dysautonomia with Selective Degeneration of Thalamic Nuclei’, New England Journal of Medicine, 315(16), pp. 997–1003. doi: 10.1056/NEJM198610163151605.

Luhr, K. M. et al. (2002) ‘Processing and degradation of exogenous prion protein by CD11c(+) myeloid dendritic cells in vitro’, J Virol. American Society for Microbiology, 76(23), pp. 12259–12264. doi: 10.1128/jvi.76.23.12259-12264.2002.

Luhr, K. M. et al. (2004) ‘Scrapie protein degradation by cysteine proteases in CD11c+ dendritic cells and GT1-1 neuronal cells’, J Virol. American Society for Microbiology, 78(9), pp. 4776–4782. doi: 10.1128/jvi.78.9.4776-4782.2004.

Luk, K. C. et al. (2009) ‘Exogenous α-synuclein fibrils seed the formation of Lewy body-like intracellular inclusions in cultured cells’, Proceedings of the National Academy of Sciences, 106(47), pp. 20051–20056. doi: 10.1073/pnas.0908005106.

Luk, K. C. et al. (2012) ‘Pathological α-synuclein transmission initiates Parkinson-like neurodegeneration in nontransgenic mice’, Science, 338(6109), pp. 949–953. doi: 10.1126/science.1227157.

Luthi-Carter, R. and Cha, J. H. J. (2003) ‘Mechanisms of transcriptional dysregulation in Huntington’s disease’, Clinical Neuroscience Research, 3(3), pp. 165–177. doi: 10.1016/S1566-2772(03)00059-8.

Ma, M. R. et al. (2016) ‘Phosphorylation induces distinct alpha-synuclein strain formation’, Scientific Reports, 6. doi: 10.1038/srep37130.

Maas, E. et al. (2007) ‘Scrapie infection of prion protein-deficient cell line upon ectopic expression of mutant prion proteins’, Journal of Biological Chemistry, 282(26), pp. 18702–18710. doi: 10.1074/jbc.M701309200.

MacMillan, D. (2013) ‘FK506 binding proteins: cellular regulators of intracellular Ca2+ signalling.’, European journal of pharmacology, 700(1–3), pp. 181–93. doi: 10.1016/j.ejphar.2012.12.029.

Maddelein, M.-L. et al. (2002) ‘Amyloid aggregates of the HET-s prion protein are infectious’, Proceedings of the National Academy of Sciences, 99(11), pp. 7402–7407. doi: 10.1073/pnas.072199199.

Mahal, S. P. et al. (2007) ‘Prion strain discrimination in cell culture: The cell panel assay’, Proceedings of the National Academy of Sciences, 104(52), pp. 20908–20913. doi: 10.1073/pnas.0710054104.

Mahal, S. P. et al. (2010) ‘Transfer of a prion strain to different hosts leads to emergence of strain variants’, Proceedings of the National Academy of Sciences, 107(52), pp. 22653–22658. doi: 10.1073/pnas.1013014108.

Mahal, S. P. et al. (2012) ‘Propagation of RML prions in mice expressing PrP devoid of GPI anchor leads to formation of a novel, stable prion strain’, PLoS Pathogens, 8(6). doi: 10.1371/journal.ppat.1002746.

Makarava, N. et al. (2010) ‘Recombinant prion protein induces a new transmissible prion disease in wild-type animals’, Acta Neuropathologica. Springer, 119(2), pp. 177–187. doi: 10.1007/s00401-009-0633-x.

Makarava, N. et al. (2011) ‘Genesis of mammalian prions: From non-infectious amyloid fibrils to a transmissible prion disease’, PLoS Pathogens. Edited by S. Supattapone. Public Library of Science, 7(12), p. e1002419. doi: 10.1371/journal.ppat.1002419.

Makarava, N. et al. (2012) ‘Stabilization of a prion strain of synthetic origin requires multiple serial passages’, Journal of Biological Chemistry, 287(36), pp. 30205–30214. doi: 10.1074/jbc.M112.392985.

Mallucci, G. et al. (2003) ‘Depleting Neuronal PrP in Prion Infection Prevents Disease and Reverses Spongiosis’, Science, 302(5646), pp. 871–874. doi: 10.1126/science.1090187.

Manzoni, C. et al. (2013) ‘Pathogenic Parkinson’s disease mutations across the functional domains of LRRK2 alter the autophagic/lysosomal response to starvation’, Biochemical and Biophysical Research Communications, 441(4), pp. 862-866. Doi: 10.1016/j.bbrc.2013.10.159.

Manzoni, C. et al. (2016) ‘mTOR independent regulation of macroautophagy by Leucine Rich Repeat Kinase 2 via Beclin-1’, Scientific Reports, 6: 35106. Doi: 10.1038/srep35106

Marbiah, M. M. et al. (2014) ‘Identification of a gene regulatory network associated with prion replication’, The EMBO Journal, 33(14), pp. 1527–1547. doi: 10.15252/embj.201387150.

Marijanovic, Z. et al. (2009) ‘Identification of an intracellular site of prion conversion’, PLoS Pathogens. Edited by N. Mabbott. Public Library of Science, 5(5), p. e1000426. doi: 10.1371/journal.ppat.1000426.

Marks, A. R. (1996) ‘Cellular functions of immunophilins.’, Physiological reviews, 76(3), pp. 631–49.

Marks, A. R. (1997) ‘Intracellular calcium-release channels: regulators of cell life and death.’, The American journal of physiology, 272(2 Pt 2), pp. H597-605.

Mashaghi, A. et al. (2016) ‘Alternative modes of client binding enable functional plasticity of Hsp70’, Nature, 539(7629), pp. 448–451. doi: 10.1038/nature20137.

Masters, C. L. et al. (2015) ‘Alzheimer’s disease’, Nature Reviews Disease Primers. Nature Publishing Group, 1, p. 15056. doi: 10.1038/nrdp.2015.56.

Mastrianni, J. A. (2010) ‘The genetics of prion diseases.’, Genetics in medicine: official journal of the American College of Medical Genetics, 12(4), pp. 187–95. doi: 10.1097/GIM.0b013e3181cd7374.

Matsusue, E. et al. (2004) ‘White matter lesions in panencephalopathic type of Creutzfeldt-Jakob disease: MR imaging and pathologic correlations’, American Journal of Neuroradiology, 25(6), pp. 910–918.

Mattsson, N. et al. (2016) ‘Selective vulnerability in neurodegeneration: Insights from clinical variants of Alzheimer’s disease’, Journal of Neurology, Neurosurgery and Psychiatry. BMJ Publishing Group Ltd, 87(9), pp. 1000–1004. doi: 10.1136/jnnp-2015-311321.

McBride, P. A. et al. (1998) ‘Heparan sulfate proteoglycan is associated with amyloid plaques and neuroanatomically targeted PrP pathology throughout the incubation period of scrapie-infected mice’, Experimental Neurology, 149(2), pp. 447–454. doi: 10.1006/exnr.1997.6740.

Mead, S. et al. (2003) ‘Balancing selection at the prion protein gene consistent with prehistoric Kurulike epidemics’, Science, 300(5619), pp. 640–643. doi: 10.1126/science.1083320.

Mead, S. et al. (2009) ‘Genetic risk factors for variant Creutzfeldt-Jakob disease: a genome-wide association study’, The Lancet Neurology, 8(1), pp. 57–66. doi: 10.1016/S1474-4422(08)70265-5.

Mead, S. et al. (2012) ‘Genome-wide association study in multiple human prion diseases suggests genetic risk factors additional to PRNP’, Human molecular genetics, 21(8), pp. 1897-906. Doi: 10.1093/hmg/ddr607.

Mealer, R. G. et al. (2014) ‘Rhes, a Striatal-selective Protein Implicated in Huntington Disease, Binds Beclin-1 and activates autophagy’, Journal of Biological Chemistry, 289(6), pp. 3547–3554. doi: 10.1074/jbc.M113.536912.

Mealer, R. G., Subramaniam, S. and Snyder, S. H. (2013) ‘Rhes Deletion Is Neuroprotective in the 3-Nitropropionic Acid Model of Huntington’s Disease’, Journal of Neuroscience, 33(9), pp. 4206–4210. doi: 10.1523/JNEUROSCI.3730-12.2013.

Medori, R. et al. (1992) ‘Fatal Familial Insomnia, a Prion Disease with a Mutation at Codon 178 of the Prion Protein Gene’, New England Journal of Medicine, 326(7), pp. 444–449. doi: 10.1056/NEJM199202133260704.

Mesulam, M. et al. (2008) ‘Alzheimer and frontotemporal pathology in subsets of primary progressive aphasia’, Annals of Neurology, 63(6), pp. 709–719. doi: 10.1002/ana.21388.

Meyer-Luehmann, M. et al. (2006) ‘Exogenous induction of cerebral β-amyloidogenesis is governed by agent and host’, Science, 313(5794), pp. 1781–1784. doi: 10.1126/science.1131864.

Migliaccio, R. et al. (2009) ‘Clinical syndromes associated with posterior atrophy: Early age at onset AD spectrum’, Neurology, 73(19), pp. 1571–1578. doi: 10.1212/WNL.0b013e3181c0d427.

Mizutani, T. (1981) ‘Neuropathology of Creutzfeldt-Jakob Disease in Japan’, Pathology International. Blackwell Publishing Ltd, 31(6), pp. 903–922. doi: 10.1111/j.1440-1827.1981.tb02006.x.

Moda, F. et al. (2017) ‘Synthetic mammalian prions’, Neuromethods. American Association for the Advancement of Science, 129(5684), pp. 209–228. doi: 10.1007/978-1-4939-7211-1_13.

Mok, T. et al. (2017) ‘Variant Creutzfeldt–Jakob Disease in a Patient with Heterozygosity at PRNP Codon 129’, New England Journal of Medicine. Massachusetts Medical Society, 376(3), pp. 292–294. doi: 10.1056/NEJMc1610003.

Monaco, S. et al. (2012) ‘Allelic origin of protease-sensitive and protease-resistant prion protein isoforms in Gerstmann-Sträussler-Scheinker disease with the p102l mutation’, PLoS ONE. Edited by N. Nishida, 7(2), p. e32382. doi: 10.1371/journal.pone.0032382.

Montine, T. J. et al. (2012) ‘National institute on aging-Alzheimer’s association guidelines for the neuropathologic assessment of Alzheimer’s disease: A practical approach’, Acta Neuropathologica, 123(1), pp. 1–11. doi: 10.1007/s00401-011-0910-3.

Moore, R. a, Vorberg, I. and Priola, S. a (2005) 'Species barriers in prion diseases--brief review.', Archives of virology. Supplementum, (19), pp. 187–202. doi: 10.1007/3-211-29981-5_15.

Morales, R. (2017) 'Prion strains in mammals: Different conformations leading to disease', PLoS Pathogens. Public Library of Science, 13(7), p. e1006323. doi: 10.1371/journal.ppat.1006323.

Morales, R., Abid, K. and Soto, C. (2007) 'The prion strain phenomenon: Molecular basis and unprecedented features', Biochimica et Biophysica Acta - Molecular Basis of Disease, 1772(6), pp. 681–691. doi: 10.1016/j.bbadis.2006.12.006.

Mori, K. et al. (2013) 'The C9orf72 GGGGCC repeat is translated into aggregating dipeptide-repeat proteins in FTLD/ALS', Science, 339(6125), pp. 1335-8. Doi: 10.1126/science.1232927.

Mosconi, L. et al. (2008) 'Hippocampal hypometabolism predicts cognitive decline from normal aging', Neurobiology of Aging, 29(5), pp. 676–692. doi: 10.1016/j.neurobiolaging.2006.12.008.

Munch, C., O'Brien, J. and Bertolotti, A. (2011) 'Prion-like propagation of mutant superoxide dismutase-1 misfolding in neuronal cells', Proceedings of the National Academy of Sciences, 108(9), pp. 3548–3553. doi: 10.1073/pnas.1017275108.

Muñoz-Gutiérrez, J. F. et al. (2016) 'Transcriptomic determinants of scrapie prion propagation in cultured ovine microglia', PLoS ONE, 11(1), p. e0147727. doi: 10.1371/journal.pone.0147727.

Muratore, C. R. et al. (2017) 'Cell-type Dependent Alzheimer's Disease Phenotypes: Probing the Biology of Selective Neuronal Vulnerability', Stem Cell Reports, 9(6), pp. 1868–1884. doi: 10.1016/j.stemcr.2017.10.015.

Nakagawa, T. et al. (2005) 'Cyclophilin D-dependent mitochondrial permeability transition regulates some necrotic but not apoptotic cell death.', Nature, 434(7033), pp. 652–8. doi: 10.1038/nature03317.

Nakamura, K. et al. (2012) 'Proline isomer-specific antibodies reveal the early pathogenic tau conformation in Alzheimer's disease', Cell, 149(1), pp. 232–244. doi: 10.1016/j.cell.2012.02.016.

Naslavsky, N. et al. (1997) 'Characterization of detergent-insoluble complexes containing the cellular prion protein and its scrapie isoform', Journal of Biological Chemistry, 272(10), pp. 6324–6331. doi: 10.1074/jbc.272.10.6324.

Naslavsky, N. et al. (1999) 'Sphingolipid depletion increases formation of the scrapie prion protein in neuroblastoma cells infected with prions', Journal of Biological Chemistry, 274(30), pp. 20763–20771. doi: 10.1074/jbc.274.30.20763.

Neumann, M. et al. (2006) 'Ubiquitinated TDP-43 in frontotemporal lobar degeneration and amyotrophic lateral sclerosis', Science, 314(5796), pp. 130–133. doi: 10.1126/science.1134108.

Nicoll, A. J. et al. (2010) ‘Pharmacological chaperone for the structured domain of human prion protein’, Proceedings of the National Academy of Sciences. National Academy of Sciences, 107(41), pp. 17610–17615. doi: 10.1073/pnas.1009062107.

Nishida, N. et al. (2000) ‘Successful Transmission of Three Mouse-Adapted Scrapie Strains to Murine Neuroblastoma Cell Lines Overexpressing Wild-Type Mouse Prion Protein’, Journal of Virology. American Society for Microbiology (ASM), 74(1), pp. 320–325. doi: 10.1128/JVI.74.1.320-325.2000.

Nonaka, T. et al. (2013) ‘Prion-like Properties of Pathological TDP-43 Aggregates from Diseased Brains’, Cell Reports, 4(1), pp. 124–134. doi: 10.1016/j.celrep.2013.06.007.

Oba, N. et al. (2000) ‘A case of Gerstmann-Sträussler-Scheinker disease with severe muscular atrophy and vertical gaze palsy.’, Rinsho Shinkeigaku, 40(7), pp. 726–731.

Oda, T. et al. (1995) ‘Prion disease with 144 base pair insertion in a Japanese family line’, Acta Neuropathologica. Springer-Verlag, 90(1), pp. 80–86. doi: 10.1007/BF00294463.

Oelschlegel, A. M. and Weissmann, C. (2013) ‘Acquisition of Drug Resistance and Dependence by Prions’, PLoS Pathogens. Edited by D. Westaway. Public Library of Science, 9(2), p. e1003158. doi: 10.1371/journal.ppat.1003158.

Oesch, B. et al. (1985) ‘A cellular gene encodes scrapie PrP 27-30 protein’, Cell, 40(4), pp. 735–746. doi: 10.1016/0092-8674(85)90333-2.

Orr, M. E., Sullivan, A. C. and Frost, B. (2017) ‘A Brief Overview of Tauopathy: Causes, Consequences, and Therapeutic Strategies’, Trends in Pharmacological Sciences, 38(7), pp. 637–648. doi: 10.1016/j.tips.2017.03.011.

Ossenkoppele, R. et al. (2015) ‘The behavioural/dysexecutive variant of Alzheimer’s disease: clinical, neuroimaging and pathological features’, Brain, 138(9), pp. 2732–2749. doi: 10.1093/brain/awv191.

Owen, F. et al. (1990) An in-frame insertion in the prion protein gene in familial Creutzfeldt-Jakob disease, Molecular Brain Research. doi: 10.1016/0169-328X(90)90038-F.

Owen, J. P. et al. (2007a) ‘Molecular Profiling of Ovine Prion Diseases by Using Thermolysin-Resistant PrPSc and Endogenous C2 PrP Fragments’, Journal of Virology, 81(19), pp. 10532–10539. doi: 10.1128/JVI.00640-07.

Owen, J. P. et al. (2007b) ‘Use of thermolysin in the diagnosis of prion diseases’, Molecular Biotechnology, 35(2), pp. 161–170. doi: 10.1007/BF02686111.

Palmer, M. S. et al. (1991) ‘Homozygous prion protein genotype predisposes to sporadic Creutzfeldt-Jakob disease.’, Nature, 352(6333), pp. 340–2. doi: 10.1038/352340a0.

Pan, K. M. et al. (1993) ‘Conversion of alpha-helices into beta-sheets features in the formation of the scrapie prion proteins.’, Proceedings of the National Academy of Sciences, 90(23), pp. 10962–10966. doi: 10.1073/pnas.90.23.10962.

Paquet, S. et al. (2007) ‘PrPc Does Not Mediate Internalization of PrPSc but Is Required at an Early Stage for De Novo Prion Infection of Rov Cells’, Journal of Virology, 81(19), pp. 10786–10791. doi: 10.1128/JVI.01137-07.

Parchi, P. et al. (1996) ‘Molecular basis of phenotypic variability in sporadic Creutzfeldt-Jakob disease’, Annals of Neurology, 39(6), pp. 767–778. doi: 10.1002/ana.410390613.

Parchi, P. et al. (1999) ‘Classification of sporadic Creutzfeldt-Jakob disease based on molecular and phenotypic analysis of 300 subjects’, Annals of Neurology. John Wiley & Sons, Inc., 46(2), pp. 224–233. doi: 10.1002/1531-8249(199908)46:2<224::AID-ANA12>3.0.CO;2-W.

Pastorino, L. et al. (2006) ‘The prolyl isomerase Pin1 regulates amyloid precursor protein processing and amyloid-beta production.’, Nature, 440(7083), pp. 528–34. doi: 10.1038/nature04543.

Pastrana, M. A. et al. (2006) ‘Isolation and characterization of a proteinase K-sensitive PrPSc fraction’, Biochemistry. American Chemical Society, 45(51), pp. 15710–15717. doi: 10.1021/bi0615442.

Pattison, I. H. (1966) ‘The relative susceptibility of sheep, goats and mice to two types of the goat scrapie agent.’, Research in veterinary science, 7(2), pp. 207–12.

Pattison, I. H. and Millson, G. C. (1961) ‘Scrapie Produced Experimentally in Goats With Special Reference To the Clinical Syndrome’, Journal of Comparative Pathology and Therapeutics, 71, pp. 101-IN10. doi: 10.1016/S0368-1742(61)80013-1.

Paumier, K. L. et al. (2015) ‘Intrastriatal injection of pre-formed mouse α-synuclein fibrils into rats triggers α-synuclein pathology and bilateral nigrostriatal degeneration’, Neurobiology of Disease, 82, pp. 185–199. doi: 10.1016/j.nbd.2015.06.003.

Pearce, M. M. P. et al. (2015) ‘Prion-like transmission of neuronal huntingtin aggregates to phagocytic glia in the Drosophila brain’, Nature Communications, 6, p. 6768. doi: 10.1038/ncomms7768.

Pearson, G. R. et al. (1992) ‘Feline spongiform encephalopathy: fibril and PrP studies’, The Veterinary Record, 131(14), pp. 307-10.

Pecho-Vrieseling, E. et al. (2018) ‘Author Correction: Transneuronal propagation of mutant huntingtin contributes to non–cell autonomous pathology in neurons’, Nature Neuroscience, 17(8), p. 1. doi: 10.1038/s41593-018-0201-6.

Peelaerts, W. et al. (2015) ‘α-Synuclein strains cause distinct synucleinopathies after local and systemic administration’, Nature, 522(7556), pp. 340–344. doi: 10.1038/nature14547.

Peeraer, E. et al. (2015) ‘Intracerebral injection of preformed synthetic tau fibrils initiates widespread tauopathy and neuronal loss in the brains of tau transgenic mice’, Neurobiology of Disease, 73, pp. 83–95. doi: 10.1016/j.nbd.2014.08.032.

Perez, M. et al. (2007) ‘The role of the VQIVYK peptide in tau protein phosphorylation.’, Journal of neurochemistry, 103(4), pp. 1447–60. doi: 10.1111/j.1471-4159.2007.04834.x.

Petersen, R. B. et al. (1996) ‘Effect of the D178N mutation and the codon 129 polymorphism on the metabolism of the prion protein’, Journal of Biological Chemistry, 271(21), pp. 12661–12668. doi: 10.1074/jbc.271.21.12661.

Petkova, A. T. et al. (2005) ‘Self-propagating, molecular-level polymorphism in Alzheimer’s β-amyloid fibrils’, Science, 307(5707), pp. 262–265. doi: 10.1126/science.1105850.

Pickrell, A. M. and Youle, R. J. (2015) ‘The roles of PINK1, parkin, and mitochondrial fidelity in Parkinson’s disease’, Neuron, 85(2), pp. 257-73. doi: 10.1016/j.neoron.2014.12.007

Piro JR. et al. (2009) ‘Prion Protein Glycosylation Is Not Required for strain-specific neurotropism’, Journal of Virology, 83(11), pp. 5321–5328. doi: 10.1128/JVI.02502-08.

Plaitakis, A. et al. (2001) ‘Increased incidence of sporadic Creutzfeldt-Jakob disease on the island of Crete associated with a high rate of PRNP 129-methionine homozygosity in the local population’, Annals of Neurology, 50(2), pp. 227–233. doi: 10.1002/ana.1285.

Pokrishevsky, E., Grad, L. I. and Cashman, N. R. (2016) ‘TDP-43 or FUS-induced misfolded human wild-type SOD1 can propagate intercellularly in a prion-like fashion’, Scientific Reports. Nature Publishing Group, 6(1), p. 22155. doi: 10.1038/srep22155.

Polymenidou, M. et al. (2005) ‘Coexistence of multiple PrPSctypes in individuals with Creutzfeldt-Jakob disease’, Lancet Neurology, 4(12), pp. 805–814. doi: 10.1016/S1474-4422(05)70225-8.

Pratt, W. B., Silverstein, A. M. and Galigniana, M. D. (1999) ‘A model for the cytoplasmic trafficking of signalling proteins involving the hsp90-binding immunophilins and p50cdc37.’, Cellular signalling, 11(12), pp. 839–51.

Priola, S. A. and Lawson, V. A. (2001) ‘Glycosylation influences cross-species formation of protease-resistant prion protein’, EMBO Journal. European Molecular Biology Organization, 20(23), pp. 6692–6699. doi: 10.1093/emboj/20.23.6692.

Prusiner, S. B. (1982) ‘Novel proteinaceous infectious particles cause scrapie’, Science, 216(4542), pp. 136–144. doi: 10.1126/science.6801762.

Prusiner, S. B. (1991) ‘Molecular biology of prion diseases’, Science, 252(5012), pp. 1515–1522. doi: 10.1126/science.1675487.

Prusiner, S. B. et al. (2015) ‘Evidence for α-synuclein prions causing multiple system atrophy in humans with parkinsonism’, Proceedings of the National Academy of Sciences, 112(38), pp. E5308–E5317. doi: 10.1073/pnas.1514475112.

Puoti, G. et al. (1999) ‘Sporadic Creutzfeldt-Jakob disease: co-occurrence of different types of PrP(Sc) in the same brain.’, Neurology, 53(9), pp. 2173–6. doi: 10.1212/WNL.53.9.2173.

Puoti, G. et al. (2012) ‘Sporadic human prion diseases: Molecular insights and diagnosis’, The Lancet Neurology, 11(7), pp. 618–628. doi: 10.1016/S1474-4422(12)70063-7.

Rabinovici, G. D. and Jagust, W. J. (2009) ‘Amyloid imaging in aging and dementia: Testing the amyloid hypothesis in vivo’, Behavioural Neurology, 21(1–2), pp. 117–128. doi: 10.3233/BEN-2009-0232.

Rabinovici, G. D. et al. (2010) ‘Increased metabolic vulnerability in early-onset Alzheimer’s disease is not related to amyloid burden’, Brain, 133(2), pp. 512–528. doi: 10.1093/brain/awp326.

Race, R. and Chesebro, B. (1998) ‘Scrapie infectivity found in resistant species’, Nature. Nature Publishing Group, 392(6678), p. 770. doi: 10.1038/33834.

Race, R. et al. (2001) ‘Long-Term Subclinical Carrier State Precedes Scrapie Replication and Adaptation in a Resistant Species: Analogies to Bovine Spongiform Encephalopathy and Variant Creutzfeldt-Jakob Disease in Humans’, Journal of Virology, 75(21), pp. 10106–10112. doi: 10.1128/JVI.75.21.10106-10112.2001.

Rauscher, S. et al. (2006) ‘Proline and Glycine Control Protein Self-Organization into Elastomeric or Amyloid Fibrils’, Structure, 14(11), pp. 1667–1676. doi: 10.1016/j.str.2006.09.008.

Raymond, G. J. et al. (2012) ‘Isolation of Novel Synthetic Prion Strains by Amplification in Transgenic Mice Coexpressing Wild-Type and Anchorless Prion Proteins’, Journal of Virology. American Society for Microbiology, 86(21), pp. 11763–11778. doi: 10.1128/JVI.01353-12.

Redler, R. L. et al. (2014) ‘Non-native soluble oligomers of Cu/Zn superoxide dismutase (SOD1) contain a conformational epitope linked to cytotoxicity in amyotrophic lateral sclerosis (ALS)’, Biochemistry. American Chemical Society, 53(14), pp. 2423–2432. doi: 10.1021/bi500158w.

Reitz, C. (2012) ‘Alzheimer’s disease and the amyloid cascade hypothesis: A critical review’, International Journal of Alzheimer’s Disease. Hindawi Publishing Corporation, 369808(11). doi: 10.1155/2012/369808.

Ren, P. H. et al. (2009) ‘Cytoplasmic penetration and persistent infection of mammalian cells by polyglutamine aggregates’, Nature Cell Biology, 11(2), pp. 219–225. doi: 10.1038/ncb1830.

Renton, A. E. et al. (2011) ‘A hexanucleotide repeat expansion in C9ORF72 is the cause of chromosome 9p21-linked ALS-FTD’, Neuron, 72(2), pp. 257-68. Doi: 10.1016/j.neuron.2011.09.010.

Reynolds, P. D. et al. (1999) ‘Glucocorticoid resistance in the squirrel monkey is associated with overexpression of the immunophilin FKBP51.’, The Journal of clinical endocrinology and metabolism, 84(2), pp. 663–9. doi: 10.1210/jcem.84.2.5429.

Riesner, D. (2003) ‘Biochemistry and structure of PrPC and PrPSc’, British Medical Bulletin. Oxford University Press, 66(1), pp. 21–33. doi: 10.1093/bmb/66.1.21.

Riggs, D. L. et al. (2003) 'The Hsp90-binding peptidylprolyl isomerase FKBP52 potentiates glucocorticoid signaling in vivo.', The EMBO journal, 22(5), pp. 1158–67. doi: 10.1093/emboj/cdg108.

Ritchie, D. L. et al. (2017) 'Amyloid-β accumulation in the CNS in human growth hormone recipients in the UK', Acta Neuropathologica, 134(2), pp. 221–240. doi: 10.1007/s00401-017-1703-0.

Roberson, E. D. et al. (2007) 'Reducing endogenous tau ameliorates amyloid β-induced deficits in an Alzheimer's disease mouse model', Science, 316(5825), pp. 750–754. doi: 10.1126/science.1141736.

Roberts, B. E. et al. (2009) 'A synergistic small-molecule combination directly eradicates diverse prion strain structures', Nature Chemical Biology, 5(12), pp. 936–946. doi: 10.1038/nchembio.246.

Rosano, G. L. and Ceccarelli, E. A. (2014) 'Recombinant protein expression in Escherichia coli: Advances and challenges', Frontiers in Microbiology. Frontiers Media SA, 5(APR), p. 172. doi: 10.3389/fmicb.2014.00172.

Roselli, F. and Caroni, P. (2014) 'Modeling Neuronal Vulnerability in ALS', Neuron, 83(4), pp. 758–760. doi: 10.1016/j.neuron.2014.08.010.

Rosen, D. R. et al. (1993) 'Mutations in Cu/Zn superoxide dismutase gene are associated with familial amyotrophic lateral sclerosis', Nature. Nature Publishing Group, 362(6415), pp. 59–62. doi: 10.1038/362059a0.

Rosenbloom, M. H. et al. (2011) 'Distinct clinical and metabolic deficits in PCA and AD are not related to amyloid distribution', Neurology, 76(21), pp. 1789–1796. doi: 10.1212/WNL.0b013e31821cccad.

Ross, C. A. and Tabrizi, S. J. (2011) 'Huntington's disease: From molecular pathogenesis to clinical treatment', The Lancet Neurology, 10(1), pp. 83–98. doi: 10.1016/S1474-4422(10)70245-3.

Rossor, M. N. et al. (1984) 'Neurochemical characteristics of early and late onset types of Alzheimer's disease.', British medical journal (Clinical research ed.), 288(6422), pp. 961–964. doi: 10.1136/bmj.288.6422.961.

Rossor, M. N. et al. (2010) 'The diagnosis of young-onset dementia', The Lancet Neurology, 9(8), pp. 793–806. doi: 10.1016/S1474-4422(10)70159-9.

Rubenstein, R. et al. (1991) 'Scrapie-infected spleens: Analysis of infectivity, scrapie-associated fibrils, and protease-resistant proteins', Journal of Infectious Diseases, 164(1), pp. 29–35. doi: 10.1093/infdis/164.1.29.

Rubenstein, R. et al. (1992) 'Demonstration of scrapie strain diversity in infected PC12 cells', Journal of General Virology, 73(11), pp. 3027–3031. doi: 10.1099/0022-1317-73-11-3027.

Rueli, R. H. L. H. et al. (2015) 'Increased selenoprotein P in choroid plexus and cerebrospinal fluid in Alzheimer's disease brain', Journal of Alzheimer's Disease, 44(2), pp. 379–383. doi: 10.3233/JAD-141755.

Ryan, N. S. and Rossor, M. N. (2011) ‘Defining and describing the pre-dementia stages of familial Alzheimer’s disease’, Alzheimer’s Research and Therapy, 3(5), p. 29. doi: 10.1186/alzrt91.

Sá, F. et al. (2012) ‘Differences between early and late-onset Alzheimer’s disease in neuropsychological tests’, Frontiers in Neurology. Frontiers Media SA, MAY, p. 81. doi: 10.3389/fneur.2012.00081.

Sabatini, D. M., Lai, M. M. and Snyder, S. H. (1997) ‘Neural roles of immunophilins and their ligands.’, Molecular neurobiology, 15(2), pp. 223–39. doi: 10.1007/BF02740635.

Saborío, G. P. et al. (1999) ‘Cell-lysate conversion of prion protein into its protease-resistant isoform suggests the participation of a cellular chaperone’, Biochemical and Biophysical Research Communications, 258(2), pp. 470–475. doi: 10.1006/bbrc.1999.0660.

Saborio, G. P., Permanne, B. and Soto, C. (2001) ‘Sensitive detection of pathological prion protein by cyclic amplification of protein misfolding’, Nature, 411(6839), pp. 810–813. doi: 10.1038/35081095.

Sacino, A. N. et al. (2014) ‘Intramuscular injection of α-synuclein induces CNS α-synuclein pathology and a rapid-onset motor phenotype in transgenic mice’, Proceedings of the National Academy of Sciences, 111(29), pp. 10732–10737. doi: 10.1073/pnas.1321785111.

Safar, J. et al. (1998) ‘Eight prion strains have PrPSc molecules with different conformations’, Nature Medicine. Nature Publishing Group, 4(10), pp. 1157–1165. doi: 10.1038/2654.

Safar, J. G. et al. (2005) ‘Diagnosis of human prion disease’, Proceedings of the National Academy of Sciences, 102(9), pp. 3501–3506. doi: 10.1073/pnas.0409651102.

Safar, J., Cohen, F. E. and Prusiner, S. B. (2000) ‘Quantitative traits of prion strains are enciphered in the conformation of the prion protein.’, Arch Virol Suppl, (16), pp. 227–235.

Saijo, E. et al. (2016) ‘PrP Sc -Specific Antibody Reveals C-terminal Conformational Differences between Prion Strains’, Journal of Virology. Edited by K. L. Beemon, 90(10), pp. 4905-4913. doi: 10.1128/JVI.00088-16

Saita, S., Shirane, M. and Nakayama, K. I. (2013) ‘Selective escape of proteins from the mitochondria during mitophagy.’, Nature communications, 4, p. 1410. doi: 10.1038/ncomms2400.

Sajnani, G. and Requena, J. R. (2012) ‘Prions, proteinase K and infectivity’, Prion. Taylor & Francis, 6(5), pp. 430–432. doi: 10.4161/pri.22309.

Salazar, A. M. et al. (1983) ‘Syndromes of amyotrophic lateral sclerosis and dementia: Relation to transmissible Creutzfeldt-Jakob disease’, Annals of Neurology. Little, Brown and Company, 14(1), pp. 17–26. doi: 10.1002/ana.410140104.

Sanchez, J. P. et al. (2012) ‘Genome-wide study links MTMR7 gene to variant Creutzfeldt-Jakob risk’, Neurobiology of Aging, 33(7): 1487.e21-8. Doi: 10.1016/j.neurobiolaging.2011.10.011.

Sanders, D. W. et al. (2014) ‘Distinct tau prion strains propagate in cells and mice and define different tauopathies’, Neuron, 82(6), pp. 1271–1288. doi: 10.1016/j.neuron.2014.04.047.

Sanokawa-Akakura, R. et al. (2010) ‘Control of Alzheimer’s amyloid beta toxicity by the high molecular weight immunophilin FKBP52 and copper homeostasis in Drosophila.’, PloS one. Public Library of Science, 5(1), p. e8626. doi: 10.1371/journal.pone.0008626.

Sarkar, S. and Rubinsztein, D. C. (2008) ‘Huntington’s disease: Degradation of mutant huntingtin by autophagy’, FEBS Journal, 275(17), pp. 4263–4270. doi: 10.1111/j.1742-4658.2008.06562.x.

Sasaki, K. et al. (2002) ‘Increased clusterin (apolipoprotein J) expression in human and mouse brains infected with transmissible spongiform encephalopathies’, Acta Neuropathologica, 103(3), pp. 199–208. doi: 10.1007/s004010100456.

Sato, H., Kato, T. and Arawaka, S. (2013) ‘The role of Ser129 phosphorylation of α-synuclein in neurodegeneration of Parkinson’ s disease: A review of in vivo models’, Reviews in the Neurosciences, 24(2), pp. 115–123. doi: 10.1515/revneuro-2012-0071.

Saunders, A. M. et al. (1993) ‘Association of apolipoprotein E allele ε4 with late-onset familial ans sporadic Alzheimer’s disease’, Neurology, 43(8). Doi: https://doi.org/10.1212/WNL.43.8.1467.

Saverioni, D. et al. (2013) ‘Analyses of protease resistance and aggregation state of abnormal prion protein across the spectrum of human prions’, Journal of Biological Chemistry, 288(39), pp. 27972–27985. doi: 10.1074/jbc.M113.477547.

Saxena, S. and Caroni, P. (2011) ‘Selective Neuronal Vulnerability in Neurodegenerative Diseases: From Stressor Thresholds to Degeneration’, Neuron, 71(1), pp. 35–48. doi: 10.1016/j.neuron.2011.06.031.

Scammell, J. G. (2000) ‘Steroid resistance in the squirrel monkey: an old subject revisited.’, ILAR journal / National Research Council, Institute of Laboratory Animal Resources, 41(1), pp. 19–25.

Schapira, A. H. V (2013) ‘Calcium dysregulation in Parkinson’s disease’, Brain, 136(7), pp. 2015–2016. doi: 10.1093/brain/awt180.

Schatzl, H. M. et al. (1997) ‘A hypothalamic neuronal cell line persistently infected with scrapie prions exhibits apoptosis’, J Virol, 71(11), pp. 8821–8831.

Schlumpberger, M., Prusiner, S. B. and Herskowitz, I. (2001) ‘Induction of distinct [URE3] yeast prion strains.’, Molecular and cellular biology, 21(20), pp. 7035–46. doi: 10.1128/MCB.21.20.7035-7046.2001.

Schmidpeter, P. A. M., Koch, J. R. and Schmid, F. X. (2015) ‘Control of protein function by prolyl isomerization.’, Biochimica et biophysica acta, 1850(10), pp. 1973–82. doi: 10.1016/j.bbagen.2014.12.019.

Schott, J. M. and Warren, J. D. (2012) ‘Alzheimer’s disease: Mimics and chameleons’, Practical Neurology, 12(6), pp. 358–366. doi: 10.1136/practneurol-2012-000315.

Schwarze, U. et al. (2013) ‘Mutations in FKBp10, which result in bruck syndrome and recessive forms of osteogenesis imperfecta, inhibit the hydroxylation of telopeptide lysines in bone collagen’, Human Molecular Genetics, 22(1), pp. 1–17. doi: 10.1093/hmg/dds371.

Seredenina, T., Gokce, O. and Luthi-Carter, R. (2011) ‘Decreased striatal RGS2 expression is neuroprotective in Huntington’s disease (HD) and exemplifies a compensatory aspect of HD-induced gene regulation’, PLoS ONE. Edited by X.-J. Li, 6(7), p. e22231. doi: 10.1371/journal.pone.0022231.

Serrano-Pozo, A., Frosch, M. P., et al. (2011) ‘Neuropathological alterations in Alzheimer disease’, Cold Spring Harbor Perspectives in Medicine, 1(1), pp. a006189–a006189. doi: 10.1101/cshperspect.a006189.

Shadidy, M. et al. (1999) ‘Biochemical analysis of mouse FKBP60, a novel member of the FKPB family’, Biochimica et Biophysica Acta - Gene Structure and Expression, 1446(3), pp. 295–307. doi: 10.1016/S0167-4781(99)00080-9.

Shi, Q. et al. (2012) ‘Mouse-adapted scrapie strains 139A and ME7 overcome species barrier to induce experimental scrapie in hamsters and changed their pathogenic features’, Virology Journal. BioMed Central, 9, p. 63. doi: 10.1186/1743-422X-9-63.

Shikiya, R. A. et al. (2010) ‘Coinfecting Prion Strains Compete for a Limiting Cellular Resource’, Journal of Virology, 84(11), pp. 5706–5714. doi: 10.1128/JVI.00243-10.

Shim, S. et al. (2009) ‘Peptidyl-prolyl isomerase FKBP52 controls chemotropic guidance of neuronal growth cones via regulation of TRPC1 channel opening.’, Neuron, 64(4), pp. 471–83. doi: 10.1016/j.neuron.2009.09.025.

Shirane, M. and Nakayama, K. I. (2003) ‘Inherent calcineurin inhibitor FKBP38 targets Bcl-2 to mitochondria and inhibits apoptosis.’, Nature cell biology, 5(1), pp. 28–37. doi: 10.1038/ncb894.

Shirane-Kitsuji, M. and Nakayama, K. I. (2014) ‘Mitochondria: FKBP38 and mitochondrial degradation.’, The international journal of biochemistry & cell biology, 51, pp. 19–22. doi: 10.1016/j.biocel.2014.03.007.

Shorter, J. (2010) ‘Emergence and natural selection of drug-resistant prions’, Molecular BioSystems, 6(7), pp. 1115–1130. doi: 10.1039/c004550k.

Shou, W. et al. (1998) ‘Cardiac defects and altered ryanodine receptor function in mice lacking FKBP12.’, Nature, 391(6666), pp. 489–92. doi: 10.1038/35146.

Shyng, S. L., Heuser, J. E. and Harris, D. A. (1994) ‘A glycolipid-anchored prion protein is endocytosed via clathrin-coated pits’, Journal of Cell Biology, 125(6), pp. 1239–1250. doi: 10.1083/jcb.125.6.1239.

Sigurdsson, B. (1954) ‘Rida: A Chronic Encephalitis of Sheep.’, Br. Vet. J. W.B. Saunders, 110(9), pp. 341–354. doi: 10.1016/S0007-1935(17)50172-4.

Silveira, J. R. et al. (2005) ‘The most infectious prion protein particles’, Nature. Nature Publishing Group, 437(7056), pp. 257–261. doi: 10.1038/nature03989.

Silverstein, A. M. et al. (1999) ‘Different regions of the immunophilin FKBP52 determine its association with the glucocorticoid receptor, hsp90, and cytoplasmic dynein’, Journal of Biological Chemistry. American Society for Biochemistry and Molecular Biology, 274(52), pp. 36980–36986. doi: 10.1074/jbc.274.52.36980.

Simons, K. and Ikonen, E. (1997) ‘Functional rafts in cell membranes’, Nature. Nature Publishing Group, 387(6633), pp. 569–572. doi: 10.1038/42408.

Šišková, Z. et al. (2013) ‘Brain Region Specific Pre-Synaptic and Post-Synaptic Degeneration Are Early Components of Neuropathology in Prion Disease’, PLoS ONE, 8(1). doi: 10.1371/journal.pone.0055004.

Smethurst, P. et al. (2016) ‘In vitro prion-like behaviour of TDP-43 in ALS’, Neurobiology of Disease. Elsevier, 96, pp. 236–247. doi: 10.1016/j.nbd.2016.08.007.

Snow, A. D. et al. (1989) ‘Sulfated glycosaminoglycans in amyloid plaques of prion diseases’, Acta Neuropathologica. Springer-Verlag, 77(4), pp. 337–342. doi: 10.1007/BF00687367.

Snyder, S. H. et al. (1998) ‘Neural actions of immunophilin ligands.’, Trends in pharmacological sciences, 19(1), pp. 21–6.

Solassol, J., Crozet, C. and Lehmann, S. (2003) ‘Prion propagation in cultured cells’, British Medical Bulletin, 66, pp. 87–97. doi: 10.1093/bmb/66.1.87.

Somerville, R. A. (1999) ‘Host and transmissible spongiform encephalopathy agent strain control glycosylation of PrP’, Journal of General Virology, 80(7), pp. 1865–1872. doi: 10.1099/0022-1317-80-7-1865.

Sorce, S. et al. (2014) ‘The Role of the NADPH Oxidase NOX2 in Prion Pathogenesis’, PLoS Pathogens, 10(12), p. e1004531. doi: 10.1371/journal.ppat.1004531.

Spät, A. et al. (2008) ‘High- and low-calcium-dependent mechanisms of mitochondrial calcium signalling’, Cell Calcium. Churchill Livingstone, 44(1), pp. 51–63. doi: 10.1016/j.ceca.2007.11.015.

Spielhaupter, C. and Schätzl, H. M. (2001) ‘PrPC Directly Interacts with Proteins Involved in Signaling Pathways’, Journal of Biological Chemistry, 276(48), pp. 44604–44612. doi: 10.1074/jbc.M103289200.

Spirig, T. et al. (2014) ‘Direct evidence for self-propagation of different amyloid-ß fibril conformations’, Neurodegenerative Diseases, 14(3), pp. 151–159. doi: 10.1159/000363623.

Stahl, N. et al. (1987) ‘Scrapie prion protein contains a phosphatidylinositol glycolipid’, Cell, 51(2), pp. 229–240. doi: 10.1016/0092-8674(87)90150-4.

Stefanova, N. et al. (2009) ‘Multiple system atrophy: an update’, The Lancet Neurology. Elsevier, 8(12), pp. 1172–1178. doi: 10.1016/S1474-4422(09)70288-1.

Steffan, J. S. et al. (2004) ‘SUMO Modification of Huntingtin and Huntington’s Disease Pathology’, Science, 304(5667), pp. 100–104. doi: 10.1126/science.1092194.

Stocki, P. et al. (2016) ‘Inhibition of the FKBP family of peptidyl prolyl isomerases induces abortive translocation and degradation of the cellular prion protein.’, Molecular biology of the cell, 27(5), pp. 757–67. doi: 10.1091/mbc.E15-10-0729.

Stohr, J. et al. (2012) ‘Purified and synthetic Alzheimer’s amyloid beta (Aβ) prions’, Proceedings of the National Academy of Sciences, 109(27), pp. 11025–11030. doi: 10.1073/pnas.1206555109.

Stohr, J. et al. (2014) ‘Distinct synthetic Aβ prion strains producing different amyloid deposits in bigenic mice’, Proceedings of the National Academy of Sciences, 111(28), pp. 10329–10334. doi: 10.1073/pnas.1408968111.

Storer, C. L. et al. (2011) ‘FKBP51 and FKBP52 in signaling and disease.’, Trends in endocrinology and metabolism: TEM, 22(12), pp. 481–90. doi: 10.1016/j.tem.2011.08.001.

Subramaniam, S. et al. (2009) ‘Rhes, a striatal specific protein, mediates mutant-huntingtin cytotoxicity’, Science, 324(5932), pp. 1327–1330. doi: 10.1126/science.1172871.

Subramaniam, S. et al. (2012) ‘Rhes, a striatal-enriched small G protein, mediates mTOR signaling and L-DOPA-induced dyskinesia’, Nature Neuroscience, 15(2), pp. 191–193. doi: 10.1038/nn.2994.

Sugata, H. et al. (2009) ‘A peptidyl-prolyl isomerase, FKBP12, accumulates in Alzheimer neurofibrillary tangles.’, Neuroscience letters, 459(2), pp. 96–9. doi: 10.1016/j.neulet.2009.04.062.

Sultana, R. et al. (2006) ‘Oxidative modification and down-regulation of Pin1 in Alzheimer’s disease hippocampus: A redox proteomics analysis.’, Neurobiology of aging, 27(7), pp. 918–25. doi: 10.1016/j.neurobiolaging.2005.05.005.

Summers, D. W., Douglas, P. M. and Cyr, D. M. (2009) ‘Prion propagation by Hsp40 molecular chaperones.’, Prion. Landes Bioscience, 3(June), pp. 59–64. doi: 10.4161/pri.3.2.9062.

Sun, C.-S. et al. (2015) ‘Conformational switch of polyglutamine-expanded huntingtin into benign aggregates leads to neuroprotective effect.’, Scientific reports, 5, p. 14992. doi: 10.1038/srep14992.

Sun, L. et al. (2015) ‘Familial fatal insomnia with atypical clinical features in a patient with D178N mutation and homozygosity for Met at codon 129 of the prion protein gene’, Prion. Taylor & Francis, 9(3), pp. 228–235. doi: 10.1080/19336896.2015.1054601.

Sunyach, C. et al. (2003) ‘The mechanism of internalization of glycosylphosphatidylinositol-anchored prion protein’, EMBO Journal. European Molecular Biology Organization, 22(14), pp. 3591–3601. doi: 10.1093/emboj/cdg344.

Surmeier, D. J., Obeso, J. A. and Halliday, G. M. (2017) ‘Selective neuronal vulnerability in Parkinson disease’, Nature Reviews Neuroscience, 18(2), pp. 101–113. doi: 10.1038/nrn.2016.178.

Surmeier, J. et al. (2016) ‘Life on the Edge: Determinants of Selective Neuronal Vulnerability in Parkinson’s Disease’, in Mitochondrial Dysfunction in

Neurodegenerative Disorders. Cham: Springer International Publishing, pp. 141–173. doi: 10.1007/978-3-319-28637-2_6.

Suzuki, G., Shimazu, N. and Tanaka, M. (2012) 'A yeast prion, Mod5, promotes acquired drug resistance and cell survival under environmental stress', Science, 336(6079), pp. 355–359. doi: 10.1126/science.1219491.

Suzuki, M. et al. (2012) 'Calcium leak through ryanodine receptor is involved in neuronal death induced by mutant huntingtin.', Biochemical and biophysical research communications, 429(1–2), pp. 18–23. doi: 10.1016/j.bbrc.2012.10.107.

Tamgüney, G. et al. (2008) 'Genes contributing to prion pathogenesis', Journal of General Virology, 89(7), pp. 1777–1778. doi: 10.1099/vir.0.2008/001255-0.

Tanaka, M. et al. (2006) 'The physical basis of how prion conformations determine strain phenotypes', Nature. Nature Publishing Group, 442(7102), pp. 585–589. doi: 10.1038/nature04922.

Taniwaki, Y. et al. (2000) 'Familial Creutzfeldt-Jakob disease with D178N-129M mutation of PRNP presenting as cerebellar ataxia without insomnia', Journal of Neurology Neurosurgery and Psychiatry. BMJ Publishing Group Ltd, 68(3), p. 388. doi: 10.1136/jnnp.68.3.388.

Taraboulos, A. et al. (1995) 'Cholesterol depletion and modification of COOH-terminal targeting sequence of the prion protein inhibit formation of the scrapie isoform', Journal of Cell Biology, 129(1), pp. 121–132. doi: 10.1083/jcb.129.1.121.

Taylor, D. M. et al. (1998) 'Observations on thermostable subpopulations of the unconventional agents that cause transmissible degenerative encephalopathies', Veterinary Microbiology, 64(1), pp. 33–38. doi: 10.1016/S0378-1135(98)00257-0.

Telling, G. C. et al. (1995) 'Prion propagation in mice expressing human and chimeric PrP transgenes implicates the interaction of cellular PrP with another protein', Cell, 83(1), pp. 79–90. doi: 10.1016/0092-8674(95)90236-8.

Thackray, A. M. et al. (2007) 'Mouse-Adapted Ovine Scrapie Prion Strains Are Characterized by Different Conformers of PrPSc', Journal of Virology, 81(22), pp. 12119–12127. doi: 10.1128/JVI.01434-07.

Tixador, P. et al. (2010) 'The Physical Relationship between Infectivity and Prion Protein Aggregates Is Strain-Dependent', PLoS Pathogens. Edited by N. Mabbott. Public Library of Science, 6(4), p. e1000859. doi: 10.1371/journal.ppat.1000859.

Toll, E. C., Seifalian, A. M. and Birchall, M. A. (2011) 'The role of immunophilin ligands in nerve regeneration.', Regenerative medicine, 6(5), pp. 635–52. doi: 10.2217/rme.11.43.

Tong, M. and Jiang, Y. (2015) 'FK506-Binding Proteins and Their Diverse Functions', Current Molecular Pharmacology, 9(1), pp. 48–65. doi: 10.2174/1874467208666150519113541.

Tranchant, C. et al. (1999) 'Basis of phenotypic variability in sporadic Creutzfeldt-Jakob disease.', Neurology, 52(6), pp. 1244–1249.

Tufi, R. et al. (2014) ‘Enhancing nucleotide metabolism protects against mitochondrial dysfunction and neurodegeneration in a PINK1 model of Parkinson’s disease’, Nature Cell Biology, 16(2), pp. 157–166. doi: 10.1038/ncb2901.

Turnbull, J., Powell, A. and Guimond, S. (2001) ‘Heparan sulfate: Decoding a dynamic multifunctional cell regulator’, Trends in Cell Biology, 11(2), pp. 75–82. doi: 10.1016/S0962-8924(00)01897-3.

Tyedmers, J., Madariaga, M. L. and Lindquist, S. (2008) ‘Prion switching in response to environmental stress’, PLoS Biology. Edited by J. Weissman, 6(11), pp. 2605–2613. doi: 10.1371/journal.pbio.0060294.

Tzaban, S. et al. (2002) ‘Protease-sensitive scrapie prion protein in aggregates of heterogeneous sizes’, Biochemistry. American Chemical Society, 41(42), pp. 12868–12875. doi: 10.1021/bi025958g.

Udan-Johns, M. et al. (2014) ‘Prion-like nuclear aggregation of TDP-43 during heat shock is regulated by HSP40/70 chaperones’, Human Molecular Genetics. Oxford University Press, 23(1), pp. 157–170. doi: 10.1093/hmg/ddt408.

Valente, E. M. et al. (2004) ‘Hereditary early-onset Parkinson’s disease caused by mutations in PINK1’, Science, 304(5674), pp. 1158–1160. doi: 10.1126/science.1096284.

Van de Hoef, D. L., Bonner, J. M. and Boulianne, G. L. (2013) ‘FKBP14 is an essential gene that regulates Presenilin protein levels and Notch signaling in Drosophila.’, Development (Cambridge, England), 140(4), pp. 810–9. doi: 10.1242/dev.081356.

Van Hoesen, G. W., Augustinack, J. C. and Redman, S. J. (1999) ‘Ventromedial temporal lobe pathology in dementia, brain trauma, and schizophrenia’, Annals of the New York Academy of Sciences, 877(3), pp. 575–594. doi: 10.1111/j.1749-6632.1999.tb09290.x.

Vanselow, B. K. and Keller, B. U. (2000) ‘Calcium dynamics and buffering in oculomotor neurones from mouse that are particularly resistant during amyotrophic lateral sclerosis (ALS)-related motoneurone disease’, Journal of Physiology. Wiley-Blackwell, 525(2), pp. 433–445. doi: 10.1111/j.1469-7793.2000.t01-1-00433.x.

Veith, N. M. et al. (2009) ‘Immunolocalisation of PrPSc in scrapie-infected N2a mouse neuroblastoma cells by light and electron microscopy’, European Journal of Cell Biology, 88(1), pp. 45–63. doi: 10.1016/j.ejcb.2008.08.001.

Vella, L. J. et al. (2007) ‘Packaging of prions into exosomes is associated with a novel pathway of PrP processing’, Journal of Pathology, 211(5), pp. 582–590. doi: 10.1002/path.2145.

Vervliet, T., Parys, J. B. and Bultynck, G. (2015) ‘Bcl-2 and FKBP12 bind to IP3 and ryanodine receptors at overlapping sites: the complexity of protein-protein interactions for channel regulation.’, Biochemical Society transactions, 43(3), pp. 396–404. doi: 10.1042/BST20140298.

Vey, M. et al. (1996) ‘Subcellular colocalization of the cellular and scrapie prion proteins in caveolae-like membranous domains.’, Proceedings of the National

Academy of Sciences of the United States of America, 93(25), pp. 14945–9. doi: 10.1073/pnas.93.25.14945.

Vilette, D. (2008) ‘Cell models of prion infection’, Veterinary Research, 39(4), p. 10. doi: 10.1051/vetres:2007049.

Volpicelli-Daley, L. A. et al. (2011) ‘Exogenous α-Synuclein Fibrils Induce Lewy Body Pathology Leading to Synaptic Dysfunction and Neuron Death’, Neuron, 72(1), pp. 57–71. doi: 10.1016/j.neuron.2011.08.033.

Von Lewinski, F. and Keller, B. U. (2005) ‘Ca2+, mitochondria and selective motoneuron vulnerability: Implications for ALS’, Trends in Neurosciences, 28(9), pp. 494–500. doi: 10.1016/j.tins.2005.07.001.

Vorberg, I. and Priola, S. A. (2002) ‘Molecular basis of scrapie strain glycoform variation’, Journal of Biological Chemistry. in Press, 277(39), pp. 36775–36781. doi: 10.1074/jbc.M206865200.

Vorberg, I. et al. (2004) ‘Susceptibility of Common Fibroblast Cell Lines to Transmissible Spongiform Encephalopathy Agents’, The Journal of Infectious Diseases, 189(3), pp. 431–439. doi: 10.1086/381166.

Vorberg, I., Raines, A. and Priola, S. A. (2004) ‘Acute formation of protease-resistant prion protein does not always lead to persistent scrapie infection in vitro’, Journal of Biological Chemistry, 279(28), pp. 29218–29225. doi: 10.1074/jbc.M402576200.

Wadsworth, J. D. F. and Collinge, J. (2007) ‘Update on human prion disease’, Biochimica et Biophysica Acta - Molecular Basis of Disease. Elsevier, 1772(6), pp. 598–609. doi: 10.1016/j.bbadis.2007.02.010.

Wadsworth, J. D. F. et al. (1999) ‘Strain-specific prion-protein conformation determined by metal ions’, Nature Cell Biology, 1(1), pp. 55–59. doi: 10.1038/9030.

Wadsworth, J. D. F. et al. (2003) ‘Molecular and clinical classification of human prion disease’, British Medical Bulletin. Oxford University Press, 66(1), pp. 241–254. doi: 10.1093/bmb/dg66.241.

Wadsworth, J. D. F. et al. (2004) ‘Human prion protein with valine 129 prevents expression of variant CJD phenotype’, Science, 306(5702), pp. 1793–1796. doi: 10.1126/science.1103932.

Wakabayashi, K. et al. (2007) ‘The Lewy body in Parkinson’s disease: Molecules implicated in the formation and degradation of α-synuclein aggregates’, Neuropathology, 27(5), pp. 494–506. doi: 10.1111/j.1440-1789.2007.00803.x.

Walmsley, A. R., Zeng, F. and Hooper, N. M. (2003) ‘The N-terminal region of the prion protein ectodomain contains a lipid raft targeting determinant’, Journal of Biological Chemistry. American Society for Biochemistry and Molecular Biology, 278(39), pp. 37241–37248. doi: 10.1074/jbc.M302036200.

Wan, W. et al. (2015) ‘Structural studies of truncated forms of the prion protein PrP’, Biophysical Journal, 108(6), pp. 1548–1554. doi: 10.1016/j.bpj.2015.01.008.

Wang, H. et al. (2008) ‘Direct and selective elimination of specific prions and amyloids by 4,5-dianilinophthalimide and analogs’, Proceedings of the National Academy of Sciences, 105(20), pp. 7159–7164. doi: 10.1073/pnas.0801934105.

Wang, P. and Heitman, J. (2005) ‘The cyclophilins’, Genome Biology. BioMed Central, 6(7), p. 226. doi: 10.1186/gb-2005-6-7-226.

Watts, J. C. et al. (2014) ‘Serial propagation of distinct strains of Aβ prions from Alzheimer’s disease patients’, Proceedings of the National Academy of Sciences, 111(28), pp. 10323–10328. doi: 10.1073/pnas.1408900111.

Wedemeyer, W. J., Welker, E. and Scheraga, H. A. (2002) ‘Proline cis-trans isomerization and protein folding.’, Biochemistry, 41(50), pp. 14637–44.

Weissmann, C. (2004) ‘The state of the prion’, Nature Reviews Microbiology. Nature Publishing Group, 2(11), pp. 861–871. doi: 10.1038/nrmicro1025.

Weissmann, C. (2012) ‘Mutation and selection of prions’, PLoS Pathogens, 8(3), pp. 1–4. doi: 10.1371/journal.ppat.1002582.

Weissmann, C. et al. (2011) ‘Prions on the move’, EMBO Reports, 12(11), pp. 1109–1117. doi: 10.1038/embor.2011.192.

Wells, G. A. et al. (1987) ‘A novel progressive spongiform encephalopathy in cattle’, The Veterinary Record, 121(18), pp. 419-420.

Wells, G. A. et al. (1994) ‘Infectivity in the ileum of cattle challenged orally with bovine spongiform encephalopathy’, Veterinary Record, 135(2), pp. 40–41. doi: 10.1136/vr.135.2.40.

Wells, G. A. H., Wilesmith, J. W. and McGill, I. S. (1991) ‘Bovine Spongiform Encephalopathy: A Neuropathological Perspective’, Brain Pathology, 1(2), pp. 69–78. doi: 10.1111/j.1750-3639.1991.tb00642.x.

Wenborn, A. et al. (2015) ‘A novel and rapid method for obtaining high titre intact prion strains from mammalian brain’, Scientific Reports, 5(1), p. 10062. doi: 10.1038/srep10062.

West, A. B. et al. (2005) ‘Parkinson’s disease-associated mutations inleucine-rich repeat kinase 2 augment kinase activity’, PNAS, 102(46), pp. 16842-7. Doi: 10.1073/pnas.0507360102.

West, B. (2016) ‘A loss-of-function approach to investigate the role of cholesterol in prion replication’, Doctoral thesis, UCL (University College London). UCL (University College London).

Westergard, L., Christensen, H. M. and Harris, D. A. (2007) ‘The cellular prion protein (PrPC): Its physiological function and role in disease’, Biochimica et Biophysica Acta - Molecular Basis of Disease, 1772 (6), pp. 629-644. doi: 10.1016/j.bba

Wickner, R. B. (1994) ‘[URE3] as an altered URE2 protein: Evidence for a prion analog in Saccharomyces cerevisiae’, Science, 264(5158), pp. 566–569. doi: 10.1126/science.7909170.

Wilesmith, J. W. et al. (1988) ‘Bovine spongiform encephalopathy: epidemiological studies.’, The Veterinary record. British Medical Journal Publishing Group, 123(25), pp. 638–44. doi: 10.1136/vr.123.25.638.

Wilesmith, J. W. et al. (1992) ‘Bovine spongiform encephalopathy: epidemiological features 1985 to 1990.’, The Veterinary record. British Medical Journal Publishing Group, 130(5), pp. 90–94. doi: 10.1136/vr.130.5.90.

Will, R. G. et al. (1996) ‘A new variant of Creutzfeldt-Jakob disease in the UK’, The Lancet. Elsevier, 347(9006), pp. 921–925. doi: 10.5555/uri:pii:S0140673696914129.

Will, R. G. et al. (2000) ‘Diagnosis of new variant Creutzfeldt-Jakob disease’, Annals of Neurology, 47(5), pp. 575–582. doi: 10.1002/1531-8249(200005)47:5<575::AID-ANA4>3.0.CO;2-W.

Williams, E. S. et al. (1993) ‘Neuropathology of chronic wasting disease of mule deer (Odocoileus hemionus) and elk (Cervus elaphus nelson)’, Veterinary Pathology, 30(1), pp. 36-45. Doi: 10.1177/030098589303000105.

Williams, E. S. et al. (2002) ‘Chronic wasting disease of deer and elk: A review with recommendations for management’, Journal of Wildlife management, 66(3), pp. 551-563. Doi: 10.2307/3803123.

Windl, O. et al. (1996) ‘Genetic basis of Creutzfeldt-Jakob disease in the United Kingdom: A systematic analysis of predisposing mutations and allelic variation in the PRNP gene’, Human Genetics, 98(3), pp. 259–264. doi: 10.1007/s004390050204.

Winklhofer, K. F. and Haass, C. (2010) ‘Mitochondrial dysfunction in Parkinson’s disease’, Biochimica et Biophysica Acta - Molecular Basis of Disease. Elsevier, 1802(1), pp. 29–44. doi: 10.1016/j.bbadis.2009.08.013.

Wong, C. et al. (2001) ‘Sulfated glycans and elevated temperature stimulate PrPsc-dependent cell-free formation of protease-resistant prion protein’, EMBO Journal, 20(3), pp. 377–386. doi: 10.1093/emboj/20.3.377.

Xu, F., Karnaukhova, E. and Vostal, J. G. (2008) ‘Human cellular prion protein interacts directly with clusterin protein’, Biochimica et Biophysica Acta - Molecular Basis of Disease, 1782(11), pp. 615–620. doi: 10.1016/j.bbadis.2008.08.004.

Xu, L. et al. (2017) ‘Familial Mutations May Switch Conformational Preferences in alpha-Synuclein Fibrils’, ACS Chem Neurosci, 8(4), pp. 837–849. doi: 10.1021/acschemneuro.6b00406.

Yao, Z. et al. (2011) ‘Cell metabolism affects selective vulnerability in PINK1-associated Parkinson’s disease’, Journal of Cell Science. Company of Biologists, 124(24), pp. 4194–4202. doi: 10.1242/jcs.088260.

Yoshida, N. L. et al. (2002) ‘Analysis of gene expression patterns during glucocorticoid-induced apoptosis using oligonucleotide arrays.’, Biochemical and biophysical research communications, 293(4), pp. 1254–61. doi: 10.1016/S0006-291X(02)00361-3.

Young, K. et al. (1995) ‘Gerstmann-straussler-scheinker disease with mutation at codon 102 and methionine at codon 129 of prnp in previously unreported patients’, Neurology, 45(6), pp. 1127–1134. doi: 10.1212/WNL.45.6.1127.

Yu, Z.-X. et al. (2003) ‘Mutant huntingtin causes context-dependent neurodegeneration in mice with Huntington’s disease.’, The Journal of neuroscience: the official journal of the Society for Neuroscience. Society for Neuroscience, 23(6), pp. 2193–2202. doi: 23/6/2193 [pii].

Zarei, S. et al. (2015) ‘A comprehensive review of amyotrophic lateral sclerosis’, Surgical Neurology International. Wolters Kluwer -- Medknow Publications, 6(1), p. 171. doi: 10.4103/2152-7806.169561.

Zhang, J. et al. (2008) ‘Arp11 affects dynein-dynactin interaction and is essential for dynein function in Aspergillus nidulans’, Traffic, 9(7), pp. 1073–1087. doi: 10.1111/j.1600-0854.2008.00748.x.

Zlotnik, I. and Rennie, J. C. (1963) ‘Further observations on the experimental transmission of scrapie from sheep and goats to laboratory mice’, Journal of Comparative Pathology and Therapeutics. W.B. Saunders, 73, pp. 150–163. doi: 10.1016/S0368-1742(63)80018-1.

Zuccato, C. et al. (2001) ‘Loss of huntingtin-mediated BDNF gene transcription in Huntington’s disease’, Science, 293(5529), pp. 493–498. doi: 10.1126/science.1059581.